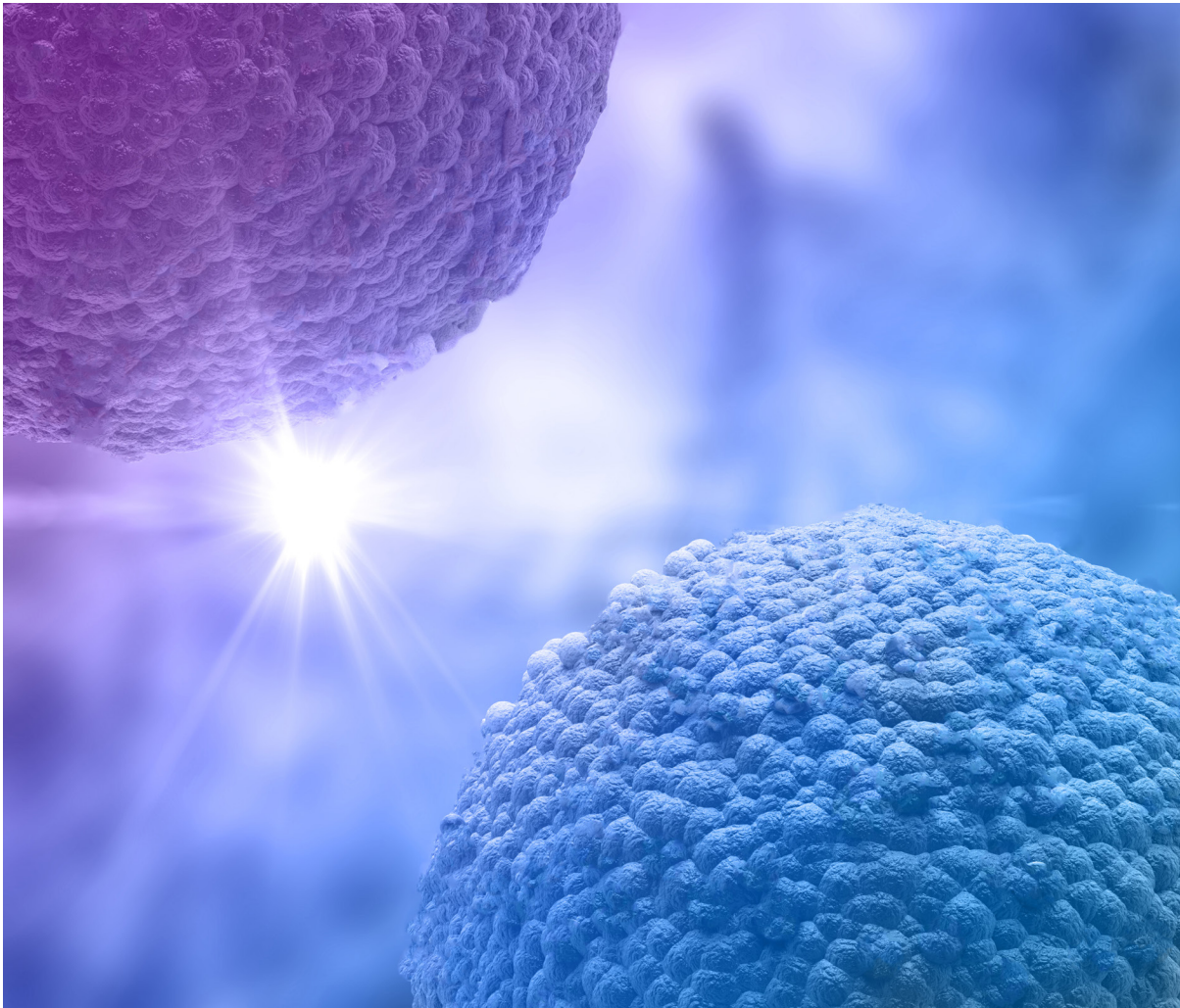


Targeting pancreatic ductal adenocarcinoma and glioblastoma with oxidative stress-mediated treatment strategies

Focus on tumor cell death and modulation of the tumor microenvironment

Jinthe Van Loenhout



Promotoren **prof. dr. Evelien Smits** | **dr. Christophe Deben** | **prof. dr. Annemie Bogaerts**

Proefschrift voorgedragen tot het behalen van de graad van doctor in de medische wetenschappen
Faculteit Geneeskunde en Gezondheidswetenschappen | Antwerpen, 2021

Jinthe Van Loenhout

Targeting pancreatic ductal adenocarcinoma and glioblastoma with oxidative stress-mediated treatment strategies

Cover design: Jinthe Van Loenhout, Natacha Hoevenaegel

Cover image: Freepik.com

The research described in this dissertation was performed at the Center for Oncological Research (CORE) at the University of Antwerp. This work was supported financially by the University of Antwerp (BOF) and the Olivia Hendrickx Research Fund.

© Copyright Jinthe Van Loenhout, 2021 – All rights reserved

Printed by D Provo nv, Bulens 23 B, B-2275, Gierle

**Targeting pancreatic ductal adenocarcinoma and
glioblastoma with oxidative stress-mediated treatment
strategies**

Focus on tumor cell death and modulation of the tumor
microenvironment

**Oxidatieve stress-gemedieerde behandelingen voor
pancreaskanker en glioblastoom**

Focus op tumorceldood en modulatie van de tumormicro-omgeving

Proefschrift voorgelegd tot het behalen van de graad van doctor in de medische
wetenschappen aan de Universiteit Antwerpen te verdedigen door

Jinthe Van Loenhout

Faculteit Geneeskunde en Gezondheidswetenschappen

Promotoren

Prof. Dr. Evelien Smits

Dr. Christophe Deben

Prof. Dr. Annemie Bogaerts

Antwerpen 2021

MEMBERS OF THE JURY

PROMOTORS

Prof. Dr. Evelien Smits, University of Antwerp

Dr. Christophe Deben, University of Antwerp

Prof. Dr. Annemie Bogaerts, University of Antwerp

INTERNAL JURY

Prof. Dr. Didier Ebo, University of Antwerp

Prof. Dr. Wim Vanden Berghe, University of Antwerp

EXTERNAL JURY

Prof. Dr. Cristina Canal, Technical University of Catalonia (UPC)

Dr. Sander Bekeschus, Leibniz Institute for Plasma Science and Technology

(INP Greifswald)

FUNDING ACKNOWLEDGMENTS



TABLE OF CONTENTS

TABLE OF CONTENTS	5
LIST OF ABBREVIATIONS	7
CHAPTER 1	9
General introduction, aims & outline of the study	9
General introduction	11
Rationale	19
Aims & outline.....	19
References	22
CHAPTER 2	27
Oxidative stress-inducing anticancer therapies: taking a closer look at their immunomodulating effects	27
Abstract.....	29
Introduction	30
Indirect and direct effects of oxidative stress-inducing therapies on the antitumoral immune response.....	38
Conclusion.....	46
References	47
CHAPTER 3	55
Cold atmospheric plasma-treated PBS eliminates immunosuppressive pancreatic stellate cells and induces immunogenic cell death of pancreatic cancer cells	55
Abstract.....	57
Introduction	58
Materials and methods.....	60
Results.....	63
Discussion	72
Conclusion.....	75
References	76
CHAPTER 4	79
Auranofin and cold atmospheric plasma synergize to trigger distinct cell death mechanisms and immunogenic responses in glioblastoma multiforme	79
Abstract.....	81
Introduction	82
Materials & methods.....	83
Results.....	90
Discussion	106
Conclusion.....	109
References	110

CHAPTER 5	113
Unraveling the <i>in vivo</i> therapeutic potential of auranofin and cold atmospheric plasma in glioblastoma	113
Abstract.....	115
Introduction.....	116
Material and methods.....	117
Results.....	120
Discussion.....	127
Conclusion.....	129
References.....	129
CHAPTER 6	131
General discussion, future challenges and future perspectives	131
General discussion.....	133
Future challenges.....	136
Future perspectives.....	139
References.....	142
SUMMARY	147
SAMENVATTING	151
DANKWOORD	155
CURRICULUM VITAE	159

LIST OF ABBREVIATIONS

AF	auranofin
Akt	protein kinase B
APC	antigen presenting cell
ANXA1	annexin A1
ATCC	American type culture collection
ATP	adenosine triphosphate
Bcl-2	B cell lymphoma 2
BSO	buthionine sulfoximine
CAP	cold atmospheric plasma
CCL	chemokine (C-C motif) ligand
CD	cluster of differentiation
CI	combination index
CNS	central nervous system
CRT	calreticulin
CTLA-4	cytotoxic T lymphocyte associated protein 4
CXCL	chemokine (C-X-C motif) ligand
DAMPs	damage-associated molecular patterns
DBD	dielectric barrier discharge
DC	dendritic cell
DFO	deferoxamine
DMSO	dimethyl sulfoxide
ELISA	enzyme-linked immunosorbent assay
E:T	effector:target
ER	endoplasmic reticulum
ERK	extracellular signal-regulated kinase
FBS	fetal bovine serum
FDA	Food and Drug Administration
Fer-1	ferrostatin-1
FFPE	formalin-fixed paraffin-embedded
GBM	glioblastoma multiforme
GCU	green calibration unit
GSH	glutathione
HMGB1	high mobility group box 1
HSP	heat shock protein
ICD	immunogenic cell death
IFN	interferon
IHC	immunohistochemistry
IL	interleukin

JNK	c-Jun N-terminal kinase
MAPK	mitogen-activated protein kinases
MDSCs	myeloid-derived suppressor cells
MFI	mean fluorescence intensity
MHC	major histocompatibility complex
MICA	MHC class I chain related molecule A
mTOR	mammalian target of rapamycin
NAC	n-acetyl-cysteine
NADPH	nicotinamide adenine dinucleotide phosphate
NF- κ B	nuclear factor kappa B
NK	natural killer
NKG2D(L)	natural killer group 2D (ligand)
NOS	nitric oxide synthase
NOX	NADPH oxidase
Nrf2	nuclear factor erythroid 2-related factor 2
PBMC	peripheral blood mononuclear cells
PBS	phosphate buffered saline
PCC	pancreatic cancer cell
PDAC	pancreatic ductal adenocarcinoma
PD-(L)1	programmed death (ligand)-1
PDT	photodynamic therapy
PI	propidium iodide
PI3K	phosphatidylinositol 3-kinase
pPBS	plasma-treated phosphate buffered saline
PSC	pancreatic stellate cell
PTEN	phosphatase and tensin homolog
RCU	red calibration unit
RNS	reactive nitrogen species
ROS	reactive oxygen species
SOD	superoxide dismutase
STAT3	signal transducer and activator of transcription 3
STING	stimulator of interferon genes
TAM	tumor-associated macrophage
TGF- β	transforming growth factor- β
TILs	tumor infiltrating lymphocytes
TLR	toll-like receptor
TME	tumor microenvironment
TNF- α	tumor necrosis factor- α
Tregs	regulatory T cells
Trx	thioredoxin
TrxR	thioredoxin reductase

CHAPTER 1

General introduction, aims & outline of the study

Partly published as: Laurie Freire Boullosa*, **Jinthe Van Loenhout***, Christophe Deben*. Chapter 4 – Endogenous antioxidants in the prognosis and treatment of lung cancer. In: Preedy VR, Patel VB, editors. Cancer (Second Edition). San Diego: Academic Press; 2021. p. 39-48

(*All authors contributed equally)

General introduction

'Cold' immunogenic tumors

Within the last decade, immunotherapy has been established as a breakthrough in cancer therapy. This has mainly been driven by the clinical data and approval of several checkpoint inhibitors (e.g. anti-CTLA-4 and anti-PD-1/L1), with more than two thousand ongoing clinical trials with these antibodies as monotherapy or in combination with other therapies (1). Immune checkpoint inhibitors are based on blocking an inhibitory negative feedback mechanism on effector immune cells and thereby 'releasing the brake' on the ability of a patient's immune system to fight cancer (2). The use of immune checkpoint inhibitors, such as anti-PD-1/PD-L1 and anti-CTLA-4, is clinically implemented to treat various cancer types including melanoma, non-small-cell lung cancer, renal cell cancer and head and neck cancer (3-5).

Despite the high initial promise, only a minority of cancer patients that are in need of new treatment options respond to this immunotherapy (6, 7). There is a strong correlation between tumors characterized by a high somatic mutational burden and clinical response to these immune checkpoint inhibitors (8, 9). As mutated proteins are the main source of neoantigens, high mutational burden results in a higher potential presence of neoantigens that are immunogenic, thereby explaining the presence of tumor-infiltrating lymphocytes (TILs) in the frequency of events known as the 'cancer immunity cycle' (10, 11). Consequently, this results in a better response to immune checkpoint inhibitors (12).

In contrast, pancreatic ductal adenocarcinoma (PDAC) and glioblastoma multiforme (GBM) are characterized as low or 'cold' immunogenic tumors due to their low mutational burden and low effector T cell infiltrates (Figure 1.1) (13, 14). Immune checkpoint inhibitors are shown to have low therapeutic efficacy towards these tumor types compared to high or 'hot' immunogenic tumors such as melanoma (15, 16). Besides the fact that these tumor types are irresponsive to immunotherapy, the current conventional therapies also fail, leading to a poor five-year survival rate of 5.6% for GBM and less than 8% for PDAC (17-19). Turning these low immunogenic into more immunogenic tumors is one of the major goals to improve immunotherapy and survival in these solid tumors.

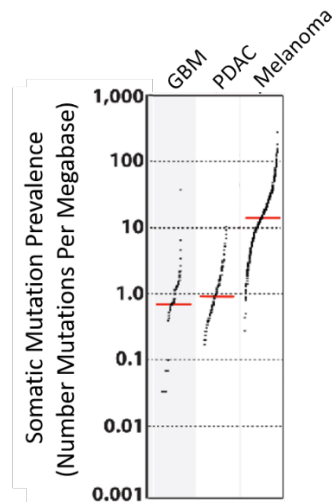


Figure 1.1. Prevalence of somatic mutations across GBM, PDAC and melanoma. Every dot represents a sample and the red horizontal lines are median numbers of mutations in the respective cancer type. The vertical axis shows the number of mutations per megabase. Figure adapted and modified from (16).

Immune suppressive tumor microenvironment in PDAC and GBM

Additionally to the low mutational burden, the tumor microenvironment (TME) is believed to be a major underlying factor for immunotherapy failure in both PDAC and GBM.

PDAC is associated with a strong desmoplastic reaction within the TME, which results in a dense fibrotic/desmoplastic stroma surrounding the tumor. This stroma acts as a mechanical and functional shield, causing diminished delivery of systemically administered anticancer agents and immune cell infiltration, as a consequence of intratumoral pressure and low microvascular density (20-22). The main orchestrators of this stromal shield are the activated pancreatic stellate cells (PSCs). These myofibroblast-like cells, also known as cancer-associated fibroblasts, enhance the development, progression, and invasion of PDAC through extensive crosstalk with pancreatic cancer cells (PCCs), resulting in reciprocal stimulation. PSCs also directly influence immune cells by secreting immunosuppressive factors, like TGF- β (23, 24). Furthermore, the immunosuppressive TME of PDAC consists of a low number of TILs and a high number of T regulatory cells (Tregs) and myeloid-derived suppressor cells (MDSCs), which can both decrease the antitumor immune response (25).

In GBM, immunotherapy has to deal with the immunological complexity that characterizes this tumor type. The brain has long been considered as immune privileged due to the presence of the blood-brain-barrier, which restricts entry of molecules and immune cells

into the brain (26). However, recent findings discovered the central nervous system (CNS) lymphatic vessels, where immune cells could travel from the brain into the regional lymph nodes, making the CNS subject to active immunosurveillance and immune responses (27, 28). Nonetheless, other factors complicate GBM immunity, such as a sparse and exhausted T cell infiltrate in combination with abundance of immunosuppressive stroma consisting of microglia, tumor-associated macrophages (TAMs), MDSCs and Tregs (13).

So, both cancer types are associated with immune escape and suppression, either directly or via the TME. Therefore, manipulation of the TME into a more immunogenic environment will be critical for any immunotherapy to gain ground in GBM and PDAC.

Improving immunotherapy in cold immunogenic tumors through immunogenic cell death

An effective way of reshaping the coldness of tumors towards an immunological hot environment is through induction of immunogenic cell death (ICD). Therapies that trigger ICD will release damage-associated molecular patterns (DAMPs) that are necessary for the recruitment and maturation of antigen presenting cells (APC), more specifically dendritic cells (DCs). Moreover, ICD-associated DAMPs and released cytokines are responsible for i) the recruitment of DCs to the tumor site (e.g. ATP), ii) guiding the interaction between DCs and dying tumor cells (e.g. ANXA1), iii) favoring phagocytosis of dying tumor cells (e.g. ecto-calreticulin (ecto-CRT), HSP70 and HSP90) by DCs, iv) the maturation of DCs and their capacity to effect cross presentation with T cells (e.g. ATP, HMGB1, type I IFN) and v) the recruitment of cytotoxic T cells into the TME (e.g. CCL2, CXCL1 and CXCL10) (Figure 1.2) (29).

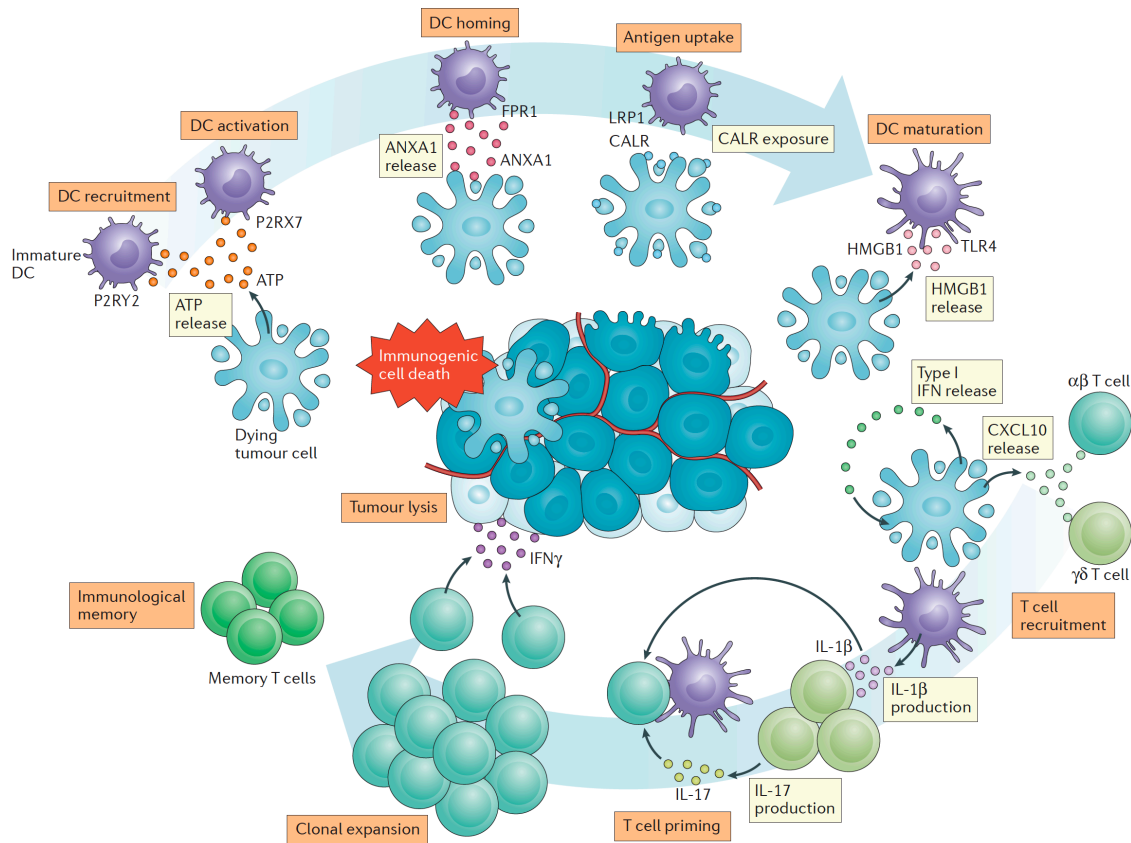


Figure 1.2. Mechanisms of therapy-induced ICD. Figure adapted from (30).

The first systematic screening for ICD inducers recognized anthracyclines (e.g. mitoxantrone) and radiotherapy as potent ICD inducers in cancer (31). Since that discovery, novel ICD inducers have been identified, which include other chemotherapeutics (e.g. bortezomib, cyclophosphamide, doxorubicin and oxaliplatin), targeted therapeutics, various physical modalities, certain oncolytic viruses and hypericin-based photodynamic therapy (32-39). The key to ICD induction for all these inducers is the concomitant and sustained induction of reactive oxygen species (ROS) and consequently endoplasmic reticulum (ER) stress. It has been shown that the induction of this oxidative stress and ER stress is crucial for elicitation of signaling pathways that mediate the emission of DAMPs (40).

Oxidative stress for cancer therapy

Modified from (41) Freire Boullosa, L.; Van Loenhout, J.; Deben, C. Chapter 4 - Endogenous antioxidants in the prognosis and treatment of lung cancer. In Cancer (Second Edition), Preedy, V.R., Patel, V.B., Eds. Academic Press: San Diego, 2021

In general, cancer cells are characterized by higher cellular ROS levels compared to their normal counterparts (42). These persistent high levels of ROS can be explained by the imbalance between oxidants and antioxidants in cancer cells, resulting in oxidative stress (43). This imbalance is due to oncogenic transformations including alteration in the tumor genetics, metabolism and microenvironment (44). For instance, hypoxia is a characteristic feature of cancer resulting from an imbalance between oxygen supply and consumption due to uncontrollable cell proliferation, altered metabolism and abnormal tumor blood vessel growth. This results in reduced transport of oxygen and nutrients (45). It is essential for cancer cells to adapt to these hypoxic conditions by altering their metabolism. Cancer cells maintain their high energy levels through a high rate of glycolysis followed by lactic acid fermentation even in the presence of abundant oxygen, which is called aerobic glycolysis or the Warburg-effect. This process is followed by oxidation in mitochondria, resulting in an increased ROS generation (46). In addition, cancer cells evolved mechanisms to protect themselves from this intrinsic oxidative stress and developed an adaptation mechanism by upregulation of pro-survival molecules and their antioxidant defense system to maintain the redox balance (43). A low to moderate increase of intracellular ROS levels may result in activation of oncogenes, which are involved in cell proliferation, and inactivation of tumor suppressor genes, angiogenesis and mitochondrial dysfunction, thereby serving as a signaling molecule in cancer survival (46). For instance, hydrogen peroxide (H_2O_2) reversibly oxidizes cysteine thiol groups of phosphatases, such as phosphatase and tensin homolog (PTEN), which cause loss of their activity and promote activation of the PI3K/Akt/mTOR survival pathway (47). Conversely, when the levels of ROS are further elevated, it can overcome the defensive antioxidant system of cancer cells and eventually causing cell death (48).

Consequently, there are two different approaches based on the redox balance to counteract cancer cells (Figure 1.3) (49). In the first approach, oxidative stress can be decreased via scavenging intracellular ROS. For example, increasing intake of antioxidants (e.g. vitamin

C and E) can deplete oxidative stress, subsequently causing growth inhibition and increased susceptibility to cell death in cancer cells. However, this antioxidant supplementation remains controversial (50). The second approach is by increasing ROS levels in cancer cells and thereby crossing the threshold of cancer cell death. This can be done either by direct production of ROS via exogenous approaches or indirectly by increasing intracellular ROS concentrations via targeted inhibition of endogenous antioxidant systems, such as glutathione (GSH) and thioredoxin (Trx), in cancer cells.

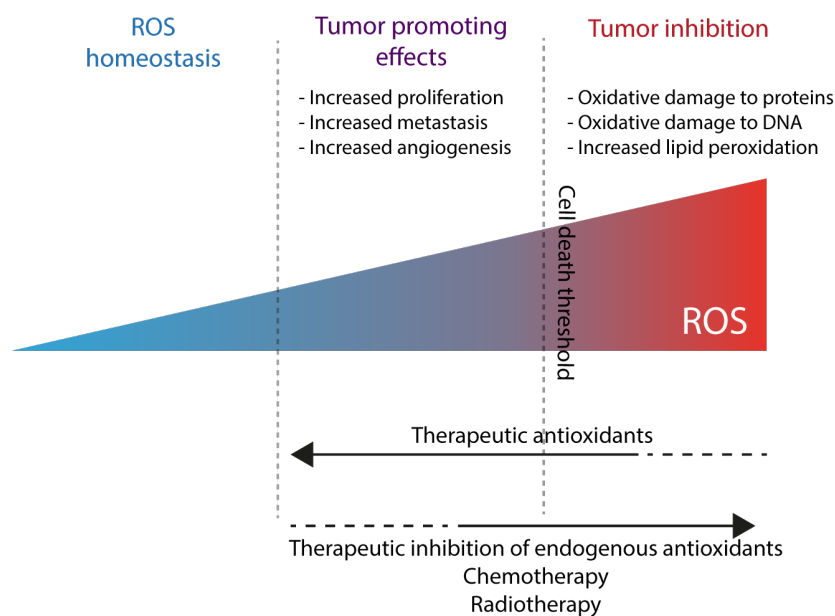


Figure 1.3. Redox balance in cancer cells. ROS can both promote and inhibit cancer cells, depending on the endogenous ROS levels. A moderate increase of ROS can have tumor promoting effects. Further elevation of ROS levels due to therapeutic interventions, can cause oxidative stress and consequently can lead to cancer cell death. Figure adapted from (41).

Cold atmospheric plasma

A novel therapeutic anti-cancer strategy to increase intracellular oxidative stress via exogenous ROS is the use of cold atmospheric plasma (CAP). To date, CAP finds its clinical applications in treatment of chronic and acute wounds, dental medicine, blood coagulation and decontamination (51, 52). CAP is a relatively young domain in the oncology field as potential treatment modality. Since the first reports about the killing effect of plasma on cancer cells in the last decade, the field of plasma-oncology has started to emerge in the research community the last couple of years (53).

Plasma, the fourth state of matter, is a partially ionized gas consisting of a variety of components such as electrical fields, various ions and electrons, thermal and UV radiation,

visible light and reactive oxygen and nitrogen species (ROS and RNS). Plasma can be distinguished into plasmas that are in thermal equilibrium (thermal plasma) and those which are not in thermal equilibrium (non-thermal plasma). In the latter case, the electrons have much higher temperature than the gas molecules. When the gas remains near room temperature, this type of non-thermal plasma is also referred to as cold atmospheric plasma (CAP). Consequently, CAP is suitable for applications to temperature-sensitive materials, such as living tissue (54).

There are several methods to produce CAP, but the most common are dielectric barrier discharge (DBD) and plasma jet devices. DBDs used for medical applications are characterized by plasma ignition in a gap between an isolated high voltage electrode and the target to be treated, having a direct contact between plasma and target. Here, atmospheric air usually serves as the working gas for plasma generation. In a plasma jet device, the electrode setup for plasma generation is usually located in or around a tube-like arrangement, in most cases inside a pen-like device, where the plasma is ignited using a flowing feeding gas, often helium or argon (54, 55).

Both devices can be used for direct CAP treatment of cancer cells or tissue (Figure 1.4). However, this direct treatment can be challenging for the delivery of CAP into the body, e.g. for deeply located tumors (56). Therefore, indirect CAP treatment through CAP-activated liquids and subsequently administration of these liquids onto the cancer cells or tissue, has gained interest for cancer treatment (57).

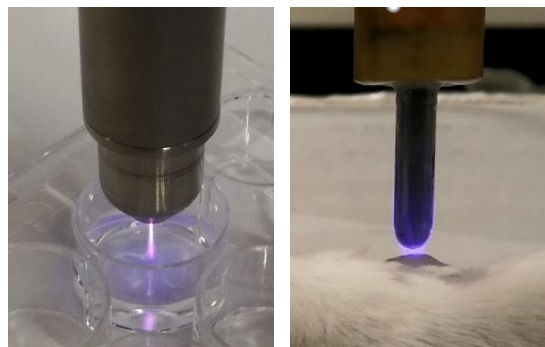


Figure 1.4. Devices used to produce CAP in plasma medicine. (Left) Indirect CAP treatment of liquids through a plasma jet device (KINPen®IND). (Right) Direct CAP treatment of tissue through a DBD device.

In CAP, ROS and RNS are the main active components achieving the desired biomedical effects. These ROS/RNS include several types of short-lived (e.g. radical hydroxyl $\cdot\text{OH}$, anion superoxide $\text{O}_2^{\cdot-}$ and singlet delta oxygen $^1\text{O}_2$) and long-lived (hydrogen peroxide H_2O_2 , nitrite NO_2^- and nitrate NO_3^-) species (58, 59). The type of plasma application (direct or indirect) has several implications with regards to physiochemical parameters that interact with the biological target. In case of direct treatment, physical factors (UV light, heat and electromagnetic field) and both short- and long-lived species are present during the treatment, while only chemical factors, and among them essentially long-lived species, should be considered in indirect treatment (60). When applied in high doses, these exogenous formed ROS and RNS will lead to intracellular stress and ultimately to cell death. This has already been proven in different cancer types (61-63).

Auranofin: a potential antioxidant inhibitor

A second mechanism of enhancing oxidative stress in cancer cells is through endogenous ROS accumulation via targeted inhibition of the elevated antioxidant defense system. One of the known protective antioxidant systems is the thioredoxin/thioredoxin reductase (Trx/TrxR) system, which can be upregulated in cancer cells and is correlated with cancer aggressiveness and drug resistance (64). TrxR is required to convert oxidized Trx into its functional reductive form, which is involved in the reduction and regulation of ROS.

Over the past years, interest has been gained in the Trx/TrxR system as a therapeutic target for cancer (65). A promising compound that interacts with TrxR activity is auranofin (AF). AF is a gold(I)-containing compound that was initially approved by the US Food and Drug Administration (FDA) for treatment of rheumatoid arthritis. AF was recently repurposed as potent anticancer drug since it targets TrxR through formation of a stable coordinative bond between its gold(I) center and the active site selenocysteine residues, and thereby perturbing cellular redox balance (66, 67). To date, the promising anticancer activity of AF has been observed in several *in vitro* and *in vivo* preclinical studies, including different cancer types (68-71).

Rationale

Despite improvements in current treatment methods, the prognosis of PDAC and GBM remains very poor. From the newly diagnosed patients, less than 8% and 5.6% of respectively PDAC and GBM patients will survive within 5 years. This makes PDAC and GBM two of the most deadliest cancer types worldwide. Both are characterized by major therapeutic hurdles for conventional treatment strategies, including incomplete surgical resection and therapy resistance, which consequently lead to high recurrence rates (72-75). Similar, these cancer types do not respond well to immunotherapy due to their immunosuppressive TME and low mutational burden.

Induction of oxidative stress due to elevated ROS levels and imbalanced redox status is considered ‘the Achilles heel’ of cancer cells and has recently been highlighted as promising target for anticancer strategies (76). Since ICD has been found to depend on the concomitant generation of ROS and activation of ER stress, ROS-inducing therapies are particularly of interest for their ability to prime an innate and subsequently adaptive immune response against tumors (77). I investigated novel oxidative stress-inducing treatment strategies to effectively eradicate PDAC and GBM cells and their ability to prime the TME to initiate an antitumoral immune response. These ROS-inducing treatment strategies might open doors to accelerate the application of immunotherapy for PDAC and GBM.

Aims & outline

The general aim of this project was to investigate a novel oxidative stress-inducing treatment strategy that targets PDAC and GBM, while modulating the TME to enhance the immunogenicity of these tumors. Thereby, I initially focused on CAP treatment as novel ROS-inducing treatment modality and additionally explored a promising combination strategy with another oxidative stress-inducing treatment that inhibits the antioxidant defense system in these cancer cells, namely auranofin (AF). With my preclinical study, I wanted to gain immunogenic and mechanistic insights into this oxidative stress-inducing treatment strategy.

This doctoral thesis is divided into six different chapters, as presented in the overview of the outline in Figure 1.5.

Chapter 2 provides a literature overview of what is known on the immunomodulating effects of different oxidative stress-inducing anticancer therapies. In this chapter I discuss the mechanistic and cellular responses of cancer cells towards exogenous and endogenous ROS-inducing treatments (e.g. radiotherapy and antioxidant inhibitors, respectively), as well as the indirect and direct immunomodulating effects, which can be both immunostimulatory and immunosuppressive.

In **chapter 3** I explored the use of CAP-treated liquids, more specifically PBS, in targeting the immunosuppressive TME and inducing ICD in PDAC. Here, I revealed the killing potential of CAP-treated PBS (pPBS) to both PCCs and the tumor-supportive PSCs. Additionally, I showed the release of danger signals necessary for induction of ICD and subsequently maturation and activation of DCs. I showed pPBS treatment of PCCs and PSCs was able to create a more immunostimulatory secretion profile in coculture with DCs.

Furthermore, the combination of exogenous ROS induction via CAP and the inhibition of the antioxidant defense system via AF, has been evaluated in **chapter 4**. As such, a synergistic antitumoral effect was observed in GBM cells after this combination strategy. In addition, I performed an in-depth analysis of the induced type of cell death and revealed the immunogenicity of this combination therapy.

As a final experimental step in **chapter 5**, I explored this combination therapy in an *in vivo* GBM model. The therapeutic response was evaluated based on tumor kinetics and survival following AF and CAP treatment.

Finally, in **chapter 6**, these results are summarized and discussed, focusing on the challenges and perspectives for future research.

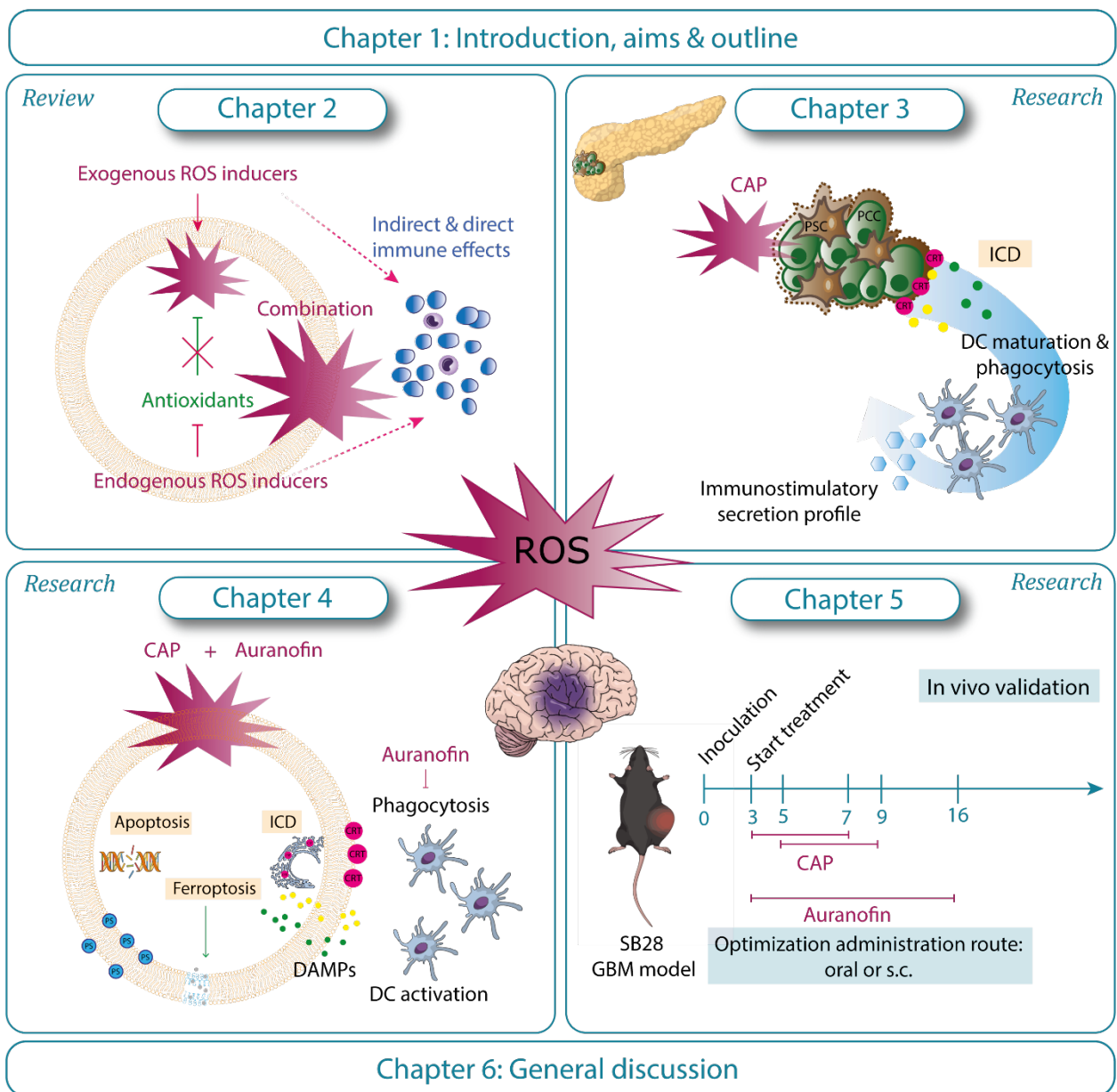


Figure 1.5. Outline of the doctoral thesis. CAP, cold atmospheric plasma; ROS, reactive oxygen species; ICD, immunogenic cell death; DAMPs, damage-associated molecular patterns; DC, dendritic cell; s.c., subcutaneous

References

1. Tang J, Yu JX, Hubbard-Lucey VM, Neftelev ST, Hodge JP, Lin Y. Trial watch: The clinical trial landscape for PD1/PDL1 immune checkpoint inhibitors. *Nature reviews Drug discovery*. 2018;17(12):854-5.
2. Pardoll DM. The blockade of immune checkpoints in cancer immunotherapy. *Nature reviews Cancer*. 2012;12(4):252-64.
3. Michielin O, van Akkooi ACJ, Ascierto PA, Dummer R, Keilholz U, clinicalguidelines@esmo.org EGCEa. Cutaneous melanoma: ESMO Clinical Practice Guidelines for diagnosis, treatment and follow-up. *Annals of oncology : official journal of the European Society for Medical Oncology*. 2019;30(12):1884-901.
4. Planchard D, Popat S, Kerr K, Novello S, Smit EF, Faivre-Finn C, et al. Metastatic non-small cell lung cancer: ESMO Clinical Practice Guidelines for diagnosis, treatment and follow-up. *Annals of oncology : official journal of the European Society for Medical Oncology*. 2018;29(Suppl 4):iv192-iv237.
5. Spranger S, Gajewski TF. Impact of oncogenic pathways on evasion of antitumour immune responses. *Nature reviews Cancer*. 2018;18(3):139-47.
6. Temel JS, Gainor JF, Sullivan RJ, Greer JA. Keeping Expectations in Check With Immune Checkpoint Inhibitors. *Journal of clinical oncology : official journal of the American Society of Clinical Oncology*. 2018;36(17):1654-7.
7. Haslam A, Prasad V. Estimation of the Percentage of US Patients With Cancer Who Are Eligible for and Respond to Checkpoint Inhibitor Immunotherapy Drugs. *JAMA Netw Open*. 2019;2(5):e192535.
8. Osipov A, Lim SJ, Popovic A, Azad NS, Laheru DA, Zheng L, et al. Tumor Mutational Burden, Toxicity, and Response of Immune Checkpoint Inhibitors Targeting PD(L)1, CTLA-4, and Combination: A Meta-regression Analysis. *Clinical cancer research : an official journal of the American Association for Cancer Research*. 2020;26(18):4842-51.
9. Klempner SJ, Fabrizio D, Bane S, Reinhart M, Peoples T, Ali SM, et al. Tumor Mutational Burden as a Predictive Biomarker for Response to Immune Checkpoint Inhibitors: A Review of Current Evidence. *The oncologist*. 2020;25(1):e147-e59.
10. Yarchoan M, Johnson BA, 3rd, Lutz ER, Laheru DA, Jaffee EM. Targeting neoantigens to augment antitumour immunity. *Nature reviews Cancer*. 2017;17(9):569.
11. Chen DS, Mellman I. Oncology meets immunology: the cancer-immunity cycle. *Immunity*. 2013;39(1):1-10.
12. Linette GP, Carreno BM. Tumor-Infiltrating Lymphocytes in the Checkpoint Inhibitor Era. *Curr Hematol Malig Rep*. 2019;14(4):286-91.
13. Buerki RA, Chheda ZS, Okada H. Immunotherapy of Primary Brain Tumors: Facts and Hopes. *Clinical cancer research : an official journal of the American Association for Cancer Research*. 2018;24(21):5198-205.
14. Woroniecka K, Chongsathidkiet P, Rhodin K, Kemeny H, Dechant C, Farber SH, et al. T-Cell Exhaustion Signatures Vary with Tumor Type and Are Severe in Glioblastoma. *Clinical cancer research : an official journal of the American Association for Cancer Research*. 2018;24(17):4175-86.
15. Vareki SM. High and low mutational burden tumors versus immunologically hot and cold tumors and response to immune checkpoint inhibitors. *J Immunother Cancer*. 2018;6.
16. Alexandrov LB, Nik-Zainal S, Wedge DC, Aparicio SA, Behjati S, Biankin AV, et al. Signatures of mutational processes in human cancer. *Nature*. 2013;500(7463):415-21.
17. Stupp R, Mason WP, van den Bent MJ, Weller M, Fisher B, Taphoorn MJ, et al. Radiotherapy plus concomitant and adjuvant temozolomide for glioblastoma. *The New England journal of medicine*. 2005;352(10):987-96.
18. Ostrom QT, Gittleman H, Truitt G, Boscia A, Kruchko C, Barnholtz-Sloan JS. CBTRUS Statistical Report: Primary Brain and Other Central Nervous System Tumors Diagnosed in the United States in 2011-2015. *Neuro-oncology*. 2018;20(suppl_4):iv1-iv86.
19. Siegel RL, Miller KD, Jemal A. Cancer statistics, 2018. *CA: a cancer journal for clinicians*. 2018;68(1):7-30.
20. Thomas D, Radhakrishnan P. Tumor-stromal crosstalk in pancreatic cancer and tissue fibrosis. *Mol Cancer*. 2019;18(1):14.

21. Watt J, Kocher HM. The desmoplastic stroma of pancreatic cancer is a barrier to immune cell infiltration. *Oncoimmunology*. 2013;2(12):e26788.
22. Heinemann V, Reni M, Ychou M, Richel DJ, Macarulla T, Ducreux M. Tumour-stroma interactions in pancreatic ductal adenocarcinoma: rationale and current evidence for new therapeutic strategies. *Cancer treatment reviews*. 2014;40(1):118-28.
23. Tang D, Wang D, Yuan Z, Xue X, Zhang Y, An Y, et al. Persistent activation of pancreatic stellate cells creates a microenvironment favorable for the malignant behavior of pancreatic ductal adenocarcinoma. *Int J Cancer*. 2013;132(5):993-1003.
24. Lunardi S, Muschel RJ, Brunner TB. The stromal compartments in pancreatic cancer: are there any therapeutic targets? *Cancer letters*. 2014;343(2):147-55.
25. Martinez-Bosch N, Vinaixa J, Navarro P. Immune Evasion in Pancreatic Cancer: From Mechanisms to Therapy. *Cancers*. 2018;10(1).
26. Engelhardt B, Ransohoff RM. The ins and outs of T-lymphocyte trafficking to the CNS: anatomical sites and molecular mechanisms. *Trends Immunol*. 2005;26(9):485-95.
27. Louveau A, Harris TH, Kipnis J. Revisiting the Mechanisms of CNS Immune Privilege. *Trends Immunol*. 2015;36(10):569-77.
28. Lim M, Xia Y, Bettgowda C, Weller M. Current state of immunotherapy for glioblastoma. *Nat Rev Clin Oncol*. 2018;15(7):422-42.
29. Galluzzi L, Vitale I, Warren S, Adjemian S, Agostinis P, Martinez AB, et al. Consensus guidelines for the definition, detection and interpretation of immunogenic cell death. *J Immunother Cancer*. 2020;8(1):e000337.
30. Galluzzi L, Buque A, Kepp O, Zitvogel L, Kroemer G. Immunogenic cell death in cancer and infectious disease. *Nature reviews Immunology*. 2017;17(2):97-111.
31. Obeid M, Tesniere A, Ghiringhelli F, Fimia GM, Apetoh L, Perfettini JL, et al. Calreticulin exposure dictates the immunogenicity of cancer cell death. *Nature medicine*. 2007;13(1):54-61.
32. Spisek R, Charalambous A, Mazumder A, Vesole DH, Jagannath S, Dhodapkar MV. Bortezomib enhances dendritic cell (DC)-mediated induction of immunity to human myeloma via exposure of cell surface heat shock protein 90 on dying tumor cells: therapeutic implications. *Blood*. 2007;109(11):4839-45.
33. Schiavoni G, Sistigu A, Valentini M, Mattei F, Sestili P, Spadaro F, et al. Cyclophosphamide synergizes with type I interferons through systemic dendritic cell reactivation and induction of immunogenic tumor apoptosis. *Cancer research*. 2011;71(3):768-78.
34. Casares N, Pequignot MO, Tesniere A, Ghiringhelli F, Roux S, Chaput N, et al. Caspase-dependent immunogenicity of doxorubicin-induced tumor cell death. *The Journal of experimental medicine*. 2005;202(12):1691-701.
35. Tesniere A, Schlemmer F, Boige V, Kepp O, Martins I, Ghiringhelli F, et al. Immunogenic death of colon cancer cells treated with oxaliplatin. *Oncogene*. 2010;29(4):482-91.
36. Koks CA, Garg AD, Ehrhardt M, Riva M, Vandenberk L, Boon L, et al. Newcastle disease virotherapy induces long-term survival and tumor-specific immune memory in orthotopic glioma through the induction of immunogenic cell death. *Int J Cancer*. 2015;136(5):E313-E25.
37. Fucikova J, Moserova I, Truxova I, Hermanova I, Vancurova I, Partlova S, et al. High hydrostatic pressure induces immunogenic cell death in human tumor cells. *Int J Cancer*. 2014;135(5):1165-77.
38. Weiss EM, Meister S, Janko C, Ebel N, Schlucker E, Meyer-Pittroff R, et al. High hydrostatic pressure treatment generates inactivated mammalian tumor cells with immunogenic features. *Journal of immunotoxicology*. 2010;7(3):194-204.
39. Garg AD, Krysko DV, Vandenabeele P, Agostinis P. Hypericin-based photodynamic therapy induces surface exposure of damage-associated molecular patterns like HSP70 and calreticulin. *Cancer immunology, immunotherapy : CII*. 2012;61(2):215-21.
40. Rufo N, Garg AD, Agostinis P. The Unfolded Protein Response in Immunogenic Cell Death and Cancer Immunotherapy. *Trends in cancer*. 2017;3(9):643-58.
41. Freire Boullosa L, Van Loenhout J, Deben C. Chapter 4 - Endogenous antioxidants in the prognosis and treatment of lung cancer. In: Preedy VR, Patel VB, editors. *Cancer (Second Edition)*. San Diego: Academic Press; 2021. p. 39-48.
42. Liou GY, Storz P. Reactive oxygen species in cancer. *Free Radic Res*. 2010;44(5):479-96.
43. Nogueira V, Hay N. Molecular pathways: reactive oxygen species homeostasis in cancer cells and implications for cancer therapy. *Clinical cancer research : an official journal of the American Association for Cancer Research*. 2013;19(16):4309-14.

44. Kim J, Kim J, Bae JS. ROS homeostasis and metabolism: a critical liaison for cancer therapy. *Exp Mol Med*. 2016;48(11):e269.
45. Vaupel P, Harrison L. Tumor hypoxia: causative factors, compensatory mechanisms, and cellular response. *The oncologist*. 2004;9 Suppl 5:4-9.
46. Kumari S, Badana AK, G MM, G S, Malla R. Reactive Oxygen Species: A Key Constituent in Cancer Survival. *Biomarker insights*. 2018;13:1177271918755391.
47. Brewer TF, Garcia FJ, Onak CS, Carroll KS, Chang CJ. Chemical Approaches to Discovery and Study of Sources and Targets of Hydrogen Peroxide Redox Signaling Through NADVII Oxidase Proteins. *Annu Rev Biochem*. 2015;84:765-90.
48. Galadari S, Rahman A, Pallichankandy S, Thayyullathil F. Reactive oxygen species and cancer paradox: To promote or to suppress? *Free radical biology & medicine*. 2017;104:144-64.
49. Raza MH, Siraj S, Arshad A, Waheed U, Aldakheel F, Alduraywish S, et al. ROS-modulated therapeutic approaches in cancer treatment. *Journal of cancer research and clinical oncology*. 2017;143(9):1789-809.
50. Singh K, Bhorl M, Kasu YA, Bhat G, Marar T. Antioxidants as precision weapons in war against cancer chemotherapy induced toxicity - Exploring the armoury of obscurity. *Saudi pharmaceutical journal : SPJ : the official publication of the Saudi Pharmaceutical Society*. 2018;26(2):177-90.
51. Brany D, Dvorska D, Halasova E, Skovierova H. Cold Atmospheric Plasma: A Powerful Tool for Modern Medicine. *International journal of molecular sciences*. 2020;21(8).
52. Dai X, Bazaka K, Richard DJ, Thompson ERW, Ostrikov KK. The Emerging Role of Gas Plasma in Oncotherapy. *Trends Biotechnol*. 2018;36(11):1183-98.
53. Fridman G, Shereshevsky A, Jost MM, Brooks AD, Fridman A, Gutsol A, et al. Floating electrode dielectric barrier discharge plasma in air promoting apoptotic behavior in melanoma skin cancer cell lines. *Plasma Chem Plasma P*. 2007;27(2):163-76.
54. Hoffmann C, Berganza C, Zhang J. Cold Atmospheric Plasma: methods of production and application in dentistry and oncology. *Med Gas Res*. 2013;3(1):21.
55. von Woedtke T, Emmert S, Metelmann HR, Rupf S, Weltmann KD. Perspectives on cold atmospheric plasma (CAP) applications in medicine. *Phys Plasmas*. 2020;27(7).
56. Mirpour S, Piroozmand S, Soleimani N, Jalali Fazarani N, Ghomi H, Fotovat Eskandari H, et al. Utilizing the micron sized non-thermal atmospheric pressure plasma inside the animal body for the tumor treatment application. *Sci Rep*. 2016;6:29048.
57. Van Boxem W, Van der Paal J, Gorbaney Y, Vanuytsel S, Smits E, Dewilde S, et al. Anti-cancer capacity of plasma-treated PBS: effect of chemical composition on cancer cell cytotoxicity. *Sci Rep*. 2017;7(1):16478.
58. Bauer G, Sersenova D, Graves DB, Machala Z. Cold Atmospheric Plasma and Plasma-Activated Medium Trigger RONS-Based Tumor Cell Apoptosis. *Sci Rep*. 2019;9(1):14210.
59. Gorbaney Y, Privat-Maldonado A, Bogaerts A. Analysis of Short-Lived Reactive Species in Plasma–Air–Water Systems: The Dos and the Do Nots. *Analytical Chemistry*. 2018;90(22):13151-8.
60. Sklias K, Santos Sousa J, Girard PM. Role of Short- and Long-Lived Reactive Species on the Selectivity and Anti-Cancer Action of Plasma Treatment In Vitro. *Cancers*. 2021;13(4).
61. Yan DY, Sherman JH, Keidar M. Cold atmospheric plasma, a novel promising anti-cancer treatment modality. *Oncotarget*. 2017;8(9):15977-95.
62. Liedtke KR, Bekeschus S, Kaeding A, Hackbarth C, Kuehn JP, Heidecke CD, et al. Non-thermal plasma-treated solution demonstrates antitumor activity against pancreatic cancer cells in vitro and in vivo. *Sci Rep*. 2017;7(1):8319.
63. Kalghatgi S, Kelly CM, Cerchar E, Torabi B, Alekseev O, Fridman A, et al. Effects of Non-Thermal Plasma on Mammalian Cells. *Plos One*. 2011;6(1).
64. Trachootham D, Alexandre J, Huang P. Targeting cancer cells by ROS-mediated mechanisms: a radical therapeutic approach? *Nature reviews Drug discovery*. 2009;8(7):579-91.
65. Biaglow JE, Miller RA. The thioredoxin reductase/thioredoxin system: novel redox targets for cancer therapy. *Cancer Biol Ther*. 2005;4(1):6-13.
66. Roder C, Thomson MJ. Auranofin: repurposing an old drug for a golden new age. *Drugs in R&D*. 2015;15(1):13-20.
67. Onodera T, Momose I, Kawada M. Potential Anticancer Activity of Auranofin. *Chemical & pharmaceutical bulletin*. 2019;67(3):186-91.

68. Boullosa LF, Van Loenhout J, Flieswasser T, De Waele J, Hermans C, Lambrechts H, et al. Auranofin reveals therapeutic anticancer potential by triggering distinct molecular cell death mechanisms and innate immunity in mutant p53 non-small cell lung cancer. *Redox biology*. 2021;101949.
69. Han Y, Chen P, Zhang Y, Lu W, Ding W, Luo Y, et al. Synergy between Auranofin and Celecoxib against Colon Cancer In Vitro and In Vivo through a Novel Redox-Mediated Mechanism. *Cancers*. 2019;11(7).
70. Topkas E, Cai N, Cumming A, Hazar-Rethinam M, Gannon OM, Burgess M, et al. Auranofin is a potent suppressor of osteosarcoma metastasis. *Oncotarget*. 2016;7(1):831-44.
71. Hou G-X, Liu P-P, Zhang S, Yang M, Liao J, Yang J, et al. Elimination of stem-like cancer cell side-population by auranofin through modulation of ROS and glycolysis. *Cell death & disease*. 2018;9(2):89.
72. Tummers WS, Groen JV, Sibinga Mulder BG, Farina-Sarasqueta A, Morreau J, Putter H, et al. Impact of resection margin status on recurrence and survival in pancreatic cancer surgery. *Br J Surg*. 2019;106(8):1055-65.
73. Gramatzki D, Roth P, Rushing EJ, Weller J, Andratschke N, Hofer S, et al. Bevacizumab may improve quality of life, but not overall survival in glioblastoma: an epidemiological study. *Annals of oncology : official journal of the European Society for Medical Oncology*. 2018;29(6):1431-6.
74. Capurso G, Sette C. Drug resistance in pancreatic cancer: New player caught in act. *EBioMedicine*. 2019;40:39-40.
75. Noch EK, Ramakrishna R, Magge R. Challenges in the Treatment of Glioblastoma: Multisystem Mechanisms of Therapeutic Resistance. *World Neurosurg*. 2018;116:505-17.
76. Perillo B, Di Donato M, Pezone A, Di Zazzo E, Giovannelli P, Galasso G, et al. ROS in cancer therapy: the bright side of the moon. *Exp Mol Med*. 2020;52(2):192-203.
77. Adkins I, Fucikova J, Garg AD, Agostinis P, Spisek R. Physical modalities inducing immunogenic tumor cell death for cancer immunotherapy. *Oncoimmunology*. 2014;3(12):e968434.

CHAPTER 2

Oxidative stress-inducing anticancer therapies: taking a closer look at their immunomodulating effects

Jinthe Van Loenhout, Marc Peeters, Annemie Bogaerts, Evelien Smits and Christophe Deben. Oxidative Stress-Inducing Anticancer Therapies: Taking a Closer Look at Their Immunomodulating Effects. *Antioxidants* 2020, 9 (12): 2076-3921

Abstract

Cancer cells are characterized by higher levels of reactive oxygen species (ROS) compared to normal cells as a result of an imbalance between oxidants and antioxidants. However, cancer cells maintain their redox balance due to their high antioxidant capacity. Recently, a high level of oxidative stress is considered a novel target for anticancer therapy. This can be induced by increasing exogenous ROS and/or inhibiting the endogenous protective antioxidant system. Additionally, the immune system has been shown to be a significant ally in the fight against cancer. Since ROS levels are important to modulate the antitumor immune response, it is essential to consider the effects of oxidative stress-inducing treatments on this response. In this chapter, we provide an overview of the mechanistic cellular responses of cancer cells towards exogenous and endogenous ROS-inducing treatments, as well as the indirect and direct antitumoral immune effects, which can be both immunostimulatory and/or immunosuppressive. For future perspectives, there is a clear need for comprehensive investigations of different oxidative stress-inducing treatment strategies and their specific immunomodulating effects, since the effects cannot be generalized over different treatment modalities. It is essential to elucidate all these underlying immune effects to make oxidative stress-inducing treatments effective anticancer therapy.

Introduction

Reactive oxygen species (ROS) is a collective term referring to unstable, reactive, partially reduced oxygen derivatives that are produced during metabolic processes within the mitochondria, peroxisomes and the endoplasmic reticulum (ER). A subset of ROS are also continuously generated by enzymatic reactions involving cyclooxygenases, nicotinamide adenine dinucleotide phosphate (NADPH) oxidases (NOX), xanthine oxidases, lipogenesis and through the iron-catalyzed Fenton reaction (1). Examples of ROS include hydrogen peroxide (H_2O_2), superoxide anion ($\text{O}_2^{\bullet-}$), singlet oxygen ($^1\text{O}_2$) and hydroxyl radical ($\bullet\text{OH}$) (2). Tight regulation of these ROS levels is crucial for cellular life. Therefore, cells benefit from a complex scavenging system based on different antioxidants, including superoxide dismutase (SOD), glutathione (GSH) peroxidase, peroxiredoxin, thioredoxin (Trx) and catalase (1). Additional to the strong antioxidant activity of the beforementioned enzymes, various non-enzymatic small-molecule antioxidants such as glutathione, ascorbic acid, vitamin E and polyphenolic compounds also act as scavengers for different types of ROS (3).

Cancer cells are characterized by increased production of ROS compared to normal cells. The persistent high levels of ROS can be explained by the imbalance between oxidants and antioxidants in cancer cells and the ongoing aerobic glycolysis by pyruvate oxidation in the mitochondria, also known as the Warburg-effect (4). This is a consequence of hypoxia in the tumor microenvironment (TME) resulting from an imbalance between oxygen supply and consumption due to uncontrollable cell proliferation, altered metabolism and abnormal tumor blood vessels growth (5). Cancer cells evolved mechanisms to protect themselves from this intrinsic oxidative stress and developed an adaptation mechanism by upregulation of pro-survival molecules and their antioxidant defense system to maintain the redox balance (6). For instance, nuclear factor erythroid 2-related factor 2 (Nrf2), which is a transcription factor in the first line of antioxidant defense against oxidative stress, is often upregulated in cancer cells and supports the cancer cell proliferation (7).

A low to moderate increase of intracellular ROS levels may result in activation of oncogenes (such as Akt), which are involved in cell proliferation, and inactivation of tumor suppressor genes, angiogenesis and mitochondrial dysfunction, thereby serving as a signaling molecule

in cancer survival (4). Conversely, when the levels of ROS are further elevated, they can overcome the defensive antioxidant system of cancer cells, causing cell death (8).

Consequently, there are two different approaches based on the redox balance to counteract cancer cells. In the first approach, oxidative stress can be decreased via scavenging intracellular ROS. For example, increasing intake of antioxidants (e.g. vitamin C and E) can deplete oxidative stress, subsequently causing growth inhibition and increased susceptibility to cell death in cancer cells, due to a crisis in energy production (9). However, this antioxidant supplementation remains controversial (10). Increasing evidence has shown that antioxidant supplementation fails to provide cancer protection and can even affect cancer mortality (11-13). These observations are further supported and rationalized by recent studies demonstrating that oxidative stress can inhibit cancer progression and metastasis and that the GSH and Trx antioxidant systems, which are under transcriptional regulation of Nrf2, may promote tumorigenesis and resistance to therapy (14).

The second approach is by increasing ROS levels in cancer cells and thereby crossing the threshold of cancer cell death. This can be done either by direct production of ROS via exogenous approaches or indirectly by increasing intracellular ROS concentrations via targeted inhibition of previously mentioned endogenous antioxidant systems in cancer cells. Several investigations are suggestive of the fact that the underlying mechanism of action and efficacy of conventional therapies (e.g. radiotherapy and chemotherapy) inducing cancer cell death, is the generation of elevated ROS levels during treatment (15-17).

In this chapter we will focus on therapies related to this second approach and how they influence the TME, more specifically the immune cell compartment, to provide an overview of the effect of ROS induction on the antitumor immune response.

Exogenous ROS generation

One mechanism of enhancing oxidative stress levels to target cancer cells is via exogenous delivery of ROS using different physical modalities (Figure 2.1).

Ionizing radiation is widely used to treat many types of cancer. During radiation, cancer cells are eradicated through free radicals such as superoxide and hydroxyl radicals which are generated by radiolysis of water in extracellular environments and indirectly damage critical targets, such as DNA (15). In addition, radiotherapy can also alter mitochondrial

membrane permeability and activate NADPH oxidase, which in turn further stimulates ROS production (18). Besides radiotherapy, other physical modalities that can induce a substantial increase in ROS levels are being investigated in cancer research, including photodynamic therapy (PDT) and cold atmospheric plasma (CAP) (19-22). PDT is a light-based oncological intervention. Here, a photosensitizer is applied and subsequently activated by light. Upon activation, exogenously produced ROS is generated (23). CAP is an ionized gas that can be produced at atmospheric pressure near room temperature. It is composed of reactive oxygen and nitrogen species, excited molecules, ions, electrons and other physical factors, such as electromagnetic fields and ultraviolet radiation (24).

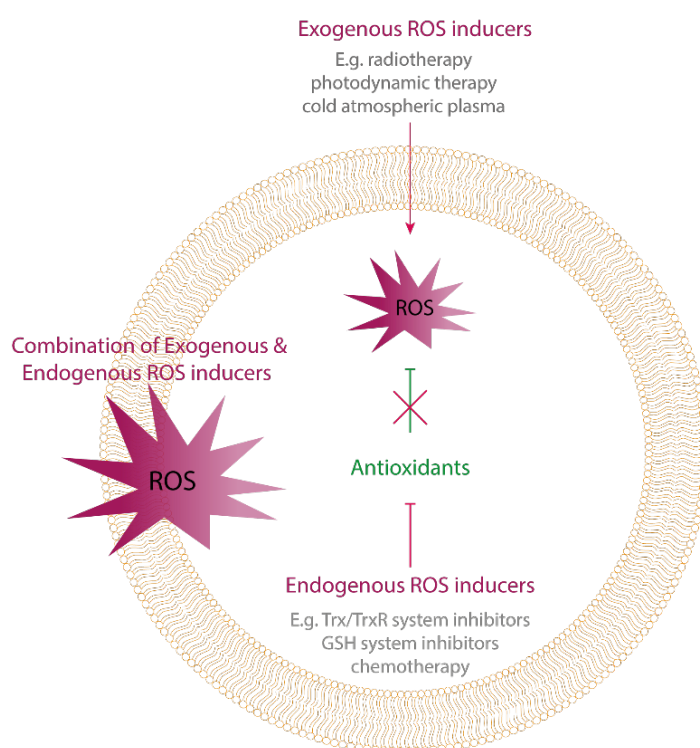


Figure 2.1. Oxidative stress-inducing treatment strategies. Oxidative stress can be induced by exogenous delivery of ROS using physical treatment modalities, as well as by targeting the endogenous antioxidant system causing an intracellular accumulation of ROS. Cancer cells counteract exogenous delivery of high ROS levels by enhancing their antioxidant capacity. Therefore, a combination of both exogenous and endogenous ROS delivery by targeting the antioxidants can be a promising anticancer strategy.

Endogenous ROS generation

The second mechanism of enhancing oxidative stress levels is via intracellular ROS accumulation through chemotherapy or targeted inhibition of the elevated antioxidant system (also Figure 2.1). A lot of chemotherapeutic agents enhance intracellular levels of ROS and can alter the redox homeostasis of cancer cells. This amplification of ROS levels towards cytotoxic levels is one of the proposed mechanisms by which multiple chemotherapeutics induce tumor regression. The level of ROS generation is different among several compounds. Agents that generate high levels of ROS include anthracyclines (e.g. doxorubicin), platinum coordination complexes (e.g. cisplatin), alkylating agents (e.g. cyclophosphamide), camptothecins, arsenic agents and topoisomerase inhibitors, while nucleoside, nucleotide analogs, antifolates, taxanes and vinca alkaloids only generate low levels of ROS (25).

There are two mechanisms for elevated ROS production during chemotherapy, namely through mitochondrial ROS generation and by inhibition of the cellular antioxidant system and thereby interfering with ROS metabolism in cancer cells (25). Several agents, including arsenic trioxide, doxorubicin and cisplatin, have been reported to induce a loss of mitochondrial membrane potential and to inhibit respiratory complexes, leading to the disruption of mitochondrial electron transport chain (ECT) and electron leakage, which is a major source of elevated ROS levels (26-28).

The other mechanism for intracellular ROS accumulation is the inhibition of the antioxidant system during chemotherapy. For instance, imexon, a small-molecule used to treat advanced cancer of the breast, lung or prostate, binds to thiols such as GSH, causing a depletion of cellular GSH and consequently an accumulation of oxidative stress in cancer cells (29). For some chemotherapeutics, more than one target site for ROS generation in cancer cells has been identified. For example, in addition to mitochondrial respiration, NADPH oxidase and thioredoxin reductase (TrxR) are other targets of arsenic trioxide induced oxidative stress, inducing apoptosis (30-32).

Besides chemotherapy, selective inhibitors that block components of the cellular antioxidant system are being studied as antitumor agents which enhance endogenous ROS production. For instance, depletion of GSH antioxidant system can also be achieved by

targeting its synthesis through buthionine sulfoximine (BSO), which has been shown to exhibit anticancer activities in various types of cancer. Furthermore, inhibitors of the X^c-cystine/glutamate antiporter (e.g. sulfasalazine) may also cause GSH depletion by inhibiting the uptake of cystine, the precursor of cysteine, which is a substrate for GSH synthesis (33). Another antioxidant is the thioredoxin/thioredoxin reductase (Trx/TrxR) system, which is shown to be upregulated in cancer cells and is correlated with cancer aggressiveness and drug resistance (30). TrxR is required to convert oxidized Trx into its functional reductive form, which can scavenge ROS (34). TrxR activity can effectively be blocked by the gold compound auranofin that is clinically used as an antirheumatic drug and functions as a thioredoxin inhibitor. In different cancer cells it has been preclinically shown to induce ROS-mediated cell death, since the ROS scavenger N-acetylcysteine prevented this cytotoxic effect (35, 36). This has led to the use of auranofin in several clinical trials involving non-small cell lung and ovarian cancer (NCT01737502 and NCT03456700). The small-molecule PX-12 is another example of an antioxidant inhibitor, since it inhibits Trx and is being used as therapy for advanced cancers in clinical trials (37, 38).

Molecular pathways involved in oxidative stress-inducing therapies

Whether ROS augment tumorigenesis or lead to apoptosis, critically depends on the intracellular ROS levels. At moderate concentration, ROS inactivate phosphatase and tensin homolog (PTEN) and unlock the PI3K-dependent recruitment of its downstream kinases, such as Akt, which will in turn activate NF- κ B, subsequently activating the cancer cell survival signaling cascade (39). For instance, hydrogen peroxide can reversibly oxidize cysteine thiol groups of PTEN which causes loss of their activity and promotes activation of the PI3K/Akt/mTOR survival pathway, consequently leading to tumor cell survival (4). Abundant high concentrations of ROS originating from exogenous and endogenous sources, produce oxidative damage to the DNA, RNA, proteins, lipids and mitochondria, initiating apoptotic cell death (Figure 2.2) (39, 40).

In line with this, it has been shown that the cellular response to exogenous sources of ROS strongly varies with the intensity of the treatment (41-43). For example, low dosages of PDT and radiotherapy have been shown to transiently activate several kinases and NF- κ B involved in survival signaling (43, 44). In these non-toxic dosages of PDT, kinases which are important to initiate autophagy were shown to be activated (44). Higher dosages of

radiation and PDT activate the mitochondrial apoptotic pathway and additionally can also produce a sustained activation of MAPK families including p38, MAPK, ERK1/2 and JNK apoptotic signaling proteins (Figure 2.2) (40, 45, 46).

Inhibition of the antioxidant system of cells could also induce apoptosis of cancer cells. Trx is a physiological inhibitor of ASK1 located upstream of the p38/MAPK pathway, and therefore disrupts the p38/MAPK dependent apoptosis. As such, an inhibitor of the Trx/TrxR system could induce apoptosis due to the phosphorylation of p38/MAPK, as well as the activation of JNK and ERK (34). Additionally, several studies have shown that Trx/TrxR inhibitors downregulate the PI3K/Akt/mTOR survival pathway, causing apoptosis of different types of cancer cells (34, 47-49). The same effect was observed using an inhibitor of the GSH antioxidant pathway (50).

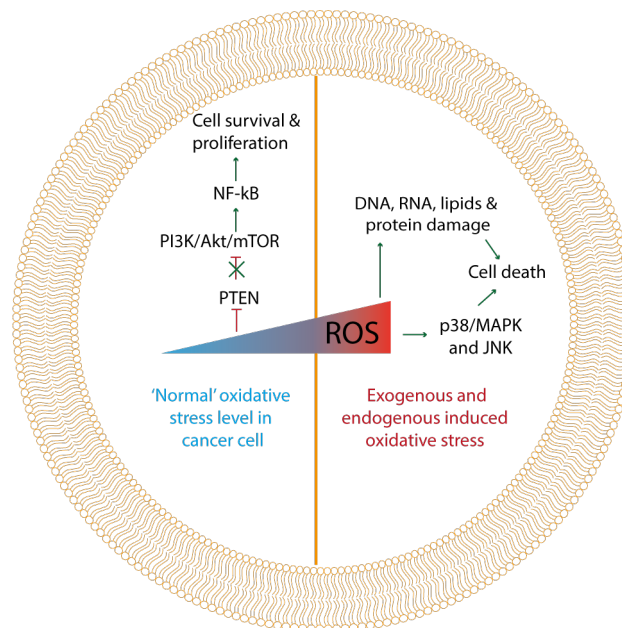


Figure 2.2. Molecular responses to oxidative stress. At moderate “normal” levels of oxidative stress in cancer cells (left side of the figure) ROS inactivate PTEN and unlock PI3K/Akt/mTOR pathway, which in turn activates NF-kB, consequently activating cancer cell survival and proliferation signaling. At high levels of oxidative stress induced by therapy, damage is produced to DNA, RNA, proteins, lipids and mitochondria, initiating apoptotic cell death. Additionally, high levels of ROS can activate p38/MAPK and JNK apoptotic signaling proteins, inducing cancer cell death.

Combinations of different oxidative stress-inducing therapies

It has been shown that radiotherapy, PDT, as well as other ROS-inducing therapies could induce acquired resistance to therapy. Here, NF- κ B is considered to be a key component in the rise of therapy-resistant cancer (43, 51). Suppression of the NF- κ B activation pathway sensitized cells to radiotherapy-induced apoptosis by increasing activation of the JNK pathway (52). Furthermore, it has been suggested that resistance to therapies that induce intracellular ROS production, such as chemotherapy (e.g. paclitaxel and doxorubicin) and radiotherapy, is correlated with an increased antioxidant capacity of cancer cells. Here, upregulation of Nrf2 after oxidative stress contributes to the therapy resistance in cancer cells (53, 54). Due to this complexity of redox homeostasis and adaptation-mediated resistance in tumor cells, ROS-inducing treatments may not always lead to an effective antitumor effect. To overcome resistance induced by oxidative stress and to maximally exploit ROS-mediated cell death mechanism as a therapeutic strategy, it would be beneficial to combine therapeutic strategies that exogenously induce ROS together with compounds that suppress the cellular antioxidant system.

In several preclinical studies, inhibition of GSH or Trx antioxidant systems, downstream of Nrf2 signaling, has been demonstrated to sensitize different types of tumor cells towards radiotherapy (55-57). BSO used to inhibit the GSH production, has shown to sensitize lung, renal and head and neck cancer to radiation. The combination of radiation and GSH depletion by BSO resulted in the activation of the JNK signaling pathway, which resulted in triggering the intrinsic apoptotic pathway (55). A combination of other agents to disrupt endogenous redox homeostasis, was also proven to improve therapeutic efficiency and overcome tumor resistance to PDT (58, 59). However, in combination with BSO, a synergistic effect with PDT was only seen when BSO alone had negligible cytotoxicity. This indicates that cancer cells with intracellular high levels of antioxidants (e.g. GSH) will be more intrinsically resistant toward antioxidant inhibitors or radiation alone, but will effectively induce cell death when these exogenous and endogenous ROS inducers are combined (59-61). Similar effects were seen when combining BSO with a platinum-based chemotherapy-inducing ROS (62). Additionally, inhibitors of the Trx/TrxR system (such as PX-12, auranofin and motexafin gadolinium) have shown similar effects to enhance the response against exogenously therapy-induced ROS (63, 64).

Hypoxia is also one of the most important causes of exogenous oxidative stress-inducing therapy failure, because of the shortage of ROS substrate oxygen. However, it is demonstrated that more ROS is produced in hypoxic conditions compared to non-hypoxic conditions. Although the specific mechanism has not been described, it appears that the source of the increased ROS levels generated under hypoxia is the mitochondria. Hypoxia increases ROS via the transfer of electrons from ubiquinone to molecular oxygen at the Qo sites of complex III of the mitochondrial electron transport chain (65). Beside mitochondria, nitric oxide synthases (NOS) and NOX have also been implicated to increase ROS production during hypoxia (66). Moreover, NO and its derivatives are a specific group of ROS synthesized by NOS. Since the inducible NOS (iNOS) is a hypoxia response gene, generation of NO is significantly increased in tumor cells under hypoxic conditions (67). As such, hypoxic tumor cells heavily rely on the antioxidant defense system to maintain ROS balance, making them vulnerable to inhibition of this antioxidant system (66). For instance, BSO produces a more pronounced GSH depletion in regions of hypoxia, since GSH levels are higher in hypoxic compared to non-hypoxic regions (68). Furthermore, auranofin was able to overcome hypoxic radiation resistance and the effect could be further amplified combining auranofin with BSO, leading to significant tumor growth delay and increased survival rate of tumor-bearing mice (56, 57). Therefore, inhibition of the antioxidant system could be effective to counteract hypoxia-induced therapy resistance (69).

Since the upregulation of NF- κ B is also a key player in acquired resistance to ROS-inducing therapy, inhibition of this transcription factor could enhance the anticancer effect. For example, auranofin has shown to decrease the expression of NF- κ B, thereby overcoming acquired therapy resistance (70, 71). Similar effects were obtained when inhibiting the GSH metabolism (72). However, it should be mentioned that activation of NF- κ B is also responsible for inflammatory responses, which can induce cross-presentation of tumor antigens and stimulate antitumor immune responses (73). This indicates that it is important to take into account the effects of exogenous and endogenous ROS-inducing therapies on the antitumoral immune system.

Indirect and direct effects of oxidative stress-inducing therapies on the antitumoral immune response

In recent years, it has become clear that the immune system is a strong ally in the fight against cancer. ROS-inducing treatments have significant effects on the immune system, which can be either immunostimulatory or, in some circumstances, immunosuppressive (74, 75). Here we will discuss direct and indirect effects of these therapies on the immune system, which are either immunostimulatory or immunosuppressive (Figure 2.3, Table 2.1).

Table 2.1. Overview of immunomodulating effects of different ROS-inducing therapies.

ROS-inducing therapy	Effect	References
Immunostimulating effects		
Indirect effects		
Radiotherapy, PDT, CAP, chemotherapy (e.g. oxaliplatin, doxorubicin)	Secretion of danger signals inducing ICD (e.g. ATP, IL-1 β , calreticulin, HMGB1, type I IFN)	(76-83)
Radiotherapy, PDT, CAP, chemotherapy (e.g. docetaxel, doxorubicin, oxaliplatin)	Secretion of chemokines attracting T cells (e.g. CXCL9, CXCL10, CCL5)	(83-90)
Radiotherapy, PDT, CAP, chemotherapy (e.g. topotecan)	Upregulation of MHC-I molecules on tumor cells	(91-95)
Radiotherapy, PDT	Upregulation of NK cell ligands (e.g. MICA, NKG2DL)	(96, 97)
Radiotherapy, GSH inhibitors (e.g. BSO)	Modulation of death receptors (e.g. Fas and CD95)	(98-100)
Trx/TrxR inhibitors (e.g. butaselen)	Downregulation of PD-L1	(101)
Radiotherapy, PDT, CAP, chemotherapy (e.g. doxorubicin, oxaliplatin), Trx inhibitor	Secretion of proinflammatory cytokines (e.g. IFN- γ , TNF- α)	(78, 93, 102, 103)
Direct effects		
Radiotherapy, PDT, Trx/TrxR inhibitors (e.g. arsenic trioxide)	Depletion of Tregs	(103-106)
CAP, Trx inhibitor	Decrease in secretion of anti-inflammatory cytokines (e.g. IL10, TGF- β)	(78, 103)
Radiotherapy, chemotherapy (e.g. cyclophosphamide), antioxidant inhibitors (e.g. noble nanoparticles)	Polarization of M2 into M1 macrophages	(107-109)

Immunosuppressive effects		
Indirect effects		
Radiotherapy, PDT, CAP, chemotherapy	Secretion of ATP modulating MDSCs	(110)
Radiotherapy	Secretion of chemokines attracting MDSCs (e.g. CXCL12)	(111, 112)
Radiotherapy, Trx/TrxR inhibitors (e.g. auranofin, arsenic trioxide)	Upregulation of PD-L1	(101, 113-115)
Radiotherapy	Secretion of anti-inflammatory cytokines (e.g. TGF- β)	(116)
Direct effects		
Radiotherapy, PDT	Accumulation of Tregs	(116, 117)
Radiotherapy	Polarization into M2 macrophages	(118)
Radiotherapy, PDT, CAP, chemotherapy (e.g. cisplatin, oxaliplatin), antioxidant inhibitors (e.g. arsenic trioxide)	Lymphocyte cytotoxicity	(87, 116, 119-122)
GSH inhibitor	Inhibition of DC maturation	(123)

Abbreviations: ATP, adenosine triphosphate; BSO, buthionine sulfoximine; CAP, cold atmospheric plasma; CCL, chemokine (C-C motif) ligand; CXCL, chemokine (C-X-C motif) ligand; DC, dendritic cell; GSH, glutathione; HMGB1, high-mobility group box 1; ICD, immunogenic cell death; IFN, interferon; IL, interleukin; MDSCs, myeloid-derived suppressor cells, MICA, MHC class I polypeptide-related sequence A; NKG2DL, natural killer group 2D ligand; PD-L1, programmed death-ligand 1; TGF- β , transforming growth factor- β ; TNF- α , tumor necrosis factor- α ; Tregs, regulatory T cells; Trx, thioredoxin; TrxR, thioredoxin reductase.

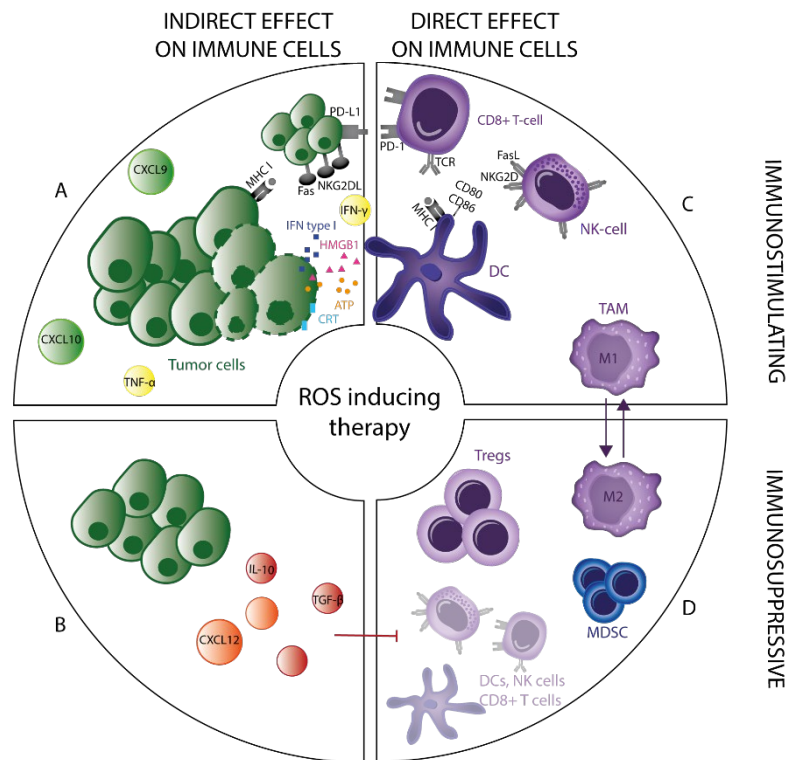


Figure 2.3. Direct and indirect immunomodulating effects of ROS-inducing therapy. The immunomodulating effects after ROS-inducing therapy can be divided into direct and indirect effects being immunostimulatory and/or immunosuppressive. **(A)** ROS-inducing therapy triggers recruitment and activation of DCs by inducing immunogenic tumor cell death (ICD). Additionally, treated tumor cells can secrete cytokines (e.g., IFN- γ and TNF- α) and chemokines (e.g., CXCL10 and CXCL9), and can modulate their surface molecules (e.g., MHC-I, PD-L1 and NKG2DL), thereby increasing their susceptibility to T cell and NK cell-mediated cytotoxicity. **(B)** Immunosuppressive cytokines (e.g., IL10 and TGF- β) and chemokines (e.g., CXCL12) can also be secreted by tumor cells treated with ROS inducers, suppressing immunostimulatory immune cells (DCs, T cells and NK cells) and promoting immunosuppressive immune cells (Tregs and MDSCs). **(C)** Depending on the intensity, ROS-inducing treatment skews TAMs towards a more antitumoral (M1) or protumoral (M2) phenotype. **(D)** T cells and NK cells are sensitive to oxidative stress-inducing treatments, compared to Tregs which are more resistant to these toxic effects.

Indirect effects on the antitumoral immune response

- Priming of an adaptive immune response

Tumor cells undergoing cell death in response to oxidative stress induced therapy have the capacity to trigger an adaptive anticancer immune response, a concept known as immunogenic cell death (ICD). This is a unique type of cell death characterized by the release of danger signals after treatment of tumor cells, leading to effective presentation of tumor antigens and subsequent priming of antigen-specific T cells. This process enhances elimination of tumor cells and generates immune memory against the tumor antigens,

thereby reducing the chance of recurrence (124). Mechanistically, ICD induction requires ROS generation and further ROS-based ER stress (125). In literature, there are already comprehensive reviews and research articles that discuss physical ROS-inducing modalities, such as radiotherapy, PDT and CAP, which have been shown to elicit effective antitumor immunity (76-80). Additionally, chemotherapeutics which have been proven to be ICD inducers (e.g. oxaliplatin and doxorubicin) are accompanied by ROS-induced cytotoxicity (81).

Danger signals released during ICD include the release of adenosine triphosphate (ATP), which attracts dendritic cells (DCs) into the tumor and can stimulate the release of interleukin (IL)-1 β , which promotes T cell priming. Moreover, calreticulin is expressed on the surface of the treated tumor cells, which promotes phagocytosis of these cells by DCs. ICD is also associated with high-mobility group box 1 (HMGB1) release, which facilitates antigen presentation and type-I interferon (IFN) secretion, mediating DC maturation (78, 82, 83). Release of ATP, however, also modulates immunosuppressive properties of myeloid-derived suppressor cells (MDSCs) and can contribute to tumor growth and inhibition of antitumor immunity (110).

- Recruitment of leukocytes

Low infiltration of effector T cells and other leukocytes (e.g. NK cells) into the tumor represents a major obstacle for cancer immunotherapy (126). Here, therapy can facilitate leukocyte infiltration by generating chemoattractants to induce leukocyte extravasation.

The most relevant signals regulating leukocyte infiltration are therapy induced chemokines secreted by treated tumor cells and/or stromal components. For instance, several exogenous ROS inducers (e.g. radiotherapy, PDT and CAP) induce CXCL9 and CXCL10 secretion, which attracts T cells and thereby enhances tumor control (83-86). By contrast, CXCL12 induced by radiotherapy can attract tumor promoting MDSCs (111, 112). This underscores the double-edged sword of oxidative stress induced therapy in the antitumor immune response. Additionally, a high dose of platinum based chemotherapy is considered immunosuppressive, causing lymphopenia and neutropenia. However, complementary to other ROS-inducing treatments, it has been shown that low dose treatment enhances the T cell response with an increased number of T cells due to secreted chemokines (CXCL9,

CXCL10 and CCL5) after treatment (87). Other chemotherapy based treatments are also able to upregulate the expression of chemokines receptors ligands in the TME, subsequently enhancing T cell recruitment (88-90).

- Modification of the related surface molecules

Susceptibility of tumor cells to T cell and NK cell-mediated cytotoxicity can be modulated by the expression pattern of surface molecules, including major histocompatibility complex (MHC)-I, MHC-II, NK cell ligands, costimulatory receptors and death receptors. The MHC class I is vital for presentation of endogenous and potentially tumor-specific antigens to cytotoxic T cells. Radiation induced MHC-I expression on tumor cells, associated with increased susceptibility to T cell-mediated killing (91-93). Similar to radiation, PDT and CAP use oxygen radicals and were shown to restore MHC-I expression in glioma and melanoma, respectively (94, 95). Additionally, PDT and radiotherapy induce MHC class I polypeptide-related sequence A (MICA) expression and upregulation of natural killer group 2D ligand (NKG2DL) on tumor cells. Both effects corresponded to increased NK cell-mediated killing of treated tumor cells (96, 97). By acting on the death receptors (e.g. Fas), the intrinsic immunogenic properties of the target cells can be altered after radiation, which consequently enhances their susceptibility to cytotoxic T cell-mediated killing (98). The same effect was seen after treatment with BSO, inducing the formation of the CD95 death inducing signaling complex (99). Other chemotherapeutic regimens, which interfere with GSH, also increased the expression of death receptors (100).

ROS-inducing treatments also modulate programmed death-ligand 1 (PD-L1) expression. However, the interplay between ROS inducers and PD-L1 expression is complex, showing that both up- and downregulation of PD-L1 expression can be induced. It is shown that different inhibitors of Trx/TrxR system decrease the PD-L1 protein level in tumor cells (101). However, the opposite effect was reported with the TrxR inhibitor auranofin (113). Like auranofin, arsenic trioxide induces PD-L1 expression in a dose-dependent manner in leukemic cells (127). Besides antioxidant depletion, PD-L1 expression was increased through PI3K/Akt and STAT3 signaling *in vivo* and *in vitro* after conventional fractionated radiotherapy (114, 115). In addition, PD-L1 expression may occur in response to tumor targeting immune cells that release IFN- γ upon recognition of the antigen expressed by tumor cells (128). Conversely, IFN- γ seems to represent the dominant effector molecule of

the antitumor immune response after radiotherapy (93). The same is true for different chemotherapeutics (such as doxorubicin and oxaliplatin) and other physical modalities inducing oxidative stress (including PDT and CAP), where IFN- γ was assessed as a reporter of T cell activity in response to treatments (102).

Many proinflammatory cytokines, including IFN- γ and tumor necrosis factor (TNF)- α , are regulated by the transcription factor NF- κ B that can attract cells of the innate and adaptive immune system to mediate antitumor immune responses (129). This highlights the paradoxical role of NF- κ B, where its activation due to intermediate levels of ROS generated during lower dosages of therapeutic strategies inducing oxidative stress (e.g. radiotherapy and PDT), enhances tumor cell growth and on the other hand activates the antitumoral immunity.

None of the described indirect effects can be generalized among all different exogenous and endogenous oxidative stress-inducing therapeutic strategies. Additionally, the effects are context and dose dependent. Further comprehensive studies are needed to fill up the gaps in the knowledge on different ROS-inducing treatments and possible combinatorial strategies concerning their specific effect on immune response priming, recruitment of leukocytes and modification of surface molecules after treatment.

Direct effects on the antitumoral immune response

- Direct effect on tumor infiltrating immunosuppressive cells

Immunosuppressive cells, including tumor associated macrophages (TAMs), regulatory T cells (Tregs) and MDSC are key components of the TME of numerous tumor types (130). There is an interaction between tumor cells and these immune cells leading to tumor immune escape. An increased number of Tregs in tumor tissue is found in a high proportion of cancer patients and is correlated with tumor progression and poor prognosis, since Tregs help to evade host immunity. In contrast to conventional CD4⁺ T cells, Tregs are more resistant to oxidative stress induced cell death (131). This could be explained by the higher expression and secretion levels of the antioxidant molecule Trx (132). It was shown that antioxidant Trx expression correlates with Treg representation in clinical samples of metastatic melanoma and that modulation of Trx influences the induction of Tregs and the generation of an immunotolerant cytokine profile. Addition of a Trx inhibitor decreased

the number of Tregs in lung lesions. Furthermore, IFN- γ increased, whereas IL-10 and transforming growth factor (TGF)- β decreased after treatment with a Trx blocking antibody (103). Arsenic trioxide, shown to inhibit TrxR, also induced selective depletion of Tregs and consequently increased the antitumor immune response (32, 104). Moreover, it was found that oxidative stress was the metabolic mechanism that controls tumor Treg cell functional behavior. Induction of Treg apoptosis through exogenous oxidative stress mediated the conversion of a large amount of ATP into adenosine via CD39 and CD73 and subsequently triggered an immunosuppressive cascade, tempering the therapeutic effect of immune checkpoint therapy (133). Beyond these effects, it was shown that radiotherapy can induce TGF- β release in the TME and consequently lead to accumulation of Tregs into the tumor tissue (116).

On the contrary, it was found that percentages of Tregs in the peripheral blood of cancer patients decreased significantly after radiotherapy (105). It was confirmed by others that the reduction was mediated by downregulation of CCL22 (106). So far, there is no consensus concerning the effect of radiotherapy on Tregs, probably because the effect of radiotherapy on Tregs is context dependent for different doses and tumor types. The same contradictory results are true for treatment with PDT (117).

Besides Tregs, certain subtypes of TAMs are also considered to have pro-tumoral functions. TAMs can differentiate from monocytes into two distinct subtypes, namely classically activated (M1) and alternatively activated (M2) macrophages with effector or suppressive function, respectively. Concerning vulnerability of TAM to oxidative stress, M2 macrophages have lower levels of ROS compared to M1 phenotype due to higher antioxidant activity, indicating that they will be more resistant to ROS-inducing treatments (134). For instance, M1 macrophages were observed to be more sensitive towards radiotherapy, compared to M2 macrophages (135). Additionally, several controversial studies have investigated the effect of chemotherapy and radiotherapy on the TAM phenotype. For example, low dose of cyclophosphamide can promote the differentiation of M2 macrophages into M1 (107). Similarly, low dose radiation promotes TAM skewing towards an M1 polarized phenotype and render them supportive of antitumor immunity (108). However, higher radiation doses can polarize TAMs to an M2 phenotype promoting tumor growth, induced by factors released from irradiated cells (118). Gold and silver

nanoparticles have been shown to modulate reactive oxygen and nitrogen species production by suppressing the antioxidant system of tumor cells. When applying these nanoparticles to TAMs, there was a downregulation of TNF- α and IL-10 and an upregulation of IL-12, resulting in a polarization from M2 to M1 macrophages, suggesting a radical shift from pro-tumorigenic to an anti-tumorigenic nature when TAMs undergo oxidative stress (109). Since polarization of TAMs is extremely dependent on the contextual signals of the TME, characterization of the oxidative stress induced factors regulating this polarization remains to be elucidated.

- Direct effect on tumor infiltrating immunostimulatory cells

Several oxidative stress-inducing treatments have the potential to increase tumor cell immunogenicity by activating ICD and secreting immunostimulatory factors that can activate innate immune responses and elicits a tumor specific adaptive immune response. In practice, however, the toxicity of these oxidative stress-inducing treatments to T cells, NK cells and DCs limits the extent of immune stimulation and can even lead to immunosuppression (136). Consequently, oxidative stress-inducing treatments can cause severe related lymphopenia that is associated with reduced patient survival (119).

For instance, the direct effect of radiation on lymphocytes is often immunosuppressive since most subsets of lymphocytes are radiosensitive (137). Similar direct effects have been demonstrated after chemotherapy, PTD and CAP (119-121). Nevertheless, the various lymphocyte subtypes differ in their sensitivity to exogenous induced oxidative stress. It has been demonstrated that memory and naïve T cells, as well as NK cells are highly sensitive, whereas effector T cells, NK-T cells and Tregs are more resistant to the toxic effects of exogenous induced oxidative stress (131, 138). Additionally, the extent of immunosuppressive properties will vary with treatment schedule and dose (136, 137). In general, activated T cells and NK cells have higher antioxidant levels (GSH and Trx), necessary to buffer the rising ROS levels upon activation and proliferation of these lymphocytes, making them less vulnerable for exogenous ROS-induced cell death (139, 140). For example, IL-2 activated NK cells were more resistant to H₂O₂-induced cell death than resting NK cells due to an upregulation of the Trx system. However, H₂O₂-induced cell death was also observed in these activated NK cells in the presence of a Trx inhibitor (140). Inhibiting the antioxidant system in T cells with arsenic trioxide also induces

apoptosis in T cells by enhancing oxidative stress, decreasing intracellular GSH releasing cytochrome c, activating caspases and downregulating Bcl-2 (122). In contrast, after Trx inhibition the expression of activation marker CD69 was significantly increased on both CD8⁺ T cells and NK cells (34).

In contrast to all lymphocyte subsets, monocytes are shown to be more resistant to exogenous ROS-induced cell death (75, 78, 121, 141). This might be explained by a stronger antioxidant defense system in phagocytes, such as monocytes and DCs, which under physiological conditions protect them against self-production of ROS during oxidative burst (142). However, depletion of the antioxidant GSH system could also inhibit DC maturation (123).

In summary, ROS-inducing treatments cause direct and indirect immune effects which can be both immunostimulatory and immunosuppressive. Current research on ROS-inducing treatments mostly focuses on one immunomodulating aspect but lacks comprehensive investigation on both stimulatory and suppressive immune effects. Additionally, it is necessary to take into account the timing and location of the effects. ROS-inducing treatments can have immediate toxic and suppressive effects on tumor infiltrating immune cells, however, can be able to attract new systemic immune cells towards the tumor, stimulating an antitumoral immune response. Therefore, it is necessary to elucidate all these challenges when investigating oxidative stress-inducing treatment modalities as novel anticancer strategy.

Conclusion

Preclinical studies have elucidated that an increase in ROS concentrations through exogenous and endogenous ROS-inducing therapies or a combination of both can be an efficient anticancer strategy. Hence, the influence of these treatments on the TME should be considered. Importantly, both the immunostimulatory as well as immunosuppressive effects have to be taken into account when investigating these anticancer modalities, because increasing ROS levels can be a double-edged sword with regards to immunomodulation and the effects cannot be generalized over different treatment modalities.

References

1. Perillo B, Di Donato M, Pezone A, Di Zazzo E, Giovannelli P, Galasso G, et al. ROS in cancer therapy: the bright side of the moon. *Exp Mol Med*. 2020;52(2):192-203.
2. de Sa Junior PL, Camara DAD, Porcacchia AS, Fonseca PMM, Jorge SD, Araldi RP, et al. The Roles of ROS in Cancer Heterogeneity and Therapy. *Oxidative medicine and cellular longevity*. 2017;2017:2467940.
3. Kurutas EB. The importance of antioxidants which play the role in cellular response against oxidative/nitrosative stress: current state. *Nutr J*. 2016;15(1):71.
4. Kumari S, Badana AK, G MM, G S, Malla R. Reactive Oxygen Species: A Key Constituent in Cancer Survival. *Biomarker insights*. 2018;13:1177271918755391.
5. Vaupel P, Harrison L. Tumor hypoxia: causative factors, compensatory mechanisms, and cellular response. *The oncologist*. 2004;9 Suppl 5:4-9.
6. Nogueira V, Hay N. Molecular pathways: reactive oxygen species homeostasis in cancer cells and implications for cancer therapy. *Clinical cancer research : an official journal of the American Association for Cancer Research*. 2013;19(16):4309-14.
7. Jaramillo MC, Zhang DD. The emerging role of the Nrf2-Keap1 signaling pathway in cancer. *Genes & development*. 2013;27(20):2179-91.
8. Galadari S, Rahman A, Pallichankandy S, Thayyullathil F. Reactive oxygen species and cancer paradox: To promote or to suppress? *Free radical biology & medicine*. 2017;104:144-64.
9. Pawlowska E, Szczepanska J, Blasiak J. Pro- and Antioxidant Effects of Vitamin C in Cancer in correspondence to Its Dietary and Pharmacological Concentrations. *Oxidative medicine and cellular longevity*. 2019;2019:7286737.
10. Singh K, Bhorl M, Kasu YA, Bhat G, Marar T. Antioxidants as precision weapons in war against cancer chemotherapy induced toxicity - Exploring the armoury of obscurity. *Saudi pharmaceutical journal : SPJ : the official publication of the Saudi Pharmaceutical Society*. 2018;26(2):177-90.
11. Fortmann SP, Burda BU, Senger CA, Lin JS, Whitlock EP. Vitamin and mineral supplements in the primary prevention of cardiovascular disease and cancer: An updated systematic evidence review for the U.S. Preventive Services Task Force. *Annals of internal medicine*. 2013;159(12):824-34.
12. Lin J, Cook NR, Albert C, Zaharris E, Gaziano JM, Van Denburgh M, et al. Vitamins C and E and beta carotene supplementation and cancer risk: a randomized controlled trial. *Journal of the National Cancer Institute*. 2009;101(1):14-23.
13. Vinceti M, Filippini T, Del Giovane C, Dennert G, Zwahlen M, Brinkman M, et al. Selenium for preventing cancer. *The Cochrane database of systematic reviews*. 2018;1:CD005195.
14. Benhar M, Shytaj IL, Stamler JS, Savarino A. Dual targeting of the thioredoxin and glutathione systems in cancer and HIV. *The Journal of clinical investigation*. 2016;126(5):1630-9.
15. Ozben T. Oxidative stress and apoptosis: impact on cancer therapy. *J Pharm Sci-US*. 2007;96(9):2181-96.
16. Kim SJ, Kim HS, Seo YR. Understanding of ROS-Inducing Strategy in Anticancer Therapy. *Oxidative medicine and cellular longevity*. 2019;2019:5381692.
17. Zhang B, Wang Y, Su Y. Peroxiredoxins, a novel target in cancer radiotherapy. *Cancer letters*. 2009;286(2):154-60.
18. Kim W, Lee S, Seo D, Kim D, Kim K, Kim E, et al. Cellular Stress Responses in Radiotherapy. *Cells*. 2019;8(9).
19. Price M, Terlecky SR, Kessel D. A role for hydrogen peroxide in the pro-apoptotic effects of photodynamic therapy. *Photochem Photobiol*. 2009;85(6):1491-6.
20. Moserova I, Truxova I, Garg AD, Tomala J, Agostinis P, Cartron PF, et al. Caspase-2 and oxidative stress underlie the immunogenic potential of high hydrostatic pressure-induced cancer cell death. *Oncoimmunology*. 2017;6(1):e1258505.
21. Yamada Y, Takano Y, Satrialdi, Abe J, Hibino M, Harashima H. Therapeutic Strategies for Regulating Mitochondrial Oxidative Stress. *Biomolecules*. 2020;10(1).
22. Turrini E, Laurita R, Stancampiano A, Catanzaro E, Calcabrini C, Maffei F, et al. Cold Atmospheric Plasma Induces Apoptosis and Oxidative Stress Pathway Regulation in T-Lymphoblastoid Leukemia Cells. *Oxidative medicine and cellular longevity*. 2017;2017.

23. Zhou Z, Song J, Nie L, Chen X. Reactive oxygen species generating systems meeting challenges of photodynamic cancer therapy. *Chem Soc Rev.* 2016;45(23):6597-626.
24. Yan D, Xu W, Yao X, Lin L, Sherman JH, Keidar M. The Cell Activation Phenomena in the Cold Atmospheric Plasma Cancer Treatment. *Sci Rep.* 2018;8(1):15418.
25. Yang H, Villani RM, Wang H, Simpson MJ, Roberts MS, Tang M, et al. The role of cellular reactive oxygen species in cancer chemotherapy. *Journal of experimental & clinical cancer research : CR.* 2018;37(1):266.
26. Yen YP, Tsai KS, Chen YW, Huang CF, Yang RS, Liu SH. Arsenic induces apoptosis in myoblasts through a reactive oxygen species-induced endoplasmic reticulum stress and mitochondrial dysfunction pathway. *Arch Toxicol.* 2012;86(6):923-33.
27. Marullo R, Werner E, Degtyareva N, Moore B, Altavilla G, Ramalingam SS, et al. Cisplatin induces a mitochondrial-ROS response that contributes to cytotoxicity depending on mitochondrial redox status and bioenergetic functions. *Plos One.* 2013;8(11):e81162.
28. Zhu H, Sarkar S, Scott L, Danelisen I, Trush MA, Jia Z, et al. Doxorubicin Redox Biology: Redox Cycling, Topoisomerase Inhibition, and Oxidative Stress. *React Oxyg Species (Apex).* 2016;1(3):189-98.
29. Moulder S, Dhillon N, Ng C, Hong D, Wheler J, Naing A, et al. A phase I trial of imexon, a pro-oxidant, in combination with docetaxel for the treatment of patients with advanced breast, non-small cell lung and prostate cancer. *Invest New Drugs.* 2010;28(5):634-40.
30. Trachootham D, Alexandre J, Huang P. Targeting cancer cells by ROS-mediated mechanisms: a radical therapeutic approach? *Nature reviews Drug discovery.* 2009;8(7):579-91.
31. Chou WC, Jie C, Kenedy AA, Jones RJ, Trush MA, Dang CV. Role of NADPH oxidase in arsenic-induced reactive oxygen species formation and cytotoxicity in myeloid leukemia cells. *Proceedings of the National Academy of Sciences of the United States of America.* 2004;101(13):4578-83.
32. Lu J, Chew EH, Holmgren A. Targeting thioredoxin reductase is a basis for cancer therapy by arsenic trioxide. *Proceedings of the National Academy of Sciences of the United States of America.* 2007;104(30):12288-93.
33. Desideri E, Ciccarone F, Ciriolo MR. Targeting Glutathione Metabolism: Partner in Crime in Anticancer Therapy. *Nutrients.* 2019;11(8).
34. Lei H, Wang G, Zhang J, Han Q. Inhibiting TrxR suppresses liver cancer by inducing apoptosis and eliciting potent antitumor immunity. *Oncol Rep.* 2018;40(6):3447-57.
35. Sobhakumari A, Love-Homan L, Fletcher EV, Martin SM, Parsons AD, Spitz DR, et al. Susceptibility of human head and neck cancer cells to combined inhibition of glutathione and thioredoxin metabolism. *Plos One.* 2012;7(10):e48175.
36. Marzano C, Gandin V, Folda A, Scutari G, Bindoli A, Rigobello MP. Inhibition of thioredoxin reductase by auranofin induces apoptosis in cisplatin-resistant human ovarian cancer cells. *Free radical biology & medicine.* 2007;42(6):872-81.
37. Ramanathan RK, Stephenson JJ, Weiss GJ, Pestano LA, Lowe A, Hiscox A, et al. A phase I trial of PX-12, a small-molecule inhibitor of thioredoxin-1, administered as a 72-hour infusion every 21 days in patients with advanced cancers refractory to standard therapy. *Invest New Drugs.* 2012;30(4):1591-6.
38. Baker AF, Adab KN, Raghunand N, Chow H, Stratton SP, Squire SW, et al. A phase IB trial of 24-hour intravenous PX-12, a thioredoxin-1 inhibitor, in patients with advanced gastrointestinal cancers. *Invest New Drugs.* 2013;31(3):631-41.
39. Aggarwal V, Tuli HS, Varol A, Thakral F, Yerer MB, Sak K, et al. Role of Reactive Oxygen Species in Cancer Progression: Molecular Mechanisms and Recent Advancements. *Biomolecules.* 2019;9(11).
40. Ryter SW, Kim HP, Hoetzel A, Park JW, Nakahira K, Wang X, et al. Mechanisms of cell death in oxidative stress. *Antioxidants & redox signaling.* 2007;9(1):49-89.
41. Piette J. Signalling pathway activation by photodynamic therapy: NF-kappa B at the crossroad between oncology and immunology. *Photoch Photobio Sci.* 2015;14(8):1510-7.
42. Maier P, Hartmann L, Wenz F, Herskind C. Cellular Pathways in Response to Ionizing Radiation and Their Targetability for Tumor Radiosensitization. *International journal of molecular sciences.* 2016;17(1).
43. Ahmed KM, Li JJ. NF-kappa B-mediated adaptive resistance to ionizing radiation. *Free radical biology & medicine.* 2008;44(1):1-13.
44. Reiners JJ, Jr., Agostinis P, Berg K, Oleinick NL, Kessel D. Assessing autophagy in the context of photodynamic therapy. *Autophagy.* 2010;6(1):7-18.

45. Kraus D, Palasuberniam P, Chen B. Targeting Phosphatidylinositol 3-Kinase Signaling Pathway for Therapeutic Enhancement of Vascular-Targeted Photodynamic Therapy. *Mol Cancer Ther.* 2017;16(11):2422-31.
46. Bundscherer L, Wende K, Ottmuller K, Barton A, Schmidt A, Bekeschus S, et al. Impact of non-thermal plasma treatment on MAPK signaling pathways of human immune cell lines. *Immunobiology.* 2013;218(10):1248-55.
47. Li H, Hu J, Wu S, Wang L, Cao X, Zhang X, et al. Auranofin-mediated inhibition of PI3K/AKT/mTOR axis and anticancer activity in non-small cell lung cancer cells. *Oncotarget.* 2016;7(3):3548-58.
48. Zheng Z, Fan S, Zheng J, Huang W, Gasparetto C, Chao NJ, et al. Inhibition of thioredoxin activates mitophagy and overcomes adaptive bortezomib resistance in multiple myeloma. *J Hematol Oncol.* 2018;11(1):29.
49. Duan D, Zhang J, Yao J, Liu Y, Fang J. Targeting Thioredoxin Reductase by Parthenolide Contributes to Inducing Apoptosis of HeLa Cells. *J Biol Chem.* 2016;291(19):10021-31.
50. Hambright HG, Meng P, Kumar AP, Ghosh R. Inhibition of PI3K/AKT/mTOR axis disrupts oxidative stress-mediated survival of melanoma cells. *Oncotarget.* 2015;6(9):7195-208.
51. Godwin P, Baird AM, Heavey S, Barr MP, O'Byrne KJ, Gately K. Targeting nuclear factor-kappa B to overcome resistance to chemotherapy. *Frontiers in oncology.* 2013;3:120.
52. Eliseev RA, Zuscik MJ, Schwarz EM, O'Keefe RJ, Drissi H, Rosier RN. Increased radiation-induced apoptosis of Saos2 cells via inhibition of NFkappaB: a role for c-Jun N-terminal kinase. *J Cell Biochem.* 2005;96(6):1262-73.
53. Telkoparan-Akillilar P, Suzen S, Saso L. Pharmacological Applications of Nrf2 Inhibitors as Potential Antineoplastic Drugs. *International journal of molecular sciences.* 2019;20(8).
54. Wu S, Lu H, Bai Y. Nrf2 in cancers: A double-edged sword. *Cancer Med.* 2019;8(5):2252-67.
55. Boivin A, Hanot M, Malesys C, Maalouf M, Rousson R, Rodriguez-Lafrasse C, et al. Transient alteration of cellular redox buffering before irradiation triggers apoptosis in head and neck carcinoma stem and non-stem cells. *Plos One.* 2011;6(1):e14558.
56. Wang H, Bouzakoura S, de Mey S, Jiang H, Law K, Dufait I, et al. Auranofin radiosensitizes tumor cells through targeting thioredoxin reductase and resulting overproduction of reactive oxygen species. *Oncotarget.* 2017;8(22):35728-42.
57. Rodman SN, Spence JM, Ronnfeldt TJ, Zhu Y, Solst SR, O'Neill RA, et al. Enhancement of Radiation Response in Breast Cancer Stem Cells by Inhibition of Thioredoxin- and Glutathione-Dependent Metabolism. *Radiat Res.* 2016;186(4):385-95.
58. Feng Z, Guo J, Liu X, Song H, Zhang C, Huang P, et al. Cascade of reactive oxygen species generation by polyprodrug for combinational photodynamic therapy. *Biomaterials.* 2020;255:120210.
59. Lee HM, Kim DH, Lee HL, Cha B, Kang DH, Jeong YI. Synergistic effect of buthionine sulfoximine on the chlorin e6-based photodynamic treatment of cancer cells. *Arch Pharm Res.* 2019;42(11):990-9.
60. Kimani SG, Phillips JB, Bruce JI, MacRobert AJ, Golding JP. Antioxidant inhibitors potentiate the cytotoxicity of photodynamic therapy. *Photochem Photobiol.* 2012;88(1):175-87.
61. Theodossiou TA, Olsen CE, Jonsson M, Kubin A, Hothersall JS, Berg K. The diverse roles of glutathione-associated cell resistance against hypericin photodynamic therapy. *Redox biology.* 2017;12:191-7.
62. Lopes-Coelho F, Gouveia-Fernandes S, Goncalves LG, Nunes C, Faustino I, Silva F, et al. HNF1beta drives glutathione (GSH) synthesis underlying intrinsic carboplatin resistance of ovarian clear cell carcinoma (OCCC). *Tumour biology : the journal of the International Society for Oncodevelopmental Biology and Medicine.* 2016;37(4):4813-29.
63. Liu X, Wang W, Yin Y, Li M, Li H, Xiang H, et al. A high-throughput drug screen identifies auranofin as a potential sensitizer of cisplatin in small cell lung cancer. *Invest New Drugs.* 2019;37(6):1166-76.
64. Smart DK, Ortiz KL, Mattson D, Bradbury CM, Bisht KS, Sieck LK, et al. Thioredoxin reductase as a potential molecular target for anticancer agents that induce oxidative stress. *Cancer research.* 2004;64(18):6716-24.
65. Sabharwal SS, Schumacker PT. Mitochondrial ROS in cancer: initiators, amplifiers or an Achilles' heel? *Nature reviews Cancer.* 2014;14(11):709-21.

66. Wang H, Jiang H, Van De Gucht M, De Ridder M. Hypoxic Radioresistance: Can ROS Be the Key to Overcome It? *Cancers*. 2019;11(1).
67. De Ridder M, Verellen D, Verovski V, Storme G. Hypoxic tumor cell radiosensitization through nitric oxide. *Nitric Oxide*. 2008;19(2):164-9.
68. Vukovic V, Nicklee T, Hedley DW. Differential effects of buthionine sulphoximine in hypoxic and non-hypoxic regions of human cervical carcinoma xenografts. *Radiother Oncol*. 2001;60(1):69-73.
69. Jiang H, Wang H, De Ridder M. Targeting antioxidant enzymes as a radiosensitizing strategy. *Cancer letters*. 2018;438:154-64.
70. Ranning PV, Di Trapani G, Vuckovic S, Tonissen KF. TrxR1 inhibition overcomes both hypoxia-induced and acquired bortezomib resistance in multiple myeloma through NF-small ka, Cyrillicbeta inhibition. *Cell cycle*. 2016;15(4):559-72.
71. Nakaya A, Sagawa M, Muto A, Uchida H, Ikeda Y, Kizaki M. The gold compound auranofin induces apoptosis of human multiple myeloma cells through both down-regulation of STAT3 and inhibition of NF-kappaB activity. *Leuk Res*. 2011;35(2):243-9.
72. Peng L, Linghu R, Chen D, Yang J, Kou X, Wang XZ, et al. Inhibition of glutathione metabolism attenuates esophageal cancer progression. *Exp Mol Med*. 2017;49(4):e318.
73. Zitvogel L, Apetoh L, Ghiringhelli F, Kroemer G. Immunological aspects of cancer chemotherapy. *Nature reviews Immunology*. 2008;8(1):59-73.
74. Mroz P, Hamblin MR. The immunosuppressive side of PDT. *Photochem Photobiol Sci*. 2011;10(5):751-8.
75. Carvalho HA, Villar RC. Radiotherapy and immune response: the systemic effects of a local treatment. *Clinics (Sao Paulo)*. 2018;73(suppl 1):e557s.
76. Adkins I, Fucikova J, Garg AD, Agostinis P, Spisek R. Physical modalities inducing immunogenic tumor cell death for cancer immunotherapy. *Oncoimmunology*. 2014;3(12):e968434.
77. Zhou J, Wang G, Chen Y, Wang H, Hua Y, Cai Z. Immunogenic cell death in cancer therapy: Present and emerging inducers. *Journal of cellular and molecular medicine*. 2019;23(8):4854-65.
78. Van Loenhout J, Flieswasser T, Freire Boullosa L, De Waele J, Van Audenaerde J, Marcq E, et al. Cold Atmospheric Plasma-Treated PBS Eliminates Immunosuppressive Pancreatic Stellate Cells and Induces Immunogenic Cell Death of Pancreatic Cancer Cells. *Cancers*. 2019;11(10).
79. Lin A, Gorbanev Y, De Backer J, Van Loenhout J, Van Boxem W, Lemièrre F, et al. Non-Thermal Plasma as a Unique Delivery System of Short-Lived Reactive Oxygen and Nitrogen Species for Immunogenic Cell Death in Melanoma Cells. *Advanced Science*. 2019:1802062.
80. Panzarini E, Inguscio V, Dini L. Immunogenic cell death: can it be exploited in PhotoDynamic Therapy for cancer? *Biomed Res Int*. 2013;2013:482160.
81. Gebremeskel S, Johnston B. Concepts and mechanisms underlying chemotherapy induced immunogenic cell death: impact on clinical studies and considerations for combined therapies. *Oncotarget*. 2015;6(39):41600-19.
82. Apetoh L, Ghiringhelli F, Tesniere A, Obeid M, Ortiz C, Criollo A, et al. Toll-like receptor 4-dependent contribution of the immune system to anticancer chemotherapy and radiotherapy. *Nature medicine*. 2007;13(9):1050-9.
83. Lamberti MJ, Mentucci FM, Roselli E, Araya P, Rivarola VA, Rumie Vittar NB, et al. Photodynamic Modulation of Type 1 Interferon Pathway on Melanoma Cells Promotes Dendritic Cell Activation. *Frontiers in immunology*. 2019;10:2614.
84. Freund E, Liedtke KR, van der Linde J, Metelmann HR, Heidecke CD, Partecke LI, et al. Physical plasma-treated saline promotes an immunogenic phenotype in CT26 colon cancer cells in vitro and in vivo. *Sci Rep*. 2019;9(1):634.
85. Sagwal SK, Pasqual-Melo G, Bodnar Y, Gandhirajan RK, Bekeschus S. Combination of chemotherapy and physical plasma elicits melanoma cell death via upregulation of SLC22A16. *Cell death & disease*. 2018;9(12):1179.
86. Lim JY, Gerber SA, Murphy SP, Lord EM. Type I interferons induced by radiation therapy mediate recruitment and effector function of CD8(+) T cells. *Cancer immunology, immunotherapy : CII*. 2014;63(3):259-71.
87. Fu D, Wu J, Lai J, Liu Y, Zhou L, Chen L, et al. T cell recruitment triggered by optimal dose platinum compounds contributes to the therapeutic efficacy of sequential PD-1 blockade in a mouse model of colon cancer. *Am J Cancer Res*. 2020;10(2):473-90.

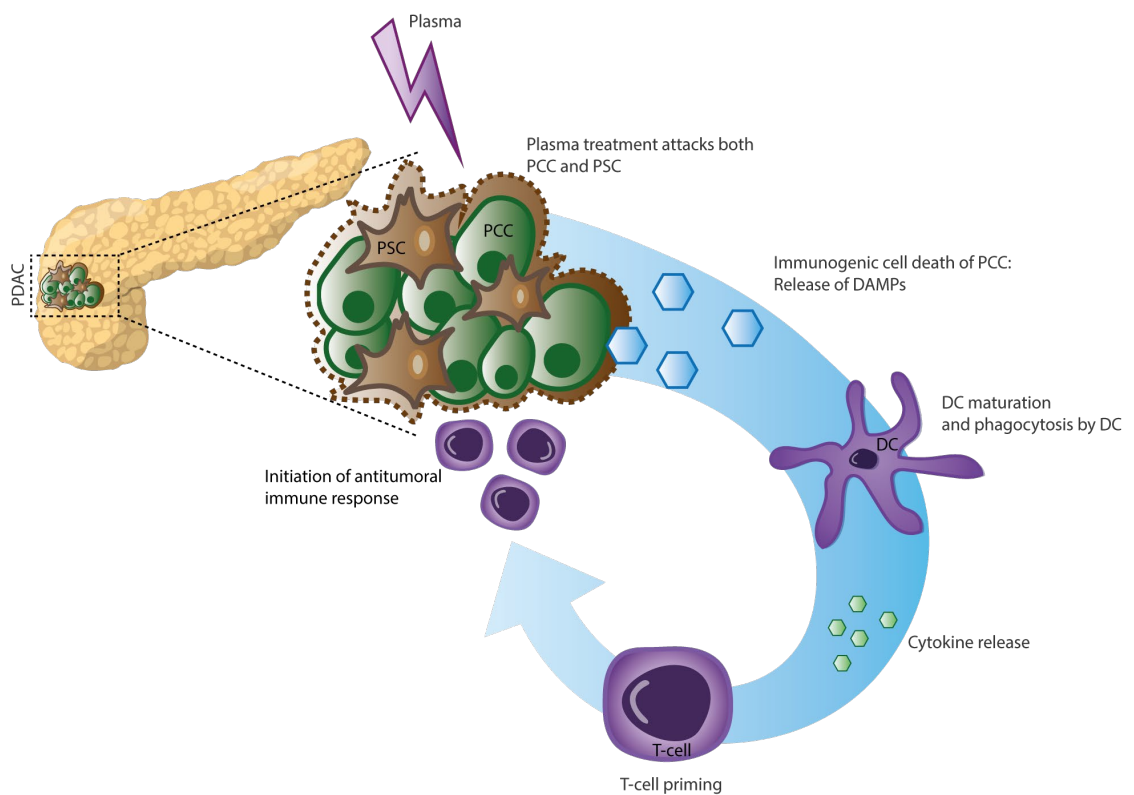
88. Gao Q, Wang S, Chen X, Cheng S, Zhang Z, Li F, et al. Cancer-cell-secreted CXCL11 promoted CD8(+) T cells infiltration through docetaxel-induced-release of HMGB1 in NSCLC. *J Immunother Cancer*. 2019;7(1):42.
89. Sauter KA, Wood LJ, Wong J, Iordanov M, Magun BE. Doxorubicin and daunorubicin induce processing and release of interleukin-1beta through activation of the NLRP3 inflammasome. *Cancer Biol Ther*. 2011;11(12):1008-16.
90. Hu J, Sun C, Bernatchez C, Xia X, Hwu P, Dotti G, et al. T-cell Homing Therapy for Reducing Regulatory T Cells and Preserving Effector T-cell Function in Large Solid Tumors. *Clinical cancer research : an official journal of the American Association for Cancer Research*. 2018;24(12):2920-34.
91. Reits EA, Hodge JW, Herberts CA, Groothuis TA, Chakraborty M, Wansley EK, et al. Radiation modulates the peptide repertoire, enhances MHC class I expression, and induces successful antitumor immunotherapy. *The Journal of experimental medicine*. 2006;203(5):1259-71.
92. Wan S, Pestka S, Jubin RG, Lyu YL, Tsai YC, Liu LF. Chemotherapeutics and radiation stimulate MHC class I expression through elevated interferon-beta signaling in breast cancer cells. *Plos One*. 2012;7(3):e32542.
93. Lugade AA, Sorensen EW, Gerber SA, Moran JP, Frelinger JG, Lord EM. Radiation-induced IFN-gamma production within the tumor microenvironment influences antitumor immunity. *Journal of immunology*. 2008;180(5):3132-9.
94. Zhang SY, Li JL, Xu XK, Zheng MG, Wen CC, Li FC. HMME-based PDT restores expression and function of transporter associated with antigen processing 1 (TAP1) and surface presentation of MHC class I antigen in human glioma. *Journal of neuro-oncology*. 2011;105(2):199-210.
95. Bekeschus S, Rodder K, Fregin B, Otto O, Lippert M, Weltmann KD, et al. Toxicity and Immunogenicity in Murine Melanoma following Exposure to Physical Plasma-Derived Oxidants. *Oxidative medicine and cellular longevity*. 2017;2017:4396467.
96. Belicha-Villanueva A, Riddell J, Bangia N, Gollnick SO. The effect of photodynamic therapy on tumor cell expression of major histocompatibility complex (MHC) class I and MHC class I-related molecules. *Lasers Surg Med*. 2012;44(1):60-8.
97. Gasser S, Orsulic S, Brown EJ, Raulet DH. The DNA damage pathway regulates innate immune system ligands of the NKG2D receptor. *Nature*. 2005;436(7054):1186-90.
98. Garnett CT, Palena C, Chakraborty M, Tsang KY, Schlom J, Hodge JW. Sublethal irradiation of human tumor cells modulates phenotype resulting in enhanced killing by cytotoxic T lymphocytes. *Cancer research*. 2004;64(21):7985-94.
99. Friesen C, Kiess Y, Debatin KM. A critical role of glutathione in determining apoptosis sensitivity and resistance in leukemia cells. *Cell death and differentiation*. 2004;11 Suppl 1:S73-85.
100. Zitvogel L, Apetoh L, Ghiringhelli F, Andre F, Tesniere A, Kroemer G. The anticancer immune response: indispensable for therapeutic success? *The Journal of clinical investigation*. 2008;118(6):1991-2001.
101. Bailly C. Regulation of PD-L1 expression on cancer cells with ROS-modulating drugs. *Life Sci*. 2020;246:117403.
102. Showalter A, Limaye A, Oyer JL, Igarashi R, Kittipatarin C, Copik AJ, et al. Cytokines in immunogenic cell death: Applications for cancer immunotherapy. *Cytokine*. 2017;97:123-32.
103. Wang X, Dong H, Li Q, Li Y, Hong A. Thioredoxin induces Tregs to generate an immunotolerant tumor microenvironment in metastatic melanoma. *Oncoimmunology*. 2015;4(9):e1027471.
104. Thomas-Schoemann A, Batteux F, Mongaret C, Nicco C, Chereau C, Annereau M, et al. Arsenic trioxide exerts antitumor activity through regulatory T cell depletion mediated by oxidative stress in a murine model of colon cancer. *Journal of immunology*. 2012;189(11):5171-7.
105. Napolitano M, D'Alterio C, Cardone E, Trotta AM, Pecori B, Rega D, et al. Peripheral myeloid-derived suppressor and T regulatory PD-1 positive cells predict response to neoadjuvant short-course radiotherapy in rectal cancer patients. *Oncotarget*. 2015;6(10):8261-70.
106. Liao C, Xiao W, Zhu N, Liu Z, Yang J, Wang Y, et al. Radiotherapy suppressed tumor-specific recruitment of regulator T cells via up-regulating microR-545 in Lewis lung carcinoma cells. *Int J Clin Exp Pathol*. 2015;8(3):2535-44.
107. Bryniarski K, Szczepanik M, Ptak M, Zemelka M, Ptak W. Influence of cyclophosphamide and its metabolic products on the activity of peritoneal macrophages in mice. *Pharmacol Rep*. 2009;61(3):550-7.

108. Klug F, Prakash H, Huber PE, Seibel T, Bender N, Halama N, et al. Low-dose irradiation programs macrophage differentiation to an iNOS(+)/M1 phenotype that orchestrates effective T cell immunotherapy. *Cancer Cell*. 2013;24(5):589-602.
109. Pal R, Chakraborty B, Nath A, Singh LM, Ali M, Rahman DS, et al. Noble metal nanoparticle-induced oxidative stress modulates tumor associated macrophages (TAMs) from an M2 to M1 phenotype: An in vitro approach. *Int Immunopharmacol*. 2016;38:332-41.
110. Bianchi G, Vuerich M, Pellegatti P, Marimpietri D, Emionite L, Marigo I, et al. ATP/P2X7 axis modulates myeloid-derived suppressor cell functions in neuroblastoma microenvironment. *Cell death & disease*. 2014;5:e1135.
111. Giordano FA, Link B, Glas M, Herrlinger U, Wenz F, Umansky V, et al. Targeting the Post-Irradiation Tumor Microenvironment in Glioblastoma via Inhibition of CXCL12. *Cancers*. 2019;11(3).
112. Eckert F, Schilbach K, Klumpp L, Bardoscia L, Sezgin EC, Schwab M, et al. Potential Role of CXCR4 Targeting in the Context of Radiotherapy and Immunotherapy of Cancer. *Frontiers in immunology*. 2018;9:3018.
113. Ranning PV, Lee AC, Sinha D, Shih YY, Mittal D, Makhale A, et al. Therapeutic cooperation between auranofin, a thioredoxin reductase inhibitor and anti-PD-L1 antibody for treatment of triple-negative breast cancer. *Int J Cancer*. 2020;146(1):123-36.
114. Gong X, Li X, Jiang T, Xie H, Zhu Z, Zhou F, et al. Combined Radiotherapy and Anti-PD-L1 Antibody Synergistically Enhances Antitumor Effect in Non-Small Cell Lung Cancer. *J Thorac Oncol*. 2017;12(7):1085-97.
115. Azad A, Yin Lim S, D'Costa Z, Jones K, Diana A, Sansom OJ, et al. PD-L1 blockade enhances response of pancreatic ductal adenocarcinoma to radiotherapy. *EMBO Mol Med*. 2017;9(2):167-80.
116. Kachikwu EL, Iwamoto KS, Liao YP, DeMarco JJ, Agazaryan N, Economou JS, et al. Radiation enhances regulatory T cell representation. *Int J Radiat Oncol Biol Phys*. 2011;81(4):1128-35.
117. Maeding N, Verwanger T, Krammer B. Boosting Tumor-Specific Immunity Using PDT. *Cancers*. 2016;8(10).
118. Tsai CS, Chen FH, Wang CC, Huang HL, Jung SM, Wu CJ, et al. Macrophages from irradiated tumors express higher levels of iNOS, arginase-I and COX-2, and promote tumor growth. *Int J Radiat Oncol Biol Phys*. 2007;68(2):499-507.
119. Grossman SA, Ellsworth S, Campian J, Wild AT, Herman JM, Laheru D, et al. Survival in Patients With Severe Lymphopenia Following Treatment With Radiation and Chemotherapy for Newly Diagnosed Solid Tumors. *J Natl Compr Canc Netw*. 2015;13(10):1225-31.
120. Hunt DW, Jiang H, Granville DJ, Chan AH, Leong S, Levy JG. Consequences of the photodynamic treatment of resting and activated peripheral T lymphocytes. *Immunopharmacology*. 1999;41(1):31-44.
121. Bekeschus S, Kolata J, Winterbourn C, Kramer A, Turner R, Weltmann KD, et al. Hydrogen peroxide: A central player in physical plasma-induced oxidative stress in human blood cells. *Free radical research*. 2014;48(5):542-9.
122. Gupta S, Yel L, Kim D, Kim C, Chiplunkar S, Gollapudi S. Arsenic trioxide induces apoptosis in peripheral blood T lymphocyte subsets by inducing oxidative stress: a role of Bcl-2. *Mol Cancer Ther*. 2003;2(8):711-9.
123. Kim HJ, Barajas B, Chan RC, Nel AE. Glutathione depletion inhibits dendritic cell maturation and delayed-type hypersensitivity: implications for systemic disease and immunosenescence. *J Allergy Clin Immunol*. 2007;119(5):1225-33.
124. Galluzzi L, Vitale I, Warren S, Adjemian S, Agostinis P, Martinez AB, et al. Consensus guidelines for the definition, detection and interpretation of immunogenic cell death. *J Immunother Cancer*. 2020;8(1):e000337.
125. Garg AD, Dudek AM, Ferreira GB, Verfaillie T, Vandenabeele P, Krysko DV, et al. ROS-induced autophagy in cancer cells assists in evasion from determinants of immunogenic cell death. *Autophagy*. 2013;9(9):1292-307.
126. Melero I, Rouzaut A, Motz GT, Coukos G. T-cell and NK-cell infiltration into solid tumors: a key limiting factor for efficacious cancer immunotherapy. *Cancer Discov*. 2014;4(5):522-6.
127. Wang X, Li J, Dong K, Lin F, Long M, Ouyang Y, et al. Tumor suppressor miR-34a targets PD-L1 and functions as a potential immunotherapeutic target in acute myeloid leukemia. *Cell Signal*. 2015;27(3):443-52.
128. Garcia-Diaz A, Shin DS, Moreno BH, Saco J, Escuin-Ordinas H, Rodriguez GA, et al. Interferon Receptor Signaling Pathways Regulating PD-L1 and PD-L2 Expression. *Cell Rep*. 2017;19(6):1189-201.

129. Broekgaarden M, Weijer R, van Gulik TM, Hamblin MR, Heger M. Tumor cell survival pathways activated by photodynamic therapy: a molecular basis for pharmacological inhibition strategies. *Cancer Metastasis Rev.* 2015;34(4):643-90.
130. Vasievich EA, Huang L. The suppressive tumor microenvironment: a challenge in cancer immunotherapy. *Mol Pharm.* 2011;8(3):635-41.
131. Mougiakakos D, Johansson CC, Kiessling R. Naturally occurring regulatory T cells show reduced sensitivity toward oxidative stress-induced cell death. *Blood.* 2009;113(15):3542-5.
132. Mougiakakos D, Johansson CC, Jitschin R, Bottcher M, Kiessling R. Increased thioredoxin-1 production in human naturally occurring regulatory T cells confers enhanced tolerance to oxidative stress. *Blood.* 2011;117(3):857-61.
133. Maj T, Wang W, Crespo J, Zhang H, Wang W, Wei S, et al. Oxidative stress controls regulatory T cell apoptosis and suppressor activity and PD-L1-blockade resistance in tumor. *Nat Immunol.* 2017;18(12):1332-41.
134. Griess B, Mir S, Datta K, Teoh-Fitzgerald M. Scavenging reactive oxygen species selectively inhibits M2 macrophage polarization and their pro-tumorigenic function in part, via Stat3 suppression. *Free radical biology & medicine.* 2020;147:48-60.
135. Leblond MM, Peres EA, Helaine C, Gerault AN, Moulin D, Anfray C, et al. M2 macrophages are more resistant than M1 macrophages following radiation therapy in the context of glioblastoma. *Oncotarget.* 2017;8(42):72597-612.
136. Wu J, Waxman DJ. Immunogenic chemotherapy: Dose and schedule dependence and combination with immunotherapy. *Cancer letters.* 2018;419:210-21.
137. Schae D, McBride WH. T lymphocytes and normal tissue responses to radiation. *Frontiers in oncology.* 2012;2:119.
138. Takahashi A, Hanson MG, Norell HR, Havelka AM, Kono K, Malmberg KJ, et al. Preferential cell death of CD8(+) effector memory (CCR7(-)CD45RA(-)) T cells by hydrogen peroxide-induced oxidative stress. *Journal of immunology.* 2005;174(10):6080-7.
139. Mak TW, Grusdat M, Duncan GS, Dostert C, Nonnenmacher Y, Cox M, et al. Glutathione Primes T Cell Metabolism for Inflammation. *Immunity.* 2017;46(6):1089-90.
140. Mimura K, Kua LF, Shimasaki N, Shiraishi K, Nakajima S, Siang LK, et al. Upregulation of thioredoxin-1 in activated human NK cells confers increased tolerance to oxidative stress. *Cancer immunology, immunotherapy : CII.* 2017;66(5):605-13.
141. Falcke SE, Ruhle PF, Deloch L, Fietkau R, Frey B, Gaipl US. Clinically Relevant Radiation Exposure Differentially Impacts Forms of Cell Death in Human Cells of the Innate and Adaptive Immune System. *International journal of molecular sciences.* 2018;19(11).
142. Seres T, Knickelbein RG, Warshaw JB, Johnston RB, Jr. The phagocytosis-associated respiratory burst in human monocytes is associated with increased uptake of glutathione. *Journal of immunology.* 2000;165(6):3333-40.

CHAPTER 3

Cold atmospheric plasma-treated PBS eliminates immunosuppressive pancreatic stellate cells and induces immunogenic cell death of pancreatic cancer cells



Jinthe Van Loenhout, Tal Flieswasser, Laurie Freire Boulosa, Jorrit De Waele, Jonas Van Audenaerde, Elly Marcq, Julie Jacobs, Abraham Lin, Eva Lion, Heleen Dewitte, Marc Peeters, Sylvia Dewilde, Filip Lardon, Annemie Bogaerts, Christophe Deben and Evelien Smits. Cold Atmospheric Plasma-Treated PBS Eliminates Immunosuppressive Pancreatic Stellate Cells and Induces Immunogenic Cell Death of Pancreatic Cancer Cells. *Cancers* 2019, 11 (10): 2072-6694

Abstract

Pancreatic ductal adenocarcinoma (PDAC) is one of the most aggressive cancers with a low response to treatment and a five-year survival rate below 5%. The ineffectiveness of treatment is partly because of an immunosuppressive tumor microenvironment (TME), which comprises tumor-supportive pancreatic stellate cells (PSCs). Therefore, new therapeutic strategies are needed to tackle both the immunosuppressive PSCs and pancreatic cancer cells (PCCs). Recently, physical cold atmospheric plasma consisting of reactive oxygen and nitrogen species has emerged as a novel treatment option for cancer. In this chapter, we investigated the cytotoxicity of plasma-treated phosphate-buffered saline (pPBS) using three PSC lines and four PCC lines and examined the immunogenicity of the induced cell death. We observed a decrease in the viability of PSCs and PCCs after pPBS treatment, with a higher efficacy in the latter. Two PCC lines expressed and released damage-associated molecular patterns characteristic of the induction of immunogenic cell death (ICD). In addition, pPBS-treated PCCs were highly phagocytosed by dendritic cells (DCs), resulting in the maturation of DC. This indicates the high potential of pPBS to trigger ICD. In contrast, pPBS induced no ICD in PSC. In general, pPBS treatment of PCCs and PSCs created a more immunostimulatory secretion profile (higher TNF- α and IFN- γ , lower TGF- β) in coculture with DC. Altogether, these data show that plasma treatment via pPBS has the potential to induce ICD in PCCs and to reduce the immunosuppressive TME created by PSCs. Therefore, these data provide a strong experimental basis for further *in vivo* validation, which might potentially open the way for more successful combination strategies with immunotherapy for PDAC.

Introduction

Pancreatic ductal adenocarcinoma (PDAC) is a devastating disease with a five-year survival below 5% making it one of the seven leading causes of cancer mortality in the world (1-4). Given its rising incidence, it is estimated that by 2030, PDAC will be among the top two most lethal cancers (5). Only 10-20% of patients are eligible for curative surgical resection due to the rapidly progressive nature of the tumor and even with adjuvant chemotherapy, the median survival rate is only 20-23 months (1, 2). The only therapeutic options for the remaining 80-90% of patients are limited to chemo- and radiotherapy, which have minimal efficacy because of therapy resistance (3).

Although immunotherapy is considered to be a major breakthrough in cancer treatment, it has not yet achieved promising outcomes in PDAC. The ineffectiveness of immunotherapy may be explained by these tumors being non-immunogenic (6-9). The immunosuppressive tumor microenvironment (TME) is believed to be a major underlying factor for immunotherapy failure. A hallmark of this TME is a desmoplastic reaction, which results in a dense fibrotic/desmoplastic structure surrounding the tumor. This dense stroma acts as a mechanical and functional shield, causing diminished delivery of systemically administered anticancer agents and immune cell infiltration, as a consequence of intratumoral pressure and low microvascular density, which results in therapy resistance (10-13). The main orchestrators of this stromal shield are the activated pancreatic stellate cells (PSCs). These myofibroblast-like cells, also known as cancer-associated fibroblasts, enhance the development, progression, and invasion of PDAC through extensive crosstalk with pancreatic cancer cells (PCCs), resulting in reciprocal stimulation. Furthermore, PSCs also directly influence immune cells by secreting immunosuppressive factors, like TGF- β (12, 14). Therefore, new treatment options that could overcome this stromal shield and consequently increase tumor immunogenicity in PDAC are necessary.

One way to enhance immunogenicity is by inducing immunogenic cell death (ICD), a form of cell death, which causes these dying cells to elicit an antitumor immune response (15). Cancer cells undergoing ICD expose proteins on their surface and release immunogenic factors, so called 'damage-associated molecular patterns' (DAMPs). Classically, there are three well-known DAMPs related to ICD. The first is surface-exposed calreticulin (ecto-

CRT) which serves as an ‘eat me’-signal. This marks tumor cells for engulfment by dendritic cells (DCs), which are professional antigen-presenting cells (16). The second DAMP is adenosine triphosphate (ATP) secreted into the extracellular environment, serving as a chemoattractant for immune cells (17). The third DAMP is high-mobility group box 1 (HMGB1) released into the extracellular milieu, which contributes to DC maturation (18, 19). Conversely, ICD is usually also accompanied by downregulation of the ‘don’t eat me’ signal CD47, which can inhibit phagocytosis of dying cancer cells (20). Altogether, these signals stimulate DCs, key players for initiating an adaptive immune response. Activated DCs will lead to the development and activation of effector T cells, capable of specifically and systemically eradicating cancer cells, and of memory T cells, which provide long-term protection against cancer recurrence (21).

Several physical methods of cancer treatment, including radiotherapy, photodynamic therapy, and high hydrostatic pressure are known inducers of ICD (22-25). The induction of oxidative stress through the production of reactive oxygen species (ROS) is the common underlying factor of these therapies. In recent years, cold atmospheric plasma (CAP), which is a partially ionized gas consisting of a variety of reactive oxygen and nitrogen species (RONS), has emerged as a novel cancer treatment (26, 27). For simplicity, CAP will be further referred to as ‘plasma’ in this chapter. These RONS can be delivered directly to the tumor or indirectly through plasma-treated liquids (27). Several studies have attributed the plasma-induced cancer cell death to the formation of exogenous and endogenous RONS, which lead to intracellular stress and ultimately cell death (27-30). Therefore, we hypothesized that plasma could also be a potent inducer of ICD.

The aim of the present study is to evaluate the potency of plasma-treated phosphate-buffered saline (pPBS) as an anticancer modality to tackle PCCs and the immunosuppressive PSCs. Therefore, we evaluated the cytotoxic effect of pPBS treatment on both PCCs and the tumor-supportive PSCs. Additionally, we examined the immunogenicity of this cytotoxic effect on PCCs and PSCs based on the release of ICD markers and activation of DCs.

Materials and methods

Cell lines and cell culture

The human PCC lines MIA-Paca-2, PANC-1, BxPC3 and Capan-2 (ATCC) were used in this study. MIA-Paca-2 and PANC-1 cells were cultured in Dulbecco's Modified Eagle Medium (DMEM; Life Technologies, 10938, Merelbeke, Belgium) supplemented with 10% fetal bovine serum (FBS, Life Technologies, 10270-106), 1% penicillin/streptomycin (Life Technologies, 15140, Merelbeke, Belgium) and 2mM L-glutamine (Life Technologies, 25030). Capan-2 and BxPC3 cells were cultured in Roswell Park Memorial Institute (RPMI) 1640 medium (Life Technologies, 52400) supplemented as described above. The human PSC lines hPSC21, hPSC128 (established at Tohoku University, Graduate School of Medicine, kindly provided by Prof. Atsushi Masamune) and RLT-PSC (established at the Faculty of Medicine of the University of Mannheim, kindly provided by Prof. Ralf Jesenofsky) were used, all cultured in DMEM-F12 (Life Technologies, 31330) supplemented as described above (31, 32). Cells were maintained in exponential growth phase at 5% CO₂ in a humidified incubator at 37°C. Cell cultures were regularly tested for absence of mycoplasma contamination using the MycoAlert detection kit (Lonza, LT07, Verviers, Belgium).

Treatment of PCCs and PSCs with cold atmospheric plasma

Cells (2×10^4 cells per mL) were treated indirectly with cold atmospheric plasma generated using the atmospheric pressure plasma jet kINPenIND® (Neoplas Tools). Argon gas is used in this setting as feeding gas (33). Two mL of PBS were treated with 1 standard liter per minute (slm) gas flow rate at a gap distance of 6mm for 5min. This 100% plasma-treated PBS (pPBS) was further diluted in PBS to final concentrations of 12.5% - 25% - 37.5% - 50% - 62.5% pPBS, which was then directly added in a 1/6 dilution in the media to the cells. Untreated PBS is used as a vehicle control for all experiments.

Analysis of cytotoxicity and ICD markers

Forty-eight hours after treatment, cells were harvested and incubated with 5% normal goat serum (NGS, Sigma-Aldrich, G9023, Overijse, Belgium), followed by washing and incubation with an Alexa Fluor 488-conjugated anti-CRT (Abcam, ab196158) antibody for 40 min. Prior to analyzing the samples, the cells were stained with Annexin V (BD, 550474)

and PI (BD, 556463) to distinguish between early apoptotic and necrotic cells. Percentage of cytotoxicity presents [%AnnV+PI- + %AnnV-PI+ + %AnnV+PI+]. Surface expression of CRT was analyzed on non-permeabilized cells (PI-). For every sample, an isotype control was used (Abcam, 199091). Flow cytometric acquisition was performed on an Accuri™ C6 instrument (BD). Extracellular ATP was measured in conditioned media (supplemented with heat inactivated FBS) 4h after treatment via ENLITEN® ATP assay system, according to the manufacturer's protocol (Promega, FF2000). The bioluminescent signal was measured using a VICTOR™ plate reader (PerkinElmer). Release of HMGB1 was analyzed 48h after treatment in the conditioned media using an enzyme-linked immunosorbent assay (IBL, ST51011). The absorption was measured using an iMARK™ plate reader (Bio-rad). Surface expression of CD47 (BD, 556046) was analyzed on non-permeabilized cells (7-AAD-, Biolegend, 420404), 48h after treatment. Flow cytometric acquisition was performed on a CytoFLEX (Beckman Coulter) instrument.

In vitro generation of human monocyte-derived DCs

Human peripheral blood mononuclear cells (PBMC) were isolated by LymphoPrep gradient separation (Sanbio, 1114547) from a buffy coat of healthy donors (Ethics Committee of the University of Antwerp, reference number 14/47/480) isolated from adult volunteer whole blood donations (supplied by the Red Cross Flanders Blood service, Belgium). Monocytes were isolated from PBMC using CD14 microbeads according to the manufacturer's protocol (Miltenyi, Biotec, 272-01). Purity after isolation was >90%. After isolation, CD14+ cells were plated at a density of 1.25-1.35 x 10⁶ cells per mL in RPMI-1640 supplemented with 2.5% human AB (hAB, Sanbio, A25761) serum, 800 U/ml granulocyte-macrophage colony stimulating factor (GM-CSF; Gentaur, 04-RHUGM-CSF) and 20 ng/ml interleukin (IL)-4 (Miltenyi, Biotec, 130-094-117) at day 0, as described before (34). Immature DCs were harvested on day 5.

Coculture of DCs and tumor cells

In order to measure the maturation and phagocytotic capacity of the immature DCs, a flow cytometric assay was used. To make a distinction between target and effector cells, they were both stained with a different fluorescent dye prior to coculturing. Labeling of immature DCs was performed as described before with minor adjustments (35). Briefly, immature DCs were labeled with 2 μM of violet-fluorescent CellTracker Violet BMQC dye

(Invitrogen, C10094, Bleiswijk, Netherlands) at a concentration of 1×10^6 cells per mL at 37°C. PCCs and PSCs were labeled with the green fluorescent membrane dye PKH67 (Sigma Aldrich, MIDI67). Labeling of tumor cells with PKH67 was carried out according to the manufacturer's instructions and performed before pPBS treatment. Four hours after pPBS treatment, effector and target cells were cocultured at a 1:1 effector:target (E:T) ratio. Forty-eight hours later, supernatant was collected and stored at -20°C for future analysis. Cells were collected and used immediately for flowcytometric detection of DC maturation markers and phagocytosis. Expression of CD80 (Biolegend, 400150, , San Diego, California, USA), CD86 (BD, 557872) and CD83 (BD, 551073) maturation markers was measured on the violet+ DC population. For every specific maturation marker an isotype control was used (BD, 555751; BD, 557872; Biolegend, 305232). Difference in mean fluorescence intensity (Δ MFI) was calculated to evaluate target upregulation after treatment. Δ MFI represents [(MFI staining treated – MFI isotype treated) – (MFI staining untreated – MFI isotype untreated)]. Phagocytosis of PKH67+ tumor cells by violet-labeled DCs was expressed as %PKH67+violet+ cells within the violet+ DC population. Acquisition was performed on a FACSAria II (BD). Data analysis was performed using FlowJo v10.1 software (TreeStar).

Cytokine secretion profile

Secreted cytokines in cocultures of pPBS-treated target cells and immature DCs were analyzed using electrochemiluminescence detection on a SECTOR3000 (MesoScale Discovery/MSD) using Discovery Workbench 4.0 software, as previously described (36). The human cytokine panel included IFN- γ , TNF- α and TGF- β . Standards and samples were measured in duplicate and the assay was performed according to the manufacturer's instructions.

Statistical analysis

Prism 8.02 software (GraphPad) was used for data comparison and graphical data representations. SPSS Statistics 25 software (IBM) was used for statistical computations. Non-parametric Kruskal-Wallis test was used to compare means between more than two groups. Nonparametric Mann-Whitney U test was used to compare means between two groups. Spearman's rank correlation coefficient was used to calculate the correlation between two variables. P-values <0.05 were considered statistically significant.

Results

pPBS induces cell death in both PCCs and PSCs

In order to initially determine a dose of pPBS treatment, which induces a significant amount of cell death in each cell line, we treated PCC and PSC lines with several dilutions of pPBS (25%, 37.5%, 50%, and 62.5%). After 48 h of treatment, we analyzed cell death with Annexin V (AnnV) and propidium iodide (PI) flow cytometric staining. All cell lines demonstrated a dose-dependent increase in AnnV-/PI+, AnnV+/PI+, and AnnV+/PI- cells, with a corresponding decrease in viable AnnV-/PI- cells (Figure 3.1 A, B and Figure 3.2). MIA-Paca-2 cells were most sensitive to the treatment, followed by Capan-2. Therefore, these two cell lines were treated with the lowest concentration of pPBS for subsequent experiments compared with all other cell lines. Overall, PSC lines were significantly less sensitive to pPBS treatment compared with PCC lines (Figure 3.1 C).

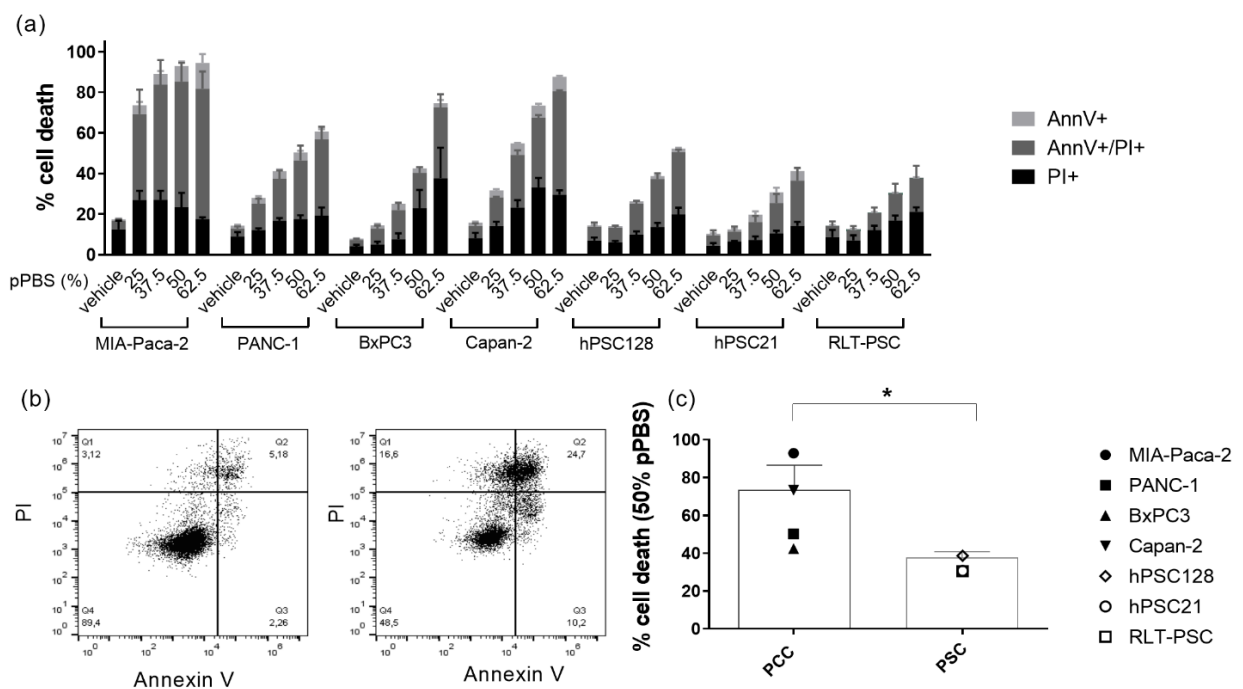


Figure 3.1. Sensitivity of pancreatic cancer cell (PCC) lines and pancreatic stellate cell (PSC) lines to different doses of plasma-treated phosphate-buffered saline (pPBS) treatment. (a) Percentage of cytotoxicity 48 h post pPBS treatment in four different PCC lines (MIA-Paca-2, PANC-1, BxPC3, Capan-2) and three different PSC lines (hPSC128, hPSC21, RLT-PSC). Subdivisions in the percentage Annexin V+, PI+, and double positive cytotoxic cells are made. (b) Dot plots showing the flow cytometric analysis of Annexin V and PI staining after 25% pPBS treatment in MIA-Paca-2 (right) compared with the untreated control (left): Q1 = AnnV-/PI+; Q2 = AnnV+/PI+; Q3 = AnnV-/PI-; Q4 = AnnV+/PI-. Representative dot plots for all other cell lines are presented in Figure 3.2. (c) The difference in sensitivity after 48 h of 50% pPBS treatment for means of all PCC lines and all PSC lines. Graphs represent mean \pm SEM of ≥ 3 independent experiments. * $p < 0.05$.

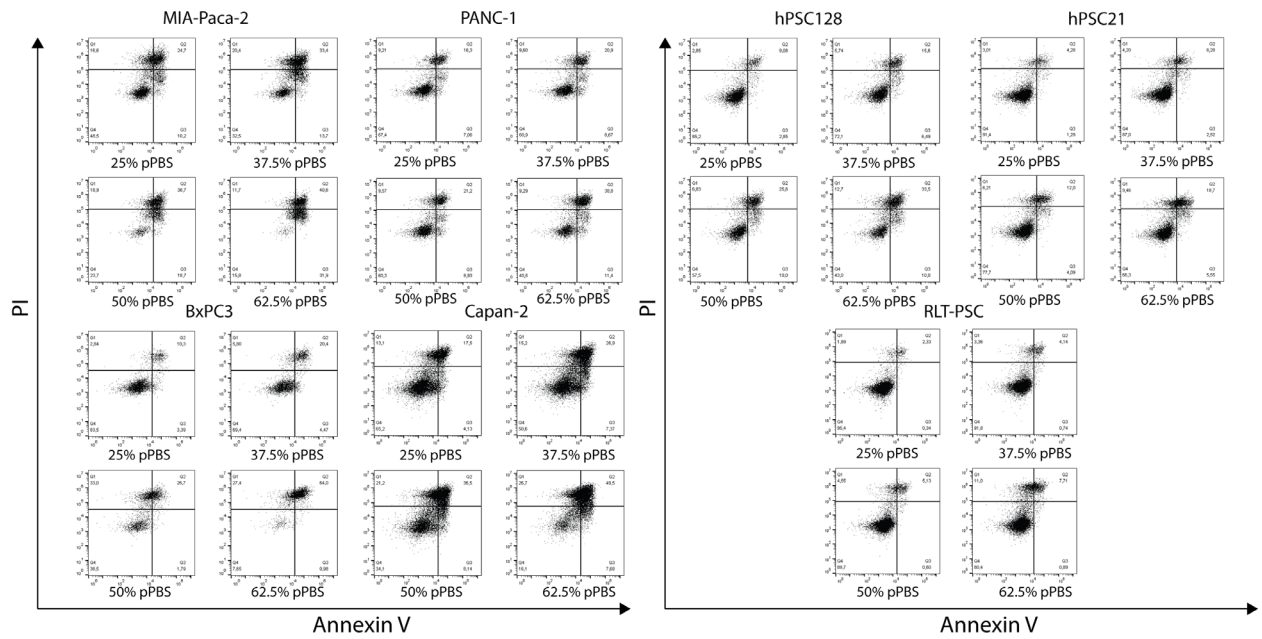


Figure 3.2. Dot plots Annexin V and PI staining. Dot plots showing the flow cytometric analysis of Annexin V and PI staining after 25%, 37.5%, 50% and 62.5% pPBS treatment in all PCC lines (left) en all PSC lines (right). Q1 = AnnV-/PI+; Q2 = AnnV+/PI+; Q3 = AnnV-/PI-; Q4 = AnnV+/PI-.

pPBS induces ICD markers on PCCs

Because therapy-induced tumor ICD is an important component to activate antitumor immunity, we investigated whether pPBS induces ICD in PCC and PSC lines. To this end, we measured the surface exposure of CRT as well as secretion of ATP and release of HMGB1 into the supernatant.

We observed a dose-dependent translocation of ecto-CRT in all PCC and two PSC lines after 48 h of pPBS treatment (Figure 3.3 A, Figure 3.4). A strong translocation was detected for MIA-Paca-2 and Capan-2 cells with a mean of 20.1% and 10.5% ecto-CRT+ cells, respectively. Less pronounced, but still significant effects on the translocation were observed for PANC-1, BxPC3, hPSC128, and hPSC21 cells. Here, even the highest concentration of pPBS exposed not more than 7.5% ecto-CRT on the cell surface. No difference in ecto-CRT was observed for RLT-PSC cells.

Next, we measured extracellular ATP levels 4 h after pPBS treatment (Figure 3.3 B). For two PCC lines, MIA-Paca-2 and PANC-1, accumulation of extracellular ATP up to five-fold from the untreated control was observed. Similar to ecto-CRT, the trend of secretion was dose-dependent. No significant accumulation was seen for the other cell lines.

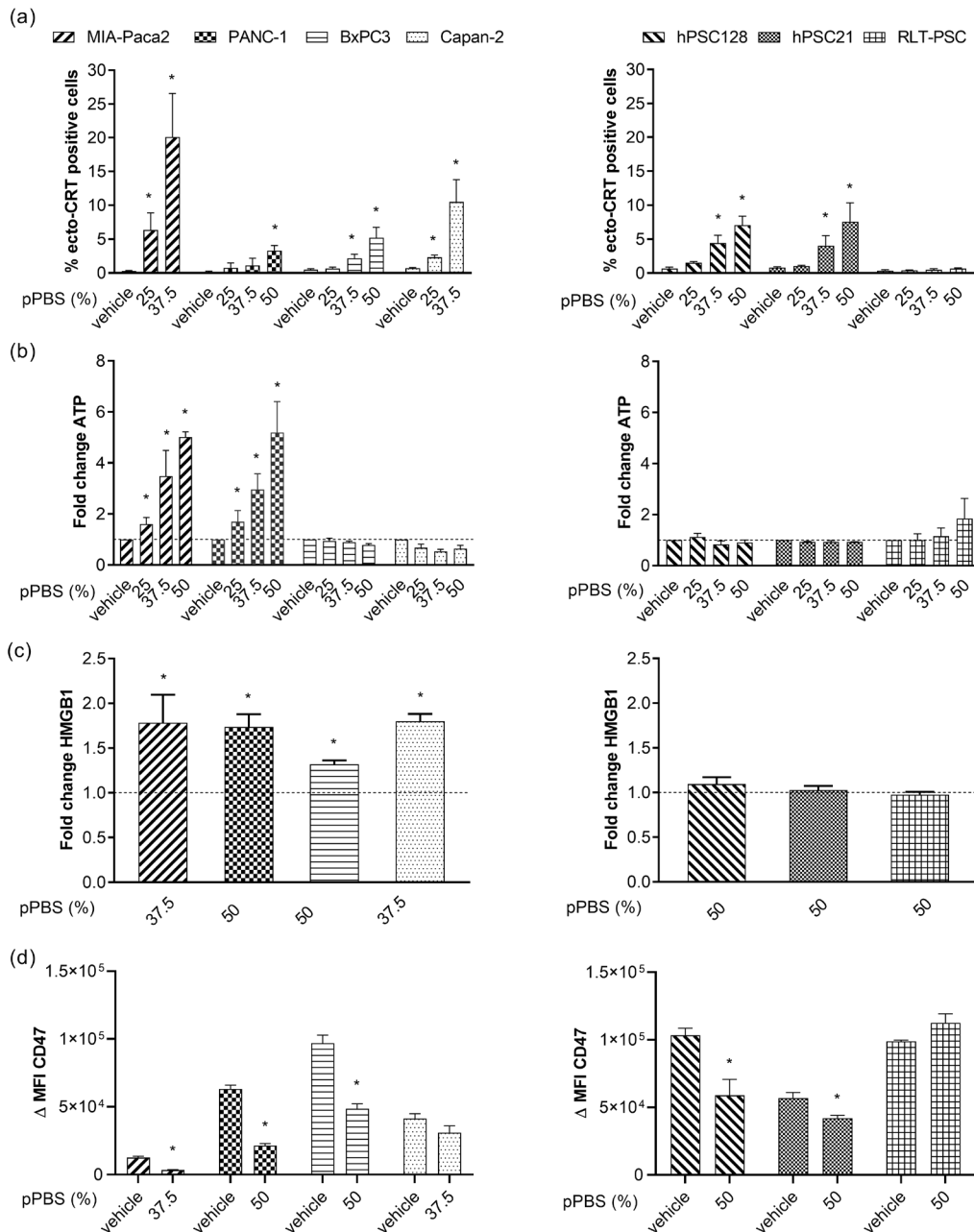


Figure 3.3. Release of immunogenic cell death (ICD) markers after pPBS treatment. (a) Percentage of surface-exposed calreticulin (ecto-CRT) positive cells after increasing the dose of pPBS treatment (25%, 37.5%, 50% pPBS). (b) Adenosine triphosphate (ATP) secretion 4 h post treatment in the supernatant. (c) High-mobility group box 1 (HMGB1) secretion 48 h post pPBS treatment in supernatant. These data demonstrate the fold change of ATP secretion (ng/mL range) against the untreated control. (d) Difference in mean fluorescence intensity (Δ MFI) of CD47 after 48 h of pPBS treatment. Δ MFI represents [(MFI staining treated – MFI isotype treated) – (MFI staining untreated – MFI isotype untreated)]. Different concentrations of pPBS treatment are used (25%, 37.5%, 50% pPBS). In the left graphs, four different PCC lines are represented (MIA-Paca-2, PANC-1, BxPC3, Capan-2), and in the right graphs, three different PSC lines are represented (hPSC128, hPSC21, RLT-PSC). Graphs represent mean \pm SEM of ≥ 3 independent experiments. * $p < 0.05$ significant difference compared with untreated conditions.

On the basis of our previous cytotoxicity results, we chose one specific dose for every cell line to evaluate HMGB1 release. As indicated above, MIA-Paca-2 and Capan-2 were the most sensitive cell lines, and thus received a dose of 37.5% pPBS, as opposed to 50% pPBS for the other cell lines. pPBS treatment induced significant release of HMGB1 in all PCC lines, with a 1.32- to 1.79-fold increase compared with the untreated control. Interestingly, no significant release was detected in the PSC lines (Figure 3.3 C). Additionally, we observed a significant downregulation of CD47 expression in all cell lines after pPBS treatment, except for Capan-2 and RLT-PSC (Figure 3.3 D).

Collectively, our results show that plasma treatment via pPBS application is able to induce events that are characteristic of ICD in PCCs. Importantly, pPBS-induced cell death in the PSC lines appears to be non-immunogenic owing to the absence of most DAMPs. For both MIA-Paca-2 and PANC-1, all four markers of ICD were significantly detected after pPBS treatment. The quantity of the examined markers was both dose and cell line dependent.

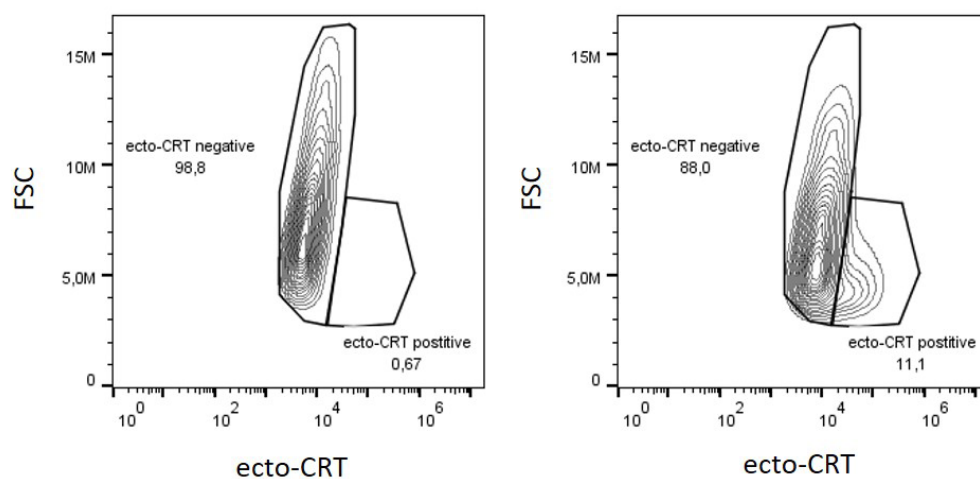


Figure 3.4. Gating strategy of surface exposure of ecto-CRT. Contour plots showing the flow cytometric analysis of ecto-CRT staining after 48h of 50% pPBS treatment (left) compared to untreated condition (right) in the BxPC3 cell line (PI- cells) showing the differences in Δ MFI (MFI treated vs MFI untreated).

pPBS-treated cells are phagocytosed by DCs

In view of the role of ecto-CRT as an ‘eat-me’ signal, we investigated the influence of pPBS-treated PCCs and PSCs on the phagocytotic capacity by immature DCs. Flow cytometric analysis revealed that pPBS-treated MIA-Paca-2, Capan-2, hPSC128, and hPSC21 were phagocytosed by immature DCs more efficiently than their untreated counterparts (Figure 3.5 A, B, Figure 3.6). This phagocytotic capacity by DCs was significantly correlated ($R =$

0.786, $p = 0.036$) with the exposure of ecto-CRT on the cell surface of the cell lines after pPBS treatment (Figure 3.5 C).

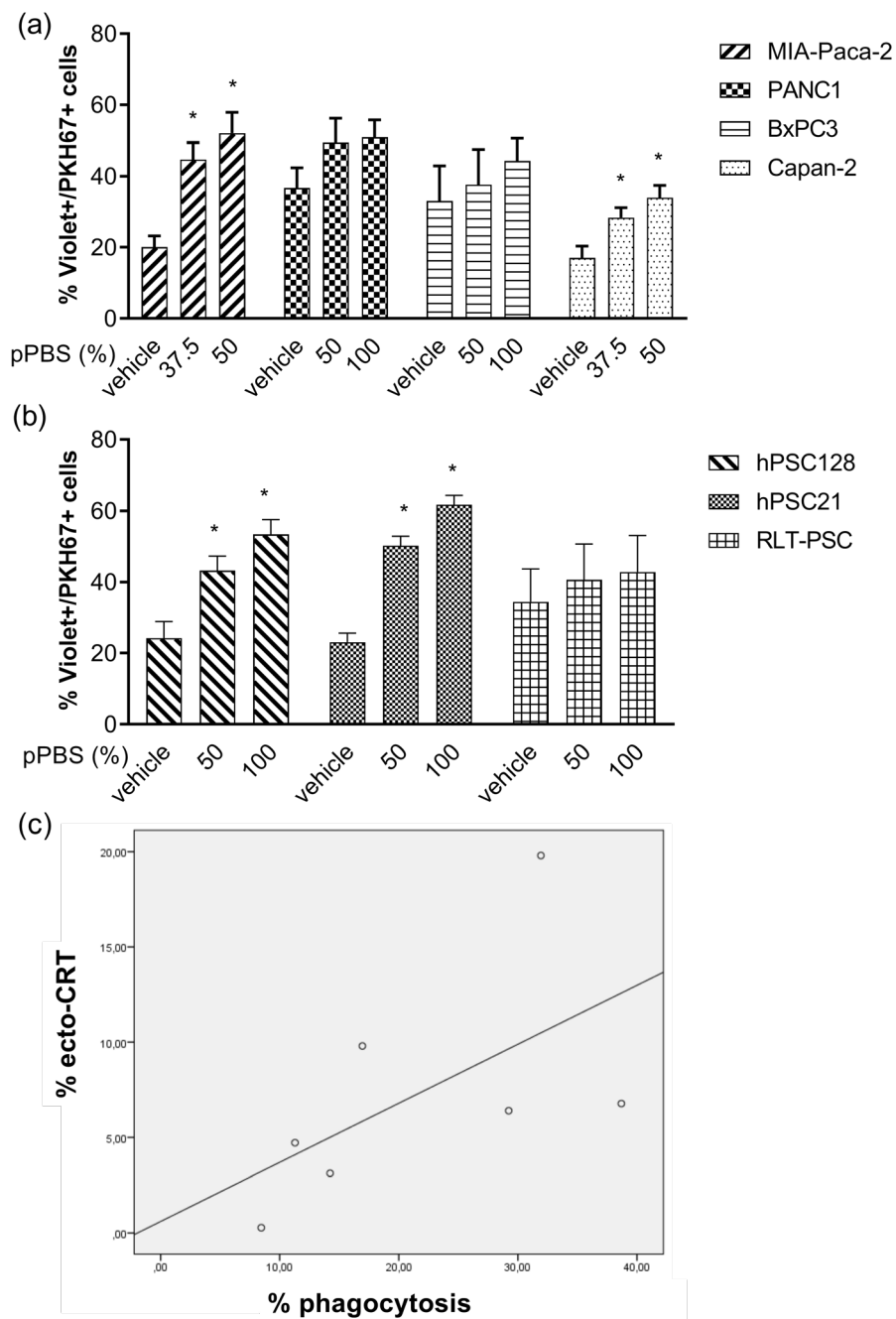


Figure 3.5. Phagocytosis of pPBS-treated PCCs and PSCs by immature dendritic cells (DCs). (a) Percentage of phagocytosis of four different PCC lines (MIA-Paca-2, PANC-1, BxPC3, Capan-2) and (b) three different PSC lines (hPSC128, hPSC21, RLT-PSC), with increasing dosage of pPBS treatment. Phagocytosis of PKH67+ tumor cells by violet-labeled DCs is expressed as the %PKH67+violet+ cells within the violet+ DC population. (c) Correlation between exposure of ecto-CRT and phagocytotic capacity of DCs in the seven cell lines ($R = 0.786$, $p = 0.036$). Graphs represent mean \pm SEM of ≥ 3 independent experiments. * $p < 0.05$ significant differences compared with untreated control.

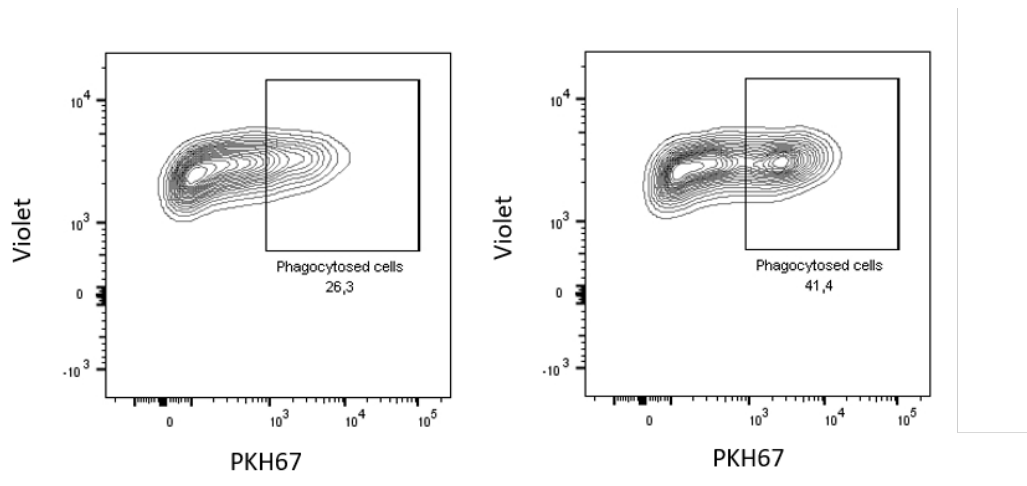


Figure 3.6. Gating strategy of phagocytosis. Contour plots showing flow cytometric analysis of percentage phagocytosis (left: MIA-Paca-2, untreated; right: MIA-Paca-2, 50% pPBS treatment). Target cells labelled with PKH67 dye and DCs labeled with CellTracker Violet BMQC dye are cocultured for 48h (E:T ratio, 1:1). Phagocytosis of the PKH67+ target cells by violet labeled DCs is expressed as the %violet+PKH67+ cells within the violet+ DC population.

pPBS treatment of PCCs increases maturation of DCs without affecting their viability

In order to initiate an effective adaptive immune response, the expression and release of DAMPs by dying tumor cells must be followed by DC phagocytosis and DC activation. The ability of DCs to initiate such an immune response depends on their maturation status upon activation. Therefore, we analyzed three different maturation markers on the cell surface of DCs: CD80, CD83, and CD86. There was a clear donor-dependent upregulation of CD86 on viable DCs after coculturing with pPBS-treated target cells (Figure 3.7 A). This variability was detected both between the cell lines and between DCs from different blood donors cultured with the same cell line. However, using DCs from different donors in coculture with pPBS-treated MIA-Paca-2 and PANC-1 cells, there was a consistent and significant upregulation of CD86. The effect was less pronounced or undetectable for CD83 and CD80 maturation markers in all cell lines (Figure 3.8 A, B). Notably, pPBS treatment of DCs alone without target cells had no significant effect on the maturation status, meaning that the observed maturation effect was the result of tumor cells dying in an immunogenic way. Furthermore, we also checked the viability of the DCs in coculture. We could not detect any significant differences in DC viability after 48 h of coculture with pPBS-treated cells compared with coculture with untreated target cells. Addition of pPBS

to monocultures of DCs also showed no significant differences in viability compared with their untreated counterparts (Figure 3.7 B).

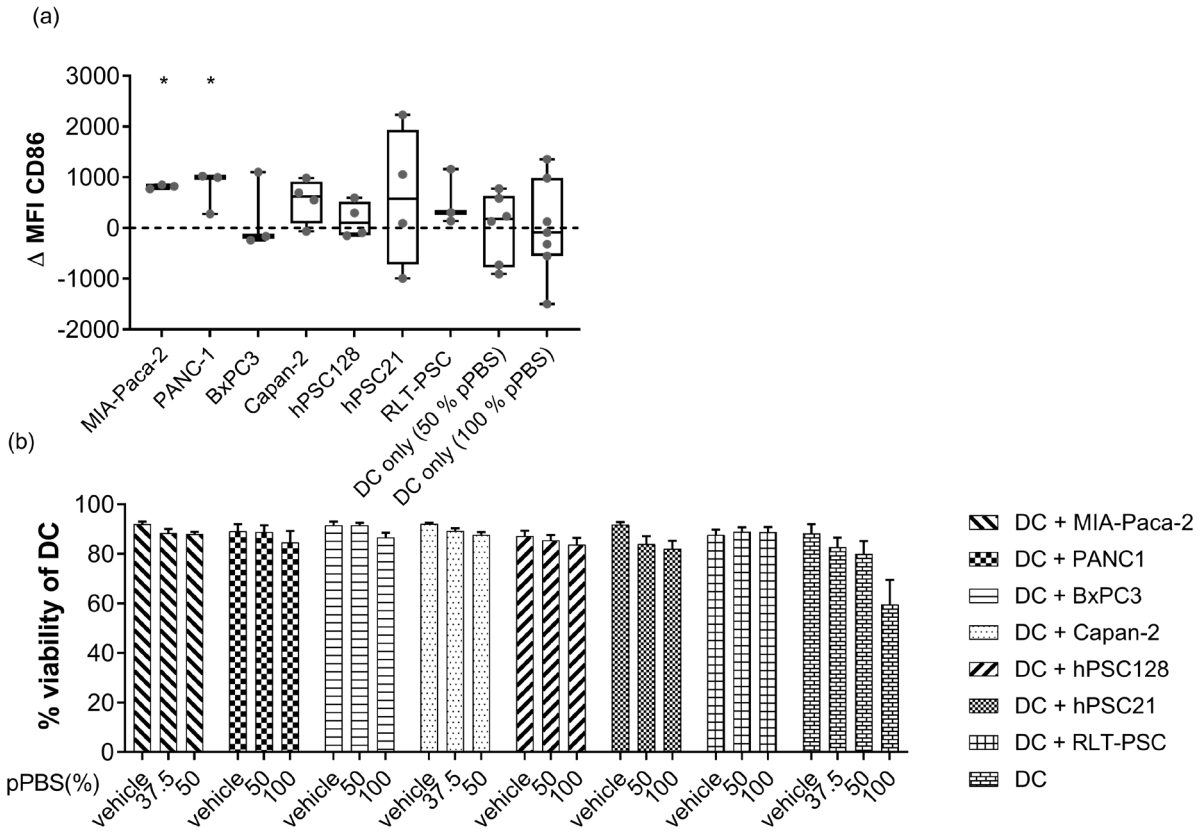


Figure 3.7. Maturation and viability of DCs after coculture with pPBS-treated PSCs and PCCs. (a) Box plot from minimum to maximum value of Δ MFI of the maturation marker CD86. CD86 expression is examined on immature DCs after 48 h of coculture of pPBS-treated PCCs and PSCs (effector/target (E/T) ratio, 1:1), and after pPBS treatment on immature DCs without coculture using flow cytometry. Δ MFI represents [(MFI staining treated – MFI isotype treated) – (MFI staining untreated – MFI isotype untreated)]. Treatment of 50% pPBS is used for MIA-Paca-2 and Capan-2, while treatment of 100% pPBS is used for PANC-1, BxPC3, hPSC128, hPSC21, and RLT-PSC. Every dot represents a different healthy donor and ≥ 3 donors were used per cell line. * $p < 0.05$ significant differences compared with untreated control. (b) Percentage of viability of DCs after 48 h coculture with pPBS-treated PCC lines (MIA-Paca-2, PANC-1, BxPC3, Capan-2) and PSC lines (hPSC128, hPSC21, RLT-PSC) or pPBS treatment alone. Graph represent mean of \pm SEM of ≥ 3 independent experiments with different donors. * $p < 0.05$ significant differences compared with untreated control.

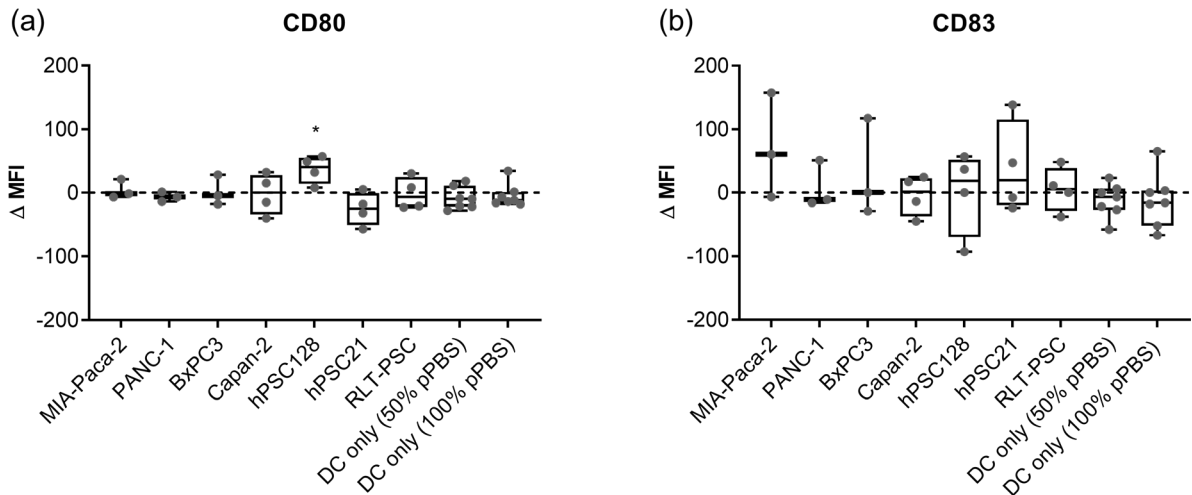


Figure 3.8. CD80 and CD83 expression on DCs after coculture with pPBS-treated PSCs and PCCs. (a) Boxplot from minimum to maximum value of Δ MFI of the maturation marker CD80. (b) Boxplot from minimum to maximum value of Δ MFI of the maturation marker CD83. CD80 and CD83 expression is examined on immature DCs after 48h of coculture of pPBS-treated PCCs and PSCs (E:T ratio, 1:1) and after pPBS treatment on immature DCs without coculture using flow cytometry. Δ MFI represents [(MFI staining treated – MFI isotype treated) – (MFI staining untreated – MFI isotype untreated)]. Treatment of 50% pPBS is used for MIA-Paca-2 and Capan-2, treatment of 100% pPBS is used for PANC-1, BxPC3, hPSC128, hPSC21 and RLT-PSC. Every dot represents a different healthy donor with ≥ 3 donors used per cell line. $p < 0.05$ significant differences compared to untreated control (*).

Secretion of cytokines after pPBS treatment

Mostly, maturation of DCs is associated with an increase in the production of proinflammatory cytokines. Therefore, we evaluated the cytokine production of TNF- α and IFN- γ by DCs in coculture with pPBS-treated PCCs and PSCs, which are both central players in the process of DC maturation and antitumoral immune responses. The interaction between DCs and pPBS-treated PCCs or PSCs induced the release of IFN- γ and TNF- α (Figure 3.9 A, B). The release of both cytokines was significant for MIA-Paca-2 and PANC-1. In BxPC3 and Capan-2 cells, IFN- γ release was also significantly increased. In addition to these proinflammatory cytokines, we evaluated a well-characterized immunosuppressive cytokine, TGF- β , which is often released in the TME (37). We observed a decrease in TGF- β release when DCs were cocultured with pPBS-treated BxPC3, hPSC128, and hPSC21 cells compared with cocultures with the untreated counterparts (Figure 3.9 C).

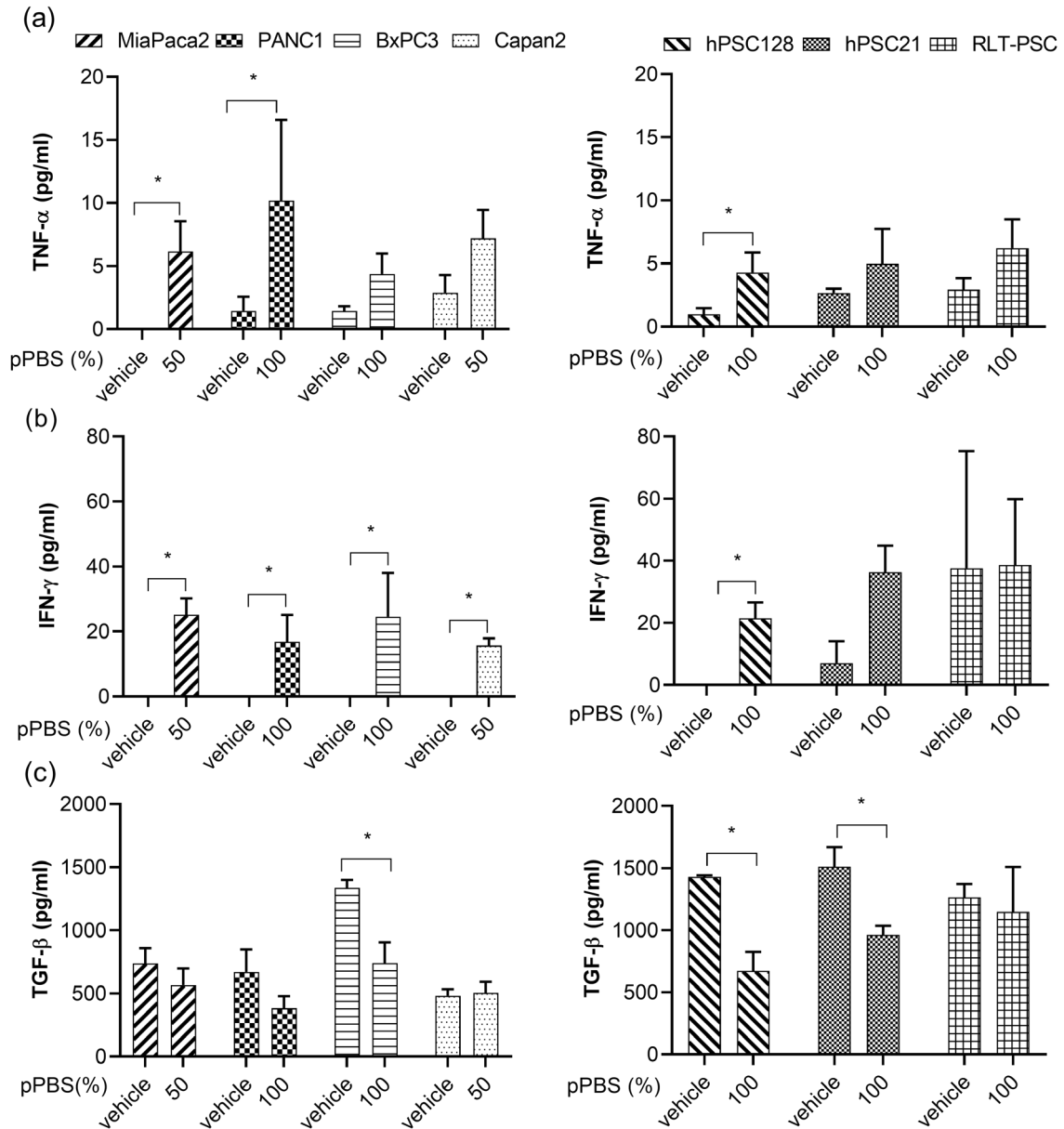


Figure 3.9. Cytokine profile released by DCs in coculture with pPBS-treated PCCs and PSCs. Graphs show the concentration of TNF- α (a), IFN- γ (b), and TGF- β (c) released in coculture of DCs with pPBS-treated PCCs (left) and PSCs (right) after 48 h. Graphs represent mean of \pm SEM of ≥ 3 independent experiments with different donors. * $p < 0.05$ significant differences compared with untreated control.

Discussion

The purpose of this study was to investigate the ability of plasma treatment via pPBS to create a more immunogenic TME for PDAC by attacking both PSCs and PCCs and inducing ICD in PCCs. Figure 3.10 gives an overview of the immunogenic signals tested after pPBS treatment in four different PCC lines and three different PSC lines.

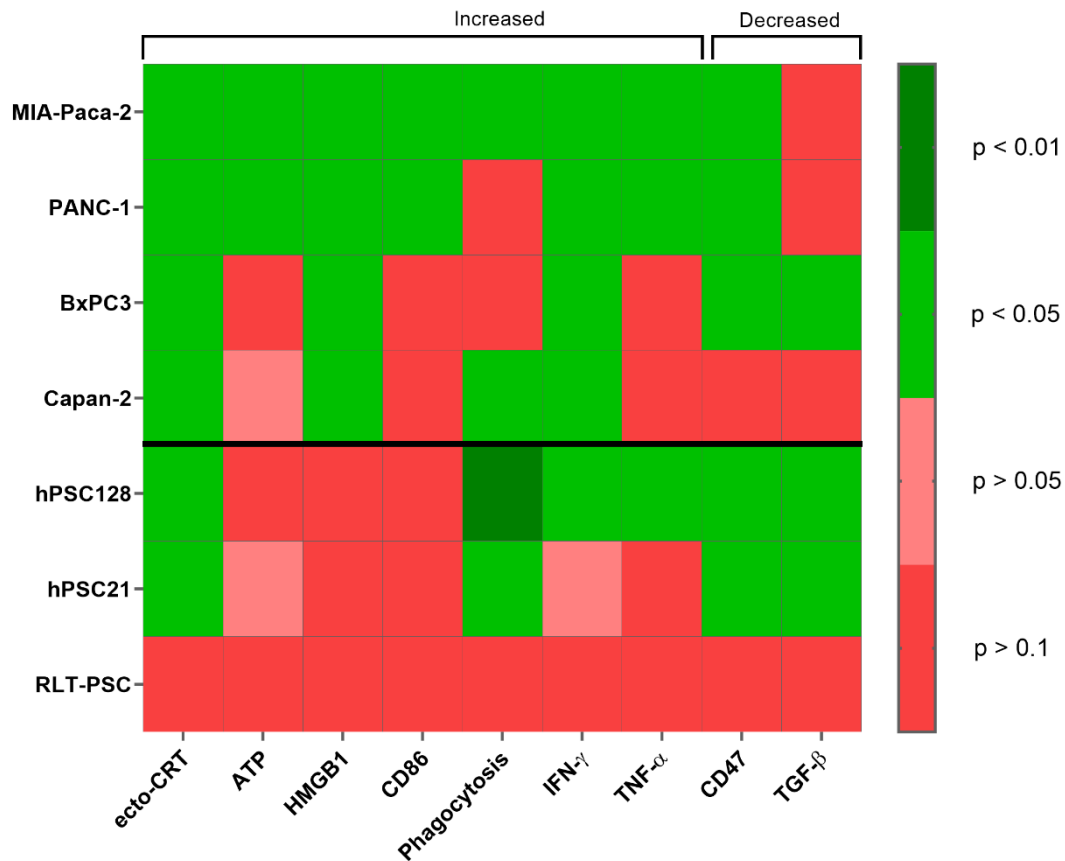


Figure 3.10. Overview of the p -values for all immunogenic signals tested. p -values are represented in a heatmap for the signals tested in previous experiments for both PCCs and PSCs. p -values are calculated using the Kruskal–Wallis or Mann–Whitney U test and are significant when <0.05 . Treated conditions for ecto-CRT, ATP, HMGB1, CD86, phagocytosis, IFN- γ , and TNF- α are significantly increased compared with untreated controls. Treated conditions for CD47 and TGF- β are significantly decreased compared with untreated control.

PDAC is known to have a low immunogenic TME profile and is often referred to as a ‘cold’ immunogenic tumor (38). Because of its low immunogenicity, immunotherapy frequently fails in this type of tumors (6, 7, 39). The dense stroma consisting of PSCs surrounding the tumor is believed to be a major underlying factor involved in failure of immunotherapy by acting as a physical barrier for drugs and immune cells (12, 13).

Additionally, PSCs secrete immunosuppressive factors, which prevent development of effective immune responses (14). Several studies showed that stromal depletion combined with immunomodulation resulted in better outcomes than immunomodulation alone in PDAC (40, 41). Therefore, we postulated that tumors can become immunogenically 'hotter' by destroying the tumor supporting PSCs with pPBS treatment.

Although the cytotoxic effect of plasma has already been investigated in PCC lines (28, 29, 42, 43) and a PSC line (43), we demonstrated the first use of pPBS to target the immunosuppressive PSCs in PDAC and investigated its immunogenic potential. Treatment with pPBS induced non-immunogenic cell death in PSC, as seen by the lack of DAMP emission, except for ecto-CRT and CD47 expression, and no significant DC maturation. This is in-line with the report of Gorchs et al., showing that cancer-associated fibroblasts in the lung do not undergo ICD after exposure to high dose radiotherapy (44). Interestingly, secretion of the immunosuppressive TGF- β decreased in cocultures of DCs with pPBS-treated PSC lines, compared to their untreated counterparts. TGF- β plays a major role in immunosuppression within the TME and is often strongly secreted by PSCs (45). TGF- β is responsible for preventing immune cell infiltration into tumor tissue and promoting tumor cell proliferation (37, 46, 47). Therefore, several ongoing efforts in this field are aimed at blocking TGF- β in the stroma in combination with anti-programmed death (PD)-1 immunotherapy for the treatment of different cancer types, including pancreatic cancer (37). Similarly, we showed that pPBS treatment could kill PSCs and thereby disrupt the physical barrier, and additionally lower their immunosuppressive capacity. These findings show that plasma treatment can be beneficial in combination with immunotherapy for PDAC treatment.

PCCs were intrinsically more sensitive to pPBS treatment compared to PSC. The delicate redox balance in PCCs may contribute to this observation. Cancer cells are characterized by increased production of ROS compared to normal cells, which promotes their tumorigenicity. This altered redox environment can increase their susceptibility to ROS-promoting therapies like pPBS by disturbing ROS homeostasis, resulting in lethal ROS levels and ultimately cancer cell death (48). Furthermore, in contrast to PSCs, four signals, which play a key role in the immunogenic potential of ICD inducers, were identified after pPBS treatment in both MIA-Paca-2 and PANC-1 tumor cells. Both Lin et al. and Freund

et al. showed similar release of DAMPs by plasma treatment using different human and murine cancer cell lines (49-52). Recently, Azzariti et al. also showed an increase of ecto-CRT and ATP in PANC-1 (53). Our study is the first to evaluate phagocytosis of plasma-treated cancer cells by DCs and DC maturation, which are both needed to confirm the immunogenic profile of tumor cells (54, 55). Phagocytosis of cancer cells by DCs improved after pPBS treatment in all PCC lines and consistent upregulation of the maturation-associated marker CD86 on DCs was observed in cocultures with pPBS-treated MIA-Paca-2 and PANC-1 cells. Both cell lines highly express ecto-CRT and released ATP and HMGB1 after treatment and showed a high downregulation in CD47 expression after treatment, resulting in more phagocytosis and DC maturation. Contrary to PSCs, we also observed an increased secretion profile of both TNF- α and IFN- γ in cocultures of DCs with pPBS-treated MIA-Paca-2 and PANC-1 cells. These data indicate a more immunogenic type of phagocytosis with higher production of proinflammatory cytokines, which is documented to lead to immunostimulatory clearance of tumor cells (20, 56, 57). Furthermore, this complements our past study where mice, inoculated with a plasma-generated, whole-cell vaccine, were protected against live tumor challenge with melanoma cancer cells (58). This strongly suggests that downstream of ICD, an adaptive immune response is triggered, which ultimately leads to the development of anti-tumor memory.

It has been shown that ATP could amplify the effects of other activators of DCs, such as TNF- α (59). This could explain the lack of DC maturation after coculture with pPBS-treated BxPC3 and Capan-2 cells, as both cell lines did not release a significant amount of ATP after pPBS treatment nor TNF- α in coculture with DCs. These observations further emphasize the importance of intrinsic differences between cell types and even cell lines when investigating immunogenicity of treatment. Similar differences between tumor cell lines have been documented by Di Blasio et al (54). Altogether, our data indicate that cocultures of pPBS-treated tumor cells and DCs are capable of releasing immunostimulatory signals in the TME, suggesting the induction of a more pronounced antitumoral immune response.

Since DCs are important players in inducing specific antitumor immune responses and are potentially present in the TME, it is also important to identify the direct effects of plasma treatment on this subtype of immune cells (60, 61). We showed that pPBS treatment had

no effect on the viability of DCs in monoculture or in coculture with PSCs and PCCs. A previous study shows that plasma induces apoptosis in PMBC in general (62). However, when looking more specific into the subpopulations of PBMC, Bekeschus et al. showed that monocytes are more resistant to plasma treatment. This could be due to a stronger antioxidant defense system in phagocytes, such as monocytes, macrophages and DCs, which under physiological conditions protects them against self-production of ROS during oxidative burst (63).

In this study, we have demonstrated that pPBS treatment may be an effective anticancer immunotherapeutic modality for PDAC by simultaneously attacking both PCCs and PSCs. Consequently, the physical barrier of PSCs might be disrupted, which could lead to more infiltration of immune cells. Together with the induction of ICD in PCCs and the reduction of immunosuppressive cytokines released by PSC, these results may potentially open the way for more successful combination strategies with immunotherapy in PDAC. In a next step, implementation of an *in vivo* model would be warranted. Nevertheless, we are convinced that our data have a high translational value, though extrapolation of *in vitro* cell line studies to the clinic should be considered with caution. Therefore, we believe that our experiments provide a strong experimental basis for further development of an *in vivo* model, which can make the translational value even stronger towards a clinical setting.

Conclusion

We conclude that plasma treatment via pPBS can attack both the PCCs and the PSCs. These data show that pPBS has the potential to induce ICD in PCCs and to reduce the immunosuppressive TME created by PSCs. Altogether, these results might potentially open the way for more successful combination strategies with immunotherapy for the treatment of PDAC.

References

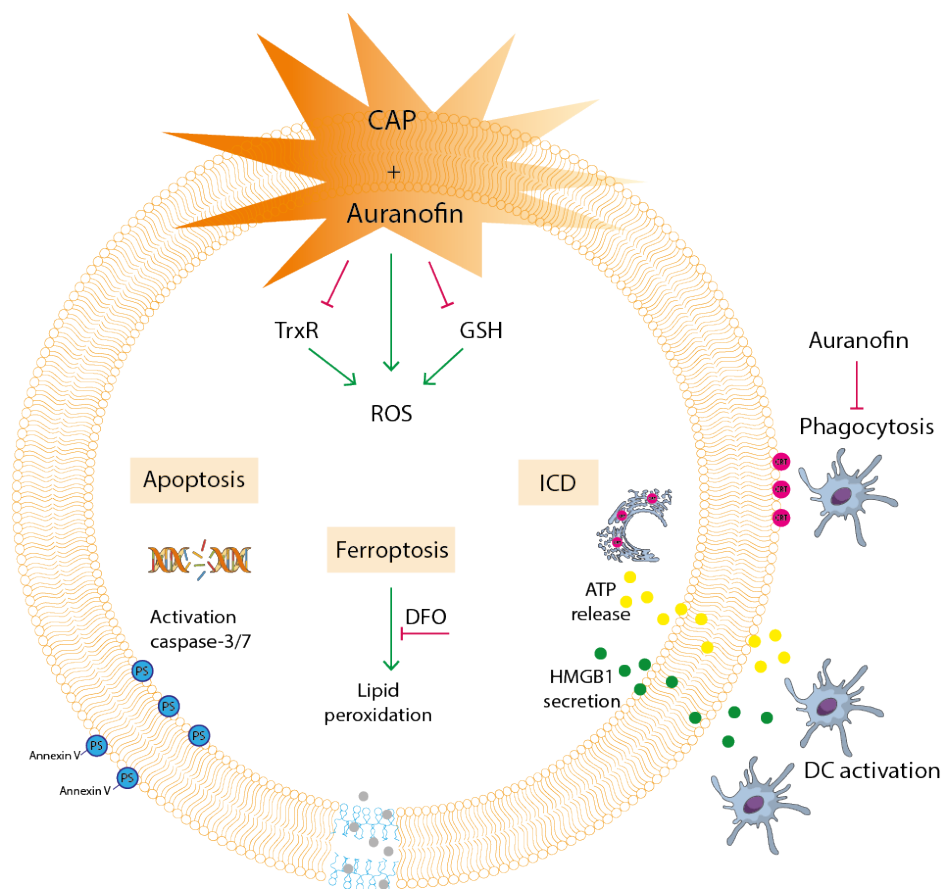
1. Ansari D, Gustafsson A, Andersson R. Update on the management of pancreatic cancer: surgery is not enough. *World journal of gastroenterology*. 2015;21(11):3157-65.
2. Chiorean EG, Coveler AL. Pancreatic cancer: optimizing treatment options, new, and emerging targeted therapies. *Drug design, development and therapy*. 2015;9:3529-45.
3. Hidalgo M, Cascinu S, Kleeff J, Labianca R, Lohr JM, Neoptolemos J, et al. Addressing the challenges of pancreatic cancer: future directions for improving outcomes. *Pancreatology : official journal of the International Association of Pancreatology*. 2015;15(1):8-18.
4. Ferlay J, Lam F., Colombet M., Mery L., Piñeros M., Znaor A., Soerjomataram I., Bray F. . *Global Cancer Observatory: Cancer Today*. Lyon, France: International Agency for Research on Cancer 2018 [
5. Rahib L, Smith BD, Aizenberg R, Rosenzweig AB, Fleshman JM, Matrisian LM. Projecting cancer incidence and deaths to 2030: the unexpected burden of thyroid, liver, and pancreas cancers in the United States. *Cancer research*. 2014;74(11):2913-21.
6. Brahmer JR, Tykodi SS, Chow LQ, Hwu WJ, Topalian SL, Hwu P, et al. Safety and activity of anti-PD-L1 antibody in patients with advanced cancer. *The New England journal of medicine*. 2012;366(26):2455-65.
7. Royal RE, Levy C, Turner K, Mathur A, Hughes M, Kammula US, et al. Phase 2 trial of single agent Ipilimumab (anti-CTLA-4) for locally advanced or metastatic pancreatic adenocarcinoma. *Journal of immunotherapy*. 2010;33(8):828-33.
8. Patnaik A, Kang SP, Rasco D, Papadopoulos KP, Ellassais-Schaap J, Beeram M, et al. Phase I Study of Pembrolizumab (MK-3475; Anti-PD-1 Monoclonal Antibody) in Patients with Advanced Solid Tumors. *Clinical cancer research : an official journal of the American Association for Cancer Research*. 2015;21(19):4286-93.
9. Herbst RS, Soria JC, Kowanetz M, Fine GD, Hamid O, Gordon MS, et al. Predictive correlates of response to the anti-PD-L1 antibody MPDL3280A in cancer patients. *Nature*. 2014;515(7528):563-7.
10. Watt J, Kocher HM. The desmoplastic stroma of pancreatic cancer is a barrier to immune cell infiltration. *Oncoimmunology*. 2013;2(12):e26788.
11. Heinemann V, Reni M, Ychou M, Richel DJ, Macarulla T, Ducreux M. Tumour-stroma interactions in pancreatic ductal adenocarcinoma: rationale and current evidence for new therapeutic strategies. *Cancer treatment reviews*. 2014;40(1):118-28.
12. Lunardi S, Muschel RJ, Brunner TB. The stromal compartments in pancreatic cancer: are there any therapeutic targets? *Cancer letters*. 2014;343(2):147-55.
13. Feig C, Gopinathan A, Neeße A, Chan DS, Cook N, Tuveson DA. The pancreas cancer microenvironment. *Clinical cancer research : an official journal of the American Association for Cancer Research*. 2012;18(16):4266-76.
14. Mace TA, Bloomston M, Lesinski GB. Pancreatic cancer-associated stellate cells: A viable target for reducing immunosuppression in the tumor microenvironment. *Oncoimmunology*. 2013;2(7):e24891.
15. Rosenberg A, Mahalingam D. Immunotherapy in pancreatic adenocarcinoma-overcoming barriers to response. *Journal of gastrointestinal oncology*. 2018;9(1):143-59.
16. Obeid M, Tesniere A, Ghiringhelli F, Fimia GM, Apetoh L, Perfettini JL, et al. Calreticulin exposure dictates the immunogenicity of cancer cell death. *Nature medicine*. 2007;13(1):54-61.
17. Michaud M, Martins I, Sukkurwala AQ, Adjemian S, Ma Y, Pellegatti P, et al. Autophagy-dependent anticancer immune responses induced by chemotherapeutic agents in mice. *Science*. 2011;334(6062):1573-7.
18. Apetoh L, Ghiringhelli F, Tesniere A, Obeid M, Ortiz C, Criollo A, et al. Toll-like receptor 4-dependent contribution of the immune system to anticancer chemotherapy and radiotherapy. *Nature medicine*. 2007;13(9):1050-9.
19. Kroemer G, Galluzzi L, Kepp O, Zitvogel L. Immunogenic cell death in cancer therapy. *Annu Rev Immunol*. 2013;31:51-72.
20. Garg AD, Romano E, Rufo N, Agostinis P. Immunogenic versus tolerogenic phagocytosis during anticancer therapy: mechanisms and clinical translation. *Cell death and differentiation*. 2016;23(6):938-51.
21. Galluzzi L, Buque A, Kepp O, Zitvogel L, Kroemer G. Immunogenic cell death in cancer and infectious disease. *Nature reviews Immunology*. 2017;17(2):97-111.

22. Fucikova J, Moserova I, Truxova I, Hermanova I, Vancurova I, Partlova S, et al. High hydrostatic pressure induces immunogenic cell death in human tumor cells. *Int J Cancer*. 2014;135(5):1165-77.
23. Garg AD, Krysko DV, Vandenabeele P, Agostinis P. Hypericin-based photodynamic therapy induces surface exposure of damage-associated molecular patterns like HSP70 and calreticulin. *Cancer immunology, immunotherapy : CII*. 2012;61(2):215-21.
24. Gameiro SR, Jammeh ML, Wattenberg MM, Tsang KY, Ferrone S, Hodge JW. Radiation-induced immunogenic modulation of tumor enhances antigen processing and calreticulin exposure, resulting in enhanced T-cell killing. *Oncotarget*. 2014;5(2):403-16.
25. Garg AD, Krysko DV, Verfaillie T, Kaczmarek A, Ferreira GB, Marysael T, et al. A novel pathway combining calreticulin exposure and ATP secretion in immunogenic cancer cell death. *The EMBO journal*. 2012;31(5):1062-79.
26. Vermeulen S, De Waele J, Vanuytsel S, De Backer J, Van der Paal J, Ramakers M, et al. Cold atmospheric plasma treatment of melanoma and glioblastoma cancer cells. *Plasma Process Polym*. 2016;13(12):1195-205.
27. Yan DY, Sherman JH, Keidar M. Cold atmospheric plasma, a novel promising anti-cancer treatment modality. *Oncotarget*. 2017;8(9):15977-95.
28. Liedtke KR, Bekeschus S, Kaeding A, Hackbarth C, Kuehn JP, Heidecke CD, et al. Non-thermal plasma-treated solution demonstrates antitumor activity against pancreatic cancer cells in vitro and in vivo. *Sci Rep*. 2017;7(1):8319.
29. Partecke LI, Evert K, Haugk J, Doering F, Normann L, Diedrich S, et al. Tissue tolerable plasma (ITP) induces apoptosis in pancreatic cancer cells in vitro and in vivo. *BMC cancer*. 2012;12:473.
30. Kalghatgi S, Kelly CM, Cerchar E, Torabi B, Alekseev O, Fridman A, et al. Effects of Non-Thermal Plasma on Mammalian Cells. *Plos One*. 2011;6(1).
31. Jesnowski R, Furst D, Ringel J, Chen Y, Schroedel A, Kleeff J, et al. Immortalization of pancreatic stellate cells as an in vitro model of pancreatic fibrosis: deactivation is induced by matrigel and N-acetylcysteine. *Laboratory investigation; a journal of technical methods and pathology*. 2005;85(10):1276-91.
32. Hamada S, Masamune A, Yoshida N, Takikawa T, Shimosegawa T. IL-6/STAT3 Plays a Regulatory Role in the Interaction Between Pancreatic Stellate Cells and Cancer Cells. *Digestive diseases and sciences*. 2016;61(6):1561-71.
33. Bekeschus S, Schmidt A, Weltmann KD, von Woedtke T. The plasma jet kINPen - A powerful tool for wound healing. *Clin Plasma Med*. 2016;4(1):19-28.
34. Smits EL, Ponsaerts P, Van de Velde AL, Van Driessche A, Cools N, Lenjou M, et al. Proinflammatory response of human leukemic cells to dsRNA transfection linked to activation of dendritic cells. *Leukemia*. 2007;21(8):1691-9.
35. Lion E, Anguille S, Berneman ZN, Smits EL, Van Tendeloo VF. Poly(I:C) enhances the susceptibility of leukemic cells to NK cell cytotoxicity and phagocytosis by DC. *Plos One*. 2011;6(6):e20952.
36. De Waele J, Marcq E, Van Audenaerde JR, Van Loenhout J, Deben C, Zwaenepoel K, et al. Poly(I:C) primes primary human glioblastoma cells for an immune response invigorated by PD-L1 blockade. *Oncoimmunology*. 2018;7(3):e1407899.
37. O'Donnell JS, Teng MW, Smyth MJ. Cancer immunoediting and resistance to T cell-based immunotherapy. *Nature Reviews Clinical Oncology*. 2018:1.
38. Hilmi M, Bartholin L, Neuzillet C. Immune therapies in pancreatic ductal adenocarcinoma: Where are we now? *World journal of gastroenterology*. 2018;24(20):2137-51.
39. Schnurr M, Duewelling P, Bauer C, Rothenfusser S, Lauber K, Endres S, et al. Strategies to relieve immunosuppression in pancreatic cancer. *Immunotherapy*. 2015;7(4):363-76.
40. Van Audenaerde J. Interleukin-15 stimulates natural killer cell-mediated killing of both human pancreatic cancer and stellate cells. *Oncotarget*. 2017;8:56968-79.
41. Feig C, Jones JO, Kraman M, Wells RJ, Deonarain A, Chan DS, et al. Targeting CXCL12 from FAP-expressing carcinoma-associated fibroblasts synergizes with anti-PD-L1 immunotherapy in pancreatic cancer. *Proceedings of the National Academy of Sciences of the United States of America*. 2013;110(50):20212-7.
42. Yan DY, Cui HT, Zhu W, Nourmohammadi N, Milberg J, Zhang LG, et al. The Specific Vulnerabilities of Cancer Cells to the Cold Atmospheric Plasma-Stimulated Solutions. *Sci Rep-Uk*. 2017;7.

43. Kumar N, Attri P, Dewilde S, Bogaerts A. Inactivation of human pancreatic ductal adenocarcinoma with atmospheric plasma treated media and water: a comparative study. *Journal of Physics D: Applied Physics*. 2018;51(25):255401.
44. Gorchs L, Hellevik T, Bruun JA, Camilio KA, Al-Saad S, Stuge TB, et al. Cancer-associated fibroblasts from lung tumors maintain their immunosuppressive abilities after high-dose irradiation. *Frontiers in oncology*. 2015;5:87.
45. Wu Q, Tian Y, Zhang J, Zhang H, Gu F, Lu Y, et al. Functions of pancreatic stellate cell-derived soluble factors in the microenvironment of pancreatic ductal carcinoma. *Oncotarget*. 2017;8(60):102721-38.
46. Erdogan B, Webb DJ. Cancer-associated fibroblasts modulate growth factor signaling and extracellular matrix remodeling to regulate tumor metastasis. *Biochemical Society transactions*. 2017;45(1):229-36.
47. Neuzillet C, Tijeras-Raballand A, Cohen R, Cros J, Faivre S, Raymond E, et al. Targeting the TGFbeta pathway for cancer therapy. *Pharmacology & therapeutics*. 2015;147:22-31.
48. Reczek CR, Chandel NS. The two faces of reactive oxygen species in cancer. *Annual Review of Cancer Biology*. 2017;1:79-98.
49. Lin A, Truong B, Pappas A, Kirifides L, Oubbari A, Chen SY, et al. Uniform Nanosecond Pulsed Dielectric Barrier Discharge Plasma Enhances Anti-Tumor Effects by Induction of Immunogenic Cell Death in Tumors and Stimulation of Macrophages. *Plasma Process Polym*. 2015;12(12):1392-9.
50. Lin A, Truong B, Patel S, Kaushik N, Choi EH, Fridman G, et al. Nanosecond-Pulsed DBD Plasma-Generated Reactive Oxygen Species Trigger Immunogenic Cell Death in A549 Lung Carcinoma Cells through Intracellular Oxidative Stress. *International journal of molecular sciences*. 2017;18(5).
51. Lin AG, Xiang B, Merlino DJ, Baybutt TR, Sahu J, Fridman A, et al. Non-thermal plasma induces immunogenic cell death in vivo in murine CT26 colorectal tumors. *Oncoimmunology*. 2018;7(9):e1484978.
52. Freund E, Liedtke KR, van der Linde J, Metelmann HR, Heidecke CD, Partecke LI, et al. Physical plasma-treated saline promotes an immunogenic phenotype in CT26 colon cancer cells in vitro and in vivo. *Sci Rep*. 2019;9(1):634.
53. Azzariti A, Iacobazzi RM, Di Fonte R, Porcelli L, Gristina R, Favia P, et al. Plasma-activated medium triggers cell death and the presentation of immune activating danger signals in melanoma and pancreatic cancer cells. *Sci Rep*. 2019;9(1):4099.
54. Di Blasio S, Wortel IM, van Bladel DA, de Vries LE, Duiveman-de Boer T, Worah K, et al. Human CD1c(+) DCs are critical cellular mediators of immune responses induced by immunogenic cell death. *Oncoimmunology*. 2016;5(8):e1192739.
55. Garg AD, Vandenberk L, Koks C, Verschuere T, Boon L, Van Gool SW, et al. Dendritic cell vaccines based on immunogenic cell death elicit danger signals and T cell-driven rejection of high-grade glioma. *Science translational medicine*. 2016;8(328):328ra27.
56. Pawaria S, Binder RJ. CD91-dependent programming of T-helper cell responses following heat shock protein immunization. *Nature communications*. 2011;2:521.
57. Garg AD, Dudek AM, Ferreira GB, Verfaillie T, Vandenabeele P, Krysko DV, et al. ROS-induced autophagy in cancer cells assists in evasion from determinants of immunogenic cell death. *Autophagy*. 2013;9(9):1292-307.
58. Lin A, Gorbanev Y, De Backer J, Van Loenhout J, Van Boxem W, Lemièrre F, et al. Non-Thermal Plasma as a Unique Delivery System of Short-Lived Reactive Oxygen and Nitrogen Species for Immunogenic Cell Death in Melanoma Cells. *Advanced Science*. 2019:1802062.
59. Schnurr M, Then F, Galambos P, Scholz C, Siegmund B, Endres S, et al. Extracellular ATP and TNF-alpha synergize in the activation and maturation of human dendritic cells. *Journal of immunology*. 2000;165(8):4704-9.
60. Palucka K, Ueno H, Fay J, Banchereau J. Dendritic cells and immunity against cancer. *Journal of internal medicine*. 2011;269(1):64-73.
61. Deicher A, Andersson R, Tingstedt B, Lindell G, Bauden M, Ansari D. Targeting dendritic cells in pancreatic ductal adenocarcinoma. *Cancer cell international*. 2018;18:85.
62. Bekeschus S, Kolata J, Winterbourn C, Kramer A, Turner R, Weltmann KD, et al. Hydrogen peroxide: A central player in physical plasma-induced oxidative stress in human blood cells. *Free radical research*. 2014;48(5):542-9.
63. Seres T, Knickelbein RG, Warshaw JB, Johnston RB, Jr. The phagocytosis-associated respiratory burst in human monocytes is associated with increased uptake of glutathione. *Journal of immunology*. 2000;165(6):3333-40.

CHAPTER 4

Auranofin and cold atmospheric plasma synergize to trigger distinct cell death mechanisms and immunogenic responses in glioblastoma multiforme



Jinthe Van Loenhout, Laurie Freire Boullosa , Delphine Quatannens, Jorrit De Waele, Céline Merlin, Hilde Lambrechts, Filip Lardon, Marc Peeters, Annemie Bogaerts, Evelien Smits, Christophe Deben. Auranofin and cold atmospheric plasma synergize to trigger distinct cell death mechanisms and immunogenic responses in glioblastoma multiforme.

Submitted

Abstract

Targeting the redox balance of malignant cells via the delivery of high oxidative stress unlocks a potential therapeutic strategy against glioblastoma multiforme (GBM). We investigated a novel reactive oxygen species (ROS)-inducing combination treatment strategy by increasing exogenous ROS via cold atmospheric plasma and inhibiting the endogenous protective antioxidant system via auranofin (AF), a thioredoxin reductase 1 (TrxR) inhibitor. Sequential combination treatment of AF and cold atmospheric plasma-treated PBS (pPBS) or AF and direct plasma application, resulted in a synergistic response in 2D and 3D GBM cell cultures, respectively. Differences in baseline protein levels related to the antioxidant system explained cell line-dependent sensitivity towards the combination treatment. The highest decrease of TrxR activity and GSH levels was observed after combination treatment of AF and pPBS, compared to AF and pPBS monotherapies. This combination also led to the highest accumulation of intracellular ROS. We confirmed a ROS-mediated response to the combination of AF and pPBS, which was able to induce distinct cell death mechanisms. On the one hand, an increase in caspase-3/7 activity together with an increase in the proportion of annexin V positive cells, indicates the induction of apoptosis in the GBM cells. On the other hand, lipid peroxidation and inhibition of cell death through an iron chelator suggest the involvement of ferroptosis in the GBM cell lines. Both cell death mechanisms induced by the combination of AF and pPBS, resulted in a significant increase of danger signals (ecto-calreticulin, ATP and HMGB1) and dendritic cell maturation, indicating a potential increase in immunogenicity, though, the phagocytotic capacity of dendritic cells was inhibited by AF. Thus, our study provides a novel therapeutic strategy for GBM to enhance the efficacy of oxidative stress-inducing therapy through a combination of AF and cold atmospheric plasma.

Introduction

Glioblastoma multiforme (GBM) is the most prevalent malignant primary brain tumor, which carries an extremely poor prognosis due to its aggressive and invasive nature (1). Despite current improvements in conventional treatment, tumor recurrence is nearly inevitable, contributing to a median survival duration of only 14.6 months and a five-year survival less than 5.6% (2, 3). Therefore, the development of new treatment strategies is urgently required.

Malignant cells are characterized with higher levels of intrinsic reactive oxygen species (ROS) compared to normal cells as a consequence of e.g. altered metabolic rate and gene mutations (4). To maintain redox balance, malignant cells counter this intrinsic oxidative stress by upregulation of their antioxidant defense system (5). The difference in redox balance between malignant cells and normal cells unlocks a potential therapeutic strategy for ROS-inducing therapies (6).

We investigated a novel combinatory therapeutic strategy by inducing high oxidative stress through delivery of exogenous ROS and inhibiting endogenous protective antioxidant systems. We hypothesized that the combination of these two different ROS-modulating methods is a beneficial and promising anti-GBM treatment strategy. Firstly, cold atmospheric plasma (CAP) was used as a unique treatment method for increasing oxidative stress levels to target cancer cells via exogenous delivery of ROS and reactive nitrogen species (RNS) (7, 8). This CAP is an ionized gas that is composed of ROS and RNS, excited molecules, ions, electrons and other physical factors, such as electromagnetic fields and ultraviolet radiation (9). This plasma can be delivered directly onto the tumor or indirectly through plasma-treated liquids (10). This type of exogenous ROS-inducing therapy has already been investigated in different cancer types *in vitro* and *in vivo*, including GBM (10-13). Secondly, endogenous induction of oxidative stress was achieved with inhibition of the antioxidant defense system using auranofin (AF), a thioredoxin reductase 1 (TrxR) inhibitor. AF forms a stable coordinative bond between its gold(I) center and the active site of selenocysteine residues, which causes an increase in oxidative stress, as TrxR is an enzyme that catalyzes the reduction of thioredoxin (Trx) with electrons from NADPH in the Trx antioxidant system (14, 15). AF has also gained interest over the past years as a non-

cancer drug for new repurposing in oncology by the Repurposing Drugs in Oncology project. Several advantages of AF include oral administration, lipophilic properties and approval of the organogold compound by the Food and Drug Administration (FDA) for the treatment of rheumatoid arthritis (16). In GBM, AF is one on the nine drugs in the CUSP9 treatment protocol using re-purposed older drugs and is currently undergoing a clinical trial (NCT02770378) as add-on treatment to standard-of-care temozolomide for recurrent GBM (17). Here, AF is also used as one of the nine drugs in the combination strategy to increase ROS-mediated cell death, highlighting the potential of AF in GBM research (18).

Targeting malignant cells via different sources of ROS could be a promising novel treatment strategy for GBM. Therefore, we studied the cellular response upon combination treatment of AF with CAP to determine whether this combination enhanced the cytotoxic effect in 2D and 3D GBM cell cultures. In addition, we performed an in-depth analysis of the molecular mechanism underlying the response of different GBM cell lines to the combination of AF and plasma-treated PBS (pPBS). This study is the first to show that the response to AF is synergistically enhanced by sequential addition of pPBS or by direct plasma treatment in both 2D and 3D cell cultures, respectively. This combination was able to deliver high amounts of ROS and induced characteristics of distinct underlying mechanisms of cell death, including apoptosis and ferroptosis. Additionally, we showed that these dying cancer cells were able to initiate the release of immunogenic cell death (ICD) related damage-associated molecular patterns (DAMPs) and subsequently could enhance dendritic cell (DC) maturation. Contrary to these immunostimulatory effects, we also found that the phagocytotic capacity of the DCs was inhibited by AF.

Materials & methods

Cell lines and cell culture

The human GBM cell lines U-87 MG (kindly provided by Dr. Margaret Ashcroft, University of Cambridge), LN-229 (ATCC CRL-261) and T98G (kindly provided by Dr. Nicolas Goffart, University of Liège) were cultured in Dulbecco's Modified Eagle Medium (DMEM, Life Technologies) supplemented with 10% fetal bovine serum (FBS, Life Technologies), 1% penicillin/streptomycin (Life Technologies) and 2 mM L-glutamine

(Life Technologies). Cells were maintained in exponential growth phase at 5% CO₂ in a humidified incubator at 37 °C. T98G cells were green autofluorescent and could therefore not be considered for certain experiments. To rule out differences in sensitivity to AF due to variations in selenium concentration (19, 20), all experiments were performed using the same supplier of FBS and triplicates of TrxR activity and GSH content were performed with the same batch of treated cells and growth medium. Cell cultures were tested regularly for absence of mycoplasma contamination using the MycoAlert detection kit (Lonza). For some experiments, cells were transduced with the InCyCte® Nuclight Red Lentivirus reagent (Essen Biosciences) using the manufacturer's protocol.

Generation of spheroids

Cell suspensions were prepared at 5x10⁴ cells/mL for U-87, 6x10⁴ cells/mL for T98G and 7x10⁴ cells/mL for LN-229. Different concentrations of different cell lines were used to maintain a diameter of approximately 500 µm. Cells were seeded in an ultra-low attachment (ULA) 96-well plate (round bottom, Corning Costar) in DMEM and centrifuged for 10 min at 100x *g*. Spheroids were allowed to form and grow for 3 days at 5% CO₂ in a humidified incubator at 37 °C prior to their use in experiments.

Treatment of 2D and 3D cell cultures

Cells were incubated with AF (0-10 µM, Bio-Techne) as single agents for different time periods according to the experiment.

2D cell cultures were treated indirectly with pPBS generated using the atmospheric pressure plasma jet kINPenIND® (Neoplas Tools), as previously used in our lab and described by Van Loenhout et al. (12). Argon gas is used in this setting as feeding gas (21). Then, 2 mL of PBS was treated with one standard liter per minute (slm) gas flow rate at a gap distance of 6 mm for 5 min. This 100% plasma-treated PBS (pPBS) was further diluted in PBS to final concentrations of 25%, 50%, 62.5% pPBS, which was then directly added in a 1/6 dilution in the media of the cells. Under these conditions the 100% pPBS contained 526.91 µM H₂O₂, 56.27 µM NO₂⁻ and 37.75 µM NO₃⁻ and were determined using a colorimetric assay for H₂O₂ and fluorometric assay for NO₂⁻ and NO₃⁻. These concentrations were 4-fold diluted in the 25% pPBS treatment conditions containing 128.46 µM H₂O₂, 14.91 µM NO₂⁻ and 14.41 µM NO₃⁻. Untreated PBS is used as vehicle control for all experiments.

3D cell cultures were treated using the COST jet plasma setup, as previously optimized in our lab and described by Privat-Maldonado et al. (22). It was operated with a feed gas of He with 5% H₂O vapor mixture achieved using the split He flow by passing part of it through an H₂O-filled Drechsel flask. Before treatment, 3-day-old spheroids were washed once with PBS after removing the culture medium. Direct treatments were performed on spheroids in 200 μ L of PBS in a 96-well ULA plate for 3 min. Spheroids in 200 μ L of untreated PBS were used as vehicle controls. Under these conditions the pPBS contained 1230.82 μ M H₂O₂, 4.98 μ M NO₂⁻ and 5.03 μ M NO₃⁻ (22). Spheroids were incubated for 90 min with the treatment, after which it was replaced with the supernatant of the corresponding spheroid.

For combination treatments, 2D or 3D cell cultures were pretreated for 4 hours with AF (0-10 μ M). Afterwards 2D and 3D cell cultures were treated with pPBS and plasma, respectively, as described.

Cell death assays and synergism

For 2D cell cultures, cell death was determined using the IncuCyte ZOOM® life cell analysis system (Sartorius). All experiments were performed at least three independent times. NuLight red lentiviral transduced GBM cell lines were seeded at a density of 2x10⁴ cells/mL in a 96-well plate. After overnight incubation, cells were treated with mono- and/or combination treatment of AF (0-7.5 μ M) and pPBS (25 %, 50% and 62.5 %), in the presence of IncuCyte® Cytotox Green reagent (50 nM, Essen BioScience). Treatment of cells was done in absence or presence of desired cell death inhibitors, with a preincubation of 1 hours for n-acetyl-cysteine (NAC, 5 mM, Sigma-Aldrich), catalase (20 μ g/mL, Sigma-Aldrich) ferrostatin-1 (Fer-1, 1 μ M, Sigma-Aldrich) and a preincubation of 4 hours with deferoxamine (DFO, 100 μ M for LN-229 and T98G cells and 50 μ M for U87 cells, Sigma-Aldrich). Plates were incubated in the temperature- and CO₂-controlled IncuCyte® Live-Cell Analysis System (Sartorius) for 72 hours. Cell death was monitored by taking images every 24 hours to limit phototoxicity. For analysis, green object count (1/mm²), red object count (1/mm²) and green-red overlapping object count (1/mm²) were determined with the IncuCyte ZOOM® software. The percentage of cell death was calculated using the formula: [green object count / ((red object count + green object count) – overlapping object count)]

*100. The percentage of survival was calculated using the red object count, which was normalized towards the untreated control.

Caspase-3/7 activity was also determined using the IncuCyte ZOOM® life cell analysis system in the presence of Caspase-3/7 Green apoptosis reagent (2.5 µM, Essen Bioscience). The percentage of caspase-3/7 positive cells was calculated using the formula: $[\text{green object count} / ((\text{red object count} + \text{green object count}) - \text{overlapping object count})] * 100$.

For 3D cell cultures, spheroids were treated with mono- and/or combination treatments of AF (0-10 µM) and plasma using the COST jet device. Microscopic images were taken with the IncuCyte® system at different time points. End-point viability of spheroids was assessed after 72 hours using the CellTiterGlo® 3D Cell Viability assay (Promega) according to the manufacturer's protocol. The luminescent signal was measured using Spark®Cyto (Tecan).

In order to determine the presence of a synergistic effect, the combination index (CI) was analyzed according to the Additive Model based on ratio value between the found and the expected combination effect as calculated from the exposure of the individual treatments (23).

ROS measurement

Cells were seeded in 96-well plates, incubated overnight and exposed to mono- and/or combination treatment of AF (0 – 7.5 µM) and plasma (25 %, 50% and 62.5% pPBS). Immediately following treatment, 2.5 µM CellROX Green reagent (Invitrogen) was added to U-87 and LN-229 cells and 5 µM CellROX Red reagent (Invitrogen) was added to T98G cells. Afterwards, the plate was transferred to the temperature- and CO₂-controlled IncuCyte ZOOM®. ROS was monitored over time by pictures that were taken at 4 h, 24 hours after treatment. For analysis, average green calibrated unit (GCU) and average red calibrated unit (RCU) was plotted for every cell line after 4 hours and 24 hours.

Protein isolation

For protein-based experiments, cells were seeded and treated with mono- and/or combination treatment of AF and pPBS. After 4 hours of the last treatment, cells were lysed in lysis buffer (10 mM TrisHCl, 400 mM NaCl, 1mM EDTA, 0.1% NP40 and protease inhibitor). After centrifugation (10 min, 13 000 rpm, 4 °C), cleared lysates

containing the isolated proteins were harvested and kept at -20 °C. Protein concentrations were determined using the Pierce BCA protein kit (Thermo Scientific), according to the manufacturer's instructions. To determine baseline protein levels, cells were collected after sub culturing and lysed as described above.

Thioredoxin reductase activity assay

The treated and untreated control protein lysates were used to measure TrxR activity using the Thioredoxin Reductase Colorimetric Assay Kit (Cayman Chemical), according to the manufacturer's protocols. Absorbance was recorded at 405 nm with the Spark®Cyto (Tecan) during the initial 5 min of the reaction. TrxR activity was calculated using the formula provided by the protocol, whereby background measurements were subtracted from all values. An equal amount of protein was loaded for each condition as determined by the Pierce BCA protein kit.

Glutathione level quantification

Cells were seeded in 96-well plates and treated with mono- and/or combination treatment of AF and pPBS. After 4 hours and 24 hours of the last treatment, cellular concentrations of glutathione (GSH) and oxidized glutathione (GSSG) were determined using the GSH/GSSG-Glo™ Assay kit (Promega), according to the manufacturer's protocols. Luminescent intensity was measured using the Spark®Cyto (Tecan). The amount of GSH, proportional to the luminescent signal, was corrected for the number of cells present in the well.

Lipid peroxidation

Cellular lipid ROS was measured using the Image-iT™ Lipid Peroxidation Kit (Invitrogen), according to the manufacturer's instructions. Therefore, U-87 and LN-229 were treated with mono- and/or combination treatment of AF (0 - 1.5 - 2 μM) and pPBS (25% and 50% pPBS) for 48 hours, or the positive control (cumene hydroperoxide) for 2 hours. Afterwards, 10 μM of the C11-BODIPY dye was added to the culture and incubated for 30 min at 37 °C. The T98G cell line could not be included in this assay due to autofluorescence. Acquisition was performed on a CytoFLEX (BD) and FlowJo v10.1 software (TreeStar) was used to calculate the ratios C11-BODIPY red over green mean fluorescence intensity (MFI) signals.

Analysis of ICD-related markers

All GBM cell lines were seeded and treated with mono- and/or combination treatment of AF and pPBS, analysis of ICD-related markers occurred at different time points. 48 hours after treatment, cells were stained for membrane (calreticulin) CRT expression. Here, cells were harvested and incubated with 5% normal goat serum (NGS, Sigma-Aldrich), followed by washing and incubation with an AF488-conjugated anti-CRT (Abcam) for U-87 and LN-229 cell lines and with an AF647-conjugated anti-CRT antibody (Abcam) for T98G cell line (due to autofluorescence of this cell line) for 40 minutes. Prior to analysis, the cells were stained with Annexin V (AnnV; BD) and propidium iodide (PI; BD) to distinguish between early apoptotic and necrotic cells. Cell debris and necrotic cells (PI⁺) were excluded from analysis. For every sample, a corresponding isotype control was used (Abcam). Flow cytometric acquisition was performed on an Accuri™ C6 instrument (BD). Extracellular ATP release (nmol) was measured in conditioned media (supplemented with heat-inactivated FBS) 4 hours after treatment via ENLITEN® ATP assay system, according to the manufacturer's protocol (Promega). The bioluminescent signal was measured using Spark®Cyto (Tecan) device. Release of HMGB1 (ng/ml) was analyzed 48 hours after treatment using an enzyme-linked immunosorbent assay (ELISA, IBL). The absorption was measured using an iMARK™ plate reader (Bio-rad).

In vitro generation of human monocyte-derived immature DCs

Human peripheral blood mononuclear cells (PBMC) were isolated by LymphoPrep gradient separation (Sanbio, 1114547) from a buffy coat of healthy donors (Ethics Committee of the University of Antwerp, reference number 13/46/454) isolated from adult volunteer whole blood donations (supplied by the Red Cross Flanders Blood service, Belgium). Monocytes were isolated from PBMC using CD14 microbeads according to the manufacturer's protocol (Miltenyi, Biotec). Purity after isolation was >90 %. After isolation, CD14⁺ cells were plated at a density of 1.25-1.35 x 10⁶ cells per mL in 1640 RPMI supplemented with 2.5% human AB (hAB, Sanbio) serum, 800 U/ml granulocyte-macrophage colony stimulating factor (GM-CSF; Gentaur) and 20 ng/ml interleukin (IL)-4 (Miltenyi, Biotec) at day 0, as described before (24). Immature DCs were harvested on day 5.

Maturation status and phagocytotic capacity of DCs

After *in vitro* generation of DCs, GBM cell lines were labeled with the green fluorescent membrane dye PKH67 (Sigma Aldrich) and seeded in 6-well plates for overnight incubation. Labeling of tumor cells with PKH67 was carried out according to the manufacturer's instructions. On day 5, tumor cells were pretreated with AF (0 – 7.5 μ M). After 4 hours of pretreatment, tumor cells were treated with pPBS (25 %, 50% and 62.5% pPBS). In order to make a distinction between target and effector cells, immature DCs were also labeled with a fluorescent dye. Briefly, DCs were labeled with 2 μ M of violet-fluorescent CellTracker Violet BMQC dye (Invitrogen) at a concentration of 1×10^6 cells per mL at 37 °C. Four hours after pPBS treatment, effector and target cells were cocultured at a 1:1 effector:target (E:T) ratio. On day 7, cells were collected and used immediately for flow cytometric detection of DC maturation markers and phagocytosis. Expression of anti-CD86-PECy7, anti-CD80-PerCP5.5 and anti-major histocompatibility complexes class II (MHC-II)-APC were measured on the Violet+ viable (Live/Dead Near IR+) DC population. For every marker, an isotype control was used to subtract aspecific signals. Results are represented as Δ MFI ((MFI staining treated – MFI isotype treated) – (MFI staining untreated – MFI isotype untreated)) and as the percentage of DCs double positive for MHC-II and CD86. Phagocytosis of PKH67+ tumor cells by violet-labeled DCs was expressed as %PKH67+violet+ cells within the violet+ DC population. Acquisition was performed on a FACSAria II (BD). Data analysis was performed using FlowJo v10.1 software (TreeStar).

Statistical analysis

All experiments were performed at least in triplicate. Prism 9.0 software (GraphPad) was used for data comparison and graphical data representations. All statistical analyses were performed in JMP Pro 15.1 and SPSS Statistics 27 software. The interaction term of AF and plasma was statistically analyzed using linear mixed models. The non-parametric Kruskal-Wallis test was used to compare means between more than two groups. The non-parametric Mann-Whitney U test was used to compare means between two groups. *P*-values < 0.05 were considered statistically significant.

Results

The combination treatment of AF and pPBS leads to synergistic response in cell growth inhibition and cell death in GBM cell lines

In order to investigate the potential interaction between AF and pPBS, 2D cell cultures of three different GBM cell lines (LN-229, U-87 and T98G) were incubated with an 8-point titration of 0 – 7.5 μM AF for 4 hours, followed by treatment with PBS or 25% pPBS for a total of 72 hours. Induction of cell death and growth inhibition were investigated to determine EC_{50} and IC_{50} values, respectively. Dose-response survival and cytotoxicity curves (Figure 4.1 A, B) showed that all cell lines had distinct sensitivity towards mono- and combination treatments of AF and pPBS. In all cell lines, the IC_{50} values of AF single treatment and in combination with 25% pPBS were lower than the EC_{50} values, indicating that at lower concentrations cell growth is inhibited and at higher concentrations cell death is induced (Table 4.1). LN-229 ($\text{IC}_{50} = 0.762 \mu\text{M}$ AF; $\text{EC}_{50} = 2.335 \mu\text{M}$ AF) and U-87 ($\text{IC}_{50} = 0.455 \mu\text{M}$ AF; $\text{EC}_{50} = 1.739 \mu\text{M}$ AF) could be considered as sensitive cell lines compared to T98G ($\text{IC}_{50} = 2.364 \mu\text{M}$ AF; $\text{EC}_{50} = 7.395 \mu\text{M}$ AF), which was not responsive to lower concentrations of AF, indicating that T98G is a more resistant cell line towards mono- and combination treatments of AF and pPBS.

When cells were incubated with AF for 4 hours before treatment with 25% pPBS, the cytotoxic effect of AF was amplified and led to a strong synergistic effect (combination index (CI) < 1 , Figure 4.1 C, D). The effects of AF and pPBS as well as their interaction on cell death and cell survival were statistically analyzed using linear mixed models. A significant interaction indicates that the effect of pPBS on cell death and cell survival is dependent on the concentration of AF and vice versa. Table 4.1 gives a detailed overview of the synergistic effects of AF and pPBS on cell death and cell survival in all examined cell lines. The addition of pPBS to AF treatment significantly enhanced cell death compared to AF and pPBS single treatments in all cell lines. A significant interaction on inhibition of cell survival was only seen for the sensitive cell lines LN-229 and U-87. These data show that the combination of AF and pPBS synergistically enhances the induction of GBM cell death in 2D cell cultures.

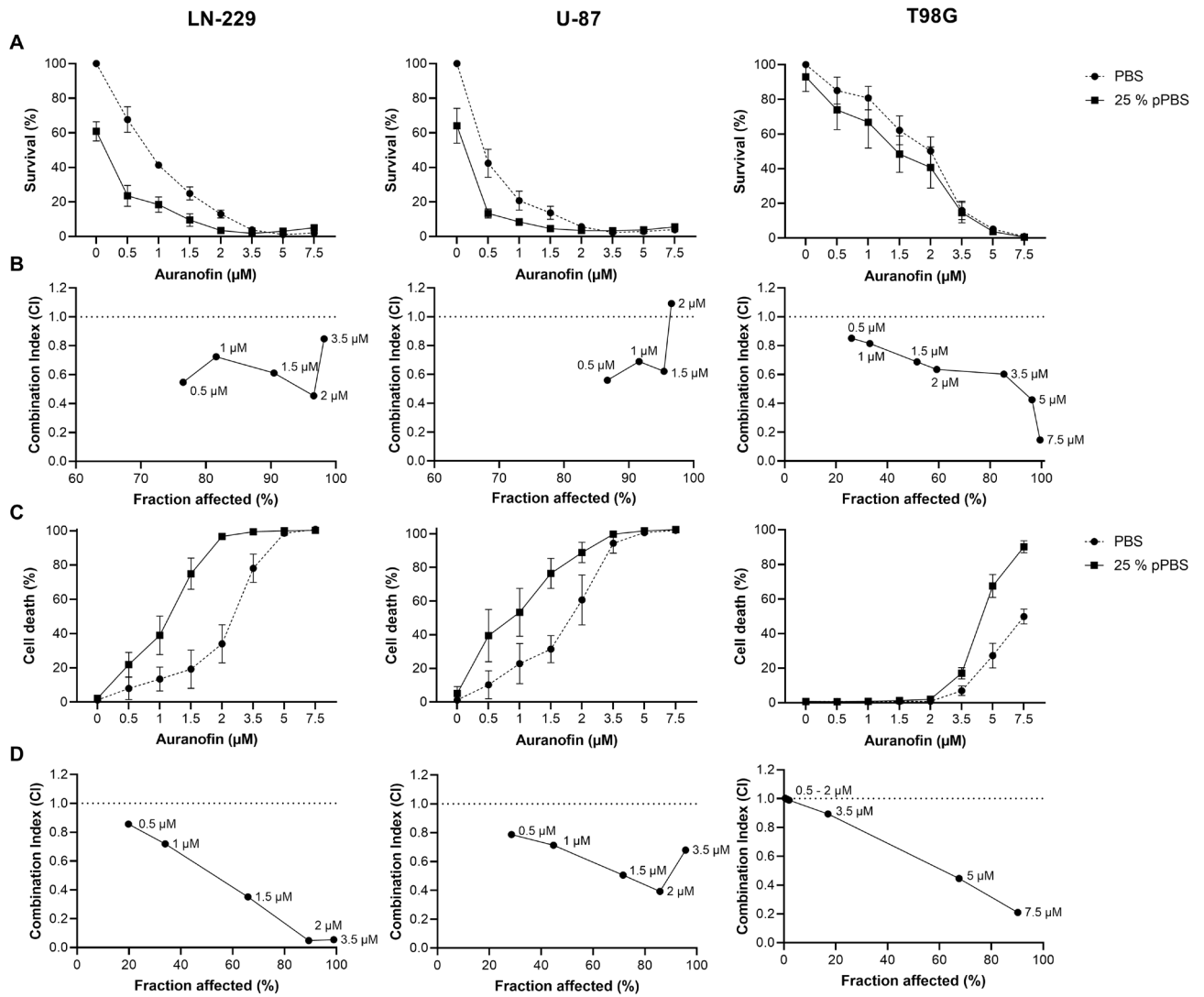


Figure 4.1 The sequential combination treatment of AF and pPBS induces a synergistic response in cell survival and cell death of GBM cell lines. (A) Dose-response survival curves after 72h of AF (0-7.5 μM) monotherapy and in combination with 25% pPBS. (B) The corresponding combination indexes (CI) for each AF concentration based on survival. (C) Dose-response curves of the cytotoxic effect after 72 hours of AF (0-7.5 μM) monotherapy and in combination with 25% pPBS. (D) The corresponding combination indexes for each AF concentration based on cytotoxicity. CI > 1 indicates an antagonistic effect, CI = 1 an additive effect and CI < 1 a synergistic effect. Fraction affected indicates the fraction of cells (in percentages) affected by AF. The supporting data and statistics for this figure can be found in table 1. Graphs represent mean \pm SEM of ≥ 3 independent experiments.

Table 4.1. Cell death, cell inhibition and synergism of AF and pPBS combination treatment of GBM cell lines

(A) Cell inhibition and treatment synergism			
Treatment	LN-229		
	IC50	p-value	CI (1.5 μM AF + 25% pPBS)
<i>AF</i>	0.762 (\pm 0.034)	/	/
<i>AF + 25% pPBS</i>	0.350 (\pm 0.064)	<0.0001	0.611 (\pm 0.214)
	U-87		
	IC50	p-value	CI (1.5 μM AF + 25% pPBS)
<i>AF</i>	0.455 (\pm 0.088)	/	/
<i>AF + 25% pPBS</i>	0.183 (\pm 0.0092)	<0.0001	0.6211 (\pm 0.227)
	T98G		
	IC50	p-value	CI (5 μM AF + 25% pPBS)
<i>AF</i>	2.364 (\pm 0.234)	/	/
<i>AF + 25% pPBS</i>	1.599 (\pm 0.239)	0.8865	0.687 (\pm 0.074)
(B) Cell death and treatment synergism			
Treatment	LN-229		
	EC50	p-value	CI (1.5 μM AF + 25% pPBS)
<i>AF</i>	2.335 (\pm 0.142)	/	/
<i>AF + 25% pPBS</i>	1.037 (\pm 0.065)	<0.0001	0.460 (\pm 0.155)
	U-87		
	EC50	p-value	CI (1.5 μM AF + 25% pPBS)
<i>AF</i>	1.739 (\pm 0.117)	/	/
<i>AF + 25% pPBS</i>	0.755 (\pm 0.098)	0.00015	0.506 (\pm 0.105)
	T98G		
	EC50	p-value	CI (5 μM AF + 25% pPBS)
<i>AF</i>	7.395 (\pm 0.269)	/	/
<i>AF + 25% pPBS</i>	4.487 (\pm 0.078)	<0.0001	0.446 (\pm 0.077)

(A) Cell inhibition and synergism of AF and pPBS combination treatment. The table gives an overview of the IC50-values (\pm SE) of AF after AF monotherapy (normalized to PBS) and in combination with 25% pPBS (normalized to 25% pPBS) for each cell line. IC50-values represent the concentration of AF where the survival response is reduced by half. The average combination index (CI \pm SEM) based on cell inhibition is provided for one concentration of AF (1.5 μ M for LN-229 and U-87, and 5 μ M for T98G) for the combination therapy. (B) Cell death and synergism of AF and pPBS combination treatment. The table gives an overview of the EC50-values (\pm SE) of AF after AF monotherapy and in combination with 25% pPBS for each cell line. EC50-values represent the concentration of AF that gives half-maximal cytotoxic response. The average combination index (CI \pm SEM) based on cell death response is provided for one concentration of AF (1.5 μ M for LN-229 and U-87, and 5 μ M for T98G) for the combination treatment. CI > 1 indicates an antagonistic effect, CI = 1 an additive effect and CI < 1 a synergistic effect. *p < 0.05: significant interaction between AF and pPBS, using linear mixed models.

The combination treatment of AF and pPBS causes alterations in protein targets related to the antioxidant defense system

To further investigate the observed difference in sensitivity between the GBM cell lines, baseline expression levels of GSH and TrxR activity were determined (Figure 4.2 A, B). Statistically, a significant difference between GSH levels of the sensitive cell lines (LN-229 and U-87) and GSH levels of the more resistant T98G was observed. Additionally, T98G cells showed the highest baseline TrxR activity compared to baseline levels of U-87 and LN-229 cell lines. However, there was only a significant difference in baseline levels between T98G and the U-87 cell line (Figure 4.2 B). These differences in baseline levels of GSH and TrxR activity might explain the observed difference in sensitivity between cell lines towards mono- and combination treatment of AF and pPBS.

Next, alterations in key regulators of the ROS scavenging system were examined upon mono- and combination treatments of AF and pPBS to elucidate the mechanism of action. Since LN-229 and U-87 cell lines were considered sensitive compared to T98G, a lower concentration of 1.5 μM AF was used for sensitive cell lines and a higher concentration of 5 μM AF was used for T98G cells, to examine the combinatorial effects of AF and 25% pPBS. GBM cells were treated with AF for 4 hours, followed by 25% pPBS for 4 hours. The total GSH levels (Figure 4.2 C) were stable in LN-229 and decreased upon statistically significant oxidation of GSH in U-87 and T98G, represented as GSH/GSSG ratio (Figure 4.2 D), after treatment with AF alone or in combination with 25% pPBS. In U-87 and T98G, sequential combination treatment led to the highest decrease in total GSH and GSH/GSSG ratio compared to AF/pPBS single treatments. This indicates that high levels of the available GSH becomes oxidized after combination of AF and pPBS, resulting in an exhaustion of the GSH system. Higher doses of AF single treatment (2 μM for LN-229 and U-87; or 7.5 μM for T98G) showed similar effects compared to the combination treatment. In contrast, increasing the dose of pPBS alone (50% for LN-229 and U-87; or 62.5% for T98G) induced only a minor decrease in total GSH, which was significant in the LN-229 cells (Figure 4.3 A,B).

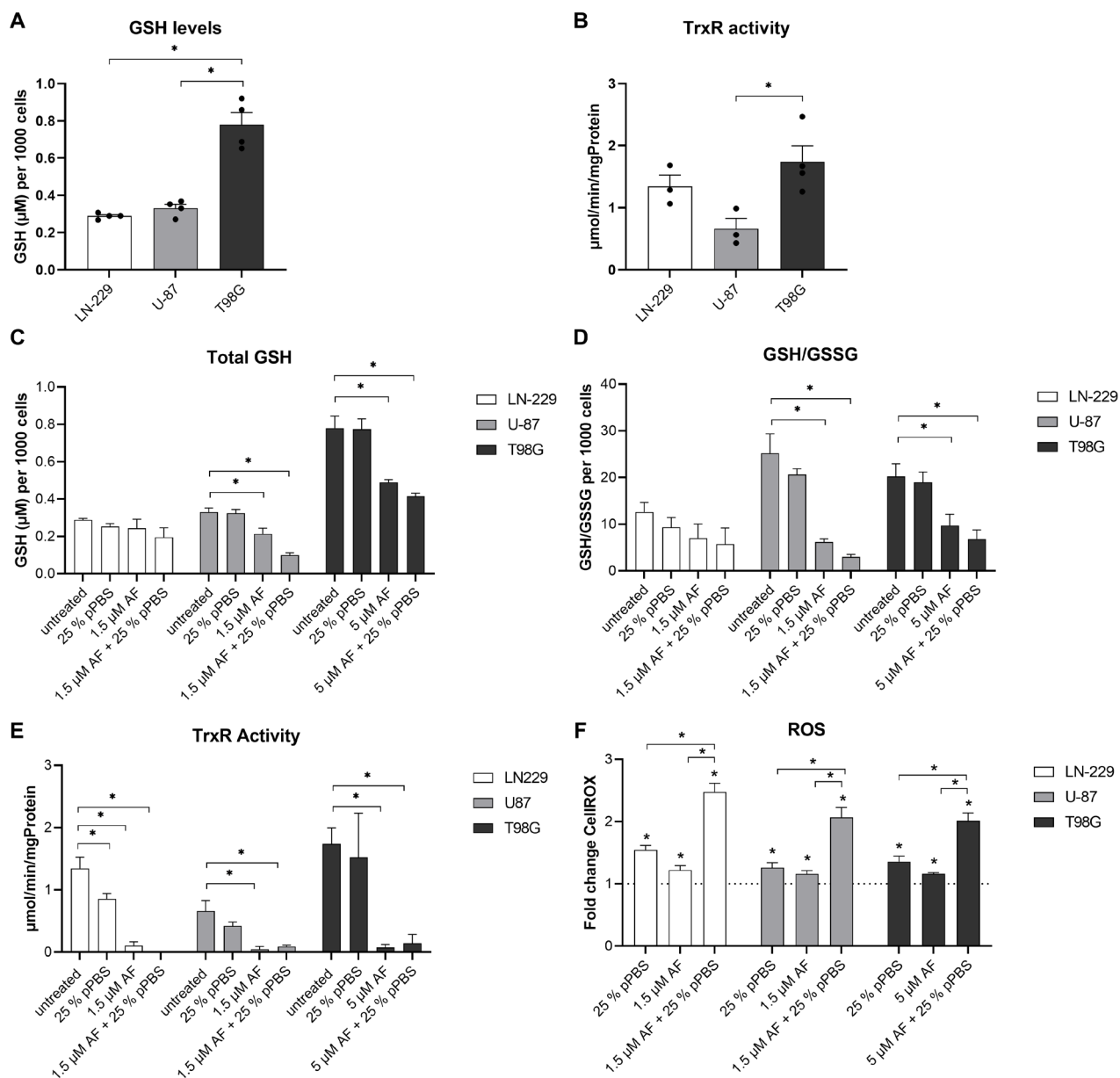


Figure 4.2. The effect of combination treatment of AF and pPBS on protein targets related to the antioxidant defense system. (A) Baseline GSH protein levels of LN-229, U-87 and T98G cells normalized towards 1000 cells (B) Baseline TrxR activity of LN-229, U-87 and T98G cells. (C) GSH protein levels normalized towards 1000 cells after 4 hours of treatment with monotherapies and combination therapy of AF (1.5 μM or 5 μM) and 25% pPBS. (D) Ratio GSH/GSSG normalized towards 1000 cells after 4 hours of treatment with monotherapies and the combination of AF (1.5 μM or 5 μM) and 25% pPBS. (E) TrxR activity after 4 hours of treatment with monotherapies and combination therapy of AF (1.5 μM or 5 μM) and 25% pPBS. (F) Intracellular ROS levels shown as fold change of CellROX Calibration Units (CU), relative towards untreated after 4 hours of treatment with monotherapies and combination therapy of AF (1.5 μM or 5 μM) and 25% pPBS. Graphs represent mean \pm SEM of ≥ 3 independent experiments. * $p \leq 0.05$ denotes statistically significant difference compared with untreated control.

AF was verified as a TrxR inhibitor since TrxR activity was fully depleted after 4 hours of treatment with 1.5 μM AF or in the combination with pPBS (Figure 4.2 E). A similar inhibitory effect was also observed with higher doses of AF (2 μM for LN-229 and U-87; or 7.5 μM for T98G) (Figure 4.3 C). pPBS alone (both 25% and 50%; or 62.5% pPBS) showed only a slight decrease in TrxR activity in LN299 cells (Figure 4.2 E and Figure 4.3 C).

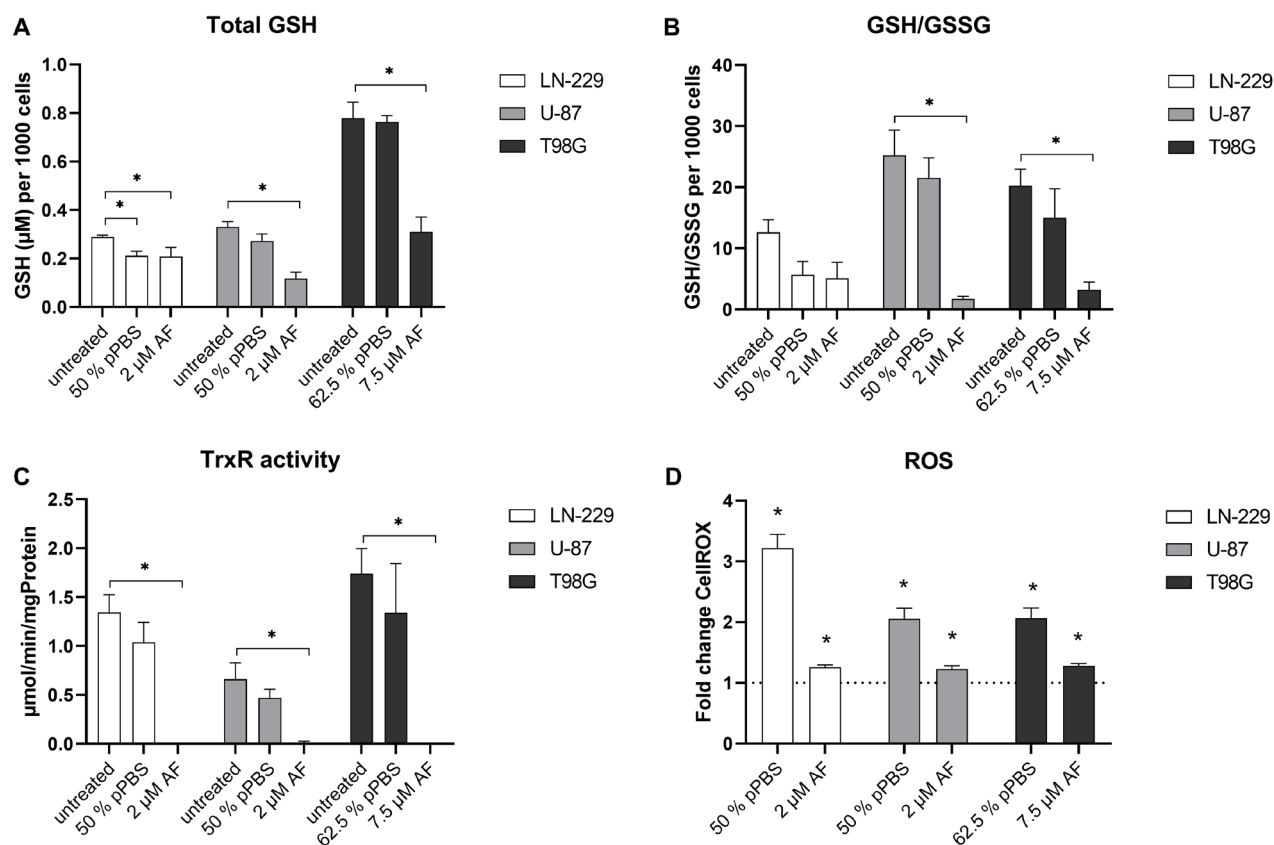


Figure 4.3. The effect of monotherapies of AF or pPBS on protein targets related to the antioxidant defense system. (A) GSH protein levels per 1000 cells after 4 hours of treatment with monotherapies of AF (2 μM or 7.5 μM) and 50% pPBS. (B) Ratio GSH/GSSG per 1000 cells after 4 hours of treatment with monotherapies of AF (2 μM or 7.5 μM) and 50% pPBS. (C) TrxR activity after 4 hours of treatment with monotherapies of AF (2 μM or 7.5 μM) and 50% pPBS. (D) Intracellular ROS levels shown as fold change of CellROX Green Calibration Units (GCU) for U-87 and LN-229 and CellROX Red Calibration Units (RCU) for T98G cells, relative towards untreated after 4 hours of treatment with monotherapies of AF (2 μM or 7.5 μM) and 50% pPBS. Graphs represent mean \pm SEM of ≥ 3 independent experiments. * $p \leq 0.05$ denotes statistically significant difference compared with untreated control.

AF (both 1.5 μM or 5 μM ; and 2 μM or 7.5 μM) alone as well as pPBS (25%) single treatment caused a significant accumulation of intracellular ROS in all GBM cells. This accumulation was significantly more pronounced after 4 hours of AF and pPBS combination treatment (Figure 4.2 F). This shows that both therapies enhance each other

for intracellular ROS accumulation. Similar high ROS accumulations were observed when treating the cells with a higher dose of pPBS (50% for LN-229 and U-87; or 62.5% for T98G), confirming the role of exogenous ROS inducers since minimal or no effects on antioxidant levels were observed (Figure 4.3 D). After a prolonged treatment period of 24 hours, the intracellular ROS levels reverted to baseline levels in the T98G cell line in both mono- and combination treatments, in contrast to LN-229 and U-87 cell lines (Figure 4.4 A). In line with the stronger baseline GSH levels and TrxR activity, T98G is suggested to have a stronger antioxidant capacity, explaining the resistance towards this ROS-inducing combination therapy. In order to investigate if ROS overproduction was involved in the enhanced cell death induced by the combination of AF and pPBS, N-acetyl cysteine (NAC), a thiol-reducing antioxidant agent, was used to scavenge ROS. The cell death induced by AF and pPBS was completely rescued by NAC pretreatment in all GBM cells, further suggesting the involvement of ROS (Figure 4.4 B). Since hydrogen peroxide (H_2O_2) was the most abundant long-lived ROS present in pPBS treatment, we further evaluated the reliance of H_2O_2 in the killing mechanisms after combination treatment. Addition of catalase, a H_2O_2 -scavenger, abolished the cytotoxic effect induced by pPBS treatment alone in both LN-229 and U-87. However, catalase did not fully suppress the cytotoxic potential when pPBS was combined with AF or in case of AF monotreatment in the U-87 cell line. In the LN-229 cell line, catalase showed stronger inhibition of the killing effect after combination treatment and AF monotreatment compared to U-87 cells (Figure 4.4 C).

Together, these data show that AF is a potent inhibitor of TrxR activity in GBM cells, which saturates their GSH system leading to a modest increase in intracellular ROS levels. While pPBS by itself had limited effect on the TrxR activity and the GSH system, inhibition of the antioxidant system by AF significantly increased intracellular ROS accumulation following pPBS treatment.

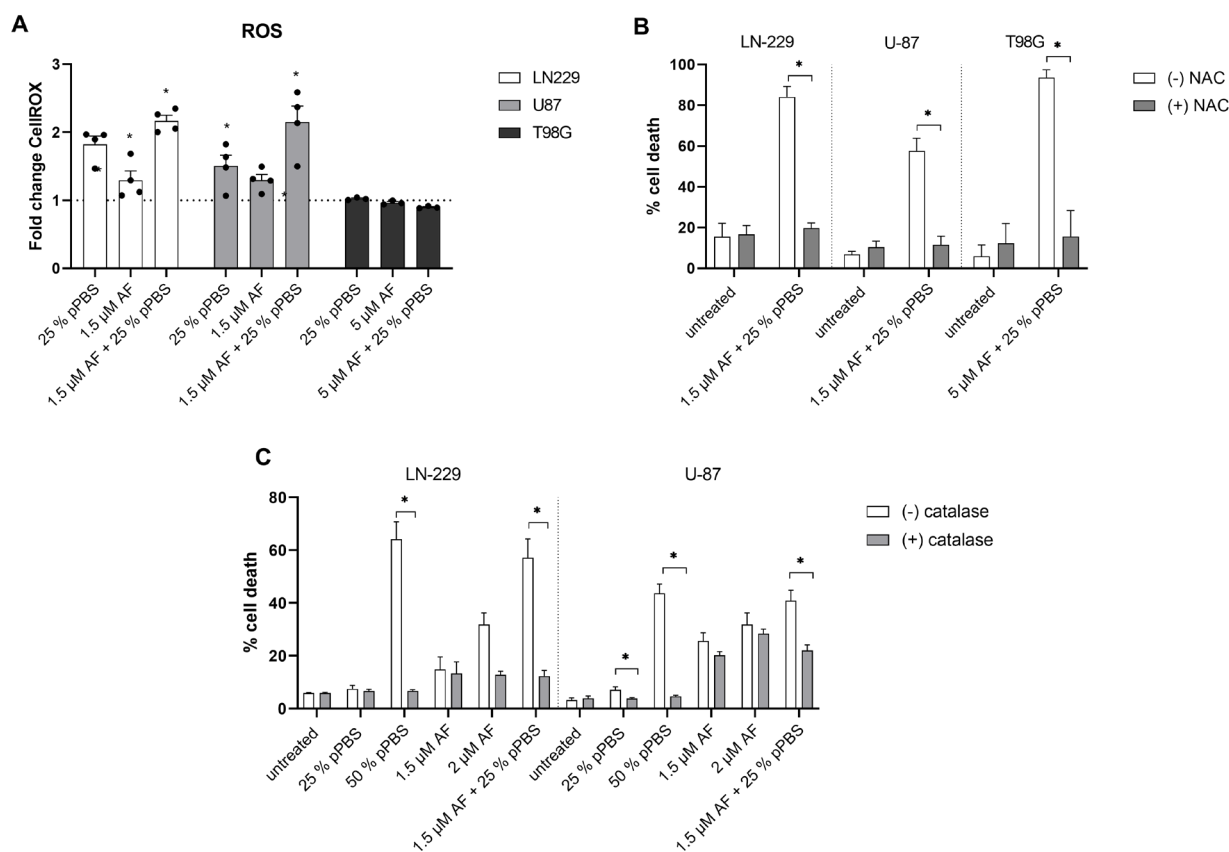


Figure 4.4. The effect on intracellular ROS levels after combination treatment of AF and pPBS. (A) Intracellular ROS levels are shown as fold change of CellROX Green Calibration Units (GCU) for U-87 and LN-229 and CellROX Red Calibration Units (RCU) for T98G cells, relative towards untreated cells after 24 hours of treatment with monotherapies or combination treatment of AF (1.5 μ M or 5 μ M) and 25% pPBS. * $p \leq 0.05$ denotes statistically significant difference compared with untreated control. (B) Percentage of cell death in the absence or presence of NAC pretreatment, after 48 hours of treatment with combination of AF and pPBS. (C) Percentage of cell death in the absence or presence of catalase pretreatment, after 48 hours of treatment. Graphs represent mean \pm SEM of ≥ 3 independent experiments. * $p \leq 0.05$ denotes statistically significant difference.

The combination of AF and pPBS induces apoptotic and ferroptotic characteristics

Next, we unraveled the underlying type of induced cancer cell death after combination treatment of AF and pPBS. In order to investigate the effect of the mono- and combination treatment on cell apoptosis, Annexin V/PI expression and caspase 3/7 activity were determined. A significant time-dependent increase in caspase 3/7 positive U-87 and LN229 cells was observed after combination treatment, which was higher compared to AF/pPBS single treatments (Figure 4.5 A, B). T98G cells are green autofluorescent and therefore not compatible with the caspase 3/7 reagent and thus not considered within this experiment.

Additionally, a significant increase of Annexin V⁺/PI⁺ and Annexin V⁺/PI⁻ proportions of apoptotic cells was observed after 48 hours of combination treatment of AF and pPBS in all cell lines (Figure 4.5 C, D).

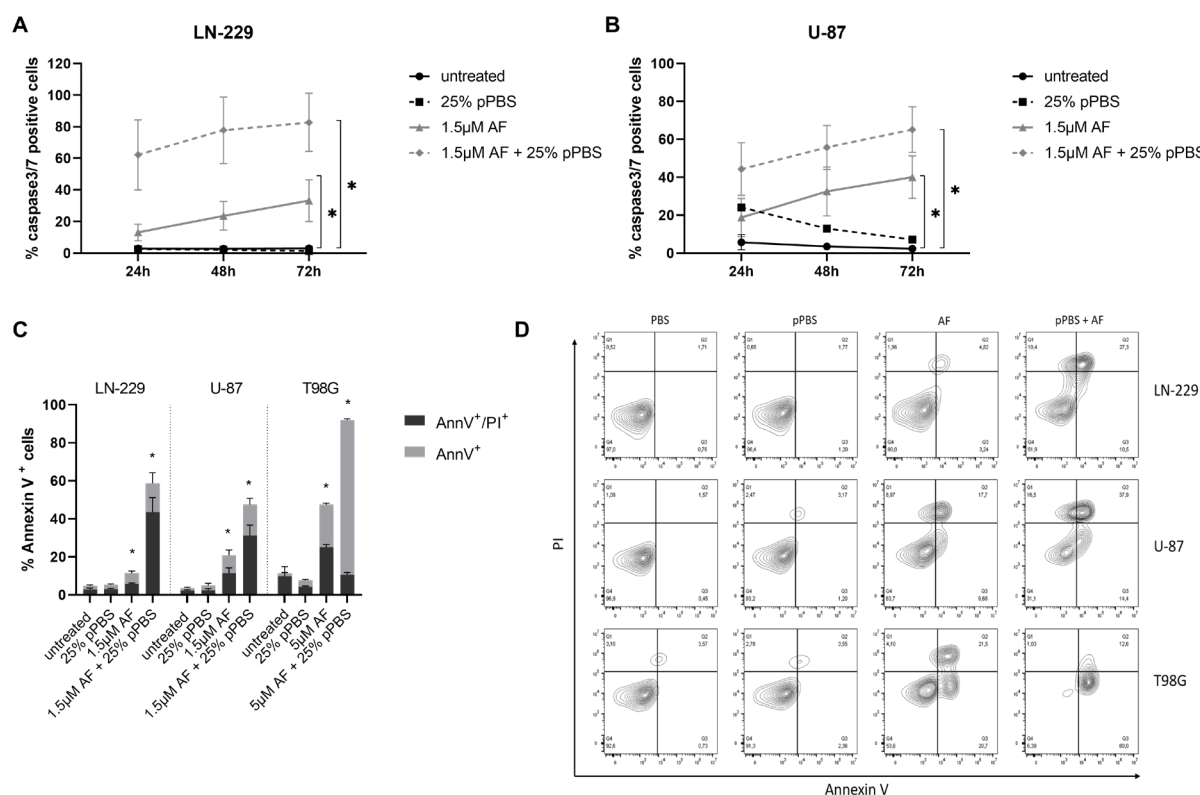


Figure 4.5. The combination treatment of AF and pPBS induces apoptotic cell death in GBM cell lines. (A) Percentage of caspase-3/7 green positive LN-229 cells after 24, 48 and 72 hours of treatment. (B) Percentage of caspase-3/7 green positive U-87 cells after 24, 48 and 72 hours of treatment. (C) Percentage of Annexin V⁺ cells after 48 hours of treatment, subdivisions of AnnV⁺/PI⁻ and AnnV⁺/PI⁺ are made. (D) Representative contour plots showing the flow cytometric analysis of Annexin V and PI staining after 48 hours of treatment. Q1 = AnnV⁺/PI⁺, Q2 = AnnV⁺/PI⁻, Q3 = AnnV⁻/PI⁻, Q4 = AnnV⁻/PI⁺. Graphs represent mean \pm SEM of ≥ 3 independent experiments. * $p \leq 0.05$ denotes statistically significant difference compared with untreated control.

ROS are known to interact with lipids leading to lipid peroxidation, which can result in ferroptotic cell death. Lipid peroxidation increased significantly after treatment with the combination of AF and pPBS, in U-87 and LN-229 cell line (Figure 4.6 A, B). Moreover, deferoxamine (DFO), an inhibitor of lipid peroxidation, was able to inhibit this process in LN-229 cells (Figure 4.6 C). Again, T98G was excluded in the flow cytometric examination of lipid peroxidation due to its autofluorescence, however, T98G could be included for cell death analysis after inhibition with DFO. Interestingly, combination treatment-induced cell death was inhibited by DFO in LN-229 and T98G cells, which was not observed in the U-87 cell line (Figure 4.6 D). A lower concentration of DFO (50 μ M) was added to the U-87

cell line, because the higher concentration (100 μM) used in LN-229 and T98G cells showed a cytotoxic effect on U-87 cells. This could explain why no inhibition was observed in the U-87 cell line. Another inhibitor, Fer-1 was not able to inhibit the combination treatment-induced cell death. However, Fer-1 also failed to inhibit treatment-induced lipid peroxidation, showing that DFO is a more potent inhibitor (Figure 4.7).

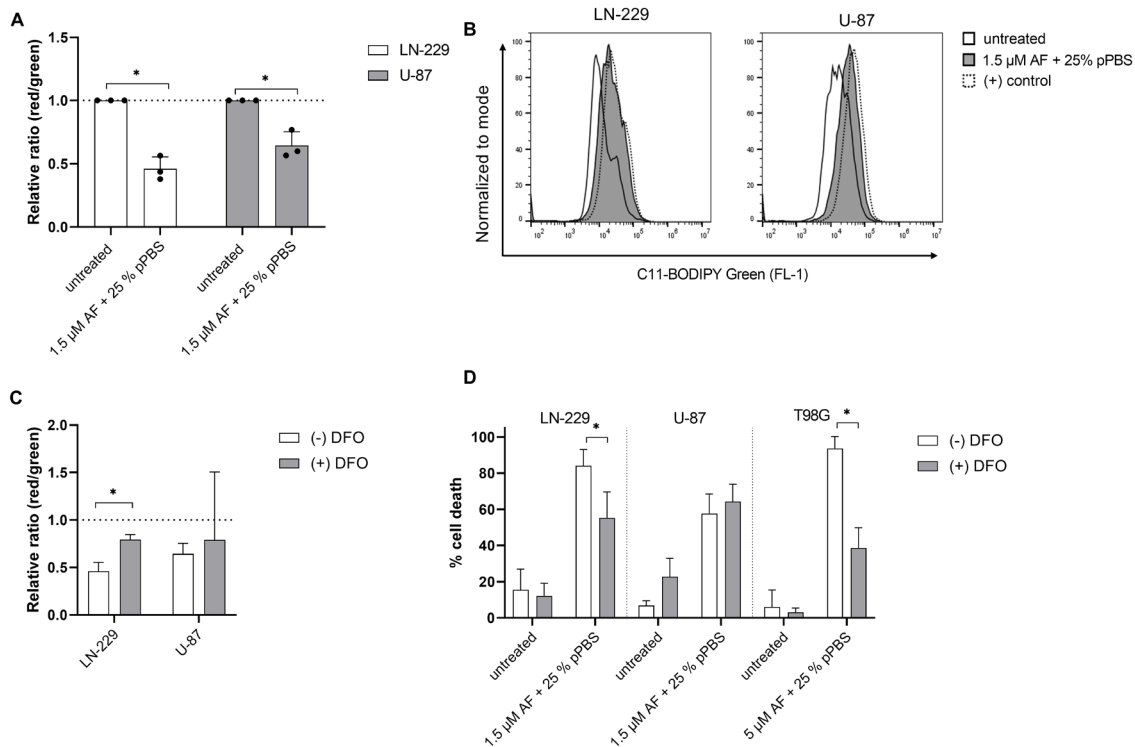


Figure 4.6. The combination treatment of AF and pPBS induces ferroptotic characteristics in GBM cell lines. (A) Lipid peroxidation presented as relative ratio of red/green MFI signal after flow cytometric analysis of the C11-BODIPY 581/591 reagent after 48 hours of treatment of AF (1.5 μM or 5 μM) in combination with 25% pPBS. (B) Representative overlay histograms of C11 BODIPY green signal (FL-1) after combination treatment of 1.5 μM AF with 25% pPBS for 48 hours or cumene hydroperoxide (positive control) for 2 hours. (C) Lipid peroxidation presented as relative ratio of red/green MFI signal of the C11-BODIPY 581/591 reagent in absence or in presence of DFO (100 μM) after 48 hours of combination treatment with 1.5 μM AF and 25% pPBS. (D) Percentage of cell death after 48 hours of treatment of AF (1.5 μM or 5 μM) in combination with 25% pPBS in the absence and presence of DFO (100 μM), an inhibitor of ferroptosis. Graphs represent mean \pm SD of ≥ 3 independent experiments. * $p \leq 0.05$ denotes statistically significant difference compared with untreated control.

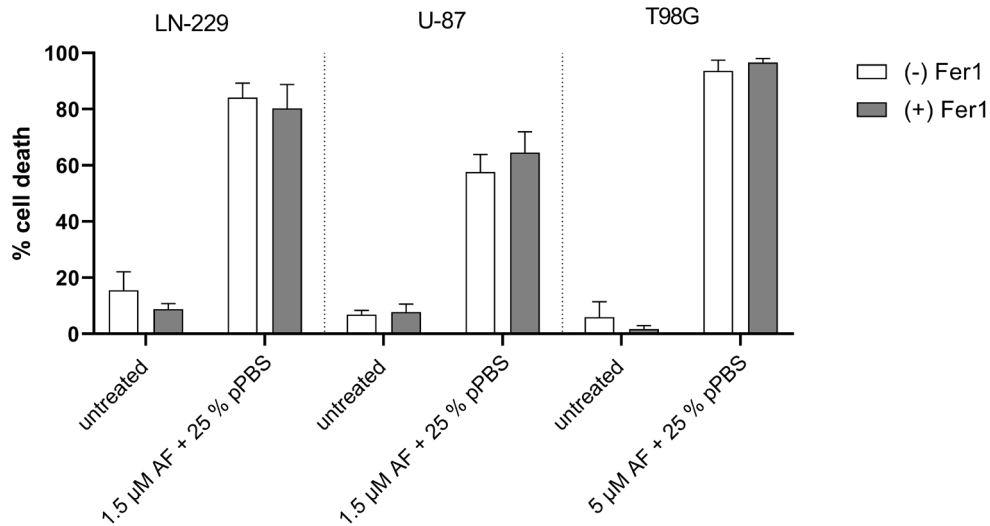


Figure 4.7. The effect of ferrostatin-1 on cell death induced via combination treatment of AF and pPBS in GBM cell lines. Percentage of cell death after 48 hours of treatment of AF (1.5 μ M or 5 μ M) in combination with 25% pPBS in the absence and presence of Fer-1 (1 μ M), an inhibitor of ferroptosis. Graphs represent mean \pm SEM of \geq 3 independent experiments.

Together, these results suggest that the combination of AF and pPBS is able to induce distinct types of cell death, including apoptosis and ferroptosis.

The combination treatment of AF and pPBS induces immunogenic cell death in GBM cells

Since different cancer treatments have the capacity to elicit ICD, depending on their ability to produce ROS and cause oxidative stress, we investigated the potential of our sequential combination strategy to elicit ICD. Three important hallmarks of ICD were elevated in all three GBM cell lines, following combination treatment with AF and pPBS, which include surface expression of CRT (ecto-CRT), extracellular ATP and HMGB1 release (Figure 4.8 A–C). However, there was no statistically significant release and expression of these danger signals when GBM cells were treated with pPBS alone (Figure 4.10 A-C).

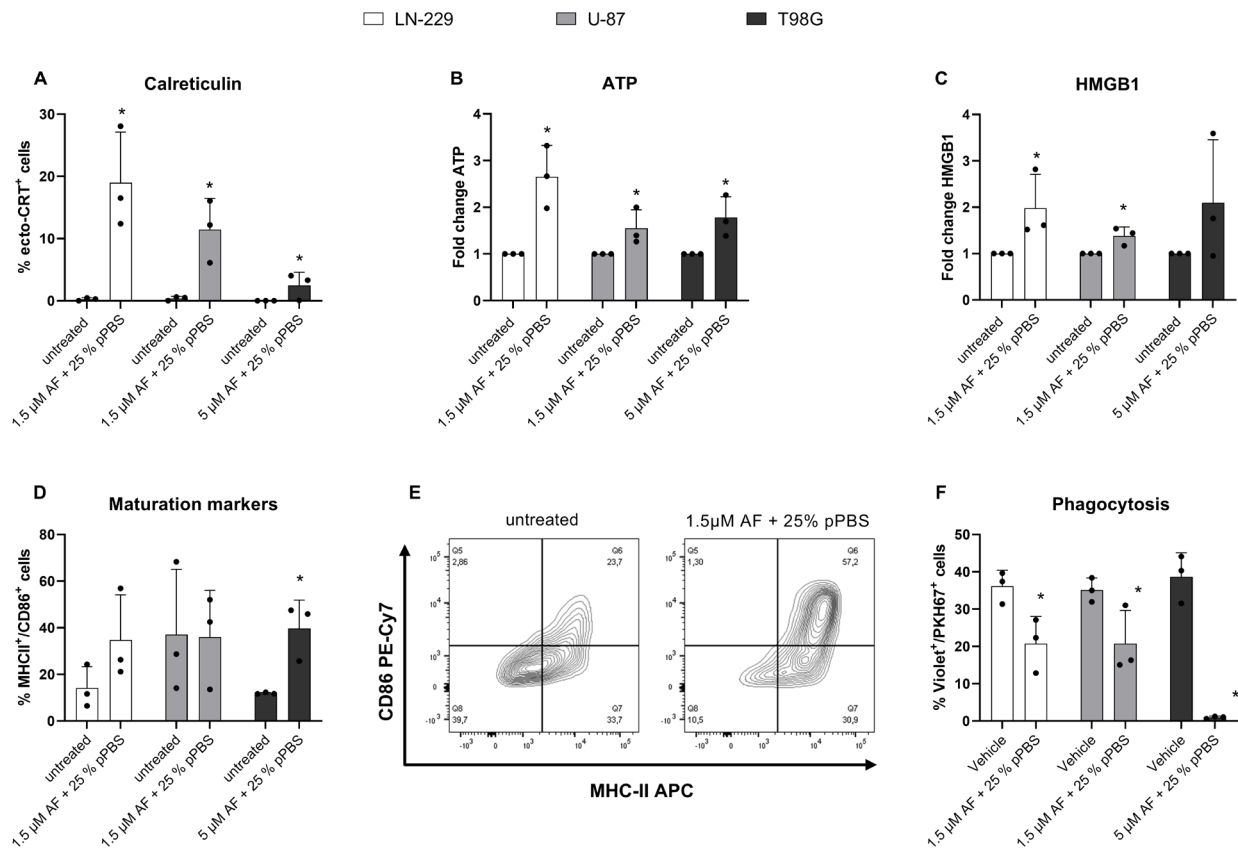


Figure 4.8. The effect of AF and pPBS combination treatment on release of ICD danger signals and DC maturation and phagocytosis. (A) Percentage of surface-exposed calreticulin (ecto-CRT) positive cells after 48 hours of combination treatment with AF (1.5 μM or 5 μM) and pPBS (25%). (B) Secretion of ATP after 4 hours of combination treatment with AF (1.5 μM or 5 μM) and pPBS (25%). These data represent the fold change of ATP secretion (nM range). (C) Secretion of HMGB1 after 48 hours of combination treatment with AF (1.5 μM or 5 μM) and pPBS (25%). These data represent the fold change of ATP secretion (ng/mL range). (D) Percentage of MHC-II/CD86 double positive DCs after 48 hours of co-culture with AF (1.5 μM or 5 μM) and pPBS (25%) combination-treated LN-229, U-87 or T98G cells (E:T ratio 1:1) using flow cytometry. (E) Representative contour plots of DC population double positive for MHC-II and CD86 in coculture with either PBS-treated and combination-treated LN-229. (F) Percentage of phagocytosis after 48 hours of violet-labeled DCs in co-culture with AF (1.5 μM or 5 μM) and pPBS (25%) combination-treated PKH67-labeled GBM cells (E:T ratio 1:1). Phagocytosis of PKH67+ tumor cells by violet-labeled DCs is expressed as %PKH67+violet+ cells within the violet+ DC population. Graphs represent mean ± SD of ≥ 3 independent experiments. *p ≤ 0.05 denotes statistically significant difference compared with untreated control.

Expression and release of these ICD-associated danger signals by dying tumor cells contribute to the activation and maturation of DCs to initiate an effective antitumor immune response. To this end, we investigated if the combination strategy of AF and pPBS could induce DC maturation. We observed an increase in mature CD86+/MHCII+ DC population (Figure 4.9 A) after coculture with treated LN-229 and T98G cell lines (Figure 4.8 D, E). No increase in DC maturation was observed with U-87 cells. Additionally, we

investigated the influence of treated GBM cells on the phagocytotic capacity by immature DCs. Flow cytometric analysis revealed that phagocytosis by immature DCs was significantly inhibited after treatment of AF in combination with pPBS (Figure 4.8 F). AF was shown to be responsible for this effect, since AF single treatment also caused inhibition of phagocytosis (Figure 4.9 B). After treatment with pPBS alone, no increase in DC maturation or phagocytosis by DCs was observed in coculture with GBM cells (Figure 4.10 E).

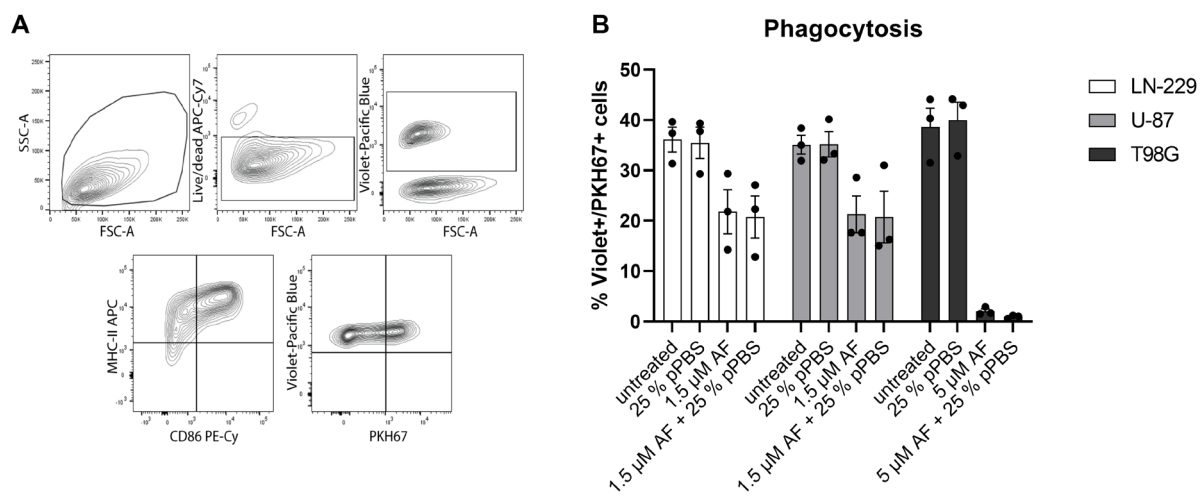


Figure 4.9. Gating strategy and effect of monotherapies on phagocytosis of GBM cells. (A) Gating strategy of maturation of DCs and phagocytosis by DCs. (B) Percentage of phagocytosis after 48 hours of violet-labeled DCs in co-culture with PKH67-labeled GBM cells (E:T ratio 1:1) after treatment with monotherapies and combination therapy of AF (1.5 μ M or 5 μ M) and pPBS (25%). Phagocytosis of PKH67+ tumor cells by violet-labeled DCs is expressed as %PKH67+violet+ cells within the violet+ DC population. Graphs represent mean \pm SEM of ≥ 3 independent experiments. * $p \leq 0.05$ denotes statistically significant difference compared with untreated control.

Collectively, our results show that combination of AF and pPBS induced release of the most important *in vitro* hallmarks of ICD and was able to induce DC maturation in two GBM cell lines. However, caution should be taken when using AF to induce an effective antitumor immune response since this compound has the capacity to inhibit DC phagocytosis *in vitro*.

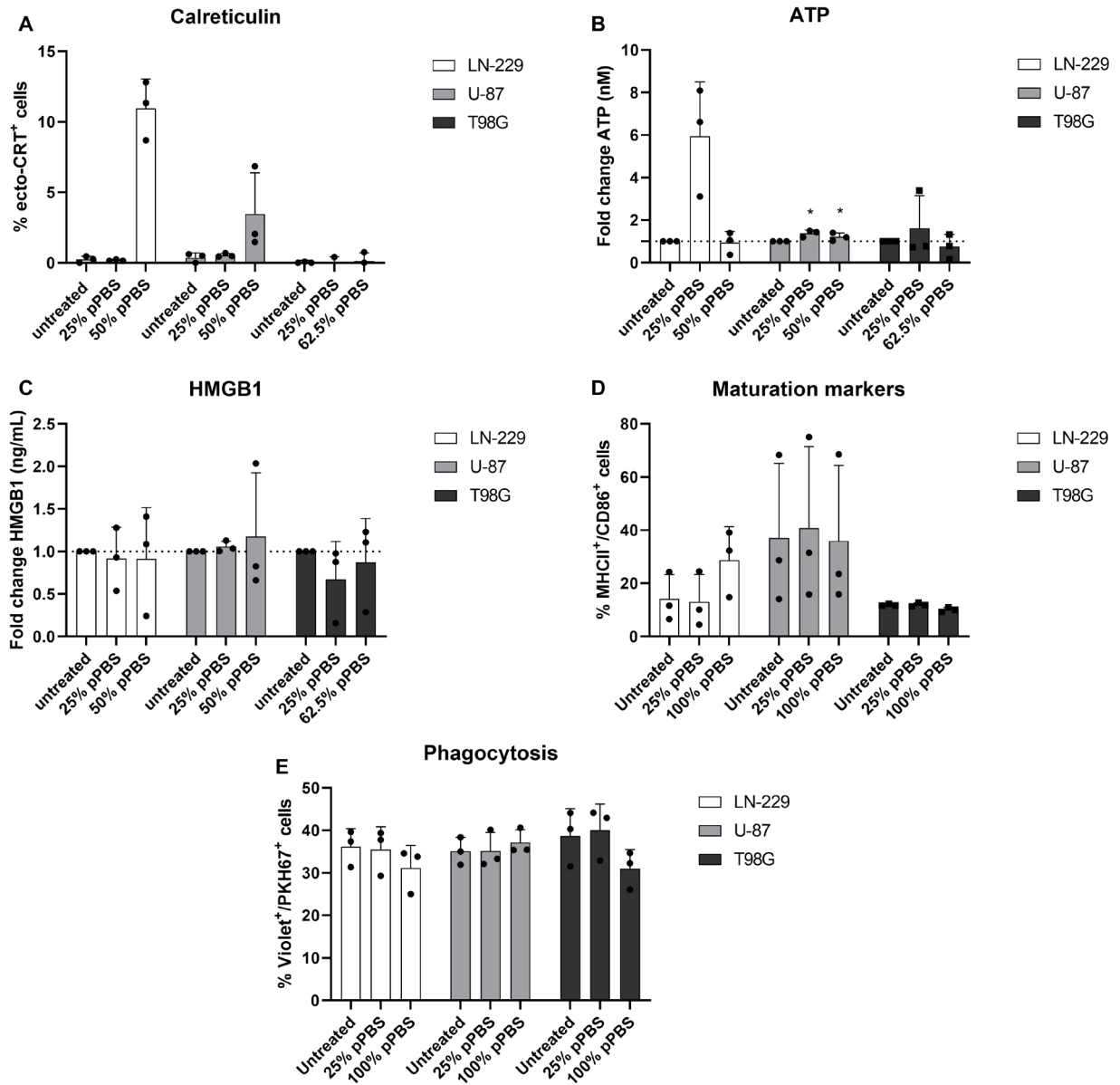


Figure 4.10. The effect of pPBS monotreatment on induction of ICD, DC maturation and phagocytosis. (A) Percentage of surface-exposed calreticulin (ecto-CRT) positive cells after 48 hours of monotreatment with pPBS. (B) Secretion of ATP after 4 hours of monotreatment with pPBS. These data represent the fold change of ATP secretion (nM range). (C) Secretion of HMGB1 after 48 hours of monotreatment with pPBS. These data represent the fold change of ATP secretion (ng/mL range). (D) Percentage of MHC-II/CD86 double positive DCs after 48 hours of co-culture with pPBS-treated GBM cells (E:T ratio 1:1) using flow cytometry. (E) Percentage of phagocytosis after 48 hours of violet-labeled DCs in co-culture with pPBS-treated PKH67-labeled GBM cells (E:T ratio 1:1). Phagocytosis of PKH67+ tumor cells by violet-labeled DCs is expressed as %PKH67+violet+ cells within the violet+ DC population. Graphs represent mean \pm SD of ≥ 3 independent experiments. * $p \leq 0.05$ denotes statistically significant difference compared with untreated control.

The combination treatment of AF and plasma leads to synergistic inhibition of 3D spheroid growth

Finally, we examined the combination strategy in a 3D single spheroid model, using higher concentrations of AF (3.5 μM – 7.5 μM for sensitive cell lines and 10 – 15 μM for the resistant cell line). Since indirect pPBS treatment had little or no effect on the viability of spheroids (Figure 4.11), a direct plasma treatment method was used, previously optimized in our lab and described by Privat-Maldonado et al (22). After 4 hours of AF treatment, the supernatant with the compound was replaced with PBS, followed by a single direct 3 minute exposure to plasma and further incubation for 90 minutes. Afterwards, PBS was replaced by the supernatant, containing AF, of the corresponding spheroid for a total of 72 hours. A decrease in cell survival was observed after mono- and combination treatments of AF and plasma (Figure 4.12 A,B). The interaction of AF and plasma was only significant with higher AF concentrations in LN-229 (7.5 μM AF) and T98G (10 and 12.5 μM AF) cell lines, as shown in Figure 4.12 A,B. Additionally, the combination index showed that the effect of AF was synergistically enhanced by plasma, however, only in combination with higher AF concentrations (CI < 1 with 7.5 μM for LN-229 and U-87 or 15 μM for T98G). In combination with lower concentrations of AF, the effect on cell survival showed even to be antagonistic (CI > 1, Figure 4.12 C).

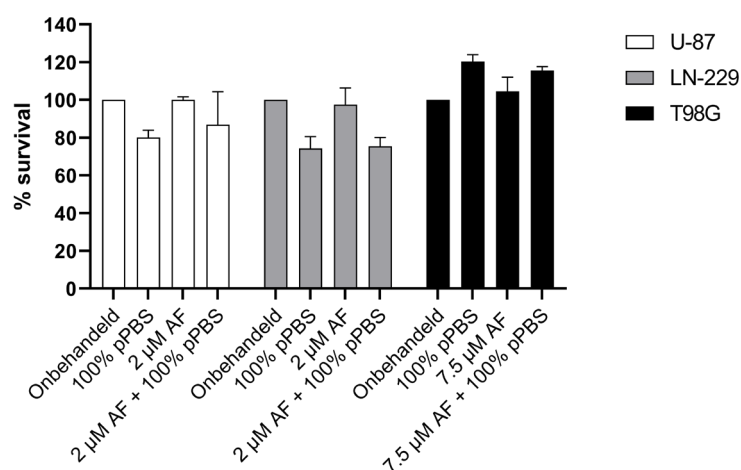


Figure 4.11. The effect of pPBS and AF on survival of GBM spheroids. Dose-response survival curves after 72 hours of AF (2 or 7.5 μM) and pPBS (100%) monotreatment and combination treatment. Graphs represent mean \pm SEM of ≥ 3 independent experiments. No statistical significant interaction between AF and pPBS was observed.

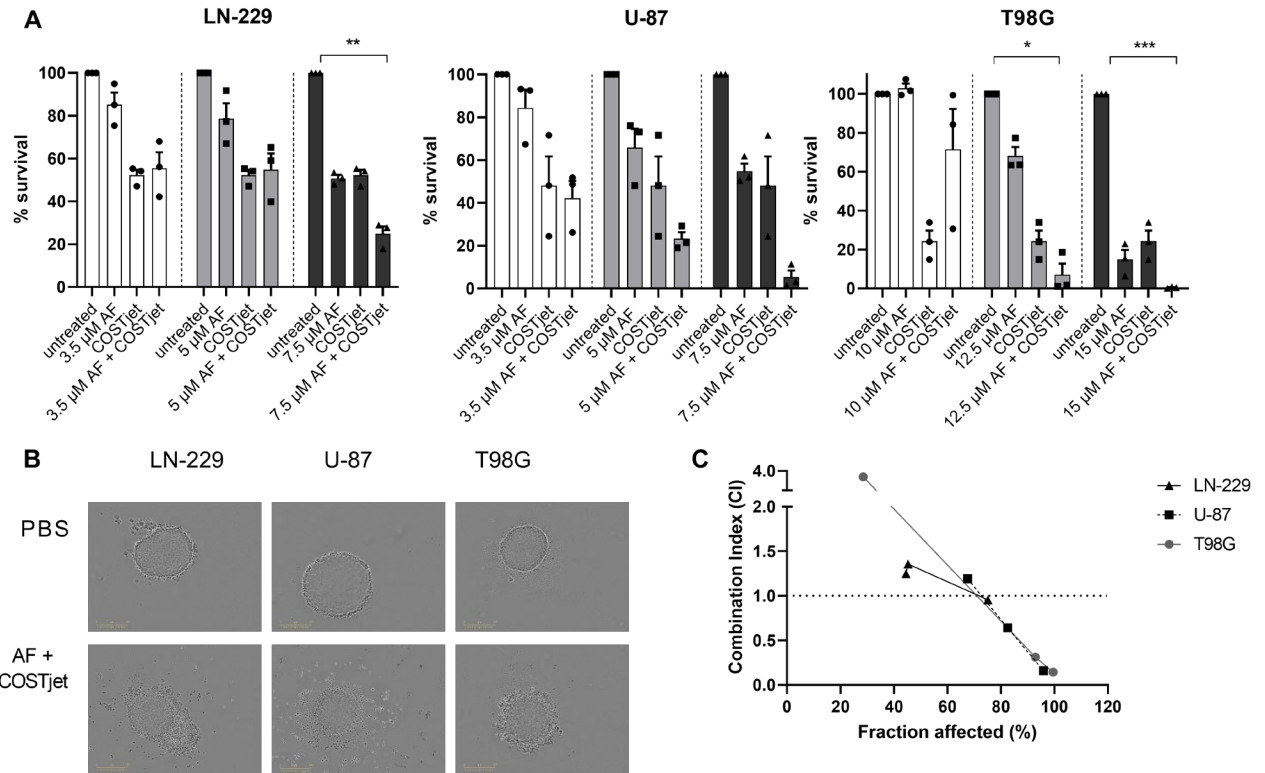


Figure 4.12. The effect of the sequential combination treatment of AF and plasma on survival of GBM spheroids. (A) Dose-response survival curves after 72h of AF (3.5 – 15 μM) and plasma (COST jet) single treatments and the combination of AF and plasma. Graphs represent mean ± SEM of ≥ 3 independent experiments. P-values represented as * < 0.05; ** < 0.01; *** < 0.001 denotes significant interaction between AF and plasma. (B) Representative microscopic images after 72h of untreated and combination treated GBM cells (7.5 μM AF + COST jet for U-87, LN-229 and 15 μM + COST jet for T98G). (C) The corresponding combination index (CI) for each AF concentration. CI > 1 indicates an antagonistic effect, CI = 1 an additive effect and CI < 1 a synergistic effect.

Discussion

Oxidative stress due to elevated ROS levels and an inability to balance the intracellular redox state is considered the ‘Achilles heel’ of cancer cells and has recently been highlighted as a promising target for anticancer strategies (4, 25). In this study, we hypothesized that increasing oxidative stress through a combination strategy of delivering exogenous ROS and inhibiting the protective antioxidant system, could result in a synergistic and promising anti-GBM treatment strategy. Therefore we used cold atmospheric plasma as a novel anti-cancer therapy to disturb ROS homeostasis in cancer cells via delivery of exogenous ROS, as previously described in different tumor types, including GBM (12, 26). Additionally, AF was selected as inhibitor of the antioxidant defense system through inhibition of TrxR. The TrxR levels in GBM patients are 31% higher in circulating blood and 5 times higher in GBM tissue compared to matched controls, both indicating a significant pathophysiological role for TrxR in GBM and emphasizing the therapeutic potential of AF (27). In this context, AF has already shown to be a promising partner to be combined with temozolomide in a novel treatment strategy for GBM (18, 28).

Our results indicated that pPBS synergistically enhances the therapeutic effect of AF in three different GBM cell lines, thereby confirming our hypothesis. The synergistic effects of AF and plasma were further investigated *in vitro* in 3D tumor spheroids. This spheroid model is characterized with biophysical properties of solid tumors such as oxygen and nutrient gradients, which are relevant when investigating oxidative-stress inducing treatment strategies (29). For the treatment of 3D spheroids we used a different plasma device, which has already been shown effective when directly treating GBM spheroids (22). This direct plasma treatment method generates a higher concentration of ROS, which we showed to be necessary for effectivity in spheroids. Synergistic effects between AF and pPBS or AF and direct plasma treatment were observed in 2D cell cultures and 3D spheroids, respectively. Interestingly, in lower AF concentrations the combinatorial effect was shown to be antagonistic in 3D spheroids. We hypothesize that in combination with lower concentrations of AF, the accumulation of intracellular ROS was too small, causing GBM spheroids to adapt by enhancing their protective antioxidant system. Indeed it has been reported that radiation-induced oxidative stress was considerably less in spheroids as compared to monolayers and corresponded with an increase in radioresistance, due to

alterations in intracellular ROS levels and redox status (e.g. activity of antioxidant enzymes) during spheroid development (30, 31). In order to be effective *in vivo*, it might be that high dosages of AF are required to treat cancer, even in combination with other therapies (32, 33).

Differences in sensitivity were observed between different GBM cell lines, with T98G being more resistant compared to LN-229 and U-87 cell lines. This could be explained by higher GSH baseline levels and TrxR activity and corresponding lower ROS levels in the resistant T98G cell line. Consistently, it was shown that T98G was more resistant to temozolomide chemotherapy as a result of lower ROS levels and higher total antioxidant capacity and GSH concentration (34). Therefore, increasing exogenous ROS levels together with inhibition of the antioxidant defense system could overcome this therapy resistance.

The role of ROS was investigated to elucidate on the underlying mechanisms of cell death after mono and combination treatment. We demonstrated a high intracellular ROS accumulation after treatment with the combination of AF and pPBS. We confirmed this ROS-mediated response *in vitro*, as the ROS scavenger NAC reversed the combination treatment-mediated cell death in all GBM cell lines. However, catalase only rescued the pPBS-induced cell death, revealing that exogenous H₂O₂ was the primary mediator of the pPBS-induced cell death, as previously described (35, 36). In the LN-229 cell line, catalase also showed a strong inhibition after combination treatment and AF monotreatment. Such an inhibition was less pronounced in the U-87 cell line after combination treatment or AF monotreatment, showing H₂O₂-independent effects contributing to the killing capacity after AF treatment alone and in combination with pPBS. In addition to catalase, the Trx/TrxR and GSH antioxidant systems are partly responsible for the removal of endogenous H₂O₂. Besides H₂O₂, the Trx and GSH systems participate in the reduction of different kinds of endogenous ROS and RNS (37). Since AF showed to inhibit these two antioxidant systems, incomplete removal of H₂O₂ and other types of ROS might explain why catalase did not completely abolish AF- and combination-induced cell death.

Next, we demonstrated a high intracellular ROS accumulation after treatment with the combination of AF and pPBS. We confirmed this ROS-mediated response *in vitro*, as the ROS scavenger NAC reversed the combination treatment-mediated cell death in all GBM cell lines. Accumulation of intrinsic ROS has shown to be important not only for induction

of apoptosis, but also ferroptosis (38). Therefore, we did a more in-depth analysis of the underlying ROS-mediated cell death mechanism after treatment with AF and pPBS. We discovered that this ROS-inducing combination treatment sensitized GBM cells for caspase-3/7-dependent apoptosis, based on an increase of caspase-3/7- and Annexin V-positive cells, as well as ferroptosis, due to lipid peroxidation and cell death inhibition by an iron chelating agent, DFO. Contrary to DFO, the level of protection against cell death by Fer-1 was incomplete as Fer-1 failed to protect cells from lipid peroxidation. Previously, we already showed that DFO and Fer-1 were able to partially prevent cell death in non-small cell lung cancer after AF treatment alone (39). Excessive ROS induced after combination treatment of AF and pPBS could explain this incomplete protection of Fer-1 (40). To date, previous studies have reported that AF and pPBS induce cancer cell death through ROS-mediated endoplasmic reticulum (ER) stress and activation of the apoptotic pathway in different cancer types (36, 41-44). Other findings indicate that both treatments are linked to ferroptosis triggered by ROS accumulation leading to iron-mediated lipid peroxidation and cell death (36, 45). Recently, our research group also demonstrated the induction of ferroptosis and apoptosis in non-small cell lung cancer after AF treatment (39). However, we are the first to show that the combination of both treatment types sensitizes GBM cells for apoptotic and ferroptotic cell death.

Furthermore, we demonstrated the immunogenic potential of the AF and pPBS combination treatment-induced apoptotic and ferroptotic cell death in GBM cells. Besides the immunogenic potential of apoptosis, it was recently described that ferroptosis is a novel approach for the induction of antitumor immunity triggered by ferroptosis-dependent ICD (46, 47). It has been suggested that cancer cells dying through distinct ICD-inducing mechanisms, might achieve a superior antitumor immune response (46). The induction of oxidative stress through the production of ROS is the common underlying factor in different ICD-inducing therapies (48). Since the induced cytotoxic effect in our study was clearly dependent on the high accumulation of intracellular ROS, we investigated if the combination of AF and pPBS was able to elicit different ICD-related DAMPs and subsequently stimulate maturation and phagocytosis by DCs. In a previous study report, we already showed the release of several ICD markers and subsequent maturation of DC and phagocytosis by DCs, after pPBS treatment in pancreatic cancer cells (12). Here, we

also reported a significant release of danger signals and maturation of DCs after combination treatment of AF and pPBS in a GBM cell panel. However, the phagocytotic capacity of DCs was inhibited after combination treatment. A similar inhibition of phagocytosis was observed after AF monotherapy, suggesting that AF was responsible for the effect. This is in line with other studies showing that AF could inhibit phagocytosis (49). This can be explained by the history of its use as an antirheumatoid arthritis drug linked to inhibition of pro-inflammatory mediators and oxidative burst in monocytes and granulocytes necessary for effective phagocytosis (50). Based on our results AF could have both pro- and anti-inflammatory effects, warranting investigation of this AF and plasma combination in an *in vivo* setting.

Conclusion

Altogether, the effectiveness of the combination treatment of AF and plasma to synergistically eradicate GBM cells was shown through different ROS-dependent molecular mechanisms, being apoptosis and ferroptosis. Both cell death mechanisms resulted in a significant increase of DAMPs and maturation of DCs *in vitro*, indicating the potential antitumoral immunogenic effect. Contrary to these immunostimulatory effects, a potential inhibitory effect on the phagocytotic capacity of DCs due to AF should be taken into consideration for future research when exploring combination strategies with AF. In conclusion, our study provides a novel therapeutic strategy for GBM to enhance the efficacy of oxidative stress-inducing therapy through a combination of increasing exogenous ROS and inhibiting the protective antioxidant system.

References

1. Taylor OG, Brzozowski JS, Skelding KA. Glioblastoma Multiforme: An Overview of Emerging Therapeutic Targets. *Frontiers in oncology*. 2019;9:963.
2. Stupp R, Mason WP, van den Bent MJ, Weller M, Fisher B, Taphoorn MJ, et al. Radiotherapy plus concomitant and adjuvant temozolomide for glioblastoma. *The New England journal of medicine*. 2005;352(10):987-96.
3. Ostrom QT, Patil N, Cioffi G, Waite K, Kruchko C, Barnholtz-Sloan JS. CBTRUS Statistical Report: Primary Brain and Other Central Nervous System Tumors Diagnosed in the United States in 2013-2017. *Neuro-oncology*. 2020;22(12 Suppl 2):iv1-iv96.
4. Perillo B, Di Donato M, Pezone A, Di Zazzo E, Giovannelli P, Galasso G, et al. ROS in cancer therapy: the bright side of the moon. *Exp Mol Med*. 2020;52(2):192-203.
5. Nogueira V, Hay N. Molecular pathways: reactive oxygen species homeostasis in cancer cells and implications for cancer therapy. *Clinical cancer research : an official journal of the American Association for Cancer Research*. 2013;19(16):4309-14.
6. Kim SJ, Kim HS, Seo YR. Understanding of ROS-Inducing Strategy in Anticancer Therapy. *Oxidative medicine and cellular longevity*. 2019;2019:5381692.
7. Lin A, Biscop E, Breen C, Butler SJ, Smits E, Bogaerts A. Critical Evaluation of the Interaction of Reactive Oxygen and Nitrogen Species with Blood to Inform the Clinical Translation of Nonthermal Plasma Therapy. *Oxidative medicine and cellular longevity*. 2020;2020:9750206.
8. Lin A, Gorbanev Y, De Backer J, Van Loenhout J, Van Boxem W, Lemièrè F, et al. Non-Thermal Plasma as a Unique Delivery System of Short-Lived Reactive Oxygen and Nitrogen Species for Immunogenic Cell Death in Melanoma Cells. *Advanced Science*. 2019:1802062.
9. Yan D, Xu W, Yao X, Lin L, Sherman JH, Keidar M. The Cell Activation Phenomena in the Cold Atmospheric Plasma Cancer Treatment. *Sci Rep*. 2018;8(1):15418.
10. Yan DY, Sherman JH, Keidar M. Cold atmospheric plasma, a novel promising anti-cancer treatment modality. *Oncotarget*. 2017;8(9):15977-95.
11. Vermeylen S, De Waele J, Vanuytsel S, De Backer J, Van der Paal J, Ramakers M, et al. Cold atmospheric plasma treatment of melanoma and glioblastoma cancer cells. *Plasma Process Polym*. 2016;13(12):1195-205.
12. Van Loenhout J, Flieswasser T, Freire Boullosa L, De Waele J, Van Audenaerde J, Marcq E, et al. Cold Atmospheric Plasma-Treated PBS Eliminates Immunosuppressive Pancreatic Stellate Cells and Induces Immunogenic Cell Death of Pancreatic Cancer Cells. *Cancers*. 2019;11(10).
13. Akter M, Jangra A, Choi SA, Choi EH, Han I. Non-Thermal Atmospheric Pressure Bio-Compatible Plasma Stimulates Apoptosis via p38/MAPK Mechanism in U87 Malignant Glioblastoma. *Cancers*. 2020;12(1).
14. Onodera T, Momose I, Kawada M. Potential Anticancer Activity of Auranofin. *Chem Pharm Bull (Tokyo)*. 2019;67(3):186-91.
15. Roder C, Thomson MJ. Auranofin: repurposing an old drug for a golden new age. *Drugs R D*. 2015;15(1):13-20.
16. Pantziarka P, Verbaanderd C, Sukhatme V, Rica Capistrano I, Crispino S, Gyawali B, et al. ReDO_DB: the repurposing drugs in oncology database. *Ecancermedicalscience*. 2018;12:886.
17. Skaga E, Skaga IO, Grieg Z, Sandberg CJ, Langmoen IA, Vik-Mo EO. The efficacy of a coordinated pharmacological blockade in glioblastoma stem cells with nine repurposed drugs using the CUSP9 strategy. *Journal of cancer research and clinical oncology*. 2019.
18. Kast RE, Karpel-Massler G, Halatsch ME. CUSP9* treatment protocol for recurrent glioblastoma: aprepitant, artesunate, auranofin, captopril, celecoxib, disulfiram, itraconazole, ritonavir, sertraline augmenting continuous low dose temozolomide. *Oncotarget*. 2014;5(18):8052-82.
19. Karlenius TC, Shah F, Yu WC, Hawkes HJ, Tinggi U, Clarke FM, et al. The selenium content of cell culture serum influences redox-regulated gene expression. *Biotechniques*. 2011;50(5):295-301.
20. Gibbs-Flournoy EA, Simmons SO, Bromberg PA, Dick TP, Samet JM. Monitoring intracellular redox changes in ozone-exposed airway epithelial cells. *Environ Health Perspect*. 2013;121(3):312-7.
21. Bekeschus S, Schmidt A, Weltmann KD, von Woedtke T. The plasma jet kINPen - A powerful tool for wound healing. *Clin Plasma Med*. 2016;4(1):19-28.

22. Privat-Maldonado A, Gorbaney Y, Dewilde S, Smits E, Bogaerts A. Reduction of Human Glioblastoma Spheroids Using Cold Atmospheric Plasma: The Combined Effect of Short- and Long-Lived Reactive Species. *Cancers*. 2018;10(11).
23. Deben C, Lardon F, Wouters A, Op de Beeck K, Van den Bossche J, Jacobs J, et al. APR-246 (PRIMA-1(MET)) strongly synergizes with AZD2281 (olaparib) induced PARP inhibition to induce apoptosis in non-small cell lung cancer cell lines. *Cancer letters*. 2016;375(2):313-22.
24. Smits EL, Ponsaerts P, Van de Velde AL, Van Driessche A, Cools N, Lenjou M, et al. Proinflammatory response of human leukemic cells to dsRNA transfection linked to activation of dendritic cells. *Leukemia*. 2007;21(8):1691-9.
25. Jia JJ, Geng WS, Wang ZQ, Chen L, Zeng XS. The role of thioredoxin system in cancer: strategy for cancer therapy. *Cancer chemotherapy and pharmacology*. 2019;84(3):453-70.
26. Van Boxem W, Van der Paal J, Gorbaney Y, Vanuytsel S, Smits E, Dewilde S, et al. Anti-cancer capacity of plasma-treated PBS: effect of chemical composition on cancer cell cytotoxicity. *Sci Rep*. 2017;7(1):16478.
27. Kemerdere R, Kacira T, Hanimoglu H, Kucur M, Tanriverdi T, Canbaz B. Tissue and plasma thioredoxin reductase expressions in patients with glioblastoma multiforme. *J Neurol Surg A Cent Eur Neurosurg*. 2013;74(4):234-8.
28. Kast RE, Boockvar JA, Bruning A, Cappello F, Chang WW, Cvek B, et al. A conceptually new treatment approach for relapsed glioblastoma: coordinated undermining of survival paths with nine repurposed drugs (CUSP9) by the International Initiative for Accelerated Improvement of Glioblastoma Care. *Oncotarget*. 2013;4(4):502-30.
29. Katt ME, Placone AL, Wong AD, Xu ZS, Searson PC. In Vitro Tumor Models: Advantages, Disadvantages, Variables, and Selecting the Right Platform. *Front Bioeng Biotechnol*. 2016;4:12.
30. Khaitan D, Chandna S, Arya MB, Dwarakanath BS. Establishment and characterization of multicellular spheroids from a human glioma cell line; Implications for tumor therapy. *J Transl Med*. 2006;4:12.
31. Pereira PMR, Berisha N, Bhupathiraju N, Fernandes R, Tome JPC, Drain CM. Cancer cell spheroids are a better screen for the photodynamic efficiency of glycosylated photosensitizers. *Plos One*. 2017;12(5):e0177737.
32. Fath MA, Ahmad IM, Smith CJ, Spence J, Spitz DR. Enhancement of carboplatin-mediated lung cancer cell killing by simultaneous disruption of glutathione and thioredoxin metabolism. *Clinical cancer research : an official journal of the American Association for Cancer Research*. 2011;17(19):6206-17.
33. Luo M, Shang L, Brooks MD, Jiage E, Zhu Y, Buschhaus JM, et al. Targeting Breast Cancer Stem Cell State Equilibrium through Modulation of Redox Signaling. *Cell Metab*. 2018;28(1):69-86 e6.
34. Zhu Z, Du S, Du Y, Ren J, Ying G, Yan Z. Glutathione reductase mediates drug resistance in glioblastoma cells by regulating redox homeostasis. *J Neurochem*. 2018;144(1):93-104.
35. Bekeschus S, Kolata J, Winterbourn C, Kramer A, Turner R, Weltmann KD, et al. Hydrogen peroxide: A central player in physical plasma-induced oxidative stress in human blood cells. *Free radical research*. 2014;48(5):542-9.
36. Wolff CM, Kolb JF, Weltmann KD, von Woedtke T, Bekeschus S. Combination Treatment with Cold Physical Plasma and Pulsed Electric Fields Augments ROS Production and Cytotoxicity in Lymphoma. *Cancers*. 2020;12(4).
37. Ren X, Zou L, Zhang X, Branco V, Wang J, Carvalho C, et al. Redox Signaling Mediated by Thioredoxin and Glutathione Systems in the Central Nervous System. *Antioxidants & redox signaling*. 2017;27(13):989-1010.
38. Galluzzi L, Vitale I, Aaronson SA, Abrams JM, Adam D, Agostinis P, et al. Molecular mechanisms of cell death: recommendations of the Nomenclature Committee on Cell Death 2018. *Cell death and differentiation*. 2018;25(3):486-541.
39. Boulosa LF, Van Loenhout J, Flieswasser T, De Waele J, Hermans C, Lambrechts H, et al. Auranofin reveals therapeutic anticancer potential by triggering distinct molecular cell death mechanisms and innate immunity in mutant p53 non-small cell lung cancer. *Redox biology*. 2021:101949.
40. Hassannia B, Wiernicki B, Ingold I, Qu F, Van Herck S, Tyurina YY, et al. Nano-targeted induction of dual ferroptotic mechanisms eradicates high-risk neuroblastoma. *The Journal of clinical investigation*. 2018;128(8):3341-55.

41. Li W, Yu KN, Ma J, Shen J, Cheng C, Zhou F, et al. Non-thermal plasma induces mitochondria-mediated apoptotic signaling pathway via ROS generation in HeLa cells. *Archives of biochemistry and biophysics*. 2017;633:68-77.
42. You BR, Shin HR, Han BR, Kim SH, Park WH. Auranofin induces apoptosis and necrosis in HeLa cells via oxidative stress and glutathione depletion. *Mol Med Rep*. 2015;11(2):1428-34.
43. Zou P, Chen M, Ji J, Chen W, Chen X, Ying S, et al. Auranofin induces apoptosis by ROS-mediated ER stress and mitochondrial dysfunction and displayed synergistic lethality with piperlongumine in gastric cancer. *Oncotarget*. 2015;6(34):36505-21.
44. Fan C, Zheng W, Fu X, Li X, Wong YS, Chen T. Enhancement of auranofin-induced lung cancer cell apoptosis by selenocystine, a natural inhibitor of TrxR1 in vitro and in vivo. *Cell death & disease*. 2014;5:e1191.
45. Yang L, Wang H, Yang X, Wu Q, An P, Jin X, et al. Auranofin mitigates systemic iron overload and induces ferroptosis via distinct mechanisms. *Signal Transduct Target Ther*. 2020;5(1):138.
46. Tang D, Kepp O, Kroemer G. Ferroptosis becomes immunogenic: implications for anticancer treatments. *Oncoimmunology*. 2021;10(1):1862949.
47. Efimova I, Catanzaro E, Van der Meeren L, Turubanova VD, Hammad H, Mishchenko TA, et al. Vaccination with early ferroptotic cancer cells induces efficient antitumor immunity. *J Immunother Cancer*. 2020;8(2).
48. Krysko DV, Garg AD, Kaczmarek A, Krysko O, Agostinis P, Vandenabeele P. Immunogenic cell death and DAMPs in cancer therapy. *Nature reviews Cancer*. 2012;12(12):860-75.
49. Han S, Kim K, Song Y, Kim H, Kwon J, Lee YH, et al. Auranofin, an immunosuppressive drug, inhibits MHC class I and MHC class II pathways of antigen presentation in dendritic cells. *Arch Pharm Res*. 2008;31(3):370-6.
50. Wang H, Bouzakoura S, de Mey S, Jiang H, Law K, Dufait I, et al. Auranofin radiosensitizes tumor cells through targeting thioredoxin reductase and resulting overproduction of reactive oxygen species. *Oncotarget*. 2017;8(22):35728-42.

CHAPTER 5

Unraveling the *in vivo* therapeutic potential of auranofin and cold atmospheric plasma in glioblastoma

Jinthe Van Loenhout, Laurie Freire Boulosa, Abraham Lin, Annemie Bogaerts, Evelien Smits, Christophe Deben. Unraveling the *in vivo* therapeutic potential of auranofin and cold atmospheric plasma in glioblastoma. *Manuscript in preparation*.

Abstract

Prognosis of glioblastoma multiforme (GBM) remains dismal, underscoring the need for novel therapeutic approaches. Oxidative stress has recently been highlighted as promising target for anticancer strategies. Targeting the redox balance of GBM by inducing high oxidative stress through delivery of exogenous reactive oxygen species (ROS) and inhibiting endogenous protective antioxidant system might be a beneficial and promising GBM treatment strategy. In this chapter, we describe a novel oxidative stress-mediated combination therapy in an *in vivo* SB28 tumor-bearing GBM model. Firstly, auranofin (AF), a potent thioredoxin reductase antioxidant inhibitor, was delivered in different doses and various administration routes to optimize the mode of treatment *in vivo*. Next, AF was combined with direct cold atmospheric plasma (CAP) treatment to induce exogenous ROS accumulation. We demonstrated a significant decrease in tumor volume and a significant increase in survival of SB28 tumor-bearing mice when CAP was sequentially combined with AF. This novel preclinical data support increasing oxidative stress by our sequential combination therapy of AF and CAP, to be a promising treatment strategy in GBM.

Introduction

We previously have shown (chapter 4) that a novel combinatory therapeutic strategy based on increasing exogenous reactive oxygen species (ROS) via cold atmospheric plasma (CAP) and inhibiting the endogenous protective antioxidant system via auranofin (AF), a potent thioredoxin reductase (TrxR) inhibitor, could induce ROS-mediated cell death in GBM cells, *in vitro*. This combination treatment was able to induce apoptosis and ferroptosis in GBM cells. Furthermore, both cell death mechanisms resulted in the release of danger signals and DC maturation, potentially enhancing the immunogenicity of GBM. However, phagocytosis by DCs was inhibited due to AF in coculture with GBM cells, in contrast to CAP treatment that enhanced phagocytosis by DCs in coculture with pancreatic cancer cells (chapter 3) (1). Based on these cytotoxic and immunomodulating results *in vitro*, it will be of great value to investigate the antitumoral and immunogenic effects of this combination strategy in an immunocompetent *in vivo* GBM model.

Since GBM tumors are characterized by a poorly immunogenic nature, we used an *in vivo* model with similar properties, namely the SB28 GBM mice model. This model features the poorly immunogenic tumor with low MHC-I expression and modest CD8⁺ T-cell infiltration, suggesting that it may present similar challenges for immunomodulating therapies as human GBM (2, 3).

After *in vivo* optimization of AF treatment, with our research as described here, we have confirmed AF to be a potent TrxR inhibitor through both oral and subcutaneous administration routes. Additionally, we have shown that when AF is sequentially combined with direct CAP treatment, this combination exhibits enhanced antitumor efficacy, resulting in an increased survival in SB28 tumor-bearing mice. Whether the effect is mediated by an immunological response, remains to be elucidated.

Material and methods

SB28 tumor bearing mice

Female C57BL/6J mice, age 6-10 weeks, were obtained from Jackson Laboratories and maintained at the animal core facility of the University of Antwerp. All animal procedures were conducted in accordance with and approval of the Animal Ethics Committee of the University of Antwerp under registration number 2020-20. All mice were housed in filter-top cages enriched with houses and nesting material. Mice were checked on a daily base to inspect for health and wellbeing. Mice were given at least 7 days adaption period upon arrival before being included in experiments to reduce stress levels.

The SB28 cell line was cultured in DMEM supplemented with 10% heat-inactivated FBS, 1% penicillin/streptomycin, 1% HEPES and 1% GlutaMAX and maintained at 37 °C and 5% CO₂. The cell line was routinely tested for mycoplasma contamination. The cells were used in the experiments between passage three and six after thawing.

Tumor kinetics and survival

Mice were inoculated subcutaneously into the shaved abdominal flank with 1×10^6 SB28 cells suspended in 100 μ L PBS. Tumor size was monitored with calipers and tumor volume (mm^3) was calculated using the formula $(\text{length} \times \text{width}^2)/2$. When tumors reached an average size of approximately 30 mm^3 , mice were randomized based on tumor size and divided over the different treatment groups. Tumor size was measured thrice a week. Mice were euthanized when a tumor size of 1500 mm^3 was reached.

In vivo administration of AF

AF was administered via different administration routes. Firstly, AF was administered by osmotic minipumps (Alzet, type 1002). Here, AF was dissolved in a vehicle compound composed of 50% DMSO, 40% PEG300, 10% absolute ethanol. The osmotic minipump was filled with 100 μ L of AF or the vehicle. Mice were anaesthetized using isoflurane. Hair was shaved off in the neck area and a small incision was made between the ears. Using a hemostat, a subcutaneous pocket wide enough for an osmotic minipump was created. Calculations for the required AF concentrations for the osmotic minipump were made based on the group average weight and using the online tool provided by Alzet. After

inserting the osmotic minipump, the incision was closed with 2 sterile surgical staples. The osmotic minipump offered a long-term delivery of 14 days, afterwards the osmotic minipump was removed under anesthesia. Secondly, AF was administered daily via oral gavage using a 20G flexible feeding needle for a period of 14 days. Calculations of the required AF concentrations were made per individual mouse based on its body weight for oral gavage. Toxicity of AF was measured based on total body weight, behavior and post-mortem evaluation.

In vivo administration of CAP

A microsecond-pulsed dielectric barrier discharge (DBD) system previously described (4, 5) was used for the CAP treatments. Briefly, a microsecond pulser (Megaimpulse Ltd., Russia) generated a 30 kV output pulse with rise time fixed within 1- 1.5 μ s and a pulse width of 2 μ s. The frequency of the pulses was fixed at 700 Hz and treatment was performed for 5 consecutive days. The applicator of the system was a copper electrode, covered with a quartz dielectric, and was connected to the output of the microsecond pulser. The applicator was held by hand above the tumor (approximately 1-4 mm) for treatment. Here, an electrically safe plasma was created in direct contact with the tumor, and the surrounding gas and tissue were not significantly heated. During the treatment, mice were sedated using IsoFlo® inhalation vapour.

Immunohistochemistry

Five μ m-thick sections were prepared from FFPE tumor tissue blocks. After deparaffinization and hydration through graded series of isopropanol solutions, the sections were subjected to heat-induced antigen retrieval by incubation in a low pH buffer for 20 minutes at 97°C (PT-Link) (DAKO). Subsequently, the endogenous peroxidase activity was quenched by incubating the slides in a peroxidase blocking buffer (DAKO) for 10 minutes. Incubation with primary monoclonal antibodies cleaved caspase-3 (1:200 for 35 minutes), anti-Ki67 (1:400 for 35 minutes), anti-CD4 (1:150 for 35 minutes), anti-CD8 (1:200 for 35 minutes) was performed at room temperature. The Envision Flex+ detection kit (DAKO) and Liquid DAB+ Substrate Chromogen System (DAKO) were used for signal detection according to the manufacturer's instructions. Sections were counterstained with hematoxylin, dehydrated and mounted. Positive and negative controls were included in each staining run. Positive controls consisted of mouse tissue of spleen (cleaved caspase-3,

anti-Ki67, anti-CD4, anti-CD8). Negative controls consisted of only the secondary antibody incubation.

All sections were scored and categorized by two observers. Expression of the markers CD4, CD8 and cleaved caspase in the tissue was divided into five categories for IHC scoring (0 = <1%; 1 = 1-5%; 2 = 5-10%; 3 = 10-50%; 4 = >50%). Percentage of estimated necrotic area and Ki67 positive cells were determined using measurement tools in the QuPath digital image analysis software.

Thioredoxin reductase activity assay

After dissection, tumors were disrupted in lysis buffer using a tissue homogenizer (Qiagen). Afterwards protein lysates were used to measure TrxR activity using the Thioredoxin Reductase Colorimetric Assay Kit (Cayman chemical), according to the manufacturer's protocols. Absorbance was recorded at 405 nm with the Spark®Cyto (Tecan) during the initial 5 minutes of the reaction. TrxR activity was calculated using the formula provided by the protocol, whereby background measurements were subtracted from all values. An equal amount of protein was loaded for each condition as determined by the Pierce BCA protein kit.

Statistics

Statistical differences in tumor kinetics between different treatment groups in different experiments were determined using linear mixed model analysis. Differences in survival were analyzed using a Log-rank test. To assess a difference between the TrxR activity between treatment groups and untreated groups, Mann Whitney U test was performed. Differences were considered to be significantly different if $p < 0.05$. Graphs were made using GraphPad v9 software. All statistical analyses were carried out in R studio or SPSS v27.

Results

Continuous slow release of AF treatment in SB28 tumor-bearing mice

To administer AF chronically for 14 days, osmotic minipumps were subcutaneously implanted in SB28 tumor-bearing mice to deliver 2, 10 or 15 mg/kg AF per day at the same constant rate. This delivery method was preferred over daily intraperitoneal injections with AF, since these frequent injections are causing discomfort and are shown to be more toxic for the mice. However, we showed that subcutaneous administration of high doses of AF (10 or 15 mg/kg) caused skin irritation and ulceration at the side of release of the compound (Figure 5.1 D). This was not observed when administering lower concentrations of AF (2 mg/kg) or the vehicle via an osmotic minipump. Furthermore, there was no observed delay in tumor growth and no increase in survival in the treatment groups receiving a higher dosage of AF (10 or 15 mg/kg) compared to the untreated group (Figure 5.1 A, B). Similarly, there was no difference in tumor kinetics between mice receiving 2 mg/kg AF and vehicle, after 14 days of treatment (Figure 5.1 C).

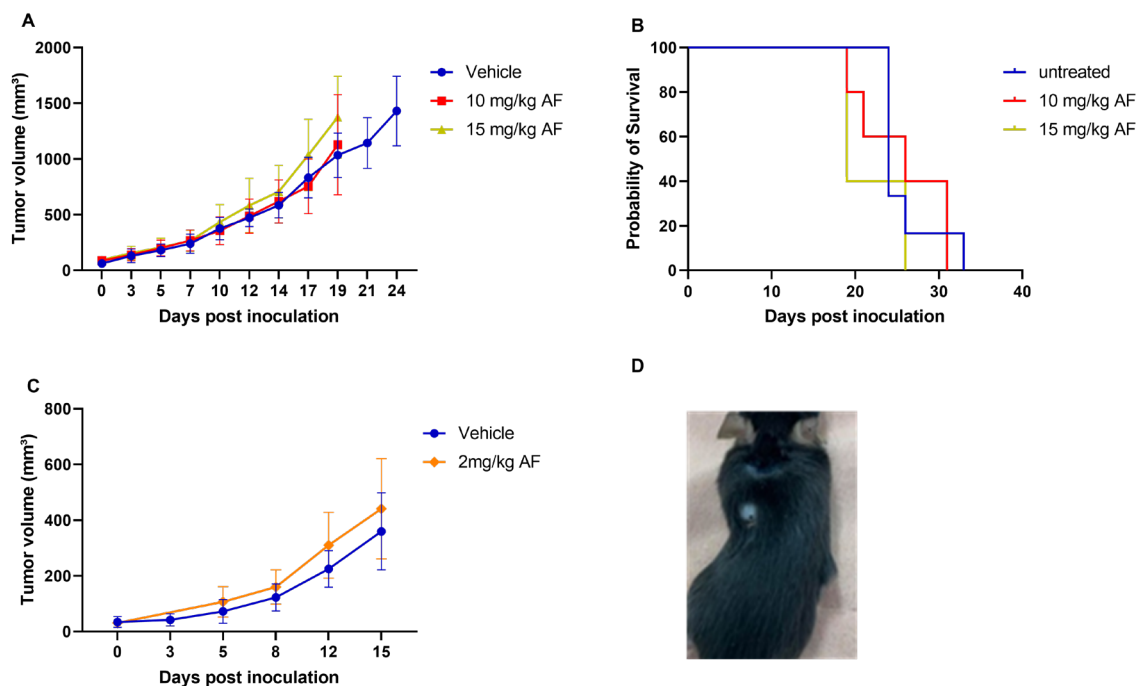


Figure 5.1 The effect of AF therapy on SB28 tumors via continuous delivery using an osmotic minipump system. (A) Tumor volume kinetics are presented (n=5 mice per group) after treatment with 10 or 15 mg/kg AF via continuous delivery of 14 days using a subcutaneously implanted osmotic minipump. (B) Survival of SB28 mice treated as indicated. (C) Tumor volume kinetics are presented (n = 5 mice per group) after treatment with 2 mg/kg AF via continuous delivery of 14 days using a subcutaneously implanted osmotic minipump. (D) Image indicating skin irritation caused by the use of a subcutaneous osmotic minipump to deliver high concentrations of AF (10 or 15 mg/kg). Data represent mean \pm SD.

Oral administration of AF treatment in SB28 tumor-bearing mice

Since delivery of high AF concentration (10 or 15 mg/kg) using the osmotic minipump system caused irritative effects, we changed the administration route to deliver these higher doses of AF. Since AF has been administered orally in rheumatoid arthritis patients in the clinic, we investigated oral administration of 10 or 15 mg/kg AF per day in SB28 tumor-bearing mice. After daily AF treatment for a period of 14 consecutive days, there was no delay in tumor growth compared to the untreated group (Figure 5.2 A). Nonetheless, there was no observed toxicity based on body weight or behavior (Figure 5.2 B) and there were no signs of local toxicity in the peritoneal cavity observed during post-mortem dissection.

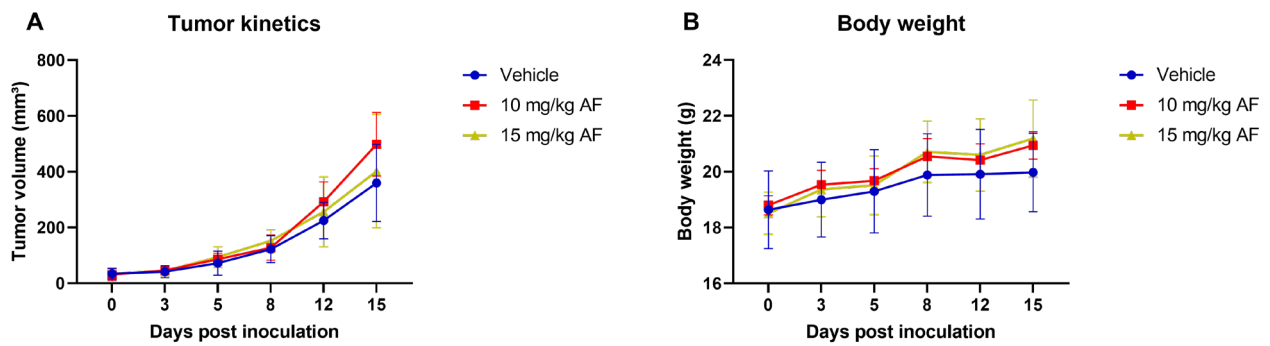


Figure 5.2. The effect of AF therapy on SB28 tumors via daily oral administration. (A) Tumor volume kinetics are presented (n=5-8 mice per group) after daily oral treatment with 10 or 15 mg/kg AF for a period of 14 days. (B) Body weight after treatment with 10 or 15 mg/kg AF. Data represent mean \pm SD.

AF inhibits TrxR in SB28 tumors

Protein lysates were isolated from disrupted SB28 tumors after 14 days of oral AF (10 or 15 mg/kg) or subcutaneous AF treatment via an osmotic minipump (2 mg/kg). AF was verified as a TrxR inhibitor since TrxR activity statistically significantly decreased in the AF-treated groups compared to the untreated group (Figure 5.3 A, B). This inhibition was the strongest in the group of mice receiving 15 mg/kg AF orally.

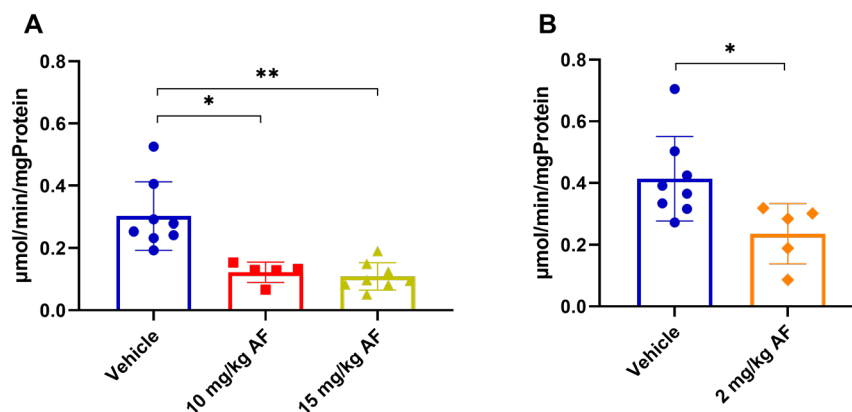


Figure 5.3. TrxR activity in SB28 tumors. (A) TrxR activity in SB28 tumors isolated from mice (n=5-8 mice per group) after 14 days of daily oral AF treatment (10 or 15 mg/kg). (B) TrxR activity in SB28 tumors isolated from mice (n=5-8 mice per group) after 14 days of continuous delivery of AF via an osmotic minipump (2 mg/kg). Data represent mean \pm SD. P-values represented as * < 0.05; ** < 0.01 denote significant difference compared to untreated control.

Effect of auranofin treatment on cell death and proliferation markers in SB28 tumors

Immunohistochemical staining of tumor sections was performed to explore the underlying cell death and proliferation effect in the tumor after AF treatment, since there were no effects on tumor kinetics. Interestingly, mice treated with 2 mg/kg of AF delivered through subcutaneous and continuous release, showed massive necrotic areas into the tumor compared to the tumors of the untreated mice (Figure 5.4 A-C). This necrotic effect was less pronounced in tumors when mice were treated with 15 mg/kg AF orally.

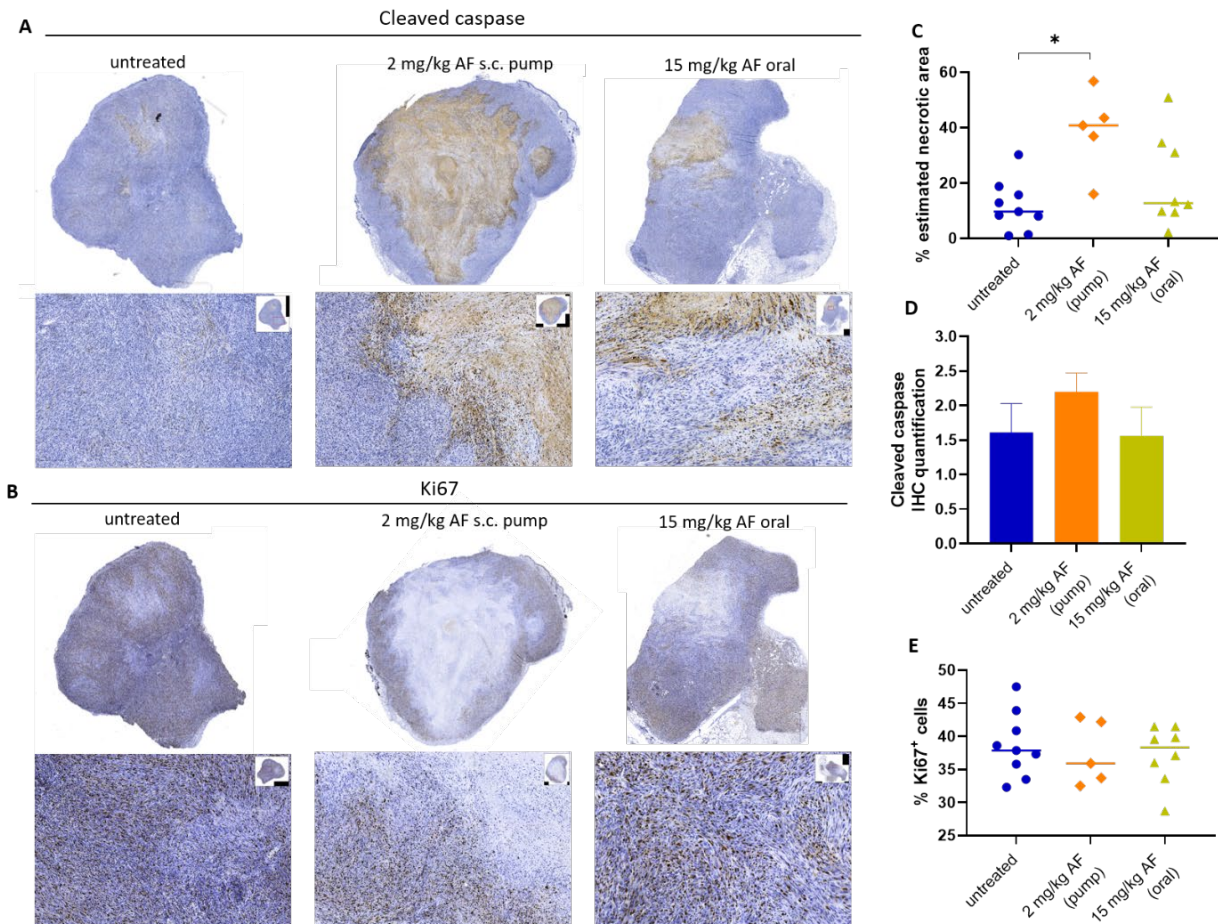


Figure 5.4. Cleaved caspase and Ki67 expression in SB28 tumors after AF treatment. (A) Immunohistochemical staining of cleaved caspase expression. (B) Immunohistochemical staining of Ki67 expression. (C) Percentage estimated necrotic area calculated on caspase positive staining. (D) IHC quantification of cleaved caspase. Data represent mean \pm SD. (E) Percentage of Ki67⁺ cells. All stainings were performed on SB28 tumors treated with vehicle or AF (2 mg/kg via subcutaneous delivery through the osmotic minipump and 15 mg/kg via oral administration) for a period of 14 days. * $p \leq 0.05$ denotes statistically significant difference compared with vehicle-treated control.

In addition to the induction of necrosis, we observed a slight increase in cleaved-caspase expression after treatment with AF (2 mg/kg), especially at the border of the necrotic areas (Figure 5.4 A, D). Minimal to no difference in proliferation (anti-Ki67) was observed between treated and untreated groups, which can be explained by the fact that Ki67 was only measured in the proliferative and viable region of the tumor without taking the necrotic area into account (Figure 5.4 B, E).

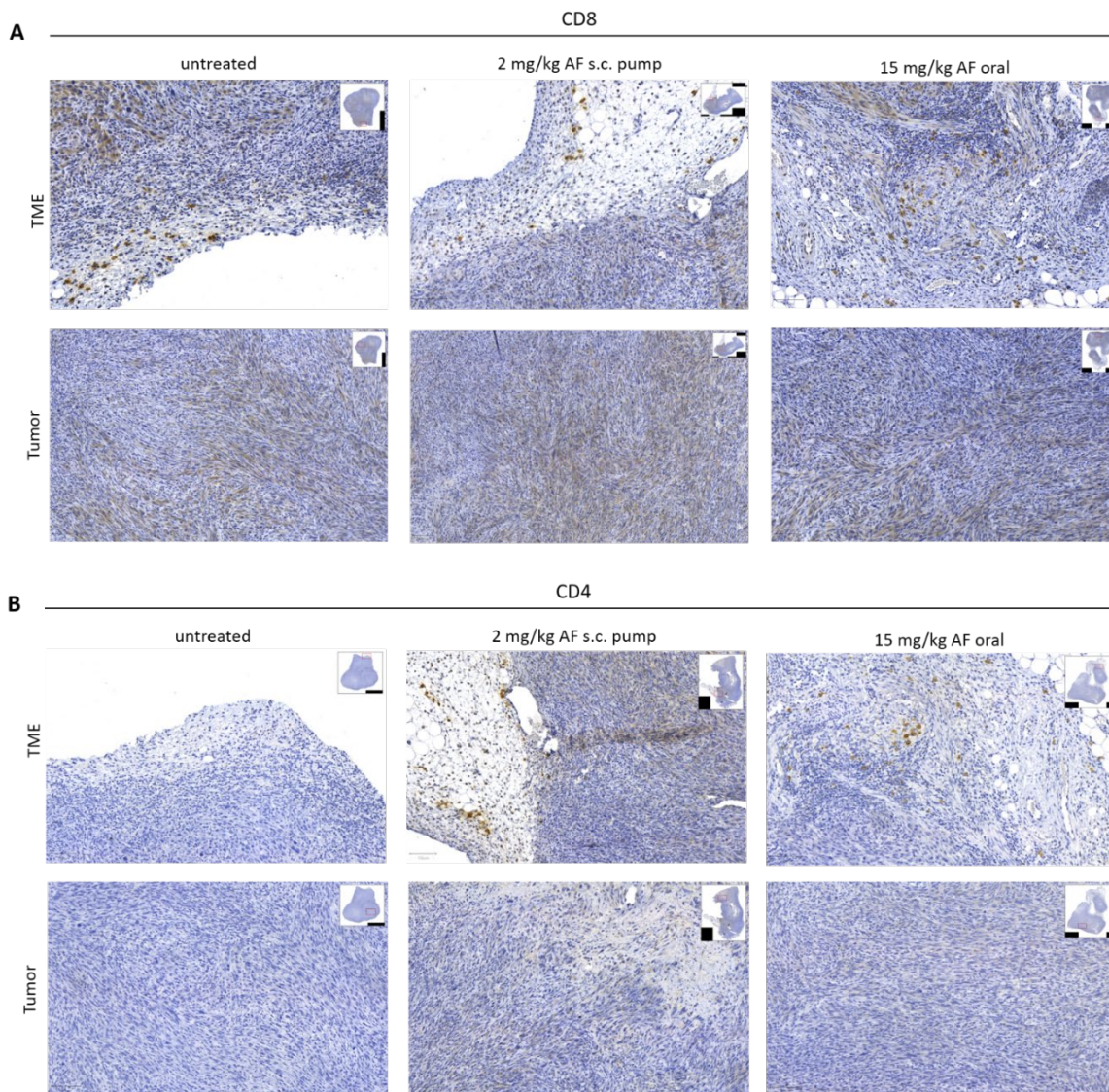


Figure 5.5. CD8 and CD4 expression in SB28 tumor after AF treatment. Immunohistochemical staining of CD8 (A) and CD4 (B) expression in TME and tumor area in SB28 tumors after treatment with vehicle and AF (2 mg/kg via subcutaneous delivery through the osmotic minipump and 15 mg/kg via oral administration) for a period of 14 days.

The necrotic cell death induced by AF in the tumor was not associated with an infiltration of CD4⁺ or CD8⁺ T cells into the tumor area. Overall, only a few CD8⁺ T cells and CD4⁺ T cells were present in the tumor microenvironment (TME) without a difference between the treated and the untreated groups (Figure 5.5 A, B).

Combination of auranofin and direct plasma application

Since we showed (chapter 4) that the combination of AF and CAP induced a synergistic ROS-mediated response *in vitro*, we further investigated whether the combined treatment of AF and CAP might lead to augmented antitumor response in the SB28 GBM-bearing mice model. The combination of AF and CAP was delivered in two different treatment schedules, either simultaneously or sequentially (Figure 5.6 A). We demonstrated that the sequential combination regimen resulted in a significantly decreased tumor volume and significantly increased survival of the SB28-bearing mice (Figure 5.6 B-G). When this sequential combination regimen was compared to the single treatments of AF and CAP, there was only a significant difference between the group receiving AF monotherapy in case of tumor volume and survival. In the simultaneous combination treatment regimen, there was no statistical significant decrease in tumor volume and no statistical significant increase in survival observed compared to the untreated group and both single treated groups.

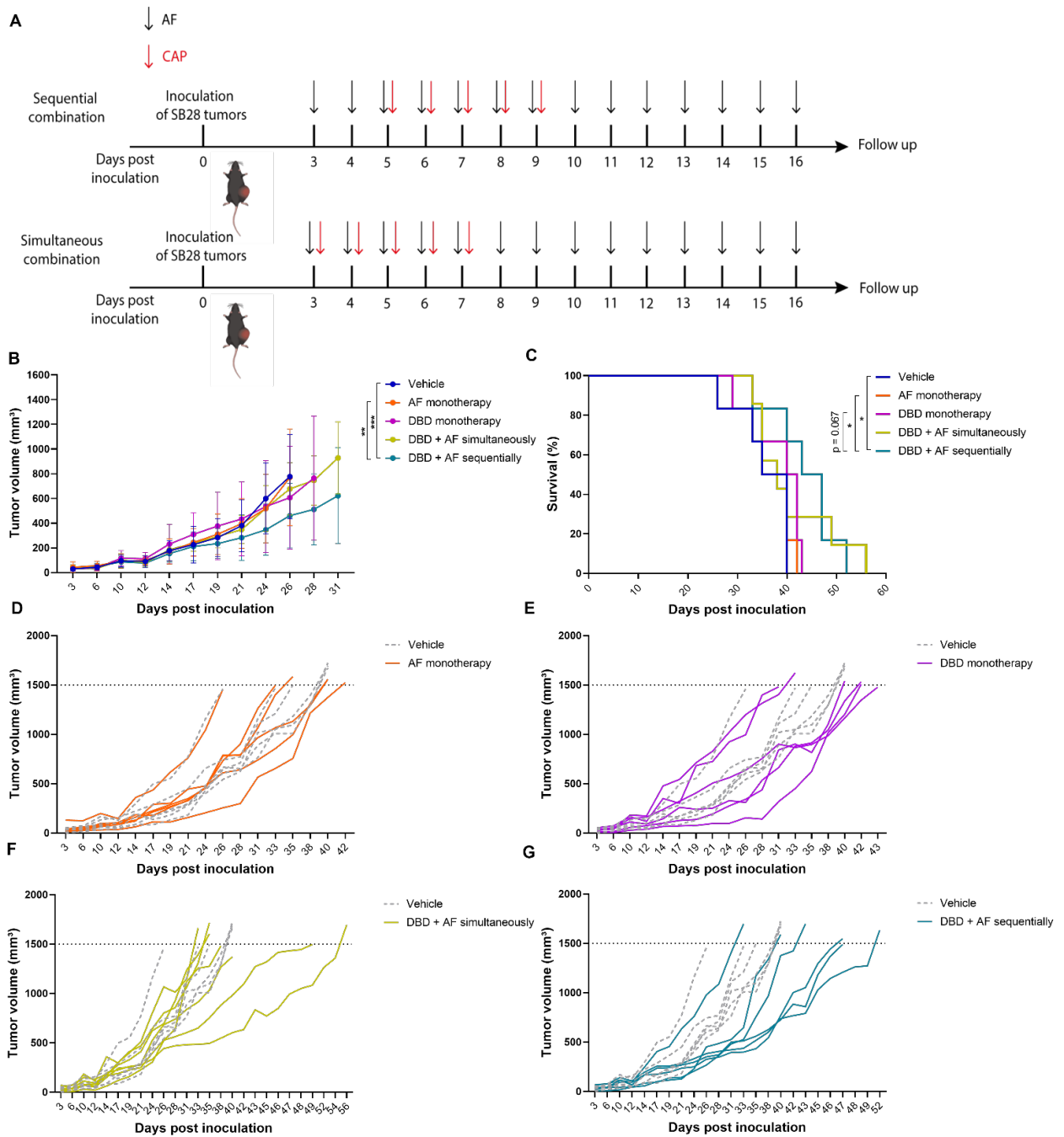


Figure 5.6. Tumor kinetics and survival after AF and CAP combination therapy. (A) Treatment schedule showing timing of AF treatment (15 mg/kg orally administered for 14 consecutive days) with black arrows and CAP treatment (direct application with DBD device for 5 consecutive days) with red arrows. (B) Tumor volume kinetics (n = 6 or 7 mice per group) after treatments as indicated. Data represent mean ± SD. (C) Survival of SB28 mice (n = 6 or 7 mice per group) after treatments as indicated. (D-G) Spaghetti plots of tumor volumes for individual mice in each treatment group (solid lines) compared to individual untreated mice (dotted lines). *p ≤ 0.05; **p ≤ 0.01; ***p ≤ 0.001 denotes statistically significant differences.

Discussion

Since the combination of AF and CAP strongly synergized *in vitro* to induce cell death and to enhance immunogenicity in different GBM cell lines (chapter 4) (6), we examined this combination therapy in an immunocompetent *in vivo* GBM-bearing mice model. Based on our *in vitro* results, we hypothesized that combining AF with CAP may result in enhanced immune activation and increased anti-tumor effects.

Before the *in vivo* validation of our combination strategy, we optimized AF treatment by testing various administration routes *in vivo*. In literature, the dose of AF varies between 1 mg/kg and 15 mg/kg and is mostly administered intraperitoneal with different treatment schedules (7-10). We noticed severe overall toxicity of mice after intraperitoneal administration of AF in a preliminary *in vivo* study and therefore opted for two different delivery methods. Firstly, we investigated continuous and slow delivery of AF through a subcutaneously implanted osmotic minipump. Here, only low doses of AF (2 mg/kg) did not cause skin irritation compared to higher doses (10 or 15 mg/kg). Secondly, we administered higher AF concentrations (10 or 15 mg/kg) orally, which was well tolerated. Oral or subcutaneous delivery of AF led to an inhibition of TrxR activity within the SB28 tumors, which was more pronounced with oral delivery of 15 mg/kg AF. This indicates that AF is a potent inhibitor of TrxR, independent on the route of administration.

Although there was no inhibition in tumor growth after AF monotherapy, AF was able to induce cell death within the tumor, which was observed as a necrotic area in the center of the tumor. These results are in line with the study of Hatem et al., showing a significant increase in tumor necrotic area without the inhibition of tumor volume after AF treatment (10 mg/kg) (11). Interestingly, we showed that the necrotic area was more pronounced after administration of a low dose of AF (2mg/kg) using the osmotic minipumps implanted subcutaneously in the mice, compared to oral administration of a high dose of AF (15 mg/kg). Whether this increase in necrotic area was due to the dosage or to the different pharmacokinetic profile during oral or continuous subcutaneous administration, remains to be elucidated. There are some reports that state that subcutaneous administration of anticancer drugs, specifically some chemotherapeutic agents, is superior to oral administration. They show a higher bioavailability and are more rapidly absorbed after

subcutaneous delivery compared to oral application (12, 13). However, we did not find any reports in literature on the pharmacokinetic profile of AF when administered subcutaneously, so follow up studies are necessary to report on differences in pharmacokinetics.

In contrast to our *in vivo* results with AF monotherapy, which showed no delay in tumor kinetics compared to the untreated group, several preclinical studies showed inhibition of tumor growth after AF treatment in various tumor models (7, 14, 15). However, several other *in vivo* studies only showed an inhibitory effect on tumor kinetics when AF was combined with other treatments, in concordance with our results (10, 11, 16, 17). In this chapter, we investigated the combination of AF, a potent TrxR inhibitor, with CAP, an exogenous ROS inducer. CAP has already been examined as efficient anticancer treatment modality in different *in vivo* tumor models, including GBM, using different devices for both direct and indirect applications (18-21). In this study, we opted for an in-house DBD device, which had already been used for direct *in vivo* CAP treatment of mice (4, 5).

Previously (chapter 4) we showed that only high AF concentrations triggered synergistic effects in combination with CAP in 3D GBM models, *in vitro* (6). Together with our *in vivo* results that showed the strongest inhibition of TrxR activity in the tumor site after oral administration of AF (15 mg/kg), we combined a high dose of orally administered AF (15 mg/kg) with CAP treatment in GBM-bearing mice. Additionally, this is in accordance with the clinical use of AF, which is an FDA approved drug in rheumatoid arthritis patients. The sequential combination regimen of orally administered AF and CAP showed a decrease in tumor volume and an increase in survival of the SB28 GBM-bearing mice model, which was significantly better than the untreated control and AF single-agent treatment group. This was in contrast with the simultaneous combination regimen, which showed no significant effect on tumor volume and survival. These results are in line with our *in vitro* data, indicating that it is important to inhibit the endogenous defense system before adding excessive amounts of exogenous ROS. Besides the promising results obtained with orally administered high doses of AF, it might be of value to further investigate subcutaneous, slow and continuous delivery of lower doses of AF in combination with direct CAP application due to its superior antitumoral effects as monotherapy, based on the amount of necrotic area inside the tumor, compared to oral administration.

Besides the anti-tumor effects, we wanted to investigate the immunological response after the combination treatment. For now, we only demonstrated no CD4⁺ or CD8⁺ T cell infiltration into the tumor site after AF monotherapy. Further analysis of immune infiltration after combination therapy still needs to be performed. Interestingly, the orthotopic SB28 GBM model showed weak immunogenicity and responsiveness towards anti-CTLA-4 and anti-PD-1 combined immunotherapy due to the poor immunogenic character of the model (2). In contrast to orthotopic SB28 tumors, subcutaneous SB28 tumors did respond towards combined anti-CTLA-4 and anti-PD-L1 therapy due to a better influx of DCs in subcutaneous tumors compared to intracranial tumors that contained abundant tumor-associated macrophages and microglia (22). Therefore, a more in-depth immune profiling and characterization of the tumor and TME is necessary to fully understand the immune response after combination treatment of AF and CAP. This characterization will be of value to provide a rationale for the combination with novel immunotherapeutic approaches.

Conclusion

In this chapter, we have shown that AF is a potent TrxR antioxidant inhibitor *in vivo* when delivered in different doses and through various administration routes. Additionally, we have shown that when AF is sequentially combined with direct CAP treatment, this combination exhibits enhanced antitumor efficacy, resulting in an increased survival in SB28 tumor-bearing mice. This novel preclinical data support increasing oxidative stress by the sequential combination therapy of AF and CAP, to be a promising treatment strategy in GBM.

References

1. Van Loenhout J, Flieswasser T, Freire Boullosa L, De Waele J, Van Audenaerde J, Marcq E, et al. Cold Atmospheric Plasma-Treated PBS Eliminates Immunosuppressive Pancreatic Stellate Cells and Induces Immunogenic Cell Death of Pancreatic Cancer Cells. *Cancers*. 2019;11(10).
2. Genoud V, Marinari E, Nikolaev SI, Castle JC, Bukur V, Dietrich PY, et al. Responsiveness to anti-PD-1 and anti-CTLA-4 immune checkpoint blockade in SB28 and GL261 mouse glioma models. *Oncoimmunology*. 2018;7(12):e1501137.
3. Majd N, de Groot J. Challenges and strategies for successful clinical development of immune checkpoint inhibitors in glioblastoma. *Expert Opin Pharmacother*. 2019;20(13):1609-24.
4. Lin A, Biscop E, Breen C, Butler SJ, Smits E, Bogaerts A. Critical Evaluation of the Interaction of Reactive Oxygen and Nitrogen Species with Blood to Inform the Clinical Translation of Nonthermal Plasma Therapy. *Oxidative medicine and cellular longevity*. 2020;2020:9750206.

5. Lin A, Razzokov J, Verswyvel H, Privat-Maldonado A, De Backer J, Yusupov M, et al. Oxidation of Innate Immune Checkpoint CD47 on Cancer Cells with Non-Thermal Plasma. *Cancers*. 2021;13(3).
6. Van Loenhout J, Freire Boullosa L, Quatannens D, De Waele J, Lardon F, Peeters M, et al. Auranofin and cold atmospheric plasma synergize to trigger distinct cell death mechanisms and to enhance immunogenicity in glioblastoma multiforme. Submitted 2021.
7. Rios Perez MV, Roife D, Dai B, Pratt M, Dobrowolski R, Kang Ya, et al. Antineoplastic effects of auranofin in human pancreatic adenocarcinoma preclinical models. *Surgery Open Science*. 2019;1(2):56-63.
8. Topkas E, Cai N, Cumming A, Hazar-Rethinam M, Gannon OM, Burgess M, et al. Auranofin is a potent suppressor of osteosarcoma metastasis. *Oncotarget*. 2016;7(1):831-44.
9. Hou G-X, Liu P-P, Zhang S, Yang M, Liao J, Yang J, et al. Elimination of stem-like cancer cell side-population by auranofin through modulation of ROS and glycolysis. *Cell death & disease*. 2018;9(2):89.
10. Ito M, Codony-Servat C, Codony-Servat J, Lligé D, Chaib I, Sun X, et al. Targeting PKC α -PAK1 signaling pathways in EGFR and KRAS mutant adenocarcinoma and lung squamous cell carcinoma. *Cell Commun Signal*. 2019;17(1):137-.
11. Hatem E, Azzi S, El Banna N, He T, Heneman-Masurel A, Vernis L, et al. Auranofin/Vitamin C: A Novel Drug Combination Targeting Triple-Negative Breast Cancer. *Journal of the National Cancer Institute*. 2018.
12. Leveque D. Subcutaneous administration of anticancer agents. *Anticancer Res*. 2014;34(4):1579-86.
13. Jeong SH, Jang JH, Lee YB. Pharmacokinetic Comparison of Three Different Administration Routes for Topotecan Hydrochloride in Rats. *Pharmaceuticals (Basel)*. 2020;13(9).
14. Raninga PV, Lee AC, Sinha D, Shih YY, Mittal D, Makhale A, et al. Therapeutic cooperation between auranofin, a thioredoxin reductase inhibitor and anti-PD-L1 antibody for treatment of triple-negative breast cancer. *Int J Cancer*. 2020;146(1):123-36.
15. Li H, Hu J, Wu S, Wang L, Cao X, Zhang X, et al. Auranofin-mediated inhibition of PI3K/AKT/mTOR axis and anticancer activity in non-small cell lung cancer cells. *Oncotarget*. 2016;7(3):3548-58.
16. Fan C, Zheng W, Fu X, Li X, Wong YS, Chen T. Enhancement of auranofin-induced lung cancer cell apoptosis by selenocystine, a natural inhibitor of TrxR1 in vitro and in vivo. *Cell death & disease*. 2014;5:e1191.
17. Han Y, Chen P, Zhang Y, Lu W, Ding W, Luo Y, et al. Synergy between Auranofin and Celecoxib against Colon Cancer In Vitro and In Vivo through a Novel Redox-Mediated Mechanism. *Cancers*. 2019;11(7).
18. Chen Z, Simonyan H, Cheng X, Gjika E, Lin L, Canady J, et al. A Novel Micro Cold Atmospheric Plasma Device for Glioblastoma Both In Vitro and In Vivo. *Cancers*. 2017;9(6).
19. Rafiei A, Sohbatzadeh F, Hadavi S, Bekeschus S, Alimohammadi M, Valadan R. Inhibition of murine melanoma tumor growth in vitro and in vivo using an argon-based plasma jet. *Clin Plasma Med*. 2020;19-20:100102.
20. Mahdikia H, Saadati F, Freund E, Gaipf US, Majidzadeh AK, Shokri B, et al. Gas plasma irradiation of breast cancers promotes immunogenicity, tumor reduction, and an abscopal effect in vivo. *Oncoimmunology*. 2020;10(1):1859731.
21. Liedtke KR, Bekeschus S, Kaeding A, Hackbarth C, Kuehn JP, Heidecke CD, et al. Non-thermal plasma-treated solution demonstrates antitumor activity against pancreatic cancer cells in vitro and in vivo. *Sci Rep*. 2017;7(1):8319.
22. Simonds EF, Lu ED, Liu EV, Tamaki W, Rancan C, Stultz J, et al. Deep immune profiling reveals targetable mechanisms of immune evasion in checkpoint blockade-refractory glioblastoma. *bioRxiv*. 2020:2020.12.01.404939.

CHAPTER 6

General discussion, future challenges and future perspectives

General discussion

Tumors are known to be capable of escaping antitumor immunity (1). One way of cancer cells to evade the immune response is accomplished by being poorly immunogenic (2). As such, cancer cells can express antigens but the immune system fails to distinguish them from tolerized self-antigens. Frequently, these poorly immunogenic tumors have low mutation rates, produce few neoantigens and have low immune cell infiltrates in their tumor microenvironment (TME) (3). Making the tumor more immunogenic might improve potent anticancer immune responses.

This thesis describes the investigation of two novel oxidative stress-mediated treatments in their capacity to target tumor cells and to increase immunogenicity of these tumor cells in two different tumor types which are characterized as low immunogenic, namely pancreatic ductal adenocarcinoma (PDAC) and glioblastoma (GBM). The common underlying therapeutic approach for both tumor types is the novel oxidative stress-mediated cold atmospheric plasma (CAP) treatment. In addition, this exogenous reactive oxygen species (ROS)-inducing treatment is combined with auranofin (AF), an endogenous antioxidant inhibitor, for the treatment of GBM. This thesis also provides a strong rationale for a combination with immunotherapeutic approaches for boosting the immunological response against PDAC and GBM.

I started this PhD project with investigating the release of immunogenic cell death (ICD)-related markers and subsequent activation of DCs in PDAC after treatment with CAP-treated PBS (pPBS) as novel oxidative stress-inducing therapy, *in vitro* (**chapter 3**). I revealed that pPBS has the potential to induce ICD in pancreatic cancer cells (PCCs) and to reduce the immunosuppressive TME by attacking the tumor-promoting pancreatic stellate cells (PSCs).

Ever since the concept of ICD was pioneered by the labs of Guido Kroemer and Laurence Zitvogel by the use of several chemotherapeutics, it has been emerged as regulated form of cell death induced by numerous ROS-inducing therapeutic strategies, now including CAP (4, 5). Our study is in line with different *in vitro* studies that indicate the release of different danger-associated molecular patterns (DAMPs) after CAP treatment (6-13). Following our results, later performed studies by others also showed maturation of DCs based on

increased expression of maturation markers (CD83, CD86 and MHC class II) in coculture with CAP-treated tumor cells (14, 15). Furthermore, several *in vivo* models have shown to increase tumor immunogenicity in melanoma, pancreatic cancer and colon cancer after CAP treatment (12, 13, 16, 17).

As reviewed in **chapter 2**, tumor cells can evolve mechanisms to protect themselves against intrinsic oxidative stress and can develop an adaptation mechanism by upregulation of pro-survival molecules and their antioxidant defense system to maintain the redox balance and to potentially become resistant towards exogenous ROS-inducing therapy. Therefore, dual targeting of tumor cells by increasing exogenous levels of ROS and inhibiting the antioxidant defense system can maximally exploit ROS-mediated cell death mechanisms as therapeutic anti-cancer strategy. In this regard, pPBS was combined with AF, a thioredoxin reductase (TrxR) inhibitor, in GBM (**chapter 4**). Additionally, it has been shown that AF-dependent inhibition of TrxR acts on the PI3K/Akt/mTOR survival pathway, causing apoptosis of cancer cells (18). Interestingly, this signaling pathway is often activated in GBM patients due to alterations of its upstream regulators or reduced expression of PTEN, the negative regulator of the pathway (19). In addition, AF blocks IL-6 signaling by inhibition of the JAK/STAT3 signaling pathway (20). Since this pathway is known to be involved in immune evasion, it is suggested that such inhibitors would be interesting to combine with immunotherapy (21).

A synergistic ROS-induced response was shown after combination of AF and pPBS treatment in 2D and 3D cell cultures. Additionally, this combination was able to elicit DAMPs and to increase immunogenicity of dying GBM cells. However, it should be kept in mind that besides the increase in maturation of DCs, the combination treatment of pPBS and AF inhibited the phagocytotic capacity of DCs in GBM. This effect was due to the presence of AF as previously shown by others (22). This can be explained by the history of its use as an antirheumatoid arthritis drug linked to inhibition of pro-inflammatory mediators and oxidative burst in monocytes and granulocytes necessary for effective phagocytosis (23). Based on our results AF could have both pro- and anti-inflammatory effects, warranting investigation of these immunomodulating effects of AF in an *in vivo* setting.

In contrast with PCC lines, pPBS single treatment did not elicit DAMPs in GBM cells, except for a statistically non-significant increase of ecto-calreticulin (ecto-CRT) for LN-229 and U-87 cells. On top, there was no increase in maturation markers or phagocytosis when pPBS-treated GBM cells were cocultured with immature DCs. This indicates that the immunogenic capacity of pPBS monotreatment is tumor type and cell line dependent with PDAC cells being more susceptible compared to GBM cells. These results provide an additional rationale to combine pPBS with AF treatment in GBM cells. In conclusion, this highlights the importance of biological variation among tumors and their different biological responses to similar treatments.

Next, the subcutaneous *in vivo* GBM mice model revealed antitumor effects after sequential combination with AF and CAP using a DBD device, which resulted in a reduction in tumor volume and an increase in survival (**chapter 5**). These results are in line with the *in vitro* results of **chapter 4** obtained in 2D and 3D cell cultures using different CAP sources (kINPenIND® and COSTjet, respectively). This indicates that several CAP sources and applications (direct or indirect) might exhibit similar effects in combination with AF in the treatment of GBM, although this remains to be verified in a comparative *in vivo* study.

We used the poorly immunogenic SB28 GBM tumor model, which is characterized with sparse T cell infiltrates, absence of MHC-I and MHC-II expression and a very low mutational load, explaining the weak immunogenicity and irresponsiveness towards anti-CTLA-4 and anti-PD-L1 combined therapy (24). As such, this SB28 mice model represents the poorly immunogenic nature comparable to the human situation. However, Simonds et al. showed that the response towards this immune checkpoint blockade was dependent on tumor site. In contrast to intracerebral orthotopic SB28 tumors, subcutaneous SB28 tumors did respond towards combined anti-CTLA-4/anti-PD-L1 therapy due to a better influx of DCs in subcutaneous tumors compared to intracranial tumors that contained abundant tumor-associated macrophages and microglia (25). This highlights the importance to further investigate the TME and identify different immune populations in the TME that might contribute to the responsiveness towards the combination therapy of AF and CAP.

In literature it has already been shown that CAP monotherapy induced higher immune cell infiltration (CD4⁺ T cells, CD8⁺ T cells and CD11c⁺ DCs) in a syngeneic melanoma and breast cancer mice model (16, 26). An increased expression of CD8⁺ T cells was

demonstrated in a similar breast cancer model following two weeks of AF monotherapy (10 mg/kg, intraperitoneal) (27). This immune characterization of the TME in our GBM model might provide a stronger rationale for future combinations with immunotherapeutic approaches, as described below. Furthermore, it will be of added value to validate the combination therapy in an orthotopic mice model.

In conclusion, these preclinical data support the idea of CAP and AF as ROS-inducing treatments to target PDAC and GBM, and potentially enhance immunogenicity of PDAC and GBM *in vitro*, but remain to be demonstrated *in vivo*.

Future challenges

Future challenges for cold atmospheric plasma (CAP) treatment

To date, CAP treatment has already found its clinical applications in wound healing, blood coagulation, ulcer prevention and decontamination (28, 29). Additionally, CAP treatment is emerging as a promising anticancer treatment that can supplement other cancer therapies (e.g. immunotherapy) and enhance their selectivity and efficacy against resistant tumors (30-32). Although the field of CAP already exists for a longer period of time, it faces different challenges with regard to cancer treatment.

It is convenient that for the clinical applications in wound healing and ulcer prevention, CAP is administered topically. However, a big challenge is the clinical treatment of non-superficial tumors within a patient. One clinical approach could be direct administration of CAP as an intra-operative adjuvant treatment. Another method could be the indirect delivery of CAP to deeply located tumors via CAP-activated liquids (33, 34). Moreover, the type (direct or indirect) of CAP application has several different implications regarding the interaction with the biological target. In case of direct CAP treatment, both short- and long-lived reactive species, as well as physical factors (UV light and in some cases electromagnetic fields) may be present during the treatment, while with indirect CAP treatment only long-lived species (such as H₂O₂ and NO₂⁻) should be considered (35). Although CAP-activated liquids have more therapeutic potential for non-superficial tumors with less toxicity, the absence of short-lived species may have an impact on the cytotoxic effect of cancer cells (9, 33, 36). Since both routes of administrations have favorable and unfavorable factors, the best choice of delivery methods remains a challenge in the field of CAP oncology.

Another major challenge is the need for more standardized and comparable CAP sources. In this project alone, three different application methods and CAP devices were considered for diverse preclinical models. Firstly, 2D monolayers were treated with CAP-treated PBS *in vitro*, using the kINPenIND® source. Secondly, 3D spheroids were directly treated with CAP using the COSTjet device, since more H₂O₂ species are delivered compared to the CAP-treated PBS necessary to inhibit spheroid survival. Finally, subcutaneous tumors *in vivo* were directly treated using a DBD source. The reason for these different CAP sources was due to feasibility issues, in-house experience (13, 37) and translational value. In case of the latter, the kINPenIND® source had the most translational value, since a similar jet device (kINPenMED®) is one of the only certified clinical CAP devices for oncological purposes until now (38). The use of different custom-made devices or modifications by different CAP research groups, including our consortium, pose a challenge with respect to comparability of the obtained results, leading to difficulties defining efficacy and long-term safety of CAP devices in a comparable and standardized manner (29). This lack of standardization represents the major limitation in the field of CAP oncology and action on this front should be taken before CAP can evolve into a potent broadly used anti-cancer treatment. Importantly, We have demonstrated that combining CAP with AF worked synergistically with each plasma device and in increasingly complex preclinical models, highlighting the robustness of this combination strategy.

In chapter 2 it is suggested that oxidative stress-inducing treatments can have pleiotropic effects, which can steer the immune response towards pro- or antitumoral immunity. In case of CAP treatment, these direct and indirect effects on immune cells still need to be investigated in more detail when combining CAP with immunotherapy. It will be of interest to reveal if CAP affects viability, polarization, activation or effector functioning of different types of innate and adaptive immune cells. Additionally, it will be important to elucidate the effect on other players of the surrounding TME. Multiple publications claim that CAP acts specifically on cancer cells, leaving the normal cells to survive the exposure (39-42). This is suggested by the impaired ability of cancer cells to deal with oxidative stress-mediated disturbances compared to normal cells (43). Such selectivity would have great clinical advantages, since both PDAC and GBM reside in vital, fragile and irreplaceable organs. While several papers claim that CAP selectively kills cancer cells *in vitro*,

retrospective analysis of these papers reveals that definitive proof is rather scarce. This is largely due to the discrepancies between treatment conditions for cancer and non-cancerous cells *in vitro*, e.g. differences in media, cell type and tissue type (40, 42, 44-46). Therefore, we recently analyzed the specificity of CAP in a controlled manner on cancer and non-cancerous counterpart cells. The result indicate that selectivity was mostly absent, also for U-87 GBM cells versus astrocytes (47). In contrast to our findings, Hasse et al. demonstrated selectivity for head and neck cancer tissue in comparison to its healthy counterpart, both derived from the same patient (48). Organoid models containing different cell types representing the TME will provide valuable information in this context. In addition, animal models might also provide a good indication whether CAP exerts collateral damage to healthy tissue and has the advantage of a functional immune system to investigate the immunomodulating effects. In our *in vivo* study, there was no observed toxicity of the direct CAP application based on body weight and behavior of the mice and there were no signs of local skin lesions at the site of the treatment.

Future challenges for auranofin (AF) treatment

Due the escalating costs and timeline required for new drug discovery and development, there is an increasing interest in repurposing well-known and well-characterized licensed non-cancer drugs to the oncology domain, as underscored by The Repurposing Drugs in Oncology project (49, 50). Here, AF is one of the compounds that is gaining interest for repurposed use in cancer research. In GBM, AF is one of the nine repurposed drugs used in the CUSP9 treatment protocol currently undergoing a clinical trial (NCT02770378) as add-on treatment to standard-of-care temozolomide for recurrent GBM (51). In this CUSP9 treatment strategy, AF is also used as one of the drugs in the combination to increase ROS-mediated cell death and was therefore of interest to our research in combination with CAP treatment (52).

Compared to the daily oral dosage of 6 mg of AF in rheumatoid arthritis patients (53), much higher doses of AF are given *in vivo* to inhibit TrxR activity in the tumor of mice. In our study, intraperitoneal injections of high dosages of AF induced acute toxicity in mice, leading to early and abrupt discontinuation of the treatment. Curiously, other groups which administered high dosages of AF in mice mentioned no signs of toxicity (54, 55). We chose for a delivery method with slow and continuous delivery of the drug, namely subcutaneous

implantation of an osmotic minipump (56). Here, a low AF concentration (2 mg/kg) was well tolerated and induced necrotic cell death. Oral administration of higher dosages of AF (10 or 15 mg/kg) was well tolerated by mice and showed a delay in tumor growth when combined with CAP. Importantly, it might be challenging to obtain sufficiently high concentrations of AF in the patient's tumor without increasing unwanted side-effects. Therefore, further in-depth validation of administration route and dosing of AF is required before clinical application in an anticancer therapeutic setting. Moreover, new technological innovations such as AF-loaded nanoparticles could offer a possible solution since they are able to enhance drug localization in the target site and minimize systemic cytotoxicity (57, 58).

Future perspectives

As proposed by Chen and Mellman, sensitizing for cancer immunotherapy can be done by interfering on different levels in the cancer immunity cycle (59). In this cycle, immunogenic tumor cell death, as induced by our ROS-mediated treatment strategy *in vitro*, is the first and imperative step to provide antigens to antigen presenting cells (APCs), more specifically DCs, for T cell priming. Further *in vivo* characterization of the TME after the ROS-inducing combination strategy of AF and CAP is necessary to provide a strong rationale for a specific combination with immunotherapeutic approaches, to ensure optimal therapeutic response. For now, I suggest some immunotherapeutic strategies that might be beneficial when combined with AF and CAP, but these are not exclusive.

One way to enhance effectivity of the ROS-inducing treatment is in combination with immunotherapeutic approaches that can boost the DC-based processes, which include antigen presentation and T cell priming and activation. For instance, the immunogenic potential of this treatment strategy can be linked with immunotherapy through DC vaccination. Here, autologous patient-derived monocytes can be differentiated into DCs and loaded with tumor-associated antigens, *ex vivo*. These tumor antigen loaded-DCs are reinjected into the patient to elicit a tumor-specific immune response (60). One approach to provide an efficient source of multiple tumor-associated antigens and adjuvants to load DCs is the use of whole tumor lysates, following treatment that enhances immunogenicity of these tumor cells (61, 62). Whole tumor lysates have the advantage of containing the full

tumor antigen repertoire, allowing DCs to naturally process the proteins and present several patient-specific tumor antigens (60). Different treatment modalities have been described to enhance the immunogenicity of cancer cells in the context of DC vaccines, all of which had the capacity to induce ICD (61, 62). For example, Garg et al. showed that inducing ICD of GBM cells after hypericin-based photodynamic treatment, instead of freeze/thawing-based necrosis, markedly improves DC vaccines by increasing immunogenicity of dying tumor cells, which they link to the release of potent DAMPs (63). Recently, it has been shown that CAP-treated tumor lysates also might be able to activate DCs in order to prime T cells and induce CD8⁺ T cell killing (15). In a clinical setting, melanoma and GBM patients have successfully been treated with DC vaccines loaded with irradiated tumor cells, however long-term antitumoral effects were limited (64, 65). Additionally, there is a clinical requirement of reaching 100% cancer cell death since subcutaneous injections of irradiated tumor cells had induced subcutaneous tumor growth in one GBM patient (66). So, the activation of anticancer immune responses following tumor treatment using ICD inducers as clearly demonstrated in several *in vivo* experimental models, has not been as apparent in the clinical studies performed so far (61). Despite the ability of DC-based vaccines to elicit immunological responses, these clinical studies have pointed to the limitation in which this approach fails to generate effective and durable clinical antitumor responses, especially when used as monotherapy (67).

Another immunotherapeutic approach to combine with ROS-inducing treatments are ligands of specific immune-related pathways that can generate a powerful adjuvant activity for enhancing adaptive immune responses (68). One possibility is the use of STING ligands, which induce the production of type I interferons (IFN) that play a particularly crucial role in the regulation of DCs. In addition to DC maturation by inducing expression of type I IFN, STING ligands can activate DCs *in vitro* and *in vivo* and enhance presentation of tumor-associated antigens to CD8⁺ T cells (69, 70). In this context, it has been demonstrated that a STING ligand is a potent adjuvant for enhancing the adaptive immune-mediated local and distant tumor control by radiotherapy in PDAC (71). Another adjuvant for ICD-inducing treatment, might be the use of Toll-like receptor (TLR)-agonists (72, 73). Our research group has already extensively examined the use of one specific TLR-agonist, namely poly(I:C), to prime GBM and awaken immune cells (74). In a clinical trial, the

combination of poly(I:C) with standard of care (radiotherapy and temozolomide) in GBM patients improved overall survival from 14.6 months, as reported by the EORTC trial, to 18.3 months (75). In this context, it would be interesting to investigate the immunogenic effect when combining poly(I:C) as adjuvant with the ROS-inducing treatment strategy to induce ICD. Thus, therapeutic strategies that activate innate immune-sensing pathways might have the potential to further increase tumor immunogenicity in combination with our treatment strategy and thereby heating up immune cold tumors that do not respond to immunotherapy.

Although the above mentioned combinatorial approaches focusing on DC-based processes might have the potential to increase tumor immunogenicity, their therapeutic effectiveness might be hampered by the presence of immunomodulatory immune checkpoint molecules in the TME (76). Furthermore, checkpoint blockade therapy alone has only shown low therapeutic efficacy in low immunogenic tumor types, such as GBM and PDAC, compared to high immunogenic tumors (77, 78). Therefore, a combination of ICD-inducing treatment to enhance tumor immunogenicity together with immune checkpoint blockade (e.g. anti-PD-(L)1) to remove inhibition of cancer cell killing by T cells, targets more than one phase of the cancer immunity cycle and might improve therapeutic response (59). As such, combining DC therapy with systemic PD-1 blockade in mice bearing GBM tumors improved survival compared to both single treatments (79). In preclinical *in vivo* studies, the combination of immune checkpoint blockade (e.g. anti-PD-(L)1 and anti-TIM-3) and radiotherapy, a potent ICD inducer, have been shown to improve antitumor immunity and survival in mice models bearing GBM or PDAC (80-82). In a clinical setting, there are approximately a dozen clinical trials evaluating the use of immune checkpoint blockade in combination with radiotherapy in GBM and PDAC, indicating the promising therapeutic option of combining ICD inducers with immune checkpoint blockade. In our case of CAP and AF treatment, the preclinical evidence for this possible combination is limited. So far, only one study examined the combination of CAP treatment with anti-PD-L1, *in vivo*. They showed delayed tumor growth and prolonged survival in a melanoma mice model compared to the untreated group and the single treated groups (83). Similarly, in case of AF only one *in vivo* study demonstrated impaired tumor growth in breast cancer tumors in combination with anti-PD-L1 (27).

In conclusion, there are several immunotherapeutic options to combine with the ROS-inducing treatment strategy that might increase immunotherapeutic efficacy in GBM and PDAC patients. In a possible follow-up study these combinations can be further explored.

References

1. Muenst S, Laubli H, Soysal SD, Zippelius A, Tzankov A, Hoeller S. The immune system and cancer evasion strategies: therapeutic concepts. *Journal of internal medicine*. 2016;279(6):541-62.
2. Beatty GL, Gladney WL. Immune escape mechanisms as a guide for cancer immunotherapy. *Clinical cancer research : an official journal of the American Association for Cancer Research*. 2015;21(4):687-92.
3. Schumacher TN, Schreiber RD. Neoantigens in cancer immunotherapy. *Science*. 2015;348(6230):69-74.
4. Galluzzi L, Humeau J, Buque A, Zitvogel L, Kroemer G. Immunostimulation with chemotherapy in the era of immune checkpoint inhibitors. *Nat Rev Clin Oncol*. 2020;17(12):725-41.
5. Garg AD, Galluzzi L, Apetoh L, Baert T, Birge RB, Bravo-San Pedro JM, et al. Molecular and Translational Classifications of DAMPs in Immunogenic Cell Death. *Frontiers in immunology*. 2015;6:588.
6. Lin A, Truong B, Pappas A, Kirifides L, Oubarri A, Chen SY, et al. Uniform Nanosecond Pulsed Dielectric Barrier Discharge Plasma Enhances Anti-Tumor Effects by Induction of Immunogenic Cell Death in Tumors and Stimulation of Macrophages. *Plasma Process Polym*. 2015;12(12):1392-9.
7. Lin A, Truong B, Patel S, Kaushik N, Choi EH, Fridman G, et al. Nanosecond-Pulsed DBD Plasma-Generated Reactive Oxygen Species Trigger Immunogenic Cell Death in A549 Lung Carcinoma Cells through Intracellular Oxidative Stress. *International journal of molecular sciences*. 2017;18(5).
8. Bekeschus S, Rodder K, Fregin B, Otto O, Lippert M, Weltmann KD, et al. Toxicity and Immunogenicity in Murine Melanoma following Exposure to Physical Plasma-Derived Oxidants. *Oxidative medicine and cellular longevity*. 2017;2017:4396467.
9. Lin A, Gorbanev Y, De Backer J, Van Loenhout J, Van Boxem W, Lemièrre F, et al. Non-Thermal Plasma as a Unique Delivery System of Short-Lived Reactive Oxygen and Nitrogen Species for Immunogenic Cell Death in Melanoma Cells. *Advanced Science*. 2019:1802062.
10. Yoon Y, Ku B, Lee K, Jung YJ, Baek SJ. Cold Atmospheric Plasma Induces HMGB1 Expression in Cancer Cells. *Anticancer Res*. 2019;39(5):2405-13.
11. Azzariti A, Iacobazzi RM, Di Fonte R, Porcelli L, Gristina R, Favia P, et al. Plasma-activated medium triggers cell death and the presentation of immune activating danger signals in melanoma and pancreatic cancer cells. *Sci Rep*. 2019;9(1):4099.
12. Freund E, Liedtke KR, van der Linde J, Metelmann HR, Heidecke CD, Partecke LI, et al. Physical plasma-treated saline promotes an immunogenic phenotype in CT26 colon cancer cells in vitro and in vivo. *Sci Rep*. 2019;9(1):634.
13. Lin AG, Xiang B, Merlino DJ, Baybutt TR, Sahu J, Fridman A, et al. Non-thermal plasma induces immunogenic cell death in vivo in murine CT26 colorectal tumors. *Oncoimmunology*. 2018;7(9):e1484978.
14. Miebach L, Freund E, Horn S, Niessner F, Sagwal SK, von Woedtke T, et al. Tumor cytotoxicity and immunogenicity of a novel V-jet neon plasma source compared to the kINPen. *Sci Rep*. 2021;11(1):136.
15. Tomić S, Petrović A, Puač N, Škoro N, Bekić M, Petrović ZL, et al. Plasma-Activated Medium Potentiates the Immunogenicity of Tumor Cell Lysates for Dendritic Cell-Based Cancer Vaccines. *Cancers*. 2021;13(7).
16. Bekeschus S, Clemen R, Niessner F, Sagwal SK, Freund E, Schmidt A. Medical Gas Plasma Jet Technology Targets Murine Melanoma in an Immunogenic Fashion. *Adv Sci (Weinh)*. 2020;7(10):1903438.
17. Rafiei A, Sohbatzadeh F, Hadavi S, Bekeschus S, Alimohammadi M, Valadan R. Inhibition of murine melanoma tumor growth in vitro and in vivo using an argon-based plasma jet. *Clin Plasma Med*. 2020;19-20:100102.
18. Li H, Hu J, Wu S, Wang L, Cao X, Zhang X, et al. Auranofin-mediated inhibition of PI3K/AKT/mTOR axis and anticancer activity in non-small cell lung cancer cells. *Oncotarget*. 2016;7(3):3548-58.

19. Brennan CW, Verhaak RG, McKenna A, Campos B, Noushmehr H, Salama SR, et al. The somatic genomic landscape of glioblastoma. *Cell*. 2013;155(2):462-77.
20. Kim NH, Lee MY, Park SJ, Choi JS, Oh MK, Kim IS. Auranofin blocks interleukin-6 signalling by inhibiting phosphorylation of JAK1 and STAT3. *Immunology*. 2007;122(4):607-14.
21. Busker S, Page B, Arner ESJ. To inhibit TrxR1 is to inactivate STAT3-Inhibition of TrxR1 enzymatic function by STAT3 small molecule inhibitors. *Redox biology*. 2020;36:101646.
22. Han S, Kim K, Song Y, Kim H, Kwon J, Lee YH, et al. Auranofin, an immunosuppressive drug, inhibits MHC class I and MHC class II pathways of antigen presentation in dendritic cells. *Arch Pharm Res*. 2008;31(3):370-6.
23. Wang H, Bouzakoura S, de Mey S, Jiang H, Law K, Dufait I, et al. Auranofin radiosensitizes tumor cells through targeting thioredoxin reductase and resulting overproduction of reactive oxygen species. *Oncotarget*. 2017;8(22):35728-42.
24. Genoud V, Marinari E, Nikolaev SI, Castle JC, Bukur V, Dietrich PY, et al. Responsiveness to anti-PD-1 and anti-CTLA-4 immune checkpoint blockade in SB28 and GL261 mouse glioma models. *Oncoimmunology*. 2018;7(12):e1501137.
25. Simonds EF, Lu ED, Liu EV, Tamaki W, Rancan C, Stultz J, et al. Deep immune profiling reveals targetable mechanisms of immune evasion in checkpoint blockade-refractory glioblastoma. *bioRxiv*. 2020:2020.12.01.404939.
26. Mahdikia H, Saadati F, Freund E, Gaipf US, Majidzadeh AK, Shokri B, et al. Gas plasma irradiation of breast cancers promotes immunogenicity, tumor reduction, and an abscopal effect in vivo. *Oncoimmunology*. 2020;10(1):1859731.
27. Raninga PV, Lee AC, Sinha D, Shih YY, Mittal D, Makhale A, et al. Therapeutic cooperation between auranofin, a thioredoxin reductase inhibitor and anti-PD-L1 antibody for treatment of triple-negative breast cancer. *Int J Cancer*. 2020;146(1):123-36.
28. Dai X, Bazaka K, Richard DJ, Thompson ERW, Ostrikov KK. The Emerging Role of Gas Plasma in Oncotherapy. *Trends Biotechnol*. 2018;36(11):1183-98.
29. Bernhardt T, Semmler ML, Schafer M, Bekeschus S, Emmert S, Boeckmann L. Plasma Medicine: Applications of Cold Atmospheric Pressure Plasma in Dermatology. *Oxidative medicine and cellular longevity*. 2019;2019:3873928.
30. Almeida ND, Klein AL, Hogan EA, Terhaar SJ, Kedda J, Uppal P, et al. Cold Atmospheric Plasma as an Adjunct to Immunotherapy for Glioblastoma Multiforme. *World Neurosurg*. 2019;130:369-76.
31. Liedtke KR, Freund E, Hermes M, Oswald S, Heidecke CD, Partecke LI, et al. Gas Plasma-Conditioned Ringer's Lactate Enhances the Cytotoxic Activity of Cisplatin and Gemcitabine in Pancreatic Cancer In Vitro and In Ovo. *Cancers*. 2020;12(1).
32. Lafontaine J, Boisvert JS, Glory A, Coulombe S, Wong P. Synergy between Non-Thermal Plasma with Radiation Therapy and Olaparib in a Panel of Breast Cancer Cell Lines. *Cancers*. 2020;12(2).
33. Saadati F, Mahdikia H, Abbaszadeh HA, Abdollahifar MA, Khoramgah MS, Shokri B. Comparison of Direct and Indirect cold atmospheric-pressure plasma methods in the B16F10 melanoma cancer cells treatment. *Sci Rep-Uk*. 2018;8.
34. Dubuc A, Monsarrat P, Virard F, Merbahi N, Sarrette JP, Laurencin-Dalicioux S, et al. Use of cold-atmospheric plasma in oncology: a concise systematic review. *Ther Adv Med Oncol*. 2018;10:1758835918786475.
35. Sklias K, Santos Sousa J, Girard PM. Role of Short- and Long-Lived Reactive Species on the Selectivity and Anti-Cancer Action of Plasma Treatment In Vitro. *Cancers*. 2021;13(4).
36. Malyavko A, Yan DY, Wang QH, Klein AL, Patel KC, Sherman JH, et al. Cold atmospheric plasma cancer treatment, direct versus indirect approaches. *Mater Adv*. 2020;1(6):1494-505.
37. Privat-Maldonado A, Gorbanev Y, Dewilde S, Smits E, Bogaerts A. Reduction of Human Glioblastoma Spheroids Using Cold Atmospheric Plasma: The Combined Effect of Short- and Long-Lived Reactive Species. *Cancers*. 2018;10(11).
38. Brany D, Dvorska D, Halasova E, Skovierova H. Cold Atmospheric Plasma: A Powerful Tool for Modern Medicine. *International journal of molecular sciences*. 2020;21(8).
39. Siu A, Volotskova O, Cheng X, Khalsa SS, Bian K, Murad F, et al. Differential Effects of Cold Atmospheric Plasma in the Treatment of Malignant Glioma. *Plos One*. 2015;10(6):e0126313.
40. Zucker SN, Zirnheld J, Bagati A, DiSanto TM, Des Soye B, Wawrzyniak JA, et al. Preferential induction of apoptotic cell death in melanoma cells as compared with normal keratinocytes using a non-thermal plasma torch. *Cancer Biol Ther*. 2012;13(13):1299-306.

41. Kaushik NK, Attri P, Kaushik N, Choi EH. A preliminary study of the effect of DBD plasma and osmolytes on T98G brain cancer and HEK non-malignant cells. *Molecules*. 2013;18(5):4917-28.
42. Wang M, Holmes B, Cheng X, Zhu W, Keidar M, Zhang LG. Cold atmospheric plasma for selectively ablating metastatic breast cancer cells. *Plos One*. 2013;8(9):e73741.
43. Liu J, Wang Z. Increased Oxidative Stress as a Selective Anticancer Therapy. *Oxidative medicine and cellular longevity*. 2015;2015:294303.
44. Kim SJ, Chung TH. Cold atmospheric plasma jet-generated RONS and their selective effects on normal and carcinoma cells. *Sci Rep-Uk*. 2016;6.
45. Guerrero-Preston R, Ogawa T, Uemura M, Shumulinsky G, Valle BL, Pirini F, et al. Cold atmospheric plasma treatment selectively targets head and neck squamous cell carcinoma cells. *Int J Mol Med*. 2014;34(4):941-6.
46. Georgescu N, Lupu AR. Tumoral and Normal Cells Treatment With High-Voltage Pulsed Cold Atmospheric Plasma Jets. *Ieee T Plasma Sci*. 2010;38(8):1949-55.
47. Biscop E, Lin A, Boxem WV, Loenhout JV, Backer J, Deben C, et al. Influence of Cell Type and Culture Medium on Determining Cancer Selectivity of Cold Atmospheric Plasma Treatment. *Cancers*. 2019;11(9).
48. Hasse S, Seebauer C, Wende K, Schmidt A, Metelmann HR, von Woedtke T, et al. Cold Argon Plasma as Adjuvant Tumour Therapy on Progressive Head and Neck Cancer: A Preclinical Study. *Appl Sci-Basel*. 2019;9(10).
49. Pantziarka P, Verbaanderd C, Sukhatme V, Rica Capistrano I, Crispino S, Gyawali B, et al. ReDO_DB: the repurposing drugs in oncology database. *Ecancermedicalscience*. 2018;12:886.
50. Zhang Z, Zhou L, Xie N, Nice EC, Zhang T, Cui Y, et al. Overcoming cancer therapeutic bottleneck by drug repurposing. *Signal Transduct Target Ther*. 2020;5(1):113.
51. Skaga E, Skaga IO, Grieg Z, Sandberg CJ, Langmoen IA, Vik-Mo EO. The efficacy of a coordinated pharmacological blockade in glioblastoma stem cells with nine repurposed drugs using the CUSP9 strategy. *Journal of cancer research and clinical oncology*. 2019.
52. Kast RE, Karpel-Massler G, Halatsch ME. CUSP9* treatment protocol for recurrent glioblastoma: aprepitant, artesunate, auranofin, captopril, celecoxib, disulfiram, itraconazole, ritonavir, sertraline augmenting continuous low dose temozolomide. *Oncotarget*. 2014;5(18):8052-82.
53. Weiss TE. Auranofin: dose-related risk to benefit. *Am J Med*. 1983;75(6A):128-32.
54. Rios Perez MV, Roife D, Dai B, Pratt M, Dobrowolski R, Kang Ya, et al. Antineoplastic effects of auranofin in human pancreatic adenocarcinoma preclinical models. *Surgery Open Science*. 2019;1(2):56-63.
55. Li H, Hu J, Wu S, Wang L, Cao X, Zhang X, et al. Auranofin-mediated inhibition of PI3K/AKT/mTOR axis and anticancer activity in non-small cell lung cancer cells. *Oncotarget*. 2016;7(3):3548-58.
56. Kurdi A, De Doncker M, Leloup A, Neels H, Timmermans JP, Lemmens K, et al. Continuous administration of the mTORC1 inhibitor everolimus induces tolerance and decreases autophagy in mice. *Br J Pharmacol*. 2016;173(23):3359-71.
57. Diez-Martinez R, Garcia-Fernandez E, Manzano M, Martinez A, Domenech M, Vallet-Regi M, et al. Auranofin-loaded nanoparticles as a new therapeutic tool to fight streptococcal infections. *Sci Rep*. 2016;6:19525.
58. Awasthi R, Roseblade A, Hansbro PM, Rathbone MJ, Dua K, Bebawy M. Nanoparticles in Cancer Treatment: Opportunities and Obstacles. *Curr Drug Targets*. 2018;19(14):1696-709.
59. Chen DS, Mellman I. Oncology meets immunology: the cancer-immunity cycle. *Immunity*. 2013;39(1):1-10.
60. Schaller TH, Sampson JH. Advances and challenges: dendritic cell vaccination strategies for glioblastoma. *Expert Rev Vaccines*. 2017;16(1):27-36.
61. Lamberti MJ, Nigro A, Mentucci FM, Rumie Vittar NB, Casolaro V, Dal Col J. Dendritic Cells and Immunogenic Cancer Cell Death: A Combination for Improving Antitumor Immunity. *Pharmaceutics*. 2020;12(3).
62. Vandenberk L, Belmans J, Van Woensel M, Riva M, Van Gool SW. Exploiting the Immunogenic Potential of Cancer Cells for Improved Dendritic Cell Vaccines. *Frontiers in immunology*. 2015;6:663.
63. Garg AD, Vandenberk L, Koks C, Verschuere T, Boon L, Van Gool SW, et al. Dendritic cell vaccines based on immunogenic cell death elicit danger signals and T cell-driven rejection of high-grade glioma. *Science translational medicine*. 2016;8(328):328ra27.

64. Cho DY, Yang WK, Lee HC, Hsu DM, Lin HL, Lin SZ, et al. Adjuvant immunotherapy with whole-cell lysate dendritic cells vaccine for glioblastoma multiforme: a phase II clinical trial. *World Neurosurg.* 2012;77(5-6):736-44.
65. Nakai N, Hartmann G, Kishimoto S, Katoh N. Dendritic cell vaccination in human melanoma: relationships between clinical effects and vaccine parameters. *Pigment Cell Melanoma Res.* 2010;23(5):607-19.
66. Wheeler CJ, Black KL, Liu G, Mazer M, Zhang XX, Pepkowitz S, et al. Vaccination elicits correlated immune and clinical responses in glioblastoma multiforme patients. *Cancer research.* 2008;68(14):5955-64.
67. Garg AD, Vara Perez M, Schaaf M, Agostinis P, Zitvogel L, Kroemer G, et al. Trial watch: Dendritic cell-based anticancer immunotherapy. *Oncoimmunology.* 2017;6(7):e1328341.
68. Li K, Qu S, Chen X, Wu Q, Shi M. Promising Targets for Cancer Immunotherapy: TLRs, RLRs, and STING-Mediated Innate Immune Pathways. *International journal of molecular sciences.* 2017;18(2).
69. Zhu Y, An X, Zhang X, Qiao Y, Zheng T, Li X. STING: a master regulator in the cancer-immunity cycle. *Mol Cancer.* 2019;18(1):152.
70. Jing W, McAllister D, Vonderhaar EP, Palen K, Riese MJ, Gershan J, et al. STING agonist inflames the pancreatic cancer immune microenvironment and reduces tumor burden in mouse models. *J Immunother Cancer.* 2019;7(1):115.
71. Baird JR, Friedman D, Cottam B, Dubensky TW, Jr., Kanne DB, Bambina S, et al. Radiotherapy Combined with Novel STING-Targeting Oligonucleotides Results in Regression of Established Tumors. *Cancer research.* 2016;76(1):50-61.
72. Cen X, Liu S, Cheng K. The Role of Toll-Like Receptor in Inflammation and Tumor Immunity. *Frontiers in pharmacology.* 2018;9:878.
73. Rodriguez-Ruiz ME, Rodriguez I, Leaman O, Lopez-Campos F, Montero A, Conde AJ, et al. Immune mechanisms mediating abscopal effects in radioimmunotherapy. *Pharmacology & therapeutics.* 2019;196:195-203.
74. De Waele J, Marcq E, Van Audenaerde JR, Van Loenhout J, Deben C, Zwaenepoel K, et al. Poly(I:C) primes primary human glioblastoma cells for an immune response invigorated by PD-L1 blockade. *Oncoimmunology.* 2018;7(3):e1407899.
75. Rosenfeld MR, Chamberlain MC, Grossman SA, Peereboom DM, Lesser GJ, Batchelor TT, et al. A multi-institution phase II study of poly-ICLC and radiotherapy with concurrent and adjuvant temozolomide in adults with newly diagnosed glioblastoma. *Neuro-oncology.* 2010;12(10):1071-7.
76. Belderbos RA, Aerts J, Vroman H. Enhancing Dendritic Cell Therapy in Solid Tumors with Immunomodulating Conventional Treatment. *Mol Ther Oncolytics.* 2019;13:67-81.
77. Vareki SM. High and low mutational burden tumors versus immunologically hot and cold tumors and response to immune checkpoint inhibitors. *J Immunother Cancer.* 2018;6.
78. Alexandrov LB, Nik-Zainal S, Wedge DC, Aparicio SA, Behjati S, Biankin AV, et al. Signatures of mutational processes in human cancer. *Nature.* 2013;500(7463):415-21.
79. Antonios JP, Soto H, Everson RG, Orpilla J, Moughon D, Shin N, et al. PD-1 blockade enhances the vaccination-induced immune response in glioma. *JCI Insight.* 2016;1(10).
80. Kim JE, Patel MA, Mangraviti A, Kim ES, Theodros D, Velarde E, et al. Combination Therapy with Anti-PD-1, Anti-TIM-3, and Focal Radiation Results in Regression of Murine Gliomas. *Clinical cancer research : an official journal of the American Association for Cancer Research.* 2017;23(1):124-36.
81. Ladomersky E, Zhai L, Lenzen A, Lauing KL, Qian J, Scholtens DM, et al. IDO1 Inhibition Synergizes with Radiation and PD-1 Blockade to Durably Increase Survival Against Advanced Glioblastoma. *Clinical cancer research : an official journal of the American Association for Cancer Research.* 2018;24(11):2559-73.
82. Azad A, Yin Lim S, D'Costa Z, Jones K, Diana A, Sansom OJ, et al. PD-L1 blockade enhances response of pancreatic ductal adenocarcinoma to radiotherapy. *EMBO Mol Med.* 2017;9(2):167-80.
83. Chen G, Chen Z, Wen D, Wang Z, Li H, Zeng Y, et al. Transdermal cold atmospheric plasma-mediated immune checkpoint blockade therapy. *Proceedings of the National Academy of Sciences of the United States of America.* 2020;117(7):3687-92.

SUMMARY

Pancreatic ductal adenocarcinoma (PDAC) and glioblastoma multiforme (GBM) are two of the most malignant solid tumor types with poor survival rates, which underscore the urgency of novel and efficacious treatment strategies. Within the last decade, immunotherapy has been established as a breakthrough in cancer therapy. This mainly has been driven by the clinical data and approval associated with several immune checkpoint inhibitors (e.g. anti-CTLA-4 and anti-PD-1/L1). Despite the clinical benefit in specific tumor types, these inhibitors have not yet fulfilled their promise in low immunogenic tumors such as PDAC and GBM.

Oxidative stress in cancer cells due to elevated reactive oxygen species (ROS) and an inability to balance intracellular redox state has recently been highlighted as promising target for anticancer treatment strategies with possible immunogenic effects. In this PhD dissertation, I investigated novel oxidative stress-mediated treatment approaches to target PDAC and GBM and to enhance immunogenicity by inducing immunogenic cell death (ICD).

In the first part of this thesis (**chapter 2**), I reviewed the mechanistic responses of cancer cells towards different oxidative stress-inducing treatment strategies and their immunomodulating effects. The resulting literature demonstrated that different exogenous and endogenous ROS-inducing therapies show direct and indirect immunomodulating effects, which can be either immunostimulatory or immunosuppressive. One of the indirect immunostimulatory effects of the ROS-mediating therapies is the capacity of inducing immunogenic cell death (ICD) in tumor cells, which can increase the immunogenicity and consequently can trigger an antitumoral immune response.

In **chapter 3**, I investigated a novel exogenous ROS-inducing treatment method, namely cold atmospheric plasma, to determine the therapeutic and ICD-inducing effects in PDAC, *in vitro*. I revealed that plasma-treated PBS (pPBS) has the potential to induce ICD in pancreatic cancer cells (PCCs) and to reduce the immunosuppressive tumor microenvironment (TME) by attacking the tumor supportive pancreatic stellate cells (PSCs). Although the cell death induced in PSCs was non-immunogenic as seen by the lack of danger-associated molecular patterns (DAMPs) emission and DC activation, I showed that pPBS could disrupt the physical barrier and lower the immunosuppressive secretion profile (lower TGF- β) of PSCs. In contrast, DAMPs were released by PCCs after treatment

with pPBS which resulted in activation and maturation of DCs and a more immunostimulatory secretion profile (higher TNF- α , IFN- γ). Hence, indirect plasma treatment via pPBS has the potential to enhance immunogenicity in PDAC by triggering ICD and by attacking the immunosuppressive PSCs.

Tumor cells can evolve adaptation mechanisms to protect themselves against intrinsic oxidative stress by upregulation of pro-survival molecules and their antioxidant defense system to maintain the redox balance. As such, tumor cells can become resistant towards exogenous ROS-inducing therapies, like plasma. Dual targeting of the redox balance of tumor cells by increasing exogenous levels of ROS and inhibiting the antioxidant defense system can maximally exploit ROS-mediated cell death mechanisms as therapeutic anticancer strategy. In this regard, cold atmospheric plasma was combined with auranofin, a thioredoxin reductase inhibitor, in GBM (**chapter 4**). A synergistic effect was shown after this combination treatment in 2D and 3D, however, in 3D only high concentrations of auranofin synergized with plasma treatment. I confirmed a ROS-mediated response after combination treatment, which was able to induce distinct cell death mechanisms, specifically apoptosis and ferroptosis. Additionally, the auranofin and plasma combined treatment strategy induced cell death, which resulted in an increased release of DAMPs. Together with the observed DC maturation, these results indicate the potential increase in immunogenicity, though, the phagocytotic capacity of DCs was inhibited by auranofin.

In **chapter 5**, I evaluated this promising oxidative stress combination therapy in GBM, *in vivo*. A decrease in tumor kinetics and an increased survival in GBM-bearing mice was observed when auranofin was sequentially combined with direct plasma treatment. No T cell infiltration was observed after auranofin monotherapy. However, further characterization of the TME after the combination therapy is necessary to provide more insight in the immunogenic effects *in vivo*.

In conclusion, this PhD dissertation comprises novel and important therapeutic and immunogenic insights in cold atmospheric plasma and auranofin as promising oxidative stress-mediated treatment strategies for low immunogenic tumors, like PDAC and GBM. These preclinical results provide a solid basis for future research towards combinations with immunotherapeutic approaches.

SAMENVATTING

Pancreaskanker en glioblastoom zijn twee kwaadaardige tumor types die gekenmerkt worden door een slechte prognose en lage overlevingskansen. Dit benadrukt de urgentie voor nieuwe doeltreffende behandelingen. De laatste tien jaar is de interesse in immuuntherapie enorm aangewakkerd door de klinische resultaten verkregen met therapeutische remmers van belangrijke immunologische ‘checkpoints’ aanwezig op kankercellen en/of immuuncellen. Ondanks goede resultaten in bepaalde kankertypes, heeft deze vorm van immuuntherapie niet het gehoopte effect in laag immunogene solide tumoren zoals pancreaskanker en glioblastoom.

Het induceren van oxidatieve stress in kankercellen is een belangrijk doelwit voor nieuwe behandelingsstrategieën, die mogelijks immunologische effecten teweeg brengen. In deze doctoraatsthesis, heb ik het therapeutische en immunologische effect van een nieuwe oxidatieve stress-geassocieerde behandelingsstrategie geëvalueerd in pancreaskanker en glioblastoom.

Het eerste deel van de thesis (**hoofdstuk 2**) beschrijft een overzicht van de mechanistische en immunologische effecten van verschillende kankerbehandelingen die oxidatieve stress kunnen verhogen in kankercellen. Deze review toont aan dat er verschillende behandelingen exogene en endogene reactieve zuurstofradicalen kunnen vrijstellen, die zowel directe als indirecte effecten hebben op het immuunsysteem. Deze immunologische effecten kunnen zowel stimulerend als remmend zijn. Een belangrijk direct en immunologisch stimulerend effect van dergelijke therapieën is het doden van kankercellen waarbij immunologische gevarensignalen worden vrijgesteld die een specifieke antitumor-immuunreactie kunnen teweegbrengen. Dit specifiek type van celdood waarbij deze vrijgestelde immunologische signalen vrijgegeven worden, wordt immunogene celdood genoemd.

In **hoofdstuk 3**, heb ik fysisch koud atmosferisch plasma onderzocht als nieuwe oxidatieve stress-geassocieerde kankerbehandeling in pancreaskanker. Hierbij toonde ik d.m.v. de vrijgestelde immunologische signalen aan, dat plasma het potentieel heeft om immunogene celdood op te wekken in pancreaskankercellen. Dit gaf vervolgens aanleiding tot fagocytose door dendritische cellen en maturatie van deze dendritische cellen. Bovendien was plasma in staat om de tumor-geassocieerde stellaatcellen met een immunologisch remmende werking aan te vallen. Deze resultaten tonen aan dat koud atmosferisch plasma in staat is

pancreaskankercellen en stercelcellen aan te vallen en bijgevolg het immunologische karakter van pancreaskanker te versterken.

Kankercellen hebben de eigenschap om zich aan te passen aan omstandigheden waarbij er te veel zuurstof aanwezig is zoals bij oxidatieve stress, door hun beschermingsmechanisme van antioxidanten te versterken. Hierdoor kan er resistentie ontstaan tegenover oxidatieve stress-geassocieerde kankerbehandelingen. Daarom zou het voordelig zijn zowel oxidatieve stress te verhogen in kankercellen als tegelijkertijd het beschermingsmechanisme van antioxidanten te blokkeren. In **hoofdstuk 4** heb ik deze behandelingsstrategie onderzocht in glioblastoom. Hierbij hebben ik koud atmosferisch plasma gecombineerd met een inhibitor van het thioredoxine reductase beschermingsmechanisme, namelijk auranofine. Deze combinatie gaf aanleiding tot een synergistische therapeutische respons in 2D- en 3D-celculturen van glioblastoom, waarbij een hoge concentratie aan zuurstofradicalen werd waargenomen. Verder werd apoptose en ferroptose van glioblastoomcellen waargenomen na behandeling met plasma en auranofine. Naast het therapeutische effect van de combinatiestrategie werden immunologische gevarensignalen vrijgesteld, die enerzijds aanleiding gaven tot maturatie van dendritische cellen. Anderzijds werd fagocytose van glioblastoomcellen door deze dendritische cellen verminderd door de aanwezigheid van auranofine.

Vervolgens heb ik in **hoofdstuk 5** de combinatie van plasma en auranofine getest in een glioblastoom muismodel. Er werd een vertraagde tumor groei en een toename in overleving waargenomen in het glioblastoom muismodel na behandeling met een sequentiële combinatie van auranofine en plasma. Er werd geen T-celinfiltratie waargenomen na behandeling met auranofine. Verdere karakterisering van de tumormicro-omgeving na de combinatiestrategie is echter nodig om meer inzicht te krijgen in de potentiële immunologische effecten *in vivo*.

Samengevat beschrijft dit doctoraatsonderzoek belangrijke therapeutische en immunologische inzichten verworven in het gebruik van koud atmosferisch plasma en auranofine als oxidatieve stress-geassocieerde kankerbehandeling gericht tegen pancreaskanker en glioblastoom. Deze preklinische resultaten vormen dan ook een sterke basis voor toekomstige veelbelovende combinaties met immuuntherapie, al dienen deze verder onderzocht te worden.

DANKWOORD

Het is onvoorstelbaar dat ik op het einde van mijn doctoraat ben gekomen. Het waren vijf fantastische jaren, die voorbij zijn gevlogen. Het was een onvergetelijke ervaring die ik voor geen geld van de wereld zou willen hebben gemist. Het rest mij enkel nog iedereen te bedanken die aan dit avontuur heeft bijgedragen.

In de eerste plaats wil ik mijn promotoren bedanken, prof. Evelien Smits, prof. Annemie Bogaerts en dr. Christophe Deben.

Evelien, merci om in mij te geloven zowel bij de start als bij de voortgang van mijn doctoraat. Je deur stond altijd open voor advies of een luisterend oor te bieden bij eender welke vraag of probleem. Jouw oprecht enthousiasme voor wetenschappelijk onderzoek is aanstekelijk en mede dankzij jouw leiderschap en begeleiding heb ik dit werk tot een mooi einde kunnen brengen. Annemie, ook jou wil ik bedanken voor de positieve feedback en waardering die ik steeds kreeg. Ondanks dat de biologische en immunologische kant van het plasma medicine onderzoek niet altijd evident is voor jou, ben je er toch meer dan goed in geslaagd mij te ondersteunen en knopen door te hakken wanneer nodig. Christophe, jouw eerlijke en directe manier van aanpak om mij te begeleiden heb ik steeds enorm gewaardeerd. Merci om mij te blijven motiveren, pushkes te blijven geven, conclusies uit mijn data te trekken, voor de talrijke keren dat ik te pas en te onpas je bureau kwam binnenwandelen, complimenten te geven waar ik zelf achter viste en zo veel meer. De onderzoeker die jij bent in hart en nieren, siert je. Om het in het Antwerps te zeggen: 'Ik mag mijn pollekes kussen met jullie als promotoren!'

Het is fantastisch om te zien hoe onze onderzoeksgroep is gegroeid en wat we daarbij allemaal verwezenlijkt hebben de voorbije jaren. Ik wil naast Evelien, ook An en Filip bedanken dat ik deel mocht uitmaken van dit geweldige CORE team. Het is jullie verdienste om ons labo te hebben laten groeien tot wat we vandaag zijn. Jullie mogen ontzettend fier zijn op zo'n onderzoeksgroep!

Ik zou ook graag de leden van mijn doctoraatsjury, prof. Didier Ebo, prof. Wim Vandenberghe, prof. Cristina Canal en dr. Sander Bekeschus, willen bedanken voor hun feedback en tijd die ze geïnvesteerd hebben in het nalezen van deze thesis. Thank you for all the feedback on this thesis.

Mijn doctoraat was niet mogelijk geweest zonder de financiële steun van het Olivia Hendrickx Research Fund. Bedankt om onderzoek naar kanker mede mogelijk te maken!

Zoals jullie weten, ben ik iemand van veel woorden en verhalen, maar toch valt er niet met woorden uit te drukken hoe ongelooflijk dankbaar ik ben. Naast de fierheid, voel ik vooral een grote portie dankbaarheid dat ik samen met jullie dit hele traject een belangrijk deel uit mijn leven mag noemen. Ik ben dankbaar voor elke kans, elk experiment, elke helpende hand, elke hobbel die we trotseerden, elk geweldig gesprek, elke fijne herinnering,... er zijn ontelbaar veel redenen! Ik ben trots deel uitgemaakt te hebben van dit ongelooflijk hecht en open team, één vol vertrouwen en talent waar ik met veel appreciatie en waardering naar opkijk. Met die verzameling aan fierheid en dankbaarheid kijk ik terug op een onvergetelijke ervaring, waar ik vandaag bedankt voor zeg!

En daarom aan iedereen die deel uitmaakt(e) van het CORE labo en de Plasma-Oncology groep, Evelien, Annemie, Deben, An, Filip, prof. Marc Peeters, prof. Sylvia Dewilde, Jorrit, Elly, Jonas, Julie, Laure, Ines, Jolien, Debbie, Ilayda, Abraham, Angela, Laurie, Tal, Delphine, Pablo, Andreas, Yannick, Hasan, Hanne, Hannah, Eline, Joey, Tias, Astrid, Kaat, Elien, Priyanka, Karen, Edgar, Steven, Wilma, Ruben, Vaso, Maxime, Maxim, Sophie, Karin, Maria, Okke, Céline, Hilde, Stofke, Howa

Aan de collega's van Hematologie, Eva, Hans, Johan, Heleen, Diana, Maarten, en al jullie overige fantastische onderzoekers

Aan mijn familie, mama & papa, Hein, Sanne & Maarten, Jens & Silke, mijn grootouders en aan al mijn vriendinnen

DANK DANK DANK

DAT JIJ ER BENT

DAT JIJ ER WAS

VOOR WAT JE DEED

EN WAT JE DOET

NIEUW OF BEKEND

VROEGER OF PAS

EN WEET

DAT IK HET NIET VERGEET

WEET JE DOET HET GOED

Jinthe

GEWOON JIJ.

CURRICULUM VITAE

Personalia

Name: Jinthe Van Loenhout

Date of Birth: 28/05/1992

Nationality: Belgian

Current affiliation: Center for Oncological Research (CORE)
Solid Tumor Immunology Group (STIG)
University of Antwerp
Universiteitsplein 1, T4.33
B-2610 Wilrijk, Belgium

Email: jinthe.vanloenhout@uantwerpen.be
vanloenhoutjinthe@gmail.com

Scientific career

2016 – present **PhD researcher**

2020 – 2021 **Part-time researcher at Karel de Grote Hogeschool**
Biomedical laboratory technology

Education

2015 – 2016 **Specific teaching program**
Didactics of biology
University of Antwerp

2015 **FELASA (cat. C)**
University of Antwerp

2013 – 2015

Master Biomedical Sciences

Major: clinical scientific research

University of Antwerp

Master dissertation

“Immune-based combination therapy to treat glioblastoma”

Supervisor: Dr. Jorrit De Waele

Promotor: Prof. Dr. Evelien Smits

2010 – 2014

Bachelor Biomedical Sciences

University of Antwerp

Scientific output

Peer-reviewed publications (A1)

2021

Jinthe Van Loenhout, Laurie Freire Boullosa, Delphine Quatannens, Jorrit De Waele, Céline Merlin, Hilde Lambrechts, Filip Lardon, Marc Peeters, Annemie Bogaerts, Evelien Smits, Christophe Deben. Auranofin and cold atmospheric plasma synergize to trigger distinct cell death mechanisms and immunogenic responses in glioblastoma multiforme. *Submitted*

Laurie Freire Boullosa, **Jinthe Van Loenhout**, Tal Flieswasser, Jorrit De Waele, Christophe Hermans, Hilde Lambrechts, Bart Cuypers, Kris Laukens, Esther Bartholomeus, Vasiliki Siozopoulou, Winnok De Vos, Marc Peeters, Evelien Smits, Christophe Deben. Auranofin reveals therapeutic anticancer potential by triggering distinct molecular cell death mechanisms and innate immunity in mutant p53 non-small cell lung cancer. *Redox Biology* – ISSN 2213-2317 – 101949 (2021)

2020

Jinthe Van Loenhout, Marc Peeters, Annemie Bogaerts, Evelien Smits, Christophe Deben. Oxidative stress-inducing anticancer therapies : taking a closer look at their immunomodulating effects. *Antioxidants* - ISSN 2076-3921 - 9:12(2020), 1188

Tal Flieswasser, **Jinthe Van Loenhout**, Laurie Freire Boullosa, Astrid Van den Eynde, Jorrit De Waele, Jonas Van Audenaerde, Filip Lardon, Evelien Smits, Patrick Pauwels, Julie Jacobs. Clinically relevant chemotherapeutics have the ability to induce immunogenic cell death in non-small cell lung cancer. *Cells* - 9:6(2020), 1474

Jonas Van Audenaerde, Elly Marcq, Bianca von Scheidt, Ashleigh S Davey, Amanda J Oliver, Jorrit De Waele, Delphine Quatannens, **Jinthe Van Loenhout**, Patrick Pauwels, Geert Roeyen, Filip Lardon, Clare Y Slaney, Marc Peeters, Michael H Kershaw, Phillip K Darcy, Smits Evelien. Novel combination immunotherapy for pancreatic cancer: potent anti-tumor effects with CD40 agonist and interleukin-15 treatment. *Clinical & Translational Immunology* - ISSN 2050-0068 - 9:8(2020), e1165

2019

Jinthe Van Loenhout, Tal Flieswasser, Laurie Freire Boullosa, Jorrit De Waele, Jonas van Audenaerde, Elly Marcq, Julie Jacobs, Abraham Lin, Eva Lion, Heleen Dewitte, Marc Peeters, Sylvia Dewilde, Filip Lardon, Annemie Bogaerts, Christophe Deben, Evelien Smits. Cold atmospheric plasma-treated PBS eliminates immunosuppressive pancreatic stellate cells and induces immunogenic cell death of pancreatic cancer cells. *Cancers* - ISSN 2072-6694 - 11:10(2019), 1597

Elly Marcq, Jonas van Audenaerde, Jorrit De Waele, Julie Jacobs, **Jinthe Van Loenhout**, Glenn Cavents, Patrick Pauwels, Jan van Meerbeeck, Evelien Smits. Building a bridge between chemotherapy and immunotherapy in malignant pleural mesothelioma : investigating the effect of chemotherapy on immune checkpoint expression. *International Journal of Molecular Sciences* - ISSN 1661-6596 - 20:17(2019), 4182

Eline Biscop, Abraham Lin, Wilma Van Boxem, **Jinthe Van Loenhout**, Joey De Backer, Christophe Deben, Sylvia Dewilde, Evelien Smits, Annemie Bogaerts. Influence of cell type and culture medium on determining cancer selectivity of cold atmospheric plasma treatment. *Cancers* - ISSN 2072-6694 - 11:9(2019), 1287

Abraham Lin, Yury Gorbanev, Joey De Backer, **Jinthe Van Loenhout**, Wilma Van Boxem, Filip Lemière, Paul Cos, Sylvia Dewilde, Evelien Smits, Annemie Bogaerts. Non-thermal plasma as a unique delivery system of short-lived reactive oxygen and nitrogen species for immunogenic cell death in melanoma cells. *Advanced Science* - ISSN 2198-3844 - 6:6(2019), 1802062

2018

Jorrit De Waele, Elly Marcq, Jonas van Audenaerde, **Jinthe Van Loenhout**, Christophe Deben, Karen Zwaenepoel, Erik Van de Kelft, David Van der Planken, Tomas Menovsky, Johan Van den Bergh, Yannick Willemen, Patrick Pauwels, Zwi Nisan Berneman, Filip Lardon, Marc Peeters, An Wouters, Evelien Smits. Poly(I:C) primes primary human glioblastoma cells for an immune response invigorated by PD-L1 blockade. *Oncoimmunology* - ISSN 2162-402X - 7:3(2018), e1407899

2017

Jonas Van Audenaerde, Jorrit De Waele, Elly Marcq, **Jinthe Van Loenhout**, Eva Lion, Johan Van den Bergh, Ralf Jesenofsky, Atsushi Masamune, Geert Roeyen, Patrick Pauwels, Filip Lardon, Marc Peeters, Evelien Smits. Interleukin-15 stimulates natural killer cell-mediated killing of both human pancreatic cancer and stellate cells. *Oncotarget* - ISSN 1949-2553 - 8:34(2017), p. 56968-56979

Other scientific publications (A2)

2021

Laurie Freire Boulosa, **Jinthe Van Loenhout**, Christophe Deben. Chapter 4 - Endogenous antioxidants in the prognosis and treatment of lung cancer. In: Preedy VR, Patel VB, editors. *Cancer* (Second Edition). San Diego: Academic Press; 2021. p. 39-48. (All authors contributed equally)

Oral presentations at scientific meetings

Jinthe Van Loenhout, Christophe Deben, Julie Jacobs, Jorrit De Waele, Jonas Van Audenaerde, Elly Marcq, Sylvia Dewilde, Annemie Bogaerts, Evelien Smits. Immunogenic potential of cold atmospheric plasma for the treatment of pancreatic cancer. 5th International Workshop on Plasma Cancer treatment (IWPCT) 2018, Greifswald, Germany, 20-21/03/2018

Jinthe Van Loenhout, Christophe Deben, Julie Jacobs, Jorrit De Waele, Jonas Van Audenaerde, Elly Marcq, Sylvia Dewilde, Annemie Bogaerts, Evelien Smits. Immunogenic potential of cold atmospheric plasma for the treatment of pancreatic cancer. Research day Tumor Immunology and Immunotherapy, Leuven, Belgium, 14/06/2018

Jinthe Van Loenhout, Christophe Deben, Julie Jacobs, Jorrit De Waele, Jonas Van Audenaerde, Elly Marcq, Tal Flieswasser, Sylvia Dewilde, Annemie Bogaerts, Evelien Smits. Can cold atmospheric plasma invigorate the immune response against pancreatic cancer. 7th Workshop on frontiers in redox biochemistry and medicine, Rostock, Germany, 23-26/09/2018

Jinthe Van Loenhout, Laurie Freire Boulosa, Delphine Quatannens, Marc Peeters, Annemie Bogaerts, Christophe Deben, Evelien Smits. Mechanistic insights into combination of different sources of ROS in glioblastoma multiforme. Presented by Evelien Smits. 6th Healthcare & Life Science & Entrepreneurship Workshop, Denmark, Copenhagen, remote only (Zoom), 29-30/04/2021

Jinthe Van Loenhout, Laurie Freire Boulosa, Delphine Quatannens, Marc Peeters, Annemie Bogaerts, Christophe Deben, Evelien Smits. Mechanistic insights into combination of different sources of ROS in glioblastoma multiforme. 7th International Workshop on Plasma for cancer Treatment (IWPCT) 2021, Barcelona, Spain (Online), 29-30/06/2021

Selected poster presentations

Jinthe Van Loenhout, Christophe Deben, Julie Jacobs, Jorrit De Waele, Jonas Van Audenaerde, Elly Marcq, Sylvia Dewilde, Annemie Bogaerts, Evelien Smits. Immunogenic potential of cold atmospheric plasma for the treatment of pancreatic cancer. EACR 2018, Amsterdam, The Netherlands, 30/06/2018 – 03/07/2018.

Jinthe Van Loenhout, Christophe Deben, Julie Jacobs, Jorrit De Waele, Jonas Van Audenaerde, Elly Marcq, Sylvia Dewilde, Annemie Bogaerts, Evelien Smits. Cold atmospheric plasma as a novel immunogenic cell death inducer in pancreatic cancer cells. EMBO workshop on phagocytosis of dying cells: molecules, mechanisms and therapeutic implications. Ghent, Belgium, 24-27/10/2018.

Jinthe Van Loenhout, Christophe Deben, Julie Jacobs, Jorrit De Waele, Jonas Van Audenaerde, Elly Marcq, Tal Flieswasser, Sylvia Dewilde, Annemie Bogaerts, Evelien Smits. Cold atmospheric plasma treatment induces immunogenic cell death in pancreatic cancer. BACR Annual Meeting 2019: Novel combinations strategies for cancer treatment – current challenges and future perspectives, Antwerp, Belgium, 1 February 2019.

Jinthe Van Loenhout, Christophe Deben, Tal Flieswasser, Laurie Freire Boulosa, Jorrit De Waele, Jonas RM Van Audenaerde, Elly Marcq, Julie Jacobs, Abraham Lin, Eva Lion, Marc Peeters, Sylvia Dewilde, Filip Lardon, Annemie Bogaerts, Evelien Smits. Targeting the immunosuppressive tumor microenvironment and inducing immunogenic cell death with cold atmospheric plasma in pancreatic cancer. 6th International Workshop on Plasma Cancer treatment (IWPCT) 2019, Antwerp, Belgium, 1-3/04/2019

Jinthe Van Loenhout, Christophe Deben, Tal Flieswasser, Laurie Freire Boulosa, Jorrit De Waele, Jonas Van Audenaerde, Elly Marcq, Julie Jacobs, Abraham Lin, Eva Lion, Marc Peeters, Sylvia Dewilde, Filip Lardon, Annemie Bogaerts, Evelien Smits. Targeting the immunosuppressive tumor microenvironment and inducing immunogenic cell death with cold atmospheric plasma in pancreatic cancer. 17th CIMT Annual Meeting taking place in Mainz, Germany from May 21-23, 2019.

Jinthe Van Loenhout, Christophe Deben, Laurie Freire Boulosa, Jorrit De Waele, Delphine Quatannens, Marc Peeters, Annemie Bogaerts, Evelien Smits. Investigation of combined ROS inducing therapies in 2D and 3D glioblastoma cell cultures. BACR Annual meeting, Brussels, Belgium January 15, 2020.

Grants

2017 – 2021 Research grant from the Olivia Hendrickx Research Foundation

2016 – 2020 BOF-DOCPRO4 fellowship
University of Antwerp